National Library
of Canada

Bibliothèque nationale
du Canada

Canadian Theses Service

Service des thèses canadiennes

Ottawa, Canada
K1A 0N4

NOTICE

The quality of this microform is heavily dependent upon the quality of the original thesis submitted for microfilming. Every effort has been made to ensure the highest quality of reproduction possible.

If pages are missing, contact the university which granted the degree.

Some pages may have indistinct print especially if the original pages were typed with a poor typewriter ribbon or if the university sent us an inferior photocopy.

Previously copyrighted materials (journal articles, published tests, etc.) are not filmed.

Reproduction in full or in part of this microform is governed by the Canadian Copyright Act, R.S.C. 1970, c. C-30.

AVIS

La qualité de cette microforme dépend grandement de la qualité de la thèse soumise au microfilmage. Nous avons tout fait pour assurer une qualité supérieure de reproduction.

S'il manque des pages, veuillez communiquer avec l'université qui a conféré le grade.

La qualité d'impression de certaines pages peut laisser à désirer, surtout si les pages originales ont été dactylographiées à l'aide d'un ruban usé ou si l'université nous a fait parvenir une photocopie de qualité inférieure.

Les documents qui font déjà l'objet d'un droit d'auteur (articles de revue, tests publiés, etc.) ne sont pas microfilmés.

La reproduction, même partielle, de cette microforme est soumise à la Loi canadienne sur le droit d'auteur, SRC 1970, c. C-30.

NL-339 (r. 88/04)

Canada

THE UNIVERSITY OF ALBERTA

Experimental Evaluation of Multivariable, Multirate Self-Tuning Control of a Binary Distillation Column

by

© Frank J. Vagi

A THESIS

SUBMITTED TO THE FACULTY OF GRADUATE STUDIES AND RESEARCH

IN PARTIAL FULFILMENT OF THE REQUIREMENTS FOR THE DEGREE

OF Master of Science

IN

Process Control

Department of Chemical Engineering

EDMONTON, ALBERTA

Fall 1988

Permission has been granted to the National Library of Canada to microfilm this thesis and to lend or sell copies of the film.

The author (copyright owner) has reserved other publication rights, and neither the thesis nor extensive extracts from it may be printed or otherwise reproduced without his/her written permission.

L'autorisation a été accordée à la Bibliothèque nationale du Canada de microfilmer cette thèse et de prêter ou de vendre des exemplaires du film.

L'auteur (titulaire du droit d'auteur) se réserve les autres droits de publication; ni la thèse ni de longs extraits de celle-ci ne doivent être imprimés ou autrement reproduits sans son autorisation écrite.

ISBN 0-315-45660-4

THE UNIVERSITY OF ALBERTA

RELEASE FORM

NAME OF AUTHOR Frank J. Vagi

TITLE OF THESIS Experimental Evaluation of Multivariable, Multirate Self-Tuning Control of a Binary Distillation Column

DEGREE FOR WHICH THESIS WAS PRESENTED Master of Science

YEAR THIS DEGREE GRANTED Fall 1988

Permission is hereby granted to THE UNIVERSITY OF ALBERTA LIBRARY to reproduce single copies of this thesis and to lend or sell such copies for private, scholarly or scientific research purposes only.

The author reserves other publication rights, and neither the thesis nor extensive extracts from it may be printed or otherwise reproduced without the author's written permission.

(SIGNED) Frank Vagi.....

PERMANENT ADDRESS:

7 Garcia Place
St Albert, Alberta
T8N 1Z7

DATED 26 AUGUST 1988

THE UNIVERSITY OF ALBERTA

FACULTY OF GRADUATE STUDIES AND RESEARCH

The undersigned certify that they have read, and recommend to the Faculty of Graduate Studies and Research, for acceptance, a thesis entitled Experimental Evaluation of Multivariable, Multirate Self-Tuning Control of a Binary Distillation Column submitted by Frank J. Vagi in partial fulfilment of the requirements for the degree of Master of Science in Process Control.

....
Dr. R. K. Wood
Supervisor

....
Dr. S. L. Shah

..Keith.....................
Dr. K. A. Stromsmoe

Date 26 August 1988

To my wife Paula,
Kevin and Lisa
with love

Abstract

This work presents the experimental evaluation of the multivariable multirate self-tuning controller (STC) on a pilot scale distillation column. Control of distillation columns remains a key concern to industry because of the energy intensive nature of the process in providing the component separation. A significant contributor to the reduced performance of many control applications is the inability to reject load disturbances within the process. It is this aspect of control which would provide the most significant improvement to industrial applications. The ability to reject disturbances effectively and retain product specification, while still maintaining an objective of minimum energy consumption, is the corner stone of this work. The evaluation of the STC is performed by comparing its performance with that of conventional Proportional Integral Derivative (PID) control. The formulation of a comparison is based on initial design techniques and well tuned results.

The STC and conventional controllers are used to provide dual composition control of the distillation column when it is subjected to disturbances composed of step changes in feed flow. The performance is quantified numerically by considering the integral of absolute error(IAE) over the duration of the test period.

The experimental results show that the Q weighting parameters in the STC formulation can be chosen with the

same open loop techniques used for PID controllers. It was found that the response of the multirate self-tuning controller provided the least value of the IAE for disturbance rejection. The response of the multirate self-tuning controller with Q weighting chosen by initial techniques provided a combined IAE result of 386.5, whereas a well tuned multirate PID controller yielded IAE results of 545. The significant improvement in disturbance rejection for the multirate self-tuning controller was provided by the dead time compensation capabilities of the self-tuning controller. Insignificant improvement was observed between conventional PID control and that of the self-tuning controller when loops with no dead time were controlled. This is demonstrated by the IAE results for the self-tuning controller of 29.6 for top composition control using IAE parameter selection methods. The PID control achieved an IAE result of 30.6 after many efforts in retuning the controllers constants.

Acknowledgements

The author wishes to thank his supervisor Dr. R. K. Wood for his support and encouragement during this research.

Special thanks are extended to Dr. A. J. Morris for providing the original source code for this work. Thanks are also extended to Dr. M. Tham for his patience, discussions and assistance during various portions of this work.

The author wishes to express his appreciation to the DACS centre staff, in particular Mr. R. L. Barton, for their assistance in using the computing facilities.

Special thanks are due to the staff in the electronic, instrumentation and machine shops, in particular Mr. D. Sutherland and Mr. K. Faulder, for their assistance in maintaining the fine operating record of the distillation column.

Thanks are extended to my fellow graduate students, especially Dr. H. K. Song, for their friendship and many hours of valuable discussions during the course of this work.

Financial support from the Department of Chemical Engineering and the Natural Sciences and Engineering Research Council during this work was greatly appreciated.

Table of Contents

Chapter Page

Abstract v

Acknowledgements vii

Nomenclature xxv

1. Introduction and Objectives 1

1.1 Introduction 1

1.2 Objectives 2

1.3 Thesis Organization 3

2. Literature Survey 5

2.1 Introduction 5

2.2 Historical Development of Self-Tuning Control 6

2.3 Applications of Self-Tuning Control 10

3. Development of Self-Tuning Controller 13

3.1 Introduction 13

3.2 Multiple Input Single Output Self-Tuning Controller 14

3.2.1 Multiple Input Single Output Control Law Formulation 14

3.2.2 Parameter Estimation 23

3.3 Multivariable Self-Tuning Controller 27

3.3.1 Multivariable Control Law Formulation 27

3.3.2 Multivariable Parameter Estimation 36

3.3.3 Extension to Multirate Control 39

3.3.4 Extension to K-incremental Self-tuning Controller 41

3.4 Control Law Implementation 44

3.4.1 Distillation Column Control Law 44

4. Experimental Implementation 47

4.1 Description of Equipment 47

4.2 Control Implementation 55

4.3 Operating System 56

4.4 Gas Chromatograph 57

5. Column Dynamics 59

5.1 Introduction 59

5.2 System Representation 60

5.3 Manipulated Variable Dynamics 61

5.4 Disturbance Dynamics 67

6. Selection of Controller Parameters 70

6.1 Introduction 70

6.2 Sample Time Selection 70

6.3 Proportional-Integral-Derivative Controller Parameters 72

6.4 Self-Tuning Controller 77

6.5 Selection of Q Weighting Parameters 79

6.6 Controller Performance Criterion 80

7. Experimental Results 85

7.1 Control of Product Compositions Using a Multiloop PID Control Strategy 86

7.1.1 Control Performance With Constants Calculated from the Ziegler-Nichols Equations 86

7.1.2 Control Performance with Constants Calculated using the Cohen-Coon Equations .93

7.1.3 Control Performance with Constants Calculated using the Integral of Absolute Error Equations 99

7.1.4 Control Performance with Constants Calculated using the Integral of Time Multiplied by the Absolute Error Equations 105

7.1.5 Summary of Column Control Performance Using a Multiloop PID Control Strategy for Calculated Controller Settings 112

7.2 Control of Product Composition Using a Multirate PID Control Strategy 114

7.2.1 Control Performance With Constants Calculated from the Ziegler-Nichols Equations 114

7.2.2 Control Performance with Constants Calculated using the Cohen-Coon Equations 120

7.2.3 Control Performance with Constants Calculated using the Integral of Absolute Error Equations 127

7.2.4 Control Performance with Constants Calculated using the Integral of Time Multiplied by the Absolute Error Equations 133

7.2.5 Summary of Column Control Performance Using a Multiloop PID Control Strategy with Multirate Sampling 139

7.2.6 The Effect of Multirate Sampling On Control Performance Using a Multiloop PID Control Strategy 140

7.3 Control of Product Composition Using a Multivariable Self-Tuning Controller Strategy ..143

7.3.1 Control Performance with Q Weighting Constants Determined With The Ziegler-Nichols Equations 145

7.3.2 Control Performance With Q Weighting Constants Determined By The Cohen-Coon Equations 152

7.3.3 Control Performance With Q Weighting Constants Calculated from the Integral of Absolute Error Equations 153

7.3.4 Control Performance With Q Weighting Constants Calculated from the Integral of Time Multiplied by the Absolute Error Equations 163

7.3.5 Comparison of The Effect of The Method of Selecting The Self-Tuning Controller Q Weighting Parameters on Column Performance 164

7.4 Evaluation of Multivariable Self-Tuning Control Using Multirate Sampling for Column Control 170

7.4.1 Control Performance with Q Weighting Constants Calculated With The Ziegler-Nichols Equations 171

7.4.2 Control Performance with Q Weighting Constants Calculated by the Cohen-Coon Equations 178

7.4.3 Control Performance with Q Weighting Constants Calculated By Integral of Absolute Error Equations 179

7.4.4 Control Performance With Q Weighting Constants Calculated from the Integral of Time Multiplied by the Absolute Error Equation 189

7.4.5 Comparison of The Effect on Control Performance of The Method of Selecting the Self-Tuning Controller Q Weighting Parameters Using The Multirate Algorithm .195

7.4.6 Effect On Control Performance of Using The Multirate Sampling Form of The Self-Tuning Control Algorithm 196

7.5 Comparison of The Control Performance Achieved Using Multiloop Conventional PID and Multivariable Self-Tuning Control 198

7.6 Column Control Behavior Using Tuned Controller Settings For PID And Self-Tuning Strategies 201

7.6.1 Performance Using a Tuned Multiloop PID Control Strategy 201

7.6.2 Performance Using a Tuned PID Control Strategy With Multirate Sampling 207

7.6.3 Multivariable Self-Tuning Column Control Behavior Using Tuned Q Weighting Parameters 213

7.6.4 Control Performance Using Multirate Self-Tuning Controller With Tuned Q Weighting Parameters 219

7.6.5 Comparison of Tuned Controller Performance 224

7.7 Effect On Column Control Performance Using Measured Feedforward Compensation with Multivariable Self-Tuning Control 228

7.8 Column Performance Using The K-Incremental Form of the Self-Tuning Controller 239

8. Conclusions 253

9. Recommendations 257

9.1 Recommended Changes and/or Additions to the Equipment 257

9.2 Recommendations for Future Research Work 259

References 262

Appendices 268

Appendix A
Differentiation of Cost Function 269

Appendix B
Source Code PROFIT.FOR 275

Appendix C
Figure Nomenclature 285

List of Tables

Table Page

4.1a Typical mass and energy balance for normal cooling water flow rate 50

4.1b Typical mass and energy balance for normal cooling water flow rate 51

4.2a Typical mass and energy balance for low cooling water flow 52

4.2b Typical mass and energy balance for low cooling water flow 53

5.1 Transfer functions: Effect of reflux flow on top and bottom composition 64

5.2 Transfer functions: Effect of steam flow on top and bottom composition 66

6.1 Controller Parameter Estimation Constants...........75

6.2 Controller settings for top composition controller...76

6.3 Controller settings for bottom composition controller...77

6.4 Q Weighting settings for top composition self-tuning controller...............................81

6.5 Q Weighting settings for bottom composition self-tuning controller...............................82

7.1.1 Multiloop PID Control Performance with Controller Constants Calculated from Ziegler-Nichols Equations..87

7.1.2 Multiloop PID Control Performance with Controller Constants Calculated from Cohen-Coon Equations.......98

7.1.3
Multiloop PID Control Performance with Controller Constants Calculated from Integral of Absolute Error Equations....................................104

7.1.4
Multiloop PID Control Performance with Controller Constants Calculated from Integral of Time Multiplied by the Absolute Error Equations..........106

7.1.5
IAE Values for Multiloop PID Control Based on Calculated Controller Constants 113

7.2.1
Multirate PID Control Performance with Controller Constants Calculated from Ziegler-Nichols Equations.119

7.2.2
Multirate PID Control Performance with Controller Constants Calculated from Cohen-Coon Equations......121

7.2.3
Multirate PID Control Performance with Controller Constants Calculated from Integral of Absolute Error Equations....................................132

7.2.4
Multirate PID Control Performance with Controller Constants Calculated from The Integral of Time Multiplied by the Absolute Error Equations..........134

7.2.5
IAE values for Multiloop PID control, with Multirate sampling, based on calculated controller settings...140

7.2.6
Comparison of Single Rate and Multirate sampling PID control.......................................141

7.3.1
Multivariable Self-Tuning Control Performance with Q Weighting Constants Calculated from Ziegler-Nichols Equations..........................146

7.3.2
Multivariable Self-Tuning Control Performance with Q Weighting Constants Calculated from Cohen-Coon Equations....................................153

7.3.3
Multivariable Self-Tuning Control Performance with Q Weighting Constants Calculated from Integral of Absolute Error Equations..............................158

7.3.4
Multivariable Self-Tuning Control Performance with Q Weighting Constants Calculated from the Integral of Time Multiplied by the Absolute Error Equations..164

7.3.5
IAE values for the Multivariable Self-Tuning Control Responses for initial parameter values 169

7.4.1
Multirate Self-Tuning Control Performance with Q Weighting Constants Calculated with Ziegler-Nichols Equations..172

7.4.2
Multirate Self-Tuning Control Performance with Q Weighting Constants Calculated with Cohen-Coon Equations..179

7.4.3
Multirate Self-Tuning Control Performance with Q Weighting Constants Calculated with Integral of Absolute Error Equations..............................184

7.4.4
Multirate Self-Tuning Control Performance with Q Weighting Constants Calculated with the Integral of Time Multiplied by the Absolute Error Equations.....189

7.4.5
IAE Values for Multirate Self-Tuning Control Based on Calculated Q Weighting Parameters...............196

7.4.6
Combined IAE Values for Single and Multirate Sampling Self-Tuning Control: Effect of Q weighting Parameter Combined IAE Values.......................197

7.5.1
Comparison of Controller Performance Bewteen Conventional PID versus Self-Tuning Control For Both Single Rate and Multirate Sampling Using Four Parameter Selection Methods 199

7.6.1
Control Performance of Multiloop PID Control With Tuned Controller Constants.............................202

7.6.2
Control Performance of Multirate Sampling PID Control With Tuned Controller Constants.............213

7.6.3
Multivariable Self-Tuning Control Performance with Tuned Q Weighting Constants.........................218

7.6.4
Multirate Self-Tuning Control Performance with Tuned Q Weighting Constants.........................224

7.6.5
Comparison of Tuned Controller Performance..........225

7.6.6
Comparison of Tuned Controller Performance and That Obtained With Calculated Constants.................225

7.6.7
Total and Individual Product Composition IAE Values for PID and STC Control Using Tuned Controller Settings...227

7.6.8
Comparison of Tuned PID Control With Self-Tuning Control Using Calculated Q Weighting Constants 227

7.7.1
Comparison of Multivariable Self-Tuning Controller Performance IAE Values.............................233

7.7.2
Comparison of Multirate Self-Tuning Controller Performance..240

7.8.1 Column Performance Using Multivariable K-Incremental Self-Tuning Control With Tuned Q Weighting Constants....245

7.8.2 Column Performance Using Multirate K-Incremental Self-Tuning Control With Tuned Q Weighting Constants250

7.8.3 Summary of Measured Feedforward Compensation IAE Totals....251

List of Figures

Figure Page

4.1 Schematic diagram of distillation column.............48

5.1 Open loop response to reflux flow 62

5.2 Open loop response to steam flow 65

5.3 Open loop response to feed flow 68

7.1 Multiloop PID; Ziegler-Nichols Response step one.....88

7.2 Multiloop PID; Ziegler-Nichols Response step two.....89

7.3 Multiloop PID; Ziegler-Nichols Response step three...90

7.4 Multiloop PID; Ziegler-Nichols Response step four....91

7.5 Multiloop PID; Cohen-Coon Response step one..........94

7.6 Multiloop PID; Cohen-Coon Response step two..........95

7.7 Multiloop PID; Cohen-Coon Response step three........96

7.8 Multiloop PID; Cohen-Coon Response step four.........97

7.9 Multiloop PID; IAE Response step one................100

7.10 Multiloop PID; IAE Response step two...............101

7.11 Multiloop PID; IAE Response step three.............102

7.12 Multiloop PID; IAE Response step four..............103

7.13 Multiloop PID; ITAE Response step one..............107

7.14 Multiloop PID; ITAE Response step two..............108

7.15 Multiloop PID; ITAE Response step three............109

7.16 Multiloop PID; ITAE Response step four.............110

7.17 Multirate PID; Ziegler-Nichols Response step one....115

7.18 Multirate PID; Ziegler-Nichols Response step two....116

7.19 Multirate PID; Ziegler-Nichols Response step three..117

7.20 Multirate PID; Ziegler-Nichols Response step four...118

7.21 Multirate PID; Cohen-Coon Response step one.........122

7.22 Multirate PID; Cohen-Coon Response step two.........123

7.23 Multirate PID; Cohen-Coon Response step three.......124

7.24 Multirate PID; Cohen-Coon Response step four........125

7.25 Multirate PID; IAE Response step one................128

7.26 Multirate PID; IAE Response step two................129

7.27 Multirate PID; IAE Response step three..............130

7.28 Multirate PID; IAE Response step four...............131

7.29 Multirate PID; ITAE Response step one...............135

7.30 Multirate PID; ITAE Response step two...............136

7.31 Multirate PID; ITAE Response step three.............137

7.32 Multirate PID; ITAE Response step four..............138

7.33 Multivariable Self-Tuning Controller; Z-N Q Weighting Response step one....................147

7.34 Multivariable Self-Tuning Controller; Z-N Q Weighting Response step two....................148

7.35 Multivariable Self-Tuning Controller; Z-N Q Weighting Response step three....................149

7.36 Multivariable Self-Tuning Controller; Z-N Q Weighting Response step four....................150

7.37 Multivariable Self-Tuning Controller; Cohen-Coon Q Weighting Response step one....................154

7.38 Multivariable Self-Tuning Controller; Cohen-Coon Q Weighting Response step two....................155

7.39 Multivariable Self-Tuning Controller; Cohen-Coon Q Weighting Response step three....................156

7.40 Multivariable Self-Tuning Controller; Cohen-Coon Q Weighting Response step four....................157

7.41 Multivariable Self-Tuning Controller; IAE Q Weighting Response step one....................159

7.42 Multivariable Self-Tuning Controller; IAE Q Weighting Response step two....................160

7.43 Multivariable Self-Tuning Controller; IAE Q Weighting Response step three....................161

7.44 Multivariable Self-Tuning Controller; IAE Q Weighting Response step four....................162

7.45 Multivariable Self-Tuning Controller; ITAE Q Weighting Response step one....................165

7.46 Multivariable Self-Tuning Controller; ITAE Q Weighting Response step two....................166

7.47 Multivariable Self-Tuning Controller; ITAE Q Weighting Response step three....................167

7.48 Multivariable Self-Tuning Controller; ITAE Q Weighting Response step four....................168

7.49 Multirate Self-Tuning Controller; Z-N Q Weighting Response step one....................173

7.50 Multirate Self-Tuning Controller; Z-N Q Weighting Response step two....................174

7.51 Multirate Self-Tuning Controller; Z-N Q Weighting Response step three....................175

7.52 Multirate Self-Tuning Controller; Z-N Q Weighting Response step four....................176

7.53 Multirate Self-Tuning Cotroller; Cohen-Coon Response step one....................180

7.54 Multirate Self-Tuning Cotroller; Cohen-Coon Response step two....................181

7.55 Multirate Self-Tuning Cotroller; Cohen-Coon Response step three....................182

7.56 Multirate Self-Tuning Cotroller; Cohen-Coon Response step four....................183

7.57 Multirate Self-Tuning Controller; IAE Response step one....................185

7.58 Multirate Self-Tuning Controller; IAE Response step two....................186

7.59 Multirate Self-Tuning Controller; IAE Response step three....................187

7.60 Multirate Self-Tuning Controller; IAE Response step four....................188

7.61 Multirate Self-Tuning Controller; ITAE Response step one....190

7.62 Multirate Self-Tuning Controller; ITAE Response step two....191

7.63 Multirate Self-Tuning Controller; ITAE Response step three....192

7.64 Multirate Self-Tuning Controller; ITAE Response step four....193

7.65 Multiloop PID Control; Tuned Constants step one....203

7.66 Multiloop PID Control; Tuned Constants step two....204

7.67 Multiloop PID Control; Tuned Constants step three....205

7.68 Multiloop PID Control; Tuned Constants step four....206

7.69 Multirate PID Control; Tuned Constants step one....208

7.70 Multirate PID Control; Tuned Constants step two....209

7.71 Multirate PID Control; Tuned Constants step three....210

7.72 Multirate PID Control; Tuned Constants step four....211

7.73 Multivariable Self-Tuning Control; Tuned Constants step one....214

7.74 Multivariable Self-Tuning Control; Tuned Constants step two....215

7.75 Multivariable Self-Tuning Control; Tuned Constants step three....216

7.76 Multivariable Self-Tuning Control; Tuned Constants step four....217

7.77 Multirate Self-Tuning Control; Tuned Constants step one....220

7.78 Multirate Self-Tuning Control; Tuned Constants step two....221

7.79 Multirate Self-Tuning Control; Tuned Constants step three....222

7.80 Multirate Self-Tuning Control; Tuned Constants step four....223

7.81 Multivariable Self-Tuning Controller; Measured Feedforward Compensation step one....229

7.82 Multivariable Self-Tuning Controller; Measured Feedforward Compensation step two....230

7.83 Multivariable Self-Tuning Controller; Measured Feedforward Compensation step three....231

7.84 Multivariable Self-Tuning Controller; Measured Feedforward Compensation step four....232

7.85 Multirate Self-Tuning Controller; Measured Feedforward Compensation step one....235

7.86 Multirate Self-Tuning Controller; Measured Feedforward Compensation step two....236

7.87 Multirate Self-Tuning Controller; Measured Feedforward Compensation step three....237

7.88 Multirate Self-Tuning Controller; Measured Feedforward Compensation step four....238

7.89 Multivariable K-Incremental Self-Tuning Controller; step one..241

7.90 Multivariable K-Incremental Self-Tuning Controller; step two..242

7.91 Multivariable K-Incremental Self-Tuning Controller; step three......................................243

7.92 Multivariable K-Incremental Self-Tuning Controller; step four.......................................244

7.93 Multirate K-Incremental Self-Tuning Controller; step one..246

7.94 Multirate K-Incremental Self-Tuning Controller; step two..247

7.95 Multirate K-Incremental Self-Tuning Controller; step three......................................248

7.96 Multirate K-Incremental Self-Tuning Controller; step four.......................................249

C.1 Definition Plot for Figure Nomenclature.............286

Nomenclature

Abbreviations:

ASCII	American Standard for Character Information Interchange
DACS	Data Acquisition, Control and Simulation
FB	Foreground/Background
GC	Gas Chromatograph
HP	Hewlett-Packard
IAE	Integral of Absolute Error
IBM	International Business Machines
IL	Interface Loop
ISE	Integral of Squared Error
ITAE	Integral of The Time Multiplied by The Absolute Error
LSI	Large Scale Integrated
MFF	Measured Feedforward Compensation
MIMO	Multi-Input Multi-Output
MISO	Multi-Input Single-Output
MV	Multivariable
MVMR	Multivariable Multirate
PID	Proportional Integral Derivative
SISO	Single-Input Single-Output
SS	Steady State
ST	Self-Tuning
STC	Self-Tuning Controller
Z-N	Ziegler-Nichols
3-C	Cohen-Coon

Polynomials in z^{-1}:

A	System output polynomial
B	System input polynomial
C	System polynomial associated with uncorrelated noise
D	System disturbance polynomial
E	Polynomial introduced with the separation of the noise into past and future terms
F	Controller polynomial associated with the output
G	Controller polynomial associated with the control input
H	Controller polynomial associated with the stochastic noise term
L	Controller polynomial associated with the feedforward disturbance terms
P	Polynomial weighting of the system output
P_d	Denominator of the output weighting polynomial
P_n	Numerator of the output weighting polynomial
Q	Control weighting polynomial
Q'	Control weighting polynomial (intermediate value)
R	Setpoint weighting polynomial

Polynomial Matrices in z^{-1}:

A	System output polynomial matrix
B	System input polynomial matrix
C	System polynomial matrix associated with uncorrelated random noise term
D	System polynomial matrix associated with the disturbance terms
E	Polynomial matrix introduced with the separation of the noise term into past and future elements
F	Controller polynomial matrix associated with system output
G	Controller polynomial matrix associated with the control effort
H	Controller polynomial matrix associated with the stochastic term
L	Controller polynomial matrix associated with the feedforward disturbance terms
P	System output weighting polynomial matrix
$\mathbf{P}_d$	Denominator of the output weighting polynomial matrix
$\mathbf{P}_n$	Numerator of the output weighting polynomial matrix
Q	Control weighting polynomial matrix
Q'	Control weighting polynomial matrix (intermediate matrix)
R	Setpoint weighting polynomial matrix

Variables:

J	Cost function
J_1	Modified cost function
J	Cost function (multivariable form)
J_1	Modified cost function (multivariable form)
ρ_1	Variance of the noise in the Kalman filter approach
ρ_2	Forgetting factor $\rho_1=\rho_2$ for recursive least squares estimation (exponential discounting factor)
s	Laplace transform variable
Pc	Covariance matrix
K	Kalman gain
Kp	Process gain
τ_1	First order time constant
θ_d	Time delay
PB	Proportional band
TI	Integral time
TD	Derivative time
Kc	Proportional constant
Ki	Integral constant
Kd	Derivative constant
t_s	Sample time

1. Introduction and Objectives

1.1 Introduction

One of the most demanding problems in the chemical industry is the saving of energy resources. Dual composition control of distillation columns can yield substantial profits from the saving in utility costs. However the presence of nonlinearities and interaction among inputs and outputs in a column has a significant effect on control of any column.

In recent years considerable effort has been made to establish better methods that would improve control performance compared to that achieved using conventional feedback proportional-integral-derivative(PID) controllers.

Kalman's original self-optimizing control system [1958] was implemented on a very crude system of analog and digital hardware. The drive, which prompted the effort to perform the task and develop a special purpose computer was that the system would be applicable to a wide range of control tasks. With the advent of today's minicomputers, the application of self-optimizing control systems (in a general sense) have expanded [Seborg et al., 1983].

Due to the nonlinear and time varying nature of distillation columns, a controller which tunes itself would provide an improvement in control [Brooks et al., 1983]. To accommodate the combined control of both top and bottom composition of a distillation column, a multivariable self-tuning controller is required.

Simulations of multivariable self-tuning controllers have been undertaken [Koivo, 1980]. However a realistic test of control system performance must involve experimental studies on a process for which only approximate process models are available, a common situation in industrial practice [Ogunnaike et al., 1983].

1.2 Objectives

The objective of this study is an extensive test and evaluation of the performance of the multivariable multirate self-tuning controller as modified by Morris et al., [1982]. The evaluation is performed on a pilot plant distillation column located in the Department of Chemical Engineering at the University of Alberta.

The basis for the evaluation is a comparison with conventional PID control. A requirement of this evaluation is that the same amount of information used to design a multiloop PID controller, will be used to specify the multivariable self-tuning controller. This will provide the author with a comparison of the degree of difficulty between the implementation of the controllers.

Self-tuning control and PID control response will be evaluated using initial parameter selection techniques based on open loop response tests. Four methods are used, two based on the one quarter decay ratio method and two based on integral minimization methods.

1.3 Thesis Organization

The material that follows is divided into eight chapters. Chapter Two consists of a literature survey of the current work done to the date of original writing (1984). Chapter Three presents the derivation of the multiple-input single-output(MISO) self-tuning controller. Following this the derivation of the multivariable self-tuning controller is presented. Extensions to multirate control form are presented, as well as extensions to the k-incremental multivariable self-tuning control [Tham, 1985]. Chapter Four briefly describes the experimental equipment, including a brief description of the microcomputer used in the control implementation. The distillation column dynamics, based on open loop step responses are presented in Chapter Five. The transfer functions used for controller parameter selections are also tabulated. Chapter Six outlines the steps used for controller parameter selection for both PID and self-tuning control.

Chapter Seven presents the experimental results based on responses for multiloop and multirate PID control as well as multivariable and multirate self-tuning control. PID and self-tuning controller responses for well tuned results are followed by a brief presentation of the response for self-tuning control with feedforward compensation(MFF) of the measurable disturbance.

Chapters Eight and Nine summarize the conclusions and recommendations which were formulated as a result of this study.

2. Literature Survey

2.1 Introduction

Most chemical processes are nonstationary (i.e. time varying). Typical examples are the decay of catalysts in a reactor or the reduction in overall heat transfer in a heat exchanger due to fouling. These types of changes lead to deterioration in control behaviour unless there is re-tuning of the controller parameters. Kalman [1958] recognized the need for a self-optimizing control system for chemical processes. At that time his control system "externally digital, internally analog" was a very specialized piece of equipment. Today, minicomputers allow for a degree of flexibility which was unknown in Kalman's era.

With the aid of low cost computing power, the implementation of self-tuning and adaptive control methods have rapidly increased [Harris and Billings, 1981]. Self-tuning controllers have been classified into two general classes [Clarke, 1981; Seborg et al., 1983]:

i. Explicit(or indirect) methods.
ii. Implicit(or direct) methods.

In the explicit approach, a process model is employed and the control calculations are based on estimated model parameters, which are used indirectly in the control law. The implicit method, directly identifies the parameters for the control law and implicitly determines the model parameters.

2.2 Historical Development of Self-Tuning Control

The idea of self-tuning control is not new. Kalman [1958] proposed the first method which could be referred to as a self-tuning controller. However, Kalman never realized the full potential of the proposal, due to insufficiently developed theory and technology. It was not until Åström and Wittenmark [1973], that the theory was revived and the current interest in the subject continued.

Åström and Wittenmark's [1973] self-tuning regulator (STR) was proposed for a constant parameter system, one for which the parameters were unknown. Their explicit approach identified the parameters of a model which were then used to calculate the minimum variance control output. Identification and control were separated following the design procedures proposed by Kalman [1958]. Åström and Wittenmark [1973] have shown that for a system with constant but unknown parameters, that, if the parameters converge, the control law obtained is the minimum variance control law. (Minimum variance control refers to the minimization of the variance of the measured output $y(t)$ at the sample instants [Clarke, 1981].) This was shown to be true even with a biased parameter estimation routine.

The self-tuning regulator algorithm [Åström and Wittenmark, 1973] attempts to minimize the variation in the system's output when the loop is randomly disturbed. It makes no attempt to ensure that setpoints are followed optimally, nor does it try to penalize excessive control action.

The restrictions of the STR were improved upon by the self-tuning controller (STC) proposed by Clarke and Gawthrop [1975]. Their self-tuning controller assumed constant but unknown parameters as did Åström and Wittenmark's STR. A cost function was proposed, which included system input, output and setpoints. Costing polynomials were included which allowed user definable weighting on the elements of the cost function. The STC method had several advantages over the self-tuning regulators; weighting of control was allowed, setpoint variation could be optimally followed, and there was no requirement to choose a system related parameter to ensure convergence.

Keviczky and Hetthessy [1977] extended the SISO controller proposed by Clarke and Gawthrop [1975] to a multivariable algorithm which identified the parameters of the multivariable structure directly. Their control algorithm was presented through implementation on a simulated system.

Morris and Nazer [1977] and Morris et al., [1977] extended Clarke and Gawthrop's [1975] algorithm to a class of multivariable interactive systems. The SISO STC was extended to include feedforward disturbance compensation and a discrete compensator in an inverse PI or PID form in the control policy. The controller was further extended to enable control of a class of multi-input multi-output systems in a decoupled form, thereby allowing regulation by individual single loop controllers. Interaction of control loops was handled as feedforward terms which allowed identification of a multivariable system in a single loop manner.

De Keyser and van Cauwenberghe [1978] presented a multivariable controller formulation which removed the constraints for the constant system parameters and assumed the process to be nonstationary. The results showed, that practical implementation was not feasible due to the computation time required in the on-line solution of the Riccati-equation.

Harris et al., [1978] applied the self-tuning regulator to a nonlinear and nonminimum phase pilot scale packed bed reactor. Harris and co-workers noted the "parameter windup" phenomenon associated with recursive least squares identification. They also suggested the necessity of using a forgetting factor (exponential discounting factor) to enable tracking of time varying parameters.

Clarke and Gawthrop [1979] extended their previous work to include feedforward and multivariable control. This was also demonstrated in the work of Morris and Nazer [1977]. Morris and Nazer [1977] also indicated stablitity and convergence properties of the self-tuning controller and noted the effect of parameter "blow-up" during long term operation.

Koivo [1980] extended the method of Clarke and Gawthrop [1975] to the multivariable form with the inclusion of setpoint changes and costing of the control action in order to limit the variation of the control signal. Costing of the control action reduced the "bang-bang" control action associated with minimum variance control. Only systems with an equal number of inputs and outputs were considered.

Lieuson [1980] conducted an experimental study of the control of a pilot scale distillation column using the multivariable formulation of the self-tuning controller [Morris and Nazer, 1977]. The multivariable control was achieved without identifying a multivariable form of the control law. Identification and control was achieved on a loop by loop basis with interaction used as feedforward terms in the control law. The self-tuning results presented were equal to or better than that of a well tuned PID controller [Morris et al., 1981].

Morris et al., [1982] extended the multivariable self-tuning controller [Morris and Nazer, 1977], to include control of systems with different sample intervals (multirate control). The restrictions of equal time delays for all loops was also removed. The multivariable, multirate self-tuning controller used a recursive factorization parameter estimator, based on the method of extended least squares. Setpoint following and feedforward control action were included in the control strategy. The formulation of the multirate self-tuning controller assumed all the sample intervals of the process to be integer multiples of the smallest sample interval.

Tanttu and Koivo [1983] presented a multivariable self-tuning controller, which would handle the problem of different delays in the control input. The restriction of equal sample times for all loops was still imposed and only simulated results were presented.

The formulation presented by Morris et al., [1982], Tham [1985] and applied in this work, to the best of the author's knowledge represent the only successful application of the multivariable, multirate self-tuning control algorithms to the control of a process system. Chien et al., [1983] presented a multirate version of the self-tuning controller, with the evaluation carried out only by simulation.

A more detailed survey of adaptive control strategies may be found in Seborg et al., [1983]. This survey includes many applications of adaptive as well as self-tuning controllers.

2.3 Applications of Self-Tuning Control

The theoretical development of self-tuning control has been accompanied by a wide variety of experimental and industrial applications. Åström and Wittenmark's [1973] paper was soon followed by industrial applications of SISO self-tuning regulators [Åström et al., 1977]. Among the applications cited were; control of a paper machine, digester, ore crusher, heat exchanger and an auto pilot for a super tanker. Sastry et al., [1977] applied a SISO self-tuning regulator to the control of the top composition of a pilot scale distillation column.

Multivariable applications of Clarke and Gawthrop's [1975] self-tuning controller, did not appear until after Morris and Nazer's [1977] extension to the multivariable form. Lieuson [1980] studied multivariable self-tuning control of the terminal compositions of a distillation column based on the algorithm presented by Morris and Nazer [1977].

Koivo et al., [1981] applied a multivariable self-tuning controller to a computer controlled, laboratory scaled concentration flow process. The control was based on a minimization of a cost function which included setpoint and control action weighting.

Morris et al., [1982] extended the multivariable self-tuning controller to a multirate formulation with evaluation of multivariable control of a pilot scale distillation column conducted only by simulation using a nonlinear distillation column model. Chien et al., [1983] also studied distillation column control using a multirate algorithm, but only simulation results were presented. To the best of the author's knowledge, the results presented in this work and Tham [1985] are the first experimental implementations of a multivariable, multirate self-tuning controller.

3. Development of Self-Tuning Controller

3.1 Introduction

The main purpose of this thesis has been the evaluation of a multivariable controller. This has involved extensions of the generalized minimum variance control law as presented by Clarke and Gawthrop [1975,1979], Morris and Nazer [1977], Morris et al., [1977], Morris et al., [1980], and Clarke et al., [1983].

This presentation will start with a derivation of the multi-input single-output (MISO) self-tuning controller and be followed by the derivation of the multivariable (MV) self-tuning controller with extensions to multirate sampling. Finally an extension of the MV self-tuning controller to the k-incremental version of the multivariable multirate (MVMR) self-tuning controller is presented. The extension of the MV self-tuning controller to the k-incremental self-tuning controller has been undertaken at the University of Newcastle Upon Tyne by Tham [1985] with it's implementation and initial experimental tests carried out at the University of Alberta. The MVMR k-incremental self-tuning controller is an extension of the k-incremental single input single output (SISO) self-tuning controller proposed by Clarke et al., [1983].

3.2 Multiple Input Single Output Self-Tuning Controller

This section presents a derivation of the MISO self-tuning controller, followed by a development of the parameter estimation technique used.

3.2.1 Multiple Input Single Output Control Law Formulation

Consider a general discrete model for a process to be represented by the following equation:

$$A(z^{-1})y(t) = z^{-k}B(z^{-1})u(t) + z^{-d}Dv(t) + C\xi(t) \qquad (3.1)$$

where $v(t)$ is a measurable disturbance at time t and $\xi(t)$ is random, zero mean, uncorrelated noise. The polynomials A, B, D and C are polynomials in the backshift operator z^{-1} with $a_0=1$, $b_0\neq 0$, and $c_0=1$. The value of z^{-k} is the system delay expressed in integer multiples of the sample period and z^{-d} is the delay associated with the measured disturbance. It is also assumed that C has roots strictly within the unit circle.

The objective is the design of a controller which minimizes the following cost function:

$$J = E\{[P(z^{-1})y(t+k)-R(z^{-1})w(t)]^2+[Q'(z^{-1})u(t)]^2|t\} \qquad (3.2)$$

where $E\{*|t\}$ is the expectation operator given information up to and including time t with $k\geq 1$. The $P(z^{-1})$, $R(z^{-1})$, and

$Q'(z^{-1})$ are transfer functions in z^{-1} to allow for general weighting on the system output $y(t)$, setpoint $w(t)$, and control effort $u(t)$, respectively which are expressed as polynomial ratios of the form:

$$P(z^{-1}) = \frac{P_n(z^{-1})}{P_d(z^{-1})}$$

In the formulation of the cost function, setpoint tracking is provided for by the term $[P(z^{-1})y(t+k)-R(z^{-1})w(t)]$. Excessive control effort is penalized by the cost function through the inclusion of a weighted control term. The strategy becomes classical minimum variance if the control term is removed from the cost function or the Q' weighting polynomial is set to zero.

Minimization of the cost function of equation 3.2 requires knowledge of future terms of the weighted output $P(z^{-1})y(t+k)$. Since this is not available, minimization of equation 3.2 in it's present form is unrealizable. In order to perform the minimization we must generate an estimated weighted output k steps ahead into the future.

Rearranging equation 3.1 of our system, yields:

$$Py(t+k)=\frac{PB}{A}u(t) + z^{k-d}\frac{PD}{A}v(t) + \frac{PC}{A}\zeta(t+k) \qquad (3.3)$$

For simplicity, the (z^{-1}) arguments have been omitted. This practice will be followed for subsequent equations within this section. Equation 3.3 will provide a realizable weighted output as long as $d \geq k$ i.e. the time delay associated with the disturbance is greater than the system delay.

Use of the separation identity [Åström, 1970] will allow the unknown noise term $\zeta(t+k)$ to be expressed in terms of known past terms and unknown future terms:

$$\frac{PC}{A}\zeta(t+k) = E\,\zeta(t+k) + \frac{F}{AP_d}\zeta(t) \tag{3.4}$$

where the polynomials E and F are of the form:

$$\begin{gathered} E(z^{-1}) = 1 + e_1 z^{-1} + \cdots + e_{n1} z^{-(n1)} \\ F(z^{-1}) = f_0 + f_1 z^{-1} + \cdots + f_{n2} z^{-(n2)} \\ n1 = k - 1 \qquad n2 = nf - 1 \\ nf = \max(\, na - 1 \,,\, nc + np_n - k \,) \end{gathered} \tag{3.5}$$

Substitution of equation 3.4 into equation 3.3 yields:

$$Py(t+k) = \frac{PB}{A}u(t) + E\zeta(t+k) + \frac{F}{AP_d}\zeta(t) + z^{k-d}\frac{PD}{A}v(t) \tag{3.6}$$

The system equation of 3.1 can be rearranged as:

$$\zeta(t) = \frac{A}{C}y(t) - z^{-k}\frac{B}{C}u(t) - z^{-d}\frac{D}{C}v(t) \tag{3.7}$$

Here $\zeta(t)$ is composed of only past and current measurable values and represents an estimation of the noise at time t. Therefore, replacing $\zeta(t)$ in equation 3.6, using equation 3.7 allows us to express our k step ahead weighted output as:

$$\begin{aligned} Py(t+k) = \frac{Fy(t)}{CP_d} &+ \left[\frac{PC}{A} - \frac{Fz^{-k}}{AP_d}\right]\frac{B}{C}\,u(t) \\ &+ \left[\frac{PC}{A} - \frac{Fz^{-k}}{AP_d}\right]\frac{Dz^{k-d}v(t)}{C} \\ &+ E\zeta(t+k) \end{aligned} \qquad (3.8)$$

Rearranging and manipulating the identity of equation 3.4 we can express it as:

$$\frac{PC}{A} - \frac{F\,z^{-k}}{AP_d} = E \qquad (3.9)$$

So equation 3.8 can now be written as:

$$Py(t+k) = \frac{F\,y(t)}{CP_d} + \frac{EB}{C}u(t) + z^{k-d}\frac{ED}{C}v(t) + E\zeta(t+k) \qquad (3.10)$$

Since $\xi(t)$ is assumed to be white noise with zero mean, therefore:

$$E\{\xi(t+k|t)\} = 0 \tag{3.11}$$

In other words the best expected value of the future noise term is zero. Defining the prediction of the weighted output by:

$$Py(t+k) = Py^*(t+k|t) + \epsilon(t+k) \tag{3.12}$$

where $Py^*(t+k|t)$ is defined as the predicted weighted output given information up to and including time t. With:

$$\epsilon(t+k) = E\xi(t+k) \tag{3.13}$$

replacement of the unknown $Py(t+k)$ term in the cost function by its prediction enables equation 3.2 to be written as:

$$\begin{aligned} J_1 = E\{[Py^*(t+k|t) + \epsilon(t+k) - Rw(t)]^2 \\ + [Q'u(t)]^2\} \end{aligned} \tag{3.14}$$

Using equation 3.11, equation 3.14 can be expressed as:

$$\begin{aligned} J_1 = E\{[Py^*(t+k|t) - Rw(t)]^2\} \\ + E\{[Q'u(t)]^2\} + \sigma^2_{t+k} \end{aligned} \tag{3.15}$$

In equation 3.15, σ^2_{t+k} is the variance of the random disturbance $\xi(t)$. Using equation 3.12 and equation 3.10 we can express the predicted weighted output as:

$$Py^*(t+k|t) = \frac{F}{CP_d}y(t) + \frac{EB}{C}u(t) + z^{k-d}\frac{ED}{C}v(t) \tag{3.16}$$

Equation 3.16 represents the weighted predicted output based on known parameters and previous measurements of process output, input and measured disturbances, y(t), u(t), and v(t) respectively.

The cost function is minimized by setting the partial derivative with respect to the current control action u(t) to zero ($\partial J_1/\partial u(t) = 0$). The time optimal control solution would require the expectation operator to be included in the minimization. Based on the single stage approach of Clarke et al., [1975] the expectation operator may be removed and the minimization becomes:

$$\frac{\partial J_1}{\partial u(t)} = 2[Py^*(t+k|t) - Rw(t)]*\frac{\partial[Py^*(t+k|t)]}{\partial u(t)} + 2\,Q'u(t)*\frac{\partial[Q'u(t)]}{\partial u(t)} \tag{3.17}$$

Note here that the term $Py^*(t+k|t)$ is a function of u(t) and is given by equation 3.16 so that:

$$\frac{\partial[Py^*(t+k|t)]}{\partial u(t)} = \frac{\partial}{\partial u(t)}\frac{EB}{C}u(t) \tag{3.18}$$

In the differentiation with respect to u(t) the polynomials E, B, and C are terms involving previous and current control actions so that:

$$\frac{\partial u(t-i)}{\partial u(t)} = 0 \qquad i \neq 0 \tag{3.19}$$

Therefore, only the first terms in the E, B, and C polynomials are involved in the differentiation.

$$\frac{\partial [Py^*(t+k|t)]}{\partial u(t)} = \frac{e_0\ b_0}{c_0} = b_0 \tag{3.20}$$

Applying equation 3.5 the minimization becomes:

$$\frac{\partial J_1}{\partial u(t)} = [Py^*(t+k|t) - Rw(t)] + \frac{q_0'\ Q'u(t)}{b_0} = 0 \tag{3.21}$$

For a new control weighting polynomial defined as:

$$\overline{Q} \equiv \frac{q_0'\ Q'}{b_0} \tag{3.22}$$

solving for u(t) from equation 3.21 yields a generalized minimum variance control law:

$$u(t) = \frac{1}{\overline{Q}}[Rw(t) - Py^*(t+k|t)] \tag{3.23}$$

The formulation of the self-tuning controller requires the step by step minimization of equation 3.21. Rather than setting equation 3.21 to zero we can define a predicted auxilliary scalar output function as:

$$\Phi^*(t+k|t) = Py^*(t+k|t) - Rw(t) + Qu(t) \tag{3.24}$$

We now base the control law calculation on setting the auxilliary scalar output function $\Phi^*(t)$ to zero at every control interval. Since the true auxilliary output function is determined from:

$$\Phi(t+k) = Py(t+k) - Rw(t) + Qu(t) \tag{3.25}$$

the error in the output function estimate, obtained by subtracting equation 3.25 from equation 3.24, substituting equation 3.12 into the result and solving for $\Phi^*(t+k|t)$ is given by:

$$\Phi^*(t+k|t) = \Phi(t+k) - E\xi(t+k) \tag{3.26}$$

The control law of equation 3.23 can be described in more detail by utilizing equation 3.16. Defining the following polynomials:

$$\begin{aligned} G &= EB \\ L &= ED \\ C &= 1 - z^{-1}H \quad nh = nc - 1 \end{aligned} \tag{3.27}$$

allows the predicted weighted output to be written as:

$$\begin{aligned} Py^*(t+k|t) &= \frac{Fy(t)}{P_d} + Gu(t) + z^{k-d}Lv(t) \\ &\quad + HPy^*(t+k-1|t-1) \end{aligned} \tag{3.28}$$

Where G, F, L and H are controller polynomials for a known system. For an unknown system these polynomials are replaced with estimates of the true polynomials; $\hat{G}$, $\hat{F}$, $\hat{L}$ and $\hat{H}$. Thus the control law of equation 3.23, making use of equation 3.28 in terms of the estimated controller polynomials becomes:

$$\begin{aligned} u(t) &= \frac{1}{Q}\Big[Rw(t) - \frac{\hat{F}y(t)}{P_d} - \hat{G}u(t) - z^{k-d}\hat{L}v(t) \\ &\quad - \hat{H}Py^*(t+k-1|t-1)\Big] \end{aligned} \tag{3.29}$$

with

$$\begin{aligned} \hat{G} &= \hat{g}_0 + \hat{g}_1 z^{-1} + \cdots + \hat{g}_n z^{-n} \\ ng &= n \end{aligned} \tag{3.30}$$

Since u(t) is not known at this time, we must therefore factor out the current control action and define:

$$\begin{aligned} \hat{G}' &= \hat{g}_1 z^{-1} + \hat{g}_2 z^{-2} + \cdots + \hat{g}_n z^{-n} \\ ng &= n \end{aligned} \tag{3.31}$$

so the current control action is calculated from:

$$u(t) = \frac{1}{[Q + \hat{g}_o]}[Rw(t) - \frac{\hat{F}y}{P_d}(t) - \hat{G}'u(t) - z^{k-d}\hat{L}v(t)$$
$$- \hat{A}Py^*(t+k-1|t-1)] \qquad (3.32)$$

Combination of equation 3.32, with a recursive parameter estimation routine, forms the basis of a self-tuning controller.

3.2.2 Parameter Estimation

With a controller structure and a method of calculating output based on controller parameters established, we must now focus on a method to estimate the parameters $\hat{F}$, $\hat{G}$, $\hat{L}$ and $\hat{A}$.

Replacement of the known controller parameters in equation 3.28 with their estimated values gives:

$$Py^*(t+k|t) = \frac{\hat{F}y}{P_d}(t) + \hat{G}u(t) + z^{k-d}\hat{L}v(t)$$
$$+ \hat{A}Py^*(t+k-1|t-1) \qquad (3.33)$$

Equation 3.33 can be represented in a more simplified form as:

$$Py^*(t+k|t) = \theta(t)X(t) \qquad (3.34)$$

where $X(t)$ is the observation vector and $\theta(t)$ the parameter vectors respectively defined as:

$$\begin{aligned} X(t) \equiv [\ & yp(t),\ yp(t-1),\ \cdots,\ yp(t-nf), \\ & u(t),\ u(t-1),\ \cdots,\ u(t-ng), \\ & v(t+k-d),\ v(t+k-d-1),\ \cdots,\ v(t+k-d-nd), \\ & Py^*(t+k-1|t-1), Py^*(t+k-2|t-2),\ \cdots, \\ & Py^*(t+k-1-nh|t-1-nh)]' \end{aligned}$$

and

$$\begin{aligned} \theta(t) \equiv [\ & \hat{f}_0,\ \hat{f}_1,\ \cdots,\ \hat{f}(nf), \\ & \hat{g}_0,\ \hat{g}_1,\ \cdots,\ \hat{g}(ng), \\ & \hat{l}_0,\ \hat{l}_1,\ \cdots,\ \hat{l}(nd), \\ & \hat{h}_0,\ \hat{h}_1,\ \cdots,\ \hat{h}(nh)] \end{aligned} \qquad (3.35)$$

where

$$yp(t) = \frac{y(t)}{P_d}$$

nf is the order of the $\hat{F}$ polynomial.

ng is the order of the $\hat{G}$ polynomial.

nd is the order of the $\hat{L}$ polynomial.

nh is the order of the $\hat{H}$ polynomial.

The weighted output of the process can be related to the input to the process by the controller polynomials. Using the definition of the predicted weighted output of the process given by equation 3.12 and substitution into equation 3.28 at time t-k, gives:

$$Py^*(t) = \frac{\hat{F}y}{P_d}(t-k) + \hat{G}u(t-k) + z^{-d}\hat{L}v(t)$$
$$+ \hat{H}Py^*(t-1|t-k-1) + E\zeta(t) \qquad (3.36)$$

Use of the definition of $X(t)$ and $\Theta(t)$ from equation 3.35, in conjunction with equation 3.36 yields a regression function of the form:

$$Py^*(t) = \Theta(t)X(t-k) + E\zeta(t) \qquad (3.37)$$

In equation 3.37, if the actual predicted weighted output $Py^*(t)$ is replaced by $Py^*(t|t-k)$ this will allow the use of a recursive least squares based identification technique.

The identification routine is applied to equation 3.37 to estimate $\Theta(t)$. The on-line estimator used is the recursive least squares(RLS) method with upper diagonal factorization of the covariance matrix [Bierman, 1976,1977]. The conventional recursive least squares identification algorithm when employed without a variable forgetting factor suffers from parameter "blow-up" [Wong et al., 1983]. Modifying Bierman's algorithm as suggested by Morris et al., [1982] yields a more numerically stable algorithm for long term operation.

The estimator used in this study is based on the following algorithm:

$$
\begin{aligned}
r &= \rho_1 + X(t-k)Pc(t)X'(t-k) \\
K(t+1) &= Pc(t)X'(t-k)/r \\
Pc(t+1) &= (Pc(t) - K(t+1)K'(t+1)r)/\rho_2 \\
\Theta(t+1) &= \Theta(t) + K(t+1)\left(\frac{y}{P_d}(t) - X(t-k)\Theta(t)\right)
\end{aligned}
\tag{3.38}
$$

where

ρ_1 is the variance of the noise as in the Kalman filter approach or $\rho_1=\rho_2$ for RLS estimation

ρ_2 is the forgetting factor $0<<\rho_2<1$

Pc is the covariance matrix

K is the Kalman gain

r is an intermediate calculated value

Actual computer implementation of the algorithm utilizes a modified form of equation 3.38 to save storage requirements for the covariance matrix Pc. This involves storing the Pc matrix as a vector since the lower triangular portion of the covariance matrix is not used in the updating. This reduction in overall storage requirements is an important factor in implementing adaptive algorithms on microcomputers.

3.3 Multivariable Self-Tuning Controller

Even though the derivation of the MISO self-tuning control law has been derived in the previous sections, a full derivation of the multivariable(MV) controller is presented in this section, including its extension to multirate sampling. The derivation is required, since disturbance feedforward compensation is added in the formulation for the MV case, compared to the MISO controller.

3.3.1 Multivariable Control Law Formulation

The multivariable system is represented by the following linear difference equation:

$$A(z^{-1})Y(t) = z^{-k_{ij}}B(z^{-1})U(t) + z^{-d_{ij}}D(z^{-1})V(t) + C(z^{-1})\Xi(t) \tag{3.39}$$

where:

$A(z^{-1})$, $B(z^{-1})$, $C(z^{-1})$ and $D(z^{-1})$ are m*m polynomial matrices in the backshift operator z^{-1}

$Y(t)$ is an m*1 vector of measurable system outputs

$U(t)$ is an m*1 vector of control inputs

$V(t)$ is an m*1 vector of measurable disturbances signals

$\Xi(t)$ is a vector of random, zero mean noise of known covariance

$z^{-k_{ij}}$ is the time delay for the ${}_i$th control input to the ${}_j$th process output expressed as an integer multiple of the sample interval t.

$z^{-d_{ij}}$ is the time delay for the ${}_{i}$th measurable disturbance, to the ${}_{j}$th process output expressed as an integer multiple of the sample time t.

Without loss of generality let us assume that the system outputs are independent of one another, as well as the noise terms so that $A(z^{-1})$ and $C(z^{-1})$ are diagonal matrices. The assumption that $A(z^{-1})$ is diagonal implies that the loop interaction terms are represented in the feedforward path [Tham, 1985]. The matrices $A(z^{-1})$ and $C(z^{-1})$ can then be assumed such that $A(0)$ and $C(0)$ are identity matrices, which is equivalent to setting $a_0=1$ and $c_0=1$ for the MISO controller.

As for the MISO controller the multi-input multi-output self-tuning control law is based upon the step by step minimization of the following performance index J with respect to the current control action $U(t)$.

$$\begin{aligned} J = E\{[P(z^{-1})Y(t+k_{ii}) - R(z^{-1})W(t)]^{\prime}[P(z^{-1})Y(t+k_{ii}) \\ - R(z^{-1})W(t)] \\ - [Q'(z^{-1})U(t)]^{\prime}[Q'(z^{-1})U(t)]\,|\,t\,\} \end{aligned} \tag{3.40}$$

In equation 3.40 $E\{*|t\}$ is the expectation operator given information up to and including time t. $W(t)$ is an $m*1$ vector of desired setpoints. $P(z^{-1})$, $R(z^{-1})$ and $Q'(z^{-1})$ are $m*m$ diagonal transfer function matrices of the form:

$$P(z^{-1}) = \frac{P_n(z^{-1})}{P_d(z^{-1})} = \frac{p_{n0} + p_{n1}z^{-1} + p_{n2}z^{-2} + \cdots}{p_{d0} + p_{d1}z^{-1} + p_{d2}z^{-2} + \cdots} \qquad (3.41)$$

The term k_{ii} represents the time delay between the $_i$th control action signal $u_i(t)$ and the $_i$th output of the process $y_i(t)$ for the $_{ii}$th loop of the process.

At time t the signals **U**(t) and **W**(t) are known so that the minimization of J with respect to **U**(t) requires the prediction of $\mathbf{P}(z^{-1})\mathbf{Y}(t+k_{ii})$ at time t. That is $\mathbf{P}(z^{-1})\mathbf{Y}^*(t+k_{ii}|t)$ given all the information up to and including time t. From equation 3.39 we can factor out the diagonal elements of the delay from both sides, then premultiplying by the inverse of the output polynomial matrix $\mathbf{A}(z^{-1})$ and premultiplying by the weighting polynomial matrix $\mathbf{P}(z^{-1})$ we have the following weighted output:

$$\begin{aligned}\mathbf{PY}(t+k_{ii}) = {} & \mathbf{PA}^{-1}[z^{k_{ii}-k_{ij}}\mathbf{BU}(t) + z^{k_{ii}-d_{ij}}\mathbf{DV}(t)] \\ & + z^{k_{ii}}\mathbf{PA}^{-1}\mathbf{C}\Xi(t)\end{aligned} \qquad (3.42)$$

For simplicity the arguments (z^{-1}) have been omitted. This practice will be followed for subsequent equations within this section. Using the identity of equation 3.4 and applying it on a loop by loop basis, it is possible to define $\mathbf{E}(z^{-1})$ and $\mathbf{F}(z^{-1})$ as diagonal polynomial matrices since **P**, **C** and **A** are diagonal polynomial matrices. We can now separate the stochastic disturbance portion in terms of past and future disturbances as:

$$z^{k_{ii}}PA^{-1}C\Xi(t) = z^{k_{ii}}E\Xi(t) + P_d^{-1}A^{-1}F\Xi(t) \qquad (3.43)$$

Substituting equation 3.43 into 3.42 allows the weighted predicted output to be expressed as:

$$\begin{aligned} PY(t+k_{ii}) &= z^{k_{ii}-k_{ij}}PA^{-1}BU(t) + z^{k_{ii}-d_{ij}}PA^{-1}DV(t) \\ &\quad + E\Xi(t+k_{ii}) + P_d^{-1}A^{-1}F\Xi(t) \qquad (3.44) \end{aligned}$$

From the difference equation 3.39 we can solve for the stochastic noise at time t, resulting in:

$$\Xi(t) = C^{-1}AY(t) - z^{-k_{ij}}C^{-1}BU(t) - z^{-d_{ij}}C^{-1}DV(t) \qquad (3.45)$$

Equation 3.45 represents an estimate of the stochastic noise term at time t. Substituting equation 3.45 into 3.44 and collecting common terms we get the following result:

$$\begin{aligned} PY(t+k_{ii}) &= C^{-1}P_d^{-1}FY(t) \\ &\quad + \left[z^{k_{ii}-k_{ij}}PA^{-1}C - z^{-k_{ij}}P_d^{-1}A^{-1}F\right] C^{-1}BU(t) \\ &\quad + \left[z^{k_{ii}-d_{ij}}PA^{-1}C - z^{-d_{ij}}P_d^{-1}A^{-1}F\right] C^{-1}DV(t) \\ &\quad + E\Xi(t+k_{ii}) \qquad (3.46) \end{aligned}$$

Since the identity of equation 3.4 can be manipulated to yield:

$$z^{k_{ii}-k_{ij}}PA^{-1}C - z^{-k_{ij}}P_d^{-1}A^{-1}F = z^{k_{ii}-k_{ij}}E \qquad (3.47)$$

and

$$z^{k_{ii}-d_{ij}}PA^{-1}C - z^{-d_{ij}}P_d^{-1}A^{-1}F = z^{k_{ii}-d_{ij}}E \qquad (3.48)$$

The terms expressed in square brackets in equation 3.46 can be replaced, so equation 3.46 simplifies to:

$$\begin{aligned} PY(t+k_{ii}) &= C^{-1}P_d^{-1}FY(t) + z^{k_{ii}-k_{ij}}C^{-1}EBU(t) \\ &\quad + z^{k_{ii}-d_{ij}}C^{-1}EDV(t) + E\Xi(t+k_{ii}) \end{aligned} \qquad (3.49)$$

Now by defining the following m*m polynomial matrices:

$$\begin{aligned} G(z^{-1}) &= E(z^{-1})B(z^{-1}) \\ L(z^{-1}) &= E(z^{-1})D(z^{-1}) \end{aligned} \qquad (3.50)$$

equation 3.49 may be expressed as:

$$\begin{aligned} PY(t+k_{ii}) &= P_d^{-1}C^{-1}FY(t) + z^{k_{ii}-k_{ij}}C^{-1}GU(t) \\ &\quad + z^{k_{ii}-d_{ij}}C^{-1}LV(t) + E\Xi(t+k_{ii}) \end{aligned} \qquad (3.51)$$

If we now define a vector of predicted weighted outputs of the process as the difference between the actual weighted output and the residual, based on the information up to and including time t, as:

$$PY^*(t+k_{ii}|t) = PY(t+k_{ii}) - E\Xi(t+k_{ii}) \qquad (3.52)$$

Then by use of this definition and assuming that the best expected value of the future noise is zero i.e. $E\{\Xi(t+k_{ii})|t\}=0$, allows the performance index of 3.40 to be expressed as:

$$J_i = E\{[PY^*(t+k_{ii}|t) - RW(t)]^t[PY^*(t+k_{ii}|t) - RW(t)] + [Q'U(t)]^t[Q'U(t)]\} + \sigma^2_{t+k_{ii}} \qquad (3.53)$$

where $\sigma^2_{t+k_{ii}}$ is a vector of the variance of the noise. In the above performance index we still require a means of evaluating $PY^*(t+k_{ii}|t)$. This can be done using equation 3.52, the weighted predicted output and equation 3.51, the weighted output, our weighted predicted output can now be expressed as:

$$PY^*(t+k_{ii}|t) = P_d^{-1}C^{-1}FY(t) + z^{k_{ii}-k_{ij}}C^{-1}GU(t) + z^{k_{ii}-d_{ij}}C^{-1}LV(t) \qquad (3.54)$$

As with equation 3.16, equation 3.54 represents the weighted predicted output based on known parameters. By defining a new m*m diagonal polynomial matrix $H(z^{-1})$ as:

$$H(z^{-1}) = zI - zC(z^{-1}) \qquad (3.55)$$

a recursive form of equation 3.54 expressed in terms of the weighted output, process outputs, control inputs, disturbances and previous predictions can be stated as:

$$\mathbf{PY}^{*}(t+k_{ii}|t) = \mathbf{P}_{d}^{-1}\mathbf{FY}(t) + z^{k_{ii}-k_{ij}}\mathbf{GU}(t) + z^{k_{ii}-d_{ij}}\mathbf{LV}(t) + \mathbf{HPY}^{*}(t+k_{ii}-1|t-1) \qquad (3.56)$$

where **F**, **G**, **L** and **H** are controller polynomial matrices based on a known system. We still require a means of calculating the current control action. To accomplish this we must minimize J_1 with respect to $\mathbf{U}(t)$, the current control action, so that $\partial J_1/\partial \mathbf{U}(t) = 0$. The time optimal control solution would require the expectation operator to be included in the differentiation. As with the MISO derivation the expectation operator may be removed and the result of the single stage minimization becomes:

$$\frac{\partial J_1}{\partial \mathbf{U}(t)} = \mathbf{C}(0)^{-1}\mathbf{E}(0)^{t}\mathbf{B}(0)^{t}(\mathbf{PY}^{*}(t+k_{ii}|t) - \mathbf{RW}(t)) + \mathbf{Q}'(0)^{t}\mathbf{Q}'\mathbf{U}(t) \qquad (3.57)$$

The minimization of the performance index without the expectation operator yields a suboptimal control strategy, and is done to simplify the mathematics involved in the differentiation. A detailed differentiation of the performance index without the expectation operator is presented in Appendix A.

By defining a new control weighting polynomial matrix as:

$$\mathbf{Q} = \mathbf{B}^{-1}(0)^{t}\mathbf{E}^{-1}(0)^{t}\mathbf{C}(0)\ \mathbf{Q}'(0)^{t}\mathbf{Q}'(z^{-1}) \tag{3.58}$$

equation 3.57 becomes:

$$\mathbf{PY}^{*}(t+k_{ii}|t) - \mathbf{RW}(t) + \mathbf{QU}(t) = 0 \tag{3.59}$$

Equation 3.59 represents a control law based on the weighted predicted output and the weighted setpoint. As with the MISO derivation we require a step by step minimization of equation 3.57. Rather than setting equation 3.59 to zero we define an auxilliary output function vector $\underline{\Phi}$ such that:

$$\underline{\Phi}(t+k_{ii}) = \mathbf{PY}(t+k_{ii}) - \mathbf{RW}(t) + \mathbf{QU}(t) \tag{3.60}$$

So the predicted auxilliary output function vector, based on the weighted predicted output is:

$$\underline{\Phi}^{*}(t+k_{ii}|t) = \mathbf{PY}^{*}(t+k_{ii}|t) - \mathbf{RW}(t) + \mathbf{QU}(t) \tag{3.61}$$

with

$$\underline{\Phi}^{*}(t+k_{ii}|t) = \underline{\Phi}(t+k_{ii}) - \mathbf{E}\Xi(t+k_{ii}) \tag{3.62}$$

Equation 3.62 is obtained by subtracting equation 3.60 from equation 3.61 and substituting equation 3.52 in the result. Setting $\underline{\Phi}^{*}(t+k_{ii}|t) = 0$ is the same restriction as equation 3.59 and yields a control law which represents the inclusion of a k_{ii} step ahead predictor in the feedback path to evaluate $\mathbf{U}(t)$. Replacing the weighted predicted output of equation 3.56 in the control law of equation 3.59 results in the following expression:

$$z^{k_{ii}-k_{ij}}\mathbf{G}\mathbf{U}(t) + \mathbf{Q}\mathbf{U}(t) = \mathbf{R}\mathbf{W}(t) - \mathbf{P}_d^{-1}\mathbf{F}\mathbf{Y}(t) - z^{k_{ii}-d_{ij}}\mathbf{L}\mathbf{V}(t) - \mathbf{H}\mathbf{P}\mathbf{Y}^*(t+k_{ii}-1|t-1) \qquad (3.63)$$

Some restrictions apply to the application of the control law formulation of equation 3.63. The delay associated with off diagonal control inputs must be larger than the delay associated with the diagonal control inputs. As well the delay associated with disturbances must be greater than the delay for control actions. These restrictions are expressed mathematically as $k_{ij} \geq k_{ii}$ for $i \neq j$, and $d_{ij} \geq k_{ii}$ for all j, since if these restrictions are not satisfied the prediction will contain future terms and will be unrealizable. These restrictions are generally applicable since in trying to control a process our control effort should be the first element to effect the output. Equation 3.63 represents a means of implementing our control law based on a fixed controller structure and known controller polynomials **F**, **G**, **L** and **H**. Replacing the controller polynomials **F**, **G**, **L** and **H** with their estimated values $\hat{\mathbf{F}}$, $\hat{\mathbf{G}}$, $\hat{\mathbf{L}}$ and $\hat{\mathbf{H}}$, obtained from a recursive parameter estimation algorithm, allows the controller to be self-tuning.

3.3.2 Multivariable Parameter Estimation

As with the MISO self-tuning controller, parameter identification must be done on-line so that the controller can track slowly moving and time varying systems. The parameter estimation is based on the ability to predict the weighted output of the process $PY(t+k_{ii})$. To do this we simplify the notation of equation 3.56 as:

$$PY^*(t+k_{ii}|t) = \underline{\Theta}(t)\underline{X}(t) \qquad (3.64)$$

where $\underline{X}(t)$ is a diagonal matrix composed of:

$$\underline{X}(t) = \begin{bmatrix} X_{11}(t) & & 0 \\ & X_{22}(t) & \\ & \cdots & \\ 0 & & X_{mm}(t) \end{bmatrix} \qquad (3.65)$$

and

$$\underline{\Theta}(t) = [\ \Theta_1(t),\ \Theta_2(t),\ \cdots,\ \Theta_m(t)]' \qquad (3.66)$$

Expressing equations 3.65 and 3.66 on a loop by loop basis, yields:

$$Py_i^*(t+k_{ii}|t) = \Theta_i(t)X_{ii}(t) \qquad (3.67)$$

Then by defining the weighted predicted output as:

$$Py_i(t+k_{ii}) = Py_i^*(t+k_{ii}|t) + E_{ii}\Xi(t+k_{ii}) \qquad (3.68)$$

Expressing equation 3.56 on a loop by loop basis, substituting the definition for the predicted output, and expressing the result at time $t-k_{ii}$, yields:

$$\begin{aligned} Py_i(t) = \frac{F_i y_i}{P_d}(t-k_{ii}) &+ G_{ii}u_i(t-k_{ii}) + G_{ij}u_j(t-k_{ij}) \\ &+ L_{ii}v_i(t-d_{ii}) + L_{ij}v_j(t-d_{ij}) \\ &+ H_i Py_i^*(t-1|t-k_{ii}-1) \\ &+ E_{ii}\Xi(t) \end{aligned} \qquad (3.69)$$

It then follows from equations 3.56, 3.64, 3.67 and 3.69 that:

$$\begin{aligned} X_{ii}(t-k_{ii}) = [\ &\frac{y_i}{P_d}(t-k_{ii}),\ \frac{y_i}{P_d}(t-k_{ii}-1),\ \cdots,\ \frac{y_i}{P_d}(t-k_{ii}-nf_i), \\ &u_i(t-k_{ii}),\ u_i(t-k_{ii}-1),\ \cdots,\ u_i(t-k_{ii}-ng_{ii}), \\ &u_j(t-k_{ij}),\ u_j(t-k_{ij}-1),\ \cdots,\ u_j(t-k_{ij}-ng_{ij}), \\ &v_i(t-d_{ii}),\ v_i(t-d_{ii}-1),\ \cdots,\ v_i(t-d_{ii}-nd_{ii}), \\ &v_j(t-d_{ij}),\ v_j(t-d_{ij}-1),\ \cdots,\ v_j(t-d_{ij}-nd_{ij}), \\ &Py_i^*(t-1|t-k_{ii}-1),\ Py_i^*(t-2|t-k_{ii}-2),\ \cdots, \\ &Py_i^*(t-1-nh_i|t-k_{ii}-1-nh_i)\ ]' \end{aligned} \qquad (3.70)$$

and

$$\begin{aligned}\theta_i(t) = [\ & f_i(0),\ f_i(1),\ \cdots,\ f_i(nf_i),\\ & g_{ii}(0),\ g_{ii}(1),\ \cdots,\ g_{ii}(ng_{ii}),\\ & g_{ij}(0),\ g_{ij}(1),\ \cdots,\ g_{ij}(ng_{ij}),\\ & l_{ii}(0),\ l_{ij}(1),\ \cdots,\ l_{ii}(nd_{ii}),\\ & l_{ij}(0),\ l_{ij}(1),\ \cdots,\ l_{ij}(nd_{ij}),\\ & h_i(0),\ h_i(1),\ \cdots,\ h_i(nh_i)'\ ] \end{aligned} \qquad (3.71)$$

where

nf_i is the order of the **F** polynomials for the ${}_i$th loop.

ng_{ii} is the order of the **G** polynomial for the ${}_i$th loop on the diagonal.

ng_{ij} is the order of the **G** polynomial for the ${}_i$th loop and the ${}_j$th element of the polynomial matrix.

nd_{ii} is the order of the **L** polynomial for the ${}_i$th loop on the diagonal.

nd_{ij} is the order of the **L** polynomial for the ${}_i$th loop and the ${}_j$th element of the polynomial matrix.

nh_i is the order of the **H** polynomial for the ${}_i$th loop.

Combinations of equations 3.70, and 3.69, substitution of $\mathbf{Py}_i^*(t|t-k_{ii})$ for $\mathbf{Py}_i(t)$, with the current parameter estimates, yields:

$$\mathbf{PY}_i^*(t|t-k_{ii}) = \Theta_i(t)\ \mathbf{X}_{ii}(t-k_{ii}) + \mathbf{E}_{ii}\Xi(t) \qquad (3.72)$$

Equation 3.72 is in a regression form which allows the parameter identification to be implemented, on a loop by loop basis. The same identification algorithm as described in section 3.2.2 is used. More information on the U-D factorization method can be found in the literature [Bierman, 1976,1977; Nazer, 1980; Wong et al., 1983].

3.3.3 Extension to Multirate Control

In multivariable control, the overall sample time chosen is usually a compromise between the different sample times of the individual loops making up the system. There are some systems where such a choice is not satisfactory. For the distillation column used in this work, the sample time, for bottoms composition control is chosen to be equal to the minimum cycle time for the gas chromatograph analysis, but this sample time is too large for good control of the top composition, for disturbance rejection. Therefore, an improvement in control performance should be achieved by selection of different sample intervals to control individual loops.

The implementation of the multirate self-tuning controller assumes that all the sample intervals of the process are integer multiples of the smallest sample interval t_s. In addition all the control signals for the interaction loops are measurable. Therefore, from equation 3.69 all the control actions $u_j(t)$ for $j=1,2,\cdots,ng_{ij}$ $j \neq i$ for the i-th loop are accessible for the time sequences $t_s(i)$, $2t_s(i)$, $3t_s(i)$, $\cdots$ etc.

The output of the i-th process loop $y_i(kt_s)$ is then written as:

$$A_{ii}y_i(kt_s) = z^{-k_{ii}}B_{ii}u_i(kt_s) + \sum_{\substack{j=1\\ j\neq i}}^{ng_{ij}} z^{-k_{ij}}B_{ij}u_j(kt_s)$$

$$+ \sum_{j=1}^{nd_{ij}} z^{-k_{ij}}D_{ij}v_j(kt_s) + C_{ii}\Xi_i(kt_s) \qquad (3.73)$$

with y_i, u_i, u_j, v_j and Ξ_i assumed known at each control interval.

The development of the control law follows the same format as the multivariable derivation. With $k_{ii}>k_{ij}$ and $k_{ii}>d_{ij}$, the control law expressed on a loop by loop basis for the i-th loop becomes:

$$[Q_i + g_{ii}(0)]u_i(t) = R_iw_i(t) - \frac{F_iy_i}{P_d}(t) \qquad (3.74)$$

$$- \sum_{k=1}^{ng_{ii}} g_{ii}(k)u_i(t-k)$$

$$- G_{ij}u_j(t+k_{ii}-k_{ij})$$

$$- L_{ij}v_j(t+k_{ii}-d_{ij})$$

$$- H_iPy_i^*(t+k_{ii}-1|t-1)$$

In section 3.3.2 the parameter estimation was represented on a loop by loop basis, so, identification and control can be performed on a loop by loop basis with the required control action being determined from equation 3.74.

For the special case where $k_{ii}=k_{ij}$, equation 3.74 is modified and the solution for the current control action requires the solution of a set of equations. Since the term $G_{ij}u_j(t)$, representing the control action from another loop would be unknown at time t.

This multirate formulation therefore allows for individual design of each loop with respect to the controller polynomials and the weighting functions **P**, **Q**, and **R**.

3.3.4 Extension to K-incremental Self-tuning Controller

In the formulation of the self-tuning controller, the assumption has been made that the noise effecting the system is of zero mean and constant covariance. If we modify this restriction to be noise of constant covariance only, such that $\Xi(t)=N(d,\sigma^2)$, then we can rewrite the multivariable difference equation 3.39 as:

$$\mathbf{AY}(t) = z^{-k_{ij}}\mathbf{BU}(t) + z^{-d_{ij}}\mathbf{DV}(t) + \mathbf{C\Xi}(t) + \mathbf{d} \qquad (3.75)$$

where all terms are as defined previously with **d** considered a constant bias term to reflect load changes, signal nonlinearity or nonzero mean noise.

Following the multivariable derivation the weighted k_{ii} step ahead prediction can be written as:

$$PY^*(t+k_{ii}|t) = P_d^{-1}FY(t) + z^{k_{ii}-k_{ij}}GU(t) + z^{k_{ii}-d_{ij}}LV(t) + HPY^*(t+k_{ii}-1|t-1) + d \qquad (3.76)$$

Now defining the k-differencing operator as:

$$\Delta_k = 1 - z^{-k_{ii}} \qquad (3.77)$$

allows equation 3.76 to be written as:

$$\begin{aligned} PY^*(t+k_{ii}|t) = PY^*(t|t-k_{ii}) &+ P_d^{-1}F\Delta_k Y(t) \qquad (3.78) \\ &+ z^{k_{ii}-k_{ij}}G\Delta_k U(t) \\ &+ z^{k_{ii}-d_{ij}}L\Delta_k V(t) \\ &+ H\Delta_k PY^*(t+k_{ii}-1|t-1) \end{aligned}$$

Note that the bias term, d does not appear since d is assumed constant, $\Delta_k d=0$.

Rearranging equation 3.78 allows the control law for the k-incremental self-tuning controller to be stated as:

$$\begin{aligned}[\mathbf{Q}_i + g_{ii}(0)\Delta_k]\mathbf{u}_i(t) = \mathbf{R}_i\mathbf{w}_i(t) &- \mathbf{P}\mathbf{y}_i^*(t|t-k_{ii}) \qquad (3.79)\\ &- \mathbf{F}_i\frac{\Delta_k \mathbf{y}_i}{\mathbf{P}_d}(t)\\ &- \sum_{k=1}^{ng_{ii}} g_{ii}(k)\Delta_k\mathbf{u}_i(t-k)\\ &- \mathbf{G}_{ij}\Delta_k\mathbf{u}_j(t+k_{ii}-k_{ij})\\ &- \mathbf{L}_{ij}\Delta_k\mathbf{v}_j(t+k_{ii}-d_{ij})\\ &- \mathbf{H}_i\Delta_k\mathbf{P}\mathbf{y}_i^*(t+k_{ii}-1|t-1)\end{aligned}$$

The parameter identification is done as per the MVMR self-tuning controller, with the observation vector being operated on by the Δ_k differencing operator, so the regression form of equation 3.72 becomes:

$$\Delta_k\mathbf{P}\mathbf{Y}_i^*(t+k_{ii}|t) = \Theta_i(t)\Delta_k\mathbf{X}_{ii}(t-k_{ii}) + \mathbf{E}_{ii}\Xi(t) \qquad (3.80)$$

As with the MVMR self-tuning controller the **G**, **F**, **L** and **H** polynomials can be specified on a loop by loop basis with individual tuning of **P**, **Q** and **R** weighting functions for each loop.

3.4 Control Law Implementation

To this point only general formulations of the MISO, MVMR, and k-incremental self-tuning controller have been presented. The derivations have been general with very few assumptions involved. In this study, the computer control of a pilot scale distillation column was accomplished with the MVMR self-tuning controller. Previous work [Lieuson, 1980] used a variation of the MISO self-tuning controller. The column has also been controlled with a variation of the MVMR k-incremental self-tuning controller [Tham, 1985]. Some of these results for the k-incremental column control are presented in the results portion of this study.

3.4.1 Distillation Column Control Law

For the distillation column control studies, the MVMR self-tuning controller has been used in a modified form. The control law has been written for a 2*2 system, with top composition control as loop one, and bottoms composition control as loop two. The multivariable system is represented by equation 3.39 with $D(z^{-1})$ as a diagonal polynomial matrix. This formulation is reasonable for the distillation column, since there is only a single disturbance, feed flow rate. Therefore, the delays $d_{ij}=0$ for $i \neq j$, as well off diagonal elements of the D matrix are zero.

The control law for the 2*2 case expressed for loop one is:

$$
\begin{aligned}
[\mathbf{Q}_1 + g_{11}(0)]u_1(t) = \mathbf{R}_1 w_1(t) - \frac{\mathbf{F}_1 y_1(t)}{\mathbf{P}_d} \qquad & (3.81) \\
- \sum_{k=1}^{ng_{11}} g_{11}(k)u_1(t-k) \\
- \mathbf{G}_{12}u_2(t+k_{11}-k_{12}) \\
- \mathbf{L}_{11}v_1(t+k_{11}-d_{11}) \\
- \mathbf{H}_1\mathbf{P}y_1^*(t+k_{11}-1|t-1)
\end{aligned}
$$

In equation 3.81 $k_{12}>k_{11}$ and $d_{11}>k_{11}$. However, if $k_{12}=k_{11}$, equation 3.81 must be modified, since the interaction term $u_2(t+k_{11}-k_{12})$ becomes $u_2(t)$. With $u_2(t)$ an unknown term, the following equation must be used to solve for $u_1(t)$ and $u_2(t)$ simultaneously:

$$
\begin{aligned}
[\mathbf{Q}_1 + g_{11}(0)]u_1(t) + g_{12}(0)u_2(t) = \mathbf{R}_1 w_1(t) - \frac{\mathbf{F}_1 y_1(t)}{\mathbf{P}_d} \\
- \sum_{k=1}^{ng_{11}} g_{11}(k)u_1(t-k) \qquad & (3.82) \\
- \sum_{k=1}^{ng_{12}} g_{12}(k)u_2(t-k) \\
- \mathbf{L}_{11}v_1(t+k_{11}-d_{11}) \\
- \mathbf{H}_1\mathbf{P}y_1^*(t+k_{11}-1|t-1)
\end{aligned}
$$

A similar equation can be formulated for loop two.

$$
\begin{aligned}
g_{21}(0)u_1(t) + [Q_2 + g_{22}(0)]u_2(t) = {} & R_2w_2(t) - \frac{F_2y_2}{P_d}(t) \\
& - \sum_{k=1}^{ng_{21}} g_{21}(k)u_1(t-k) \\
& - \sum_{k=1}^{ng_{22}} g_{22}(k)u_2(t-k) \\
& - L_{22}v_2(t+k_{22}-d_{22}) \\
& - H_2Py^*_2(t+k_{22}-1|t-1)
\end{aligned}
\tag{3.83}
$$

Equations 3.82 and 3.83 can be represented by:

$$SU(t) = T(t) \tag{3.84}$$

where T(t) denotes the right hand sides of equations 3.82 and 3.83, with:

$$S = \begin{bmatrix} Q_1 + g_{11}(0) & g_{12}(0) \\ g_{21}(0) & Q_2 + g_{22}(0) \end{bmatrix} \tag{3.85}$$

Since the control vector can be expressed as:

$$U(t) = S^{-1}T(t) \tag{3.86}$$

The solution of equation 3.86, is accomplished explicitly, for the 2*2 case, using Cramer's rule for matrix inversion.

4. Experimental Implementation

4.1 Description of Equipment

The pilot plant distillation column in the Department of Chemical Engineering at the University of Alberta is a 22.5 cm (9 inch) diameter column, that contains eight trays numbered from bottom to top. Each tray contains four bubble caps arranged in a square pattern. Tray spacing is 30.5 cm (12 inch) with feed supplied at tray four, an option is available to supply feed at tray five. Feed temperature is controlled at 61°C using a small steam heat exchanger and a Foxboro temperature controller. A schematic diagram of the distillation column is presented in Figure 4.1, with further detailed descriptions of the column and associated equipment given by Sverck [1967], Pacey [1973] and Lieuson [1980].

Several changes have been made to the column since the studies of Coppus [1980], Kan [1982] and Lieuson [1980]. Most of the changes have been to piping and preheat loops for the feed and reflux flows. A recirculation line has been added to the feed pump discharge, to maintain feed output pressure constant, at 25 psig. This helps to ensure reproducible feed flow results regardless of the feed filter condition. A regulator has been added to the steam supply to both the feed and reflux preheat loops to allow these loops to properly maintain temperatures at 61°C and 55°C respectively. Heat exchangers have been added to the return lines to the feed tank to maintain feed tank temperatures

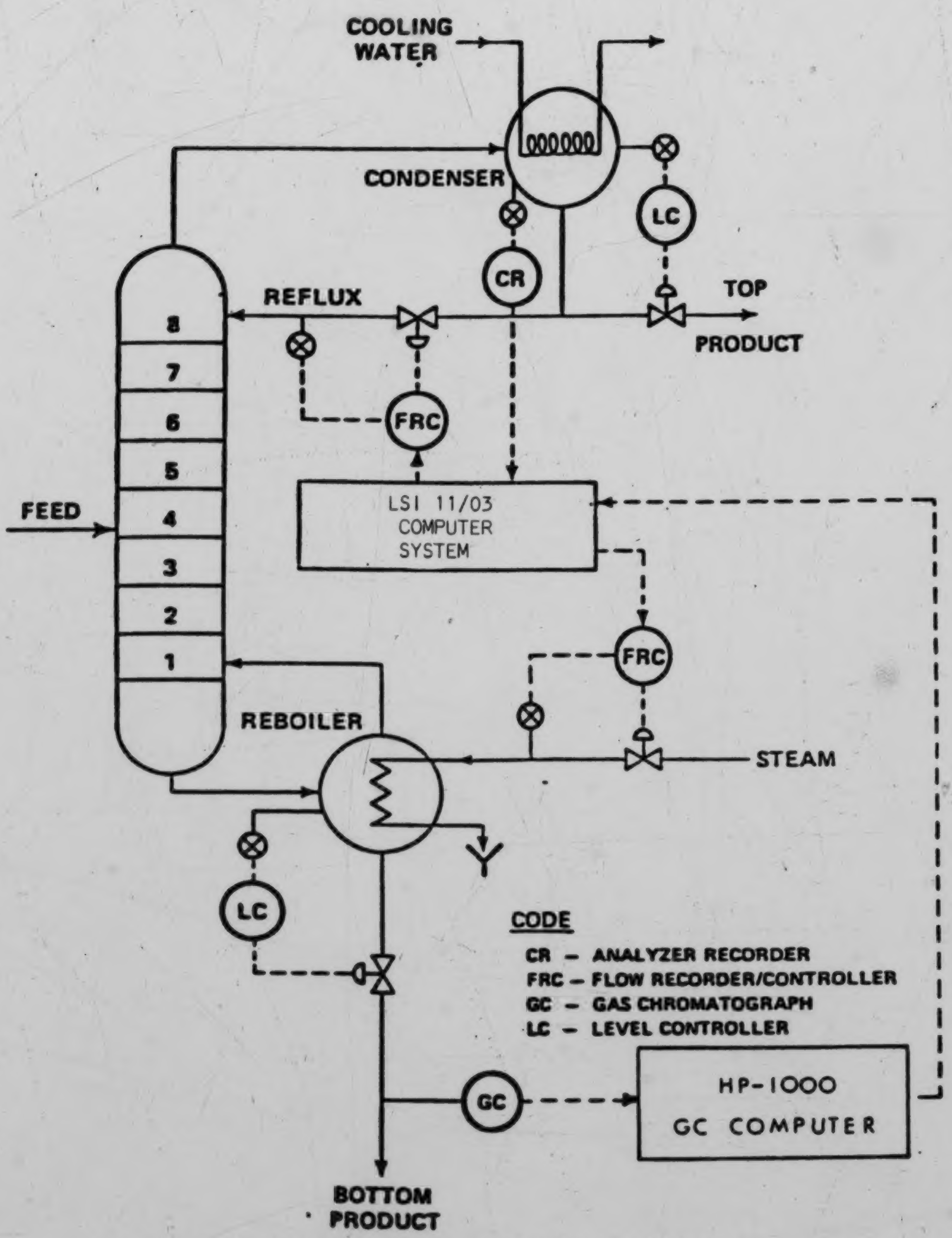
COOLING WATER
CONDENSER
LC
CR
REFLUX
TOP PRODUCT
8
7
6
5
4
3
2
1
FRC
FEED
LSI 11/03 COMPUTER SYSTEM
FRC
REBOILER
STEAM
LC
CODE
CR – ANALYZER RECORDER
FRC – FLOW RECORDER/CONTROLLER
GC – GAS CHROMATOGRAPH
LC – LEVEL CONTROLLER
GC
HP-1000 GC COMPUTER
BOTTOM PRODUCT

Figure 4.1 Schematic Diagram of Distillation Column

below 30°C. Above 30°C it was found that the water methanol mixture of the feed tank would cavitate in the feed pump causing an erratic feed flow rate. It was noted that a composition gradient as well as a temperature gradient developed in the feed tank after several days of operation. To remedy this, an in tank feed circulation system was employed to maintain constant feed composition and temperature.

Changes in the operating conditions were also made. The column was operated with the vent to atmosphere shut, so operation corresponds more closely to industrial applications, since most columns run with pressure control loops which effects the composition and steady state operation. Operating the column in this manner has caused the column steady state operating conditions to be very dependent on the temperature and amount of cooling water available, as shown by the mass and energy balances given in Tables 4.1(a,b) and 4.2(a,b).

Comparison of Tables 4.1a and 4.2a, reveals that little difference exists between the two open loop steady state operating conditions. The values of the flows have little difference, but the bottom composition differs by a significant amount. This difference is attributed to the change in cooling water flow. A reduction in cooling water flow has increased the top composition only slightly, but has had a significant effect on bottoms composition. In closed loop control this change in cooling water flow was

13 July 1983 0845 hrs

STEADY STATE CONDITIONS
(488. SAMPLES 1 SECOND INTERVAL)

FLOW DATA

	FLOW(g/s)	STANDARD DEVIATION
STEAM	11.010	0.094
REFLUX	9.048	0.050
FEED	17.845	0.090
TOP PRODUCT	7.962	0.127
BOTTOM PRODUCT	10.274	0.462
COOLING WATER	319.902	5.768

TEMPERATURE DATA

	TEMP(DEG C)	STANDARD DEVIATION
FEED INLET	61.370	0.309
REFLUX	47.700	0.000
REFLUX INLET	52.805	0.364
TOP VAPOUR	59.252	0.165
CWATER IN	11.501	0.226
CWATER OUT	26.244	0.237
STEAM IN	118.608	0.000
STEAM CONDS	100.480	0.000
REB VAPOUR	90.481	0.320
BOTTOM PRODUCT	38.189	0.292
REBOILER LIQ	92.151	0.000
FEED	29.419	0.227
CONDENSER LIQ	58.454	0.100

COMPOSITION DATA (MASS% METHANOL)

TOP = 95.087 FEED = 50.742 BOTTOM= 7.439

Table 4.1a Typical mass and energy balance for normal cooling water flow rate

MATERIAL BALANCE

	FLOW (g/s)	COMPOSITION (MASS% MEOH)	METHANOL (g/s)	WATER (g/s)
FEED	17.845	50.742	9.055	8.790
BOTTOM PRODUCT	10.274	7.439	0.764	9.509
TOP PRODUCT	7.962	95.087	7.571	0.391
% ERROR	-2.19		7.95	-12.63

ENERGY BALANCE

	ENTHALPY IN (J/s)	ENTHALPY OUT (J/s)
FEED	3898.104	
REFLUX INLET	1392.183	
STEAM	27377.020	4664.741
COOLING WATER	15388.843	35084.711
CONDENSER OUT		2961.556
BOTTOM PRODUCT		3924.632
TOTAL	48056.148	46635.641

HEAT LOSS = 1420.508 (J/s)
= 2.956 (% OF TOTAL HEAT INPUT)

Table 4.1b Typical mass and energy balance for normal cooling water flow rate

7 July 1983 1620 hrs

STEADY STATE CONDITIONS
(730. SAMPLES 1 SECOND INTERVAL)

FLOW DATA

	FLOW(g/s)	STANDARD DEVIATION
STEAM	11.065	0.043
REFLUX	8.412	0.040
FEED	17.925	0.070
TOP PRODUCT	8.629	0.077
BOTTOM PRODUCT	9.632	0.176
COOLING WATER	182.619	8.274

TEMPERATURE DATA

	TEMP(DEG C)	STANDARD DEVIATION
FEED INLET	61.531	0.332
REFLUX	47.898	0.107
REFLUX INLET	54.297	0.000
TOP VAPOUR	59.770	0.261
CWATER IN	11.923	0.205
CWATER OUT	41.635	0.569
STEAM IN	119.122	0.440
STEAM CONDS	102.644	0.274
REB VAPOUR	92.444	0.272
BOTTOM PRODUCT	37.310	0.292
REBOILER LIQ	94.305	0.440
FEED	27.301	0.446
CONDENSER LIQ	59.719	0.287

COMPOSITION DATA (MASS% METHANOL)

TOP = 95.462 FEED = 50.063 BOTTOM= 5.064

Table 4.2a Typical mass and energy balance for low cooling water flow

MATERIAL BALANCE

	FLOW (g/s)	COMPOSITION (MASS% MEOH)	METHANOL (g/s)	WATER (g/s)
FEED	17.925	50.063	8.974	8.951
BOTTOM PRODUCT	9.632	5.064	0.488	9.144
TOP PRODUCT	8.629	95.462	8.238	0.392
% ERROR	-1.88		2.77	-6.53

ENERGY BALANCE

	ENTHALPY IN (J/s)	ENTHALPY OUT (J/s)
FEED	3936.203	
REFLUX INLET	1336.308	
STEAM	27430.146	4791.877
COOLING WATER	9107.033	31774.650
CONDENSER OUT		3041.375
BOTTOM PRODUCT		3786.999
TOTAL	41809.691	38603.027

HEAT LOSS = 3206.664 (J/s)
= 7.670 (% OF TOTAL HEAT INPUT)

Table 4.2b Typical mass and energy balance for low cooling water flow

compensated for by changes in both the relux flow and steam flow, resulting in a different operating point.

Pairing of manipulated and controlled variables was based on the results of Lieuson [1980]. The energy balance configuration for the top loop control removes the dynamics of the condenser level from the top composition response [Lieuson, 1980].

Operating conditions for the column were selected for a methanol-water feed mixture containing 50% by mass methanol. Feed enters at a rate of 18 g/s and is separated into an overhead stream containing 95% by mass methanol and a bottoms stream containing 5% by mass methanol. The control objective is to minimize the effect of feed disturbances on the terminal composition, when the feed flow rate is changed by 25% from its normal steady state flow rate. It should be noted that for industrial application, changes in feed rate of 25% represent drastic changes. This magnitude of disturbance is employed since increases in flow rate of up to 15% have little effect on overhead composition. Therefore, in order to successfully demonstrate the performance and robustness of the controller, ±25% disturbances in feed rate were used for all experimental tests. Use of this large disturbance also allows for comparison with previous work [Lieuson, 1980; Kan, 1982].

The column has an extensive amount of instrumentation to measure physical parameters needed for column operation. This includes flow measurements for feed, reflux, top product, condenser cooling water, bottoms product and steam. Thermocouples are installed to measure the temperature of all flows, allowing mass and energy balance calculations to be performed.

Composition measurement is needed in order to apply control, top composition is determined by a continuous on-line capacitance probe connected to a Foxboro Dyanalog recorder, with bottoms composition analyzed by an HP-5722A gas chromatograph (GC). The GC signal is analyzed by the HP-1000 GC computer. The results are transmitted to the LSI 11/03 computer via a RS-232 serial communications line, with a program resident in the LSI which interprets the report from the HP computer to extract the value of the composition.

4.2 Control Implementation

Previous control implementations of self-tuning control have been accomplished using the IBM 1800 [Sastry, 1977] and HP-1000 computers [Lieuson, 1980]. The current self-tuning controller implementation is being accomplished using a LSI 11/03 16 bit microcomputer, using 64Kbytes of memory.

The computer is fitted with 16 single ended analog inputs for various flow and pressure measurements, 8 analog outputs for control signal outputs, 8 digital outputs for valve and GC control, and 16 thermocouple inputs for temperature measurements. Calculations are done using two word real numbers and single word integers. The computer is

5

also fitted with a line time clock to enable real time execution. Driver routines for analog inputs, analog outputs, digital outputs and thermocouple inputs are assembler coded routines, written to be FORTRAN callable. Analog outputs to the feed, reflux and steam setpoints are digitally multiplexed through one analog output channel to individual current output stations. From the current output stations the signals are converted to pneumatic signals by current to pressure converters, after which they are routed to the local flow controllers for feed, reflux and steam control.

4.3 Operating System

Previous control programs resided in multi-user main frames or mini-computers, unlike the LSI 11/03 which is not a multi-user computer. The operating environment is a single user foreground/background (FB) operating system. The foreground/background feature allows the execution of two jobs; a privileged foreground job and a secondary background job. In the current application the self-tuning controller operates in the privileged foreground job so that it has first priority on all tasks. This allows the background partition to accommodate several jobs, though only one at a time. These jobs include mass and energy balance calculations and data collection, data reformatting from binary to ASCII, data transfer programs to transfer collected data from the LSI to the University Amdhal 5860 computer for analysis. File editing and compilation can also be performed while the self-tuning controller manages the distillation column.

4.4 Gas Chromatograph

The bottoms composition is measured by an HP-5722A gas chromatograph(GC). The analog signal from the GC is received by an analog to digital converter model HP-18652A for transmission to the HP-1000 GC computer. Communication is accomplished via an interface loop (IL), used by the HP GC system.

Samples, for the GC, of the bottoms composition are obtained from the reboiler by a centrifugal pump and piping system. Normal flow in the sample piping system is from the reboiler to the pump, through a strainer and back to the reboiler. When a sample is required for analysis, a solenoid valve operated by either the event control module on the HP-1000 GC computer or a digital out from the LSI, closes and diverts flow from the pump through the GC automatic sample valve. The sample valve is an Applied Automation model twenty valve, with internal sample loop configuration and a $2\mu\ell$ sample size. Timing on the HP-1000 event control module and the LSI 11/03 is such that, flow is diverted through the GC sample valve for 30 seconds prior to actuating the valve to sample the flow. The 30 seconds is required to ensure proper purging of the valve and to ensure that an up-to-date bottoms composition is obtained. After the sample is taken, recirculation of the bottoms flow from the reboiler is returned directly to the reboiler until the next sample is required.

The overall cycle time for GC sampling is three minutes. Two minutes are used by the HP GC computer in analyzing the chromatogram. After two minutes the report is generated by the HP-1000 computer, transmission to the LSI 11/03 requires approximately 25 seconds, followed by the sample purge. The sample purge is required to return the detector current to the base line value in preparation for the next sample.

5. Column Dynamics

5.1 Introduction

In applying any type of controller or control strategy to a system, certain information about the system must be known. The information required varies depending on the complexity of the controller being implemented. Assuming the system we wish to control can be represented in the simplest form as a first order plus time delay model, three parameters are required to describe the system; process gain, time constant and time delay. This information can be obtained in many ways, one method being off-line identification of the system response used in this work. Analysis can be accomplished either graphically [Lopez et al., 1967] or by numerical search techniques [Desphande and Ash, 1981].

One of the easiest methods [Lopez et al., 1967] is to analyse the process reaction curve [Cohen and Coon, 1953] obtained from an open loop step test. Other more complicated methods, such as pulse testing [Desphande and Ash, 1981] and PRBS-testing can provide the same information. Each method has its advantages and disadvantages. For this study, open loop tests based on step responses have been chosen to determine first order plus time delay process transfer functions of the two loops involved in control of the distillation column.

5.2 System Representation

In Chapter 3 it was noted that the distillation column, is being controlled as a 2*2 system. The distillation column can therefore be described by the following transfer function matrix representation:

$$\begin{bmatrix} y_1(s) \\ y_2(s) \end{bmatrix} = \begin{bmatrix} G_{11}(s) & G_{12}(s) \\ G_{21}(s) & G_{22}(s) \end{bmatrix} \begin{bmatrix} u_1(s) \\ u_2(s) \end{bmatrix} \qquad (5.1)$$

where y_1 and y_2 designate the top composition and the bottom composition respectively and u_1 and u_2 represent the reflux and steam flow rates respectively. Since the dynamic behavior of higher order systems, such as distillation columns can be approximated by first order plus time delay transfer function representations [Lopez et al., 1967], this approach has been employed in this study. The transfer function is expressed as:

$$G_{ij}(s) = \frac{Kp\, e^{-\theta_d s}}{\tau_1 s+1} \qquad (5.2)$$

where

Kp is the process gain (wt%/g/s)

τ_1 is the first order time constant (min)

θ_d is the time delay (min)

u is the control input

y is the process output

5.3 Manipulated Variable Dynamics

The values of the process gain, time constant and time delay which will accurately describe the distillation column dynamic behavior must be determined. To do this open loop tests, for step changes in each of the inputs from their steady state value, were performed to determine each of the four transfer functions which represent the distillation column model. Positive and negative step tests were performed to determine the nonlinear characteristics of the distillation column. Reflux step tests were conducted with ±10% changes in reflux flow rates. Steam step tests were conducted with ±5% changes in flow rate. The feed flow rate tests were performed for disturbances of ±15%. All tests were conducted over a 600 minute time duration, during which time the parameter under manipulation underwent four changes in a square wave pattern. Transfer functions were obtained by use of the program PROFIT.FOR listed in Appendix B, which is a modified version of the program MODEL [Desphande and Ash, 1981] which fits a second order plus time delay model to a set of input-output process data obtained from a step test. First order models were obtained by specifying a very small initial guess for the second order time constant.

Figure 5.1 presents the response obtained when the reflux flow rate was manipulated in a square wave pattern. The data for this diagram is contained in file REFLUX2.DAT.

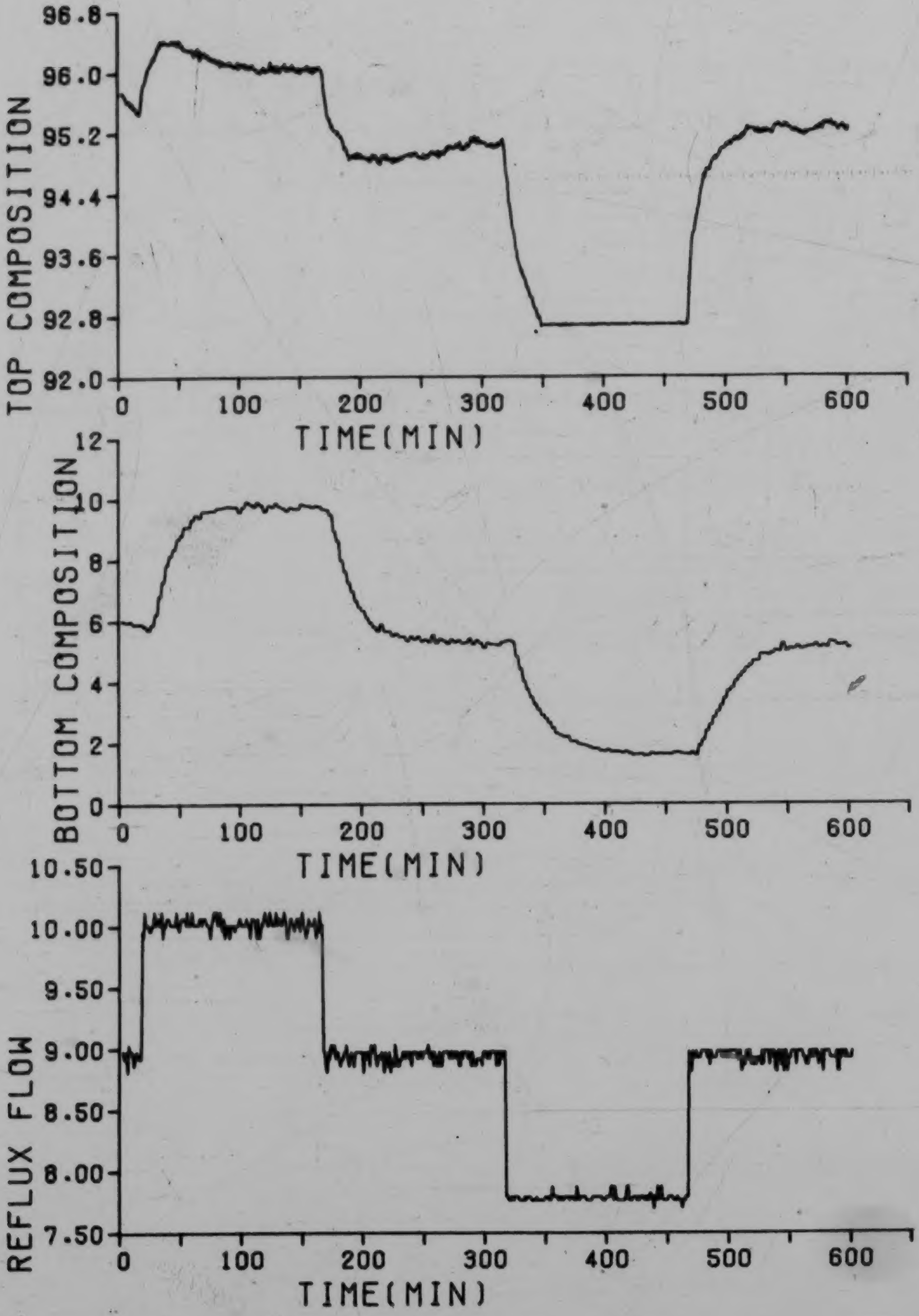

FIGURE 5.1 OPEN LOOP RESPONSE TO REFLUX FLOW

As can be seen from Figure 5.1, the lower range of the continuous analyzer for the top composition measurement was reached for the downward step in reflux flow rate. In order to obtain suitable reaction curves for the top composition response, the reflux flow was increased. This operation resulted in suitable reaction curves for the top composition response, but bottom composition approached zero, which prevented the use of the response curve for determining the transfer functions relating the effect of reflux flow rate on bottom composition. Therefore, several open loop tests were finally used to determine the $G_{11}(s)$ and $G_{21}(s)$ transfer functions. The data from two tests, data files REFLUX1.DAT and REFLUX2.DAT, were used to obtain the transfer functions. Steady state conditions for reflux, steam and feed flow were 8.9 g/s, 11.0 g/s and 18.0 g/s respectively. For brevity the other plots will not be presented, only the transfer functions obtained, are presented in Table 5.1.

Table 5.1
Transfer functions: Effect of reflux flow on top and bottom composition

Region of operation	Above Steady State(SS)		Below Steady State(SS)	
	Increase from SS	Decrease to SS	Decrease from SS	Increase to SS
$G_{11}(s)$	$\frac{1.52\ e^{-1s}}{3.265s+1}$	$\frac{1.084\ e^{-1s}}{6.151s+1}$	$\frac{1.408\ e^{-1s}}{10.964s+1}$	$\frac{1.604\ e^{-1s}}{8.35s+1}$
$G_{21}(s)$	$\frac{3.56\ e^{-12s}}{13.73s+1}$	$\frac{4.27\ e^{-6s}}{18.05s+1}$	$\frac{3.526\ e^{-6s}}{21.2s+1}$	$\frac{3.183\ e^{-9s}}{30.4s+1}$

Figure 5.2 represents the reaction curves, from step test data in data file STEAM2.DAT, for the effect of steam flow rate on top and bottom composition. Top composition response to the increase in steam rate appears to not have returned to steady state before the second step, the decrease in flow rate, was introduced. The transfer functions obtained from these process reaction curves are presented in Table 5.2.

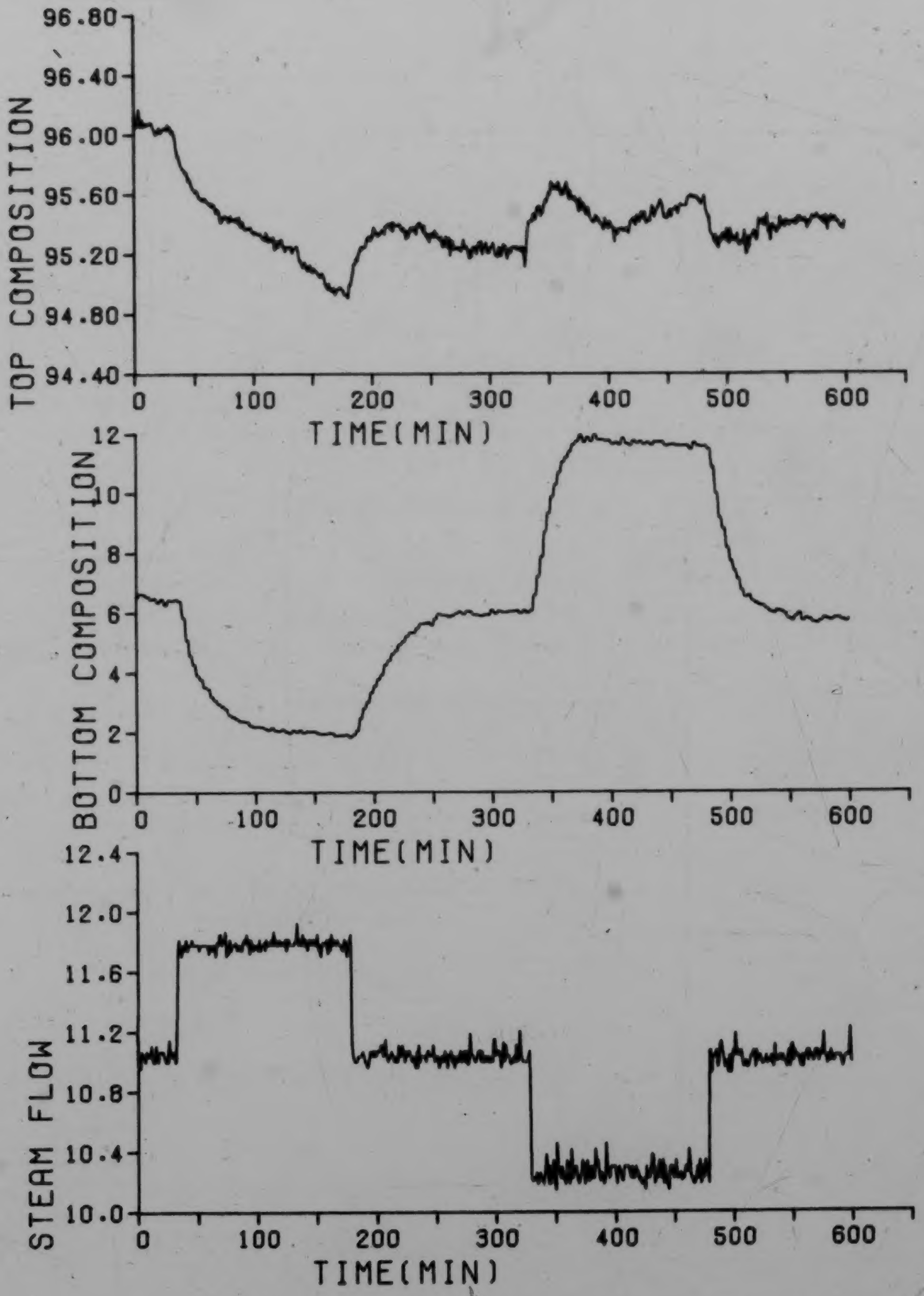

FIGURE 5.2 OPEN LOOP RESPONSE TO STEAM FLOW

Table 5.2
Transfer functions: Effect of steam flow on top and bottom composition

Region of operation	Above Steady State(SS)		Below Steady State(SS)	
	Increase from SS	Decrease to SS	Decrease from SS	Increase to SS
$G_{22}(s)$	$\frac{-5.579\ e^{-3s}}{19.95s+1}$	$\frac{-5.484\ e^{-7s}}{27.83s+1}$	$\frac{-6.416\ e^{-9s}}{12.345s+1}$	$\frac{-7.235\ e^{-6s}}{14.02s+1}$
$G_{12}(s)$	$\frac{-1.084\ e^{-1s}}{27.4s+1}$	$\frac{-.3016\ e^{-5s}}{4.902s+1}$	$\frac{-.2746\ e^{-1s}}{3.31s+1}$	$\frac{-.083\ e^{-2s}}{2.0s+1}$

The nonlinear characteristics of the distillation column are evident, by comparing the gains, time constants and time delays in Tables 5.1 and 5.2. Note as well that the nonlinear nature of the column is more pronounced in the off-diagonal, interaction transfer functions, than in the diagonal transfer functions. The process gains of G_{12} change by an order of magnitude, and the time constants and time delays vary by a considerable amount. The transfer functions as presented in Table 5.1 and 5.2 would lead to four different controller designs, depending on the direction of control action. This is not acceptable, so we must further approximate the dynamics of the column. Therefore, the parameters of the transfer functions are averaged numerically to arrive at a single transfer function matrix for future use in controller design. The final transfer function matrix is:

$$Y(s) = \begin{bmatrix} \dfrac{1.405\ e^{-1s}}{7.17s+1} & \dfrac{-.436\ e^{-3s}}{9.4035s+1} \\ \dfrac{3.635\ e^{-8s}}{20.85s+1} & \dfrac{-6.179\ e^{-6s}}{18.536s+1} \end{bmatrix} U(s) \qquad (5.3)$$

5.4 Disturbance Dynamics

To gain some insight, as to the nature of the distillation column response to feed disturbances; open loop tests were performed for step changes in feed flow rate. The reaction curves that resulted from these open loop step tests are plotted in Figure 5.3 (data file FEED4.DAT). The response of the top composition graphically indicates the nonlinearity of the distillation column with regard to feed flow rate disturbances. The response of the top composition to a decrease in feed flow rate from its steady state value results in an inverse response as displayed in the first transient response in Figure 5.3. No explanation for the occurrence of this inverse response is offered. It is presented here, only as an indication of the nonlinearity of the distillation column. This inverse response was demonstrated and reproduced in several open loop test results over the duration of this study. Work on simulation of inverse response behavior of binary and multicomponent

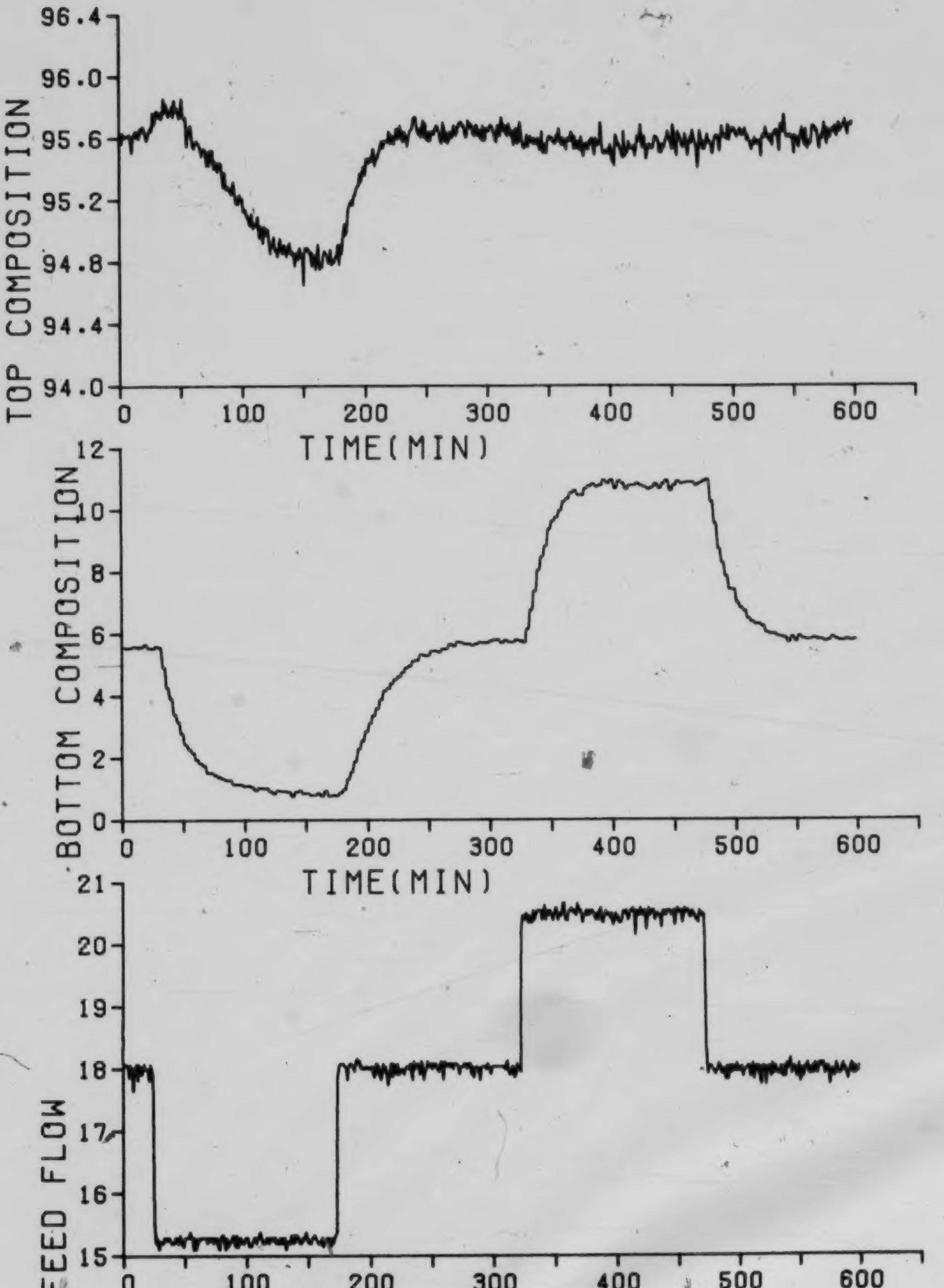

FIGURE 5.3 OPEN LOOP RESPONSE TO FEED FLOW

columns is underway [Wong, 1985]. Control of the column for this decrease in feed flow rate will prove difficult to regulate due to this inverse response. Furthermore, the top composition appears to be very sensitive to an increase in feed ~~flow to~~ steady state. It should be noted that, the reaction curves in Figure 5.3 represent the response to ±15% changes in feed flow rate. The control studies as noted in Chapter 4, are performed using ±25% changes. Open loop tests with feed changes of ±25% were attempted, but the composition response of both top and bottom products were beyond the range of both measuring devices.

6. Selection of Controller Parameters

6.1 Introduction

In Chapter Three the derivation of the multivariable multirate self-tuning controller was presented. In the derivation the structure of the controller was fixed, but the number of parameters for each of the respective controller polynomials and the value of the weighting transfer functions were not specified. The number of parameters and the value of the coefficients are left for the control engineer to specify depending on the system to be controlled. The Q weighting for the self-tuning controllers is specified on the basis of the dynamic behaviour of the distillation column established through open loop testing as discussed in the previous chapter. Settings for the proportional-integral-derivative (PID) controllers are also specified on the basis of the column dynamics.

6.2 Sample Time Selection

The minimum sample time as noted in Chapter Four for the bottoms composition loop is limited to three minutes due to the restriction of the GC cycle time. It seems reasonable to expect that improved control performance of a process would be expected if it were possible to sample as rapidly as the equipment would allow, but this practice may lead to difficulties [Dahlin, 1968]. For the distillation column a short sample time would reveal the higher order process dynamics and cause complications, such as nonminimum phase characteristics and controller ringing [Dahlin, 1968]. Stephanopoulos [1984] recommends the selection of sample times based on the dominant first order time constant according to:

$$.1\tau_1 < t_s < .2\tau_1 \qquad (6.1)$$

The dominant time constant for the top loop is 7.17 minutes (cf. equation 5.3), so the recommended sample time based on equation 6.1 would be between 0.72 minutes and 1.43 minutes. A convenient sample time of one minute was chosen for the multirate control of the top loop, since three minutes is then an integer multiple of the smallest sample time.

6.3 Proportional-Integral-Derivative Controller Parameters

Analog PID controllers have been used for many years, but with the advent of low cost microcomputers the implementation of PID control with computers requires the discrete realization of the controller [Verbruggen et al., 1975]. Analog PID control action is defined in terms of proportional band (PB), integral time (TI) and derivative time (TD). These terms, which are used in this work because of their familiarity, are related to the controller constants of discrete controllers Kc, Ki and Kd by

$$Kc = \frac{100.0}{PB} \qquad Ki = \frac{Kc}{TI} \qquad Kd = KcTD \tag{6.2}$$

For this study the discrete PID controller in the velocity form with trapezoidal approximation for the integration was implemented as:

$$\begin{aligned} u_n = u_{n-1} &+ \left[Kc + \frac{Kit_s}{2} + \frac{Kd}{t_s} \right] e_n \\ &- \left[Kc - \frac{Kit_s}{2} + 2\frac{Kd}{t_s} \right] e_{n-1} \\ &+ \frac{Kd}{t_s} e_{n-2} \end{aligned} \tag{6.3}$$

where

Kc is the proportional constant for the controller

Ki is the integral constant for the controller

Kd is the derivative constant for the controller

e_n is the error at time n

t_s is the sample time

u_n is the control action at time n

Equation 6.3 may be expressed as:

$$u_n = u_{n-1} + K_1 e_n + K_2 e_{n-1} + K_3 e_{n-2} \tag{6.4}$$

where K_1, K_2, K_3 are the coefficients of the error terms of equation 6.3. The values of K_1, K_2, K_3 are related to proportional constant, integral constant, and derivative constant by the following equations:

$$\begin{aligned} K_1 &= Kc + \frac{Kit_s}{2} + \frac{Kd}{t_s} \\ K_2 &= \frac{Kit_s}{2} - Kc - \frac{2Kd}{t_s} \\ K_3 &= \frac{Kd}{t_s} \end{aligned} \tag{6.5}$$

Many methods are available to the engineer who wishes to determine initial controller parameters for a PID controller [Haalman, 1966; Lopez et al., 1969; Pemberton, 1972; Yuwana and Seborg, 1982]. For this study, four methods will be compared with regard to the selection of initial constants for digital PI and PID controllers to accomplish control of the distillation column. These methods are those of Ziegler-Nichols(Z-N), Cohen-Coon(3-C), IAE and ITAE as summarized by Miller et al., [1967]. These four methods for the estimation of the initial constants of continuous controllers are based on a first order plus time delay model representation of an open loop process response (cf. equation 5.2). The initial estimates for each of the methods are expressed by the following equations:

$$KpKc = A(\theta_d/\tau_1)^{-B} \tag{6.6}$$

$$TI/\tau_1 = C(\theta_d/\tau_1)^{D} \tag{6.7}$$

$$TD/\tau_1 = E(\theta_d/\tau_1)^{F} \tag{6.8}$$

with the values of the constants A, B, C, D, E, and F for PI and PID controllers given in Table 6.1. For discrete controllers the time delay, in equations 6.6 to 6.8, should be evaluated with the equivalent time delay $\theta_d' = (\theta_d + t_s/2)$ in place of θ_d [Moore et al., 1969] due to the delay from sampling.

The constants of equations 6.6 to 6.8 in Table 6.1 for the Ziegler-Nichols and Cohen-Coon methods are based on a one quarter decay ratio response characteristic. The minimum integral of absolute error(IAE) and the minimum integral of the time multiplied by the absolute error(ITAE) are integral criteria described by the minimization of the following:

$$IAE = \int_0^\infty |e(t)|\, dt \tag{6.9}$$

$$ITAE = \int_0^\infty t|e(t)|\, dt \tag{6.10}$$

Table 6.1
Constants for Equations 6.6 to 6.8 [Miller et al., 1967]

Method	Mode	A	B	C	D	E	F
Z-N	PI	.900	1.000	3.333	1.000		
3-C	PI	.928	.946	.928	.583		
IAE	PI	.984	.986	1.644	.707		
ITAE	PI	.858	.977	1.484	.680		
Z-N	PID	1.200	1.0	2.0	1.0	.5	1.0
3-C	PID	1.370	.950	.740	.738	.365	.950
IAE	PID	1.435	.921	1.139	.749	.482	1.137
ITAE	PID	1.357	.947	1.176	.738	.381	.995

Miller et al., [1967] suggests criteria for determining the relative merits for use of PI versus PID control. For θ_d/τ_1 less than 0.4, PI and PID control give essentially the same results, but if θ_d/τ_1 is greater than 0.4, the use of a PID controller would offer an advantage over a PI controller. For the distillation column, reference to Tables 5.1 and 5.2, shows that ratio of the largest time delay to smallest time constant for the top loop is 0.3063 and 0.7290 for the bottom loop. These results suggest that the top loop can be satisfactorily controlled by a PI controller whereas addition of derivative action is advantageous for control of bottom composition. The initial controller settings for the discrete controllers are summarized in Tables 6.2 and 6.3.

Table 6.2
Controller settings for top composition controller

GAIN OF SYSTEM= 1.4050 wt%/g/s
TIME CONSTANT= 7.17 MINUTES
TIME DELAY= 1.0 MINUTE

SAMPLING INTERVAL= 3.0 MINUTES

		Z-N	3-C	IAE	ITAE
(P)	KC	2.041	2.305	1.812	1.093
	PB	48.989	43.383	55.177	91.509
(PI)	KC	1.837	1.790	1.979	1.711
	PB	54.432	55.880	50.525	58.429
	TI	499.950	215.998	335.787	311.853
(PID)	KC	2.450	2.653	2.695	2.620
	PB	40.824	37.693	37.102	38.174
	TI	300.000	146.288	222.570	232.479
	TD	75.000	57.712	62.582	57.452

SAMPLING INTERVAL= 1.0 MINUTE

		Z-N	3-C	IAE	ITAE
(P)	KC	3.402	3.718	2.998	1.901
	PB	29.393	26.895	33.361	52.600
(PI)	KC	3.062	2.901	3.275	2.819
	PB	32.659	34.466	30.533	35.472
	TI	299.970	160.366	234.001	220.340
(PID)	KC	4.083	4.310	4.314	4.249
	PB	24.494	23.201	23.178	23.533
	TI	180.000	100.342	151.811	159.463
	TD	45.000	35.523	35.011	34.559

Table 6.3
Controller settings for bottom composition controller

GAIN OF SYSTEM= 6.1790 wt%/g/s
TIME CONSTANT= 18.536 MINUTES
TIME DELAY= 6.0 MINUTES

SAMPLING INTERVAL= 3.0 MINUTES

		Z-N	3-C	IAE	ITAE
(P)	KC	0.400	0.456	0.356	0.211
	PB	250.013	219.304	280.964	472.889
(PI)	KC	0.360	0.353	0.389	0.337
	PB	277.793	282.901	257.318	297.172
	TI	1499.849	609.007	964.383	892.055
(PID)	KC	0.480	0.524	0.534	0.517
	PB	208.345	190.937	187.135	193.290
	TI	900.000	422.083	643.232	670.770
	TD	225.000	171.851	191.613	172.227

6.4 Self-Tuning Controller

For the self-tuning controller, specifying the number of terms in each of the F, G, H and L polynomial matrices is equivalent to specifying the model of the system. In this study no H polynomial matrix was used. For the distillation column, the system is represented by G_{11}, F_1, L_1 and G_{12} polynomials for loop one. For the process response, interaction and disturbance dynamics each approximated by first order plus time delay models, three parameters would need to be specified for each polynomial. However for the three minute sample interval, any time delay less than the three minute sample period is taken as one integer delay, so the G_{11} transfer function with a time delay of one minute, adds one parameter to the G_{11} polynomial, and the delay of two minutes associated with the G_{12} transfer function, requires the addition of one parameter to the G_{12} polynomial. Thus the top loop composition self-tuning controller parameters number 4, 3, 3 and 4 for G_{11}, F_1, L_1 and G_{12} polynomials respectively.

For the bottom composition controller (loop two), G_{22} has a six minute delay which is equivalent to two sample intervals and G_{21} has a delay of eight minutes considered to be three sample intervals, it follows that the number of parameters are 5, 3, 3 and 6 for G_{22}, F_2, L_2 and G_{21} polynomials respectively.

6.5 Selection of Q Weighting Parameters

We have specified the **G**, **F**, **L** and **H** polynomial matrices, so the selection of **P**, **Q** and **R** weighting may now be specified. Selection of **P**=**R**=**I** and **Q**=0 yields a minimum variance controller [Lieuson, 1980]. The **P** and **R** weighting will remain as identity matrices for this study, which leaves the selection of Q weighting as the final design step. Following the form presented by Morris et al., [1981] the Q weighting transfer function will be represented in the form of an inverse PID structure, that is:

$$Q = \frac{1 - z^{-1}}{q_0 + q_1 z^{-1} + q_2 z^{-2}} \tag{6.11}$$

with the terms q_0, q_1 and q_2 chosen to represent the coefficients of a discrete PI, PID controller [Verbruggen et al., 1975] according to the following relations:

$$\begin{aligned} q_0 &= Kc + \frac{Kit_s}{2} + \frac{Kd}{t_s} \\ q_1 &= \frac{Kit_s}{2} - Kc - \frac{2Kd}{t_s} \\ q_2 &= \frac{Kd}{t_s} \end{aligned} \tag{6.12}$$

The Q weighting uses the inverse form because the weighting as applied in equations 3.29 and 3.32 appears as part of the denominator. With the self-tuning controller based on the k step ahead prediction, there is effectively no delay in the closed loop characteristic equation [Lieuson, 1980; Morris et al., 1981; Nazer, 1981], which allows the Q weighting to be represented as a PI compensator. Consequently the same methods used for calculating initial controller settings for P, PI, and PID controllers can now be used to select the Q weighting coefficients. The diagonal transfer functions (cf. equation 5.3) are used without the delay terms as the basis for the calculation. The calculated values of proportional band, integral time and derivative time using equations 6.6 to 6.8 are given in Tables 6.4 and 6.5. These values are provided in this form for comparison with the PID controller constants. Equation 6.2 along with equation 6.12 are used to transform these values into the Q weighting parameters for use in equation 6.11. Since this tranformation is provided within the preprocessing portion of the implemented algorithm, for convenience, the values in Tables 6.4 and 6.5 will be referred to as the Q weighting values.

6.6 Controller Performance Criterion

To compare the performance of different types of controllers, or the performance from the same type of controller using different settings, it is convenient to use a quantitative measure of performance.

Table 6.4
Q Weighting settings for top composition self-tuning controller

GAIN OF SYSTEM= 1.4050 wt%/g/s
TIME CONSTANT= 7.17 MINUTES
TIME DELAY= 0.0 MINUTE

SAMPLING INTERVAL= 3.0 MINUTES

		Z-N	3-C	IAE	ITAE
(P)	KC	3.402	3.718	2.998	1.901
	PB	29.393	26.895	33.361	52.600
(PI)	KC	3.062	2.901	3.275	2.819
	PB	32.659	34.466	30.533	35.472
	TI	299.970	160.366	234.001	220.340
(PID)	KC	4.083	4.310	4.314	4.249
	PB	24.494	23.201	23.178	23.533
	TI	180.000	100.342	151.811	159.463
	TD	45.000	35.523	35.011	34.559

SAMPLING INTERVAL= 1.0 MINUTE

		Z-N	3-C	IAE	ITAE
(P)	KC	10.206	10.397	8.846	6.255
	PB	9.798	9.618	11.305	15.988
(PI)	KC	9.186	8.203	9.676	8.246
	PB	10.886	12.191	10.335	12.126
	TI	99.990	84.518	107.620	104.388
(PID)	KC	12.248	12.240	11.867	12.027
	PB	8.165	8.170	8.426	8.315
	TI	60.000	44.604	66.671	70.883
	TD	15.000	12.510	10.040	11.583

Table 6.5
Q Weighting settings for bottom composition self-tuning controller

GAIN OF SYSTEM= 6.1790 wt%/g/s
TIME CONSTANT= 18.536 MINUTES
TIME DELAY= 0.0 MINUTE

SAMPLING INTERVAL= 3.0 MINUTES

		Z-N	3-C	IAE	ITAE
(P)	KC	2.000	2.057	1.737	1.210
	PB	50.003	48.619	57.566	82.618
(PI)	KC	1.800	1.620	1.900	1.621
	PB	55.559	61.718	52.636	61.676
	TI	299.970	238.300	309.085	298.602
(PID)	KC	2.400	2.416	2.353	2.375
	PB	41.669	41.388	42.501	42.100
	TI	180.000	128.694	192.681	204.519
	TD	45.000	37.250	30.739	34.724

Typical common performance criteria are [Stephanopoulos, 1984]:

$$ISE = \int_0^\infty [e(t)]^2 \, dt \qquad (6.13)$$

$$IAE = \int_0^\infty |e(t)| \, dt \qquad (6.14)$$

$$ITAE = \int_0^\infty t|e(t)| \, dt \qquad (6.15)$$

The choice of criterion must obviously measure the most important performance characteristics. The integral of the squared error(ISE) is relatively insensitive to small errors, but large errors contribute heavily to the value of the integral [Lopez et al., 1967; Stephanopoulos, 1984]. Consequently, use of ISE as a criterion of performance will result in a response with small overshoots, but long settling times, since small errors contribute little to the integral. The integral of the absolute value of the error(IAE) is more sensitive to small errors, but less sensitive to large errors, when compared with ISE. IAE weights errors in the response curve equally. The integral of the time multiplied absolute error(ITAE) is insensitive to the initial and somewhat unavoidable errors, but places a heavy weight on errors of long duration. Controllers designed by the minimization of ITAE, show short total response time, short settling times and larger overshoots than with either of the other criteria [Lopez et al., 1967; Stephanopoulos, 1984].

For column composition control the elimination of offset and the minimization of the overshoot are equally important in the comparison of controller performance, so the IAE performance criterion will be used to compare the control performance for the different techniques used for estimating initial controller constants.

The continuous integral as defined by equation 6.14 is evaluated as:

$$IAE = \sum_{t=0}^{150} |e(t)*t_s| \tag{6.16}$$

which approximates the integral of absolute error for the top composition loop with t_s = 1.0 minute. For the bottom composition loop t_s=3.0 minutes and the upper limit on the summation is set to 50, which corresponds to 50 samples for a test period of 150 minutes.

7. Experimental Results

The material in this chapter is separated into eight sections. Sections 1 and 2 present the observed response of the distillation column operated under multiloop and multirate PID control with parameters based on initial selection methods as provided in Tables 6.2 and 6.3. The controlled responses under the multivariable, multirate self-tuning control strategy with the Q weighting values given in Tables 6.4 and 6.5 are presented in sections 3 and 4. The control performance for the column operated under PID control compared to the performance achieved using the self-tuning controller based on the same initial parameter selection methods are summarized in section 5. Section 6 presents the response observed for the best settings obtained for multiloop, multirate PID control and for the self-tuning control with tuned Q weighting for both multivariable, and multirate applications. Results of the performance achieved using multivariable, multirate self-tuning control with measured feedforward compensation are provided in section 7. The results of the k-incremental self-tuning controller with measured feedforward compensation are presented in section 8.

The observed column response is presented in a standard format, based on a ±25% square wave disturbance in feed flow rate for all tests. The duration of each sequence of changes, for particular controller settings is 10 hours. Each study is separated into four sections corresponding to the four steps in the square wave disturbance. The response for the key process variables are presented for a 150 minute duration for each step. The response for each step is presented using eight plots, consisting of top composition, reflux flow, feed flow, top composition IAE performance, bottom composition, steam flow, feed flow and bottom composition IAE performance. A detailed description of the plot titles and abbreviations used are provided in Appendix C.

7.1 Control of Product Compositions Using a Multiloop PID Control Strategy

Tests for control of the pilot plant distillation column using a multiloop PID control strategy were performed using a common sample time of 3.0 minutes. Conventional PID controllers using the single and multirate strategies with no feedforward compensation were studied.

7.1.1 Control Performance With Constants Calculated from the Ziegler-Nichols Equations

Table 7.1.1 provides a summary of the IAE performance values for the tests of the control performance of the pilot plant distillation column when subjected to dual composition control with conventional PID controllers using constants calculated with the Ziegler-Nichols equations. Figures 7.1 through 7.4 presents the response of the manipulated and controlled variables when subjected to the feed flow rate

Table 7.1.1
Multiloop PID Control Performance with Controller Constants Calculated from Ziegler-Nichols Equations

	IAE Values	
Step	TOP	BOTTOM
increase from steady state	8.0	255.9
decrease to steady state	21.0	267.7
decrease from steady state	49.3	421.5
increase to steady state	38.1	449.7
total	116.4	1394.8

disturbances. In Chapter 5 it was noted that increases in feed flow from steady state had very little effect on the top composition. This contributes to the good regulation of the top composition evident in Figure 7.1, which resulted in an IAE of only 8.0. The top composition varies little during the introduction of the disturbance, and as can be seen, only a slight change in the manipulated variable, reflux flow, is required to maintain the composition close to the set point, so interaction as a result of the steam change from bottom composition control is minimal. For the bottom composition a substantial deviation from the setpoint occurs at the introduction of the disturbance with a resulting IAE value of 255.9. Due to the small amount of integral action it can be seen that the controller is unable to return the bottom composition to its setpoint prior to the end of the test period.

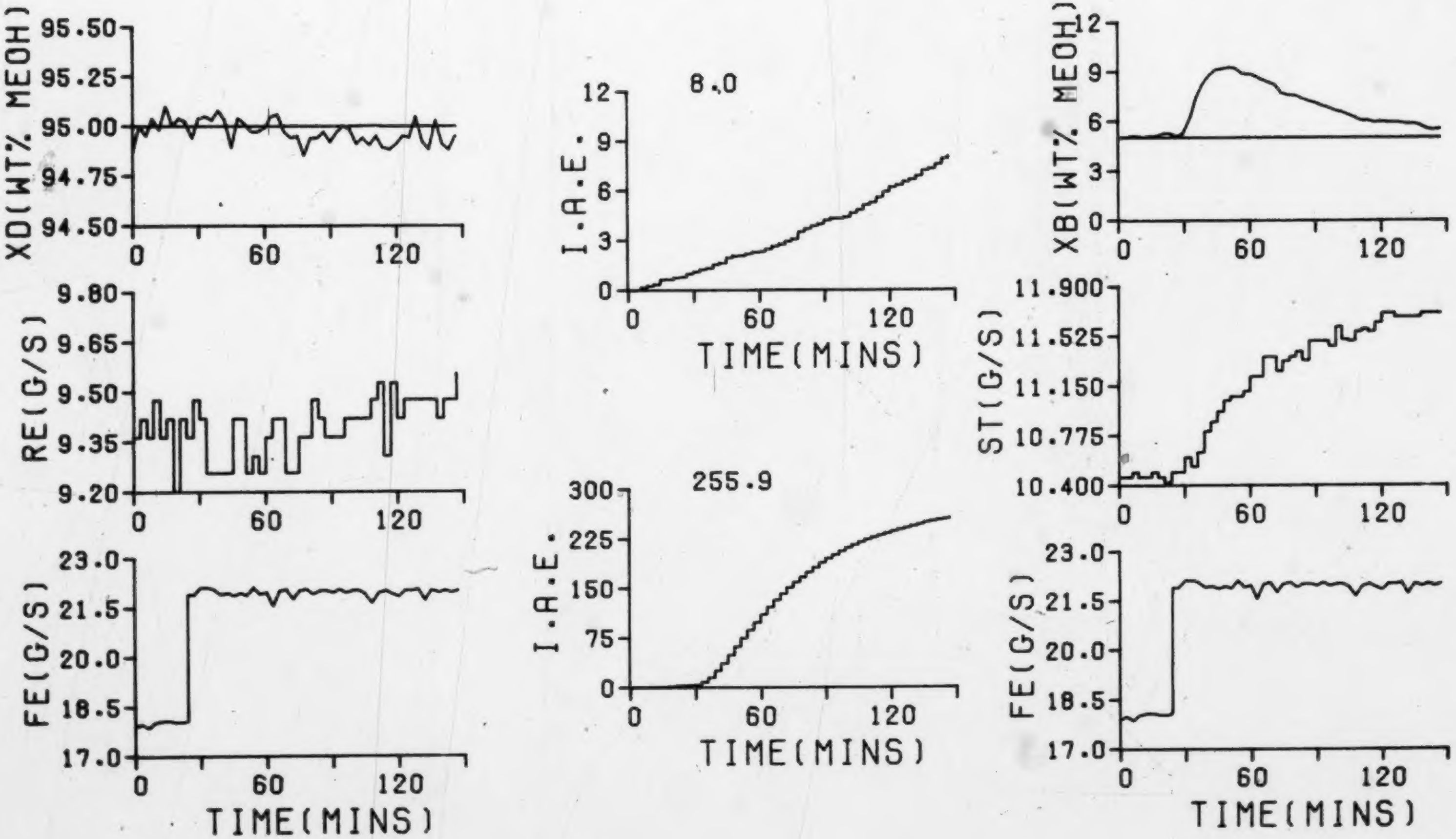

FIGURE 7.1 ML PID Z-N/PID(PB=54.432.TI=499.95.TD=0.)/TS=180.0/
PID(PB=208.345.TI=900.0.TD=225.0)/TS=180.0/

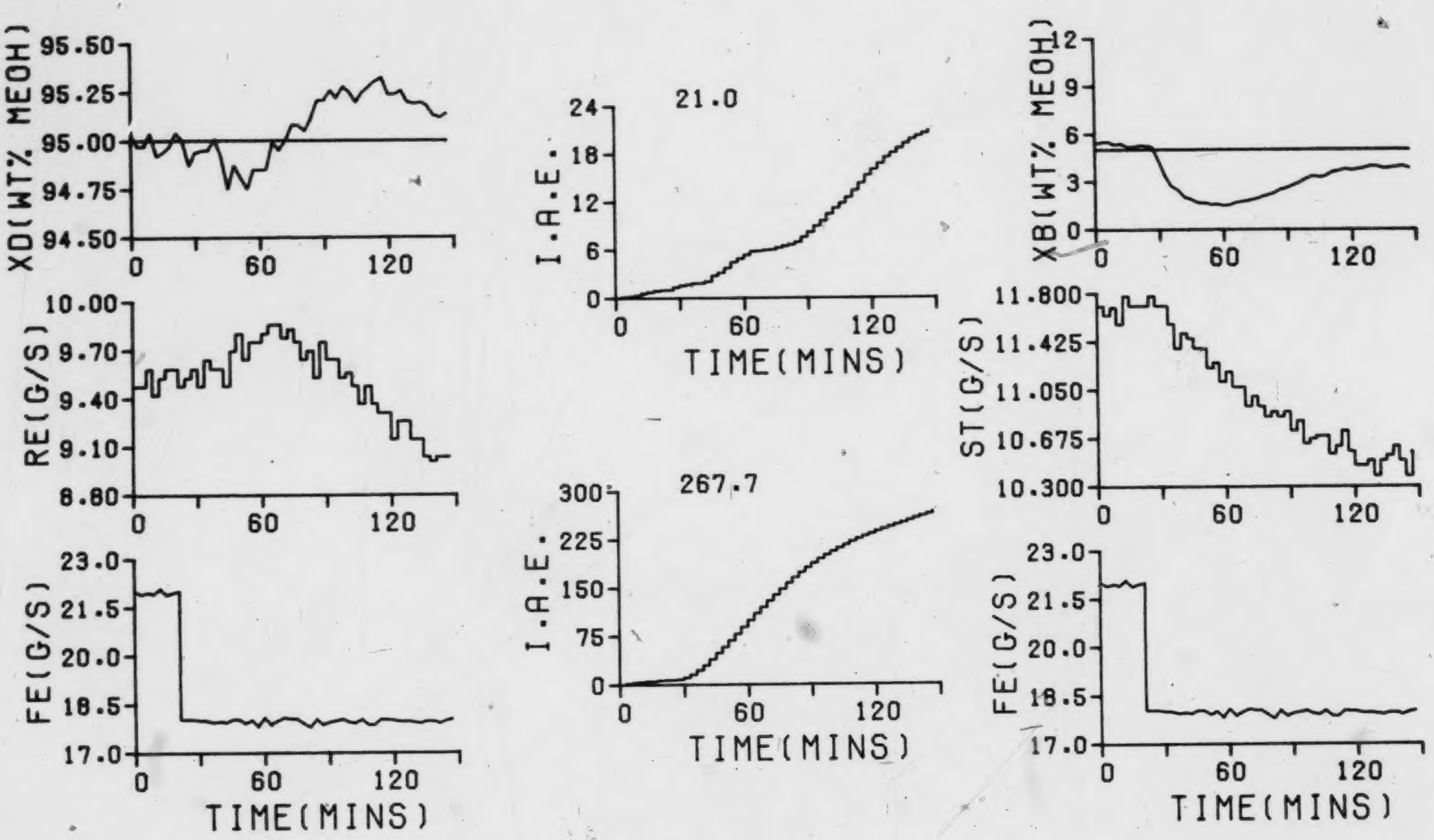

FIGURE 7.2 ML PID Z-N/PID(PB=54.432,TI=499.95,TD=0.)/TS=180.0/ PID(PB=208.345,TI=900.0,TD=225.0)/TS=180.0/

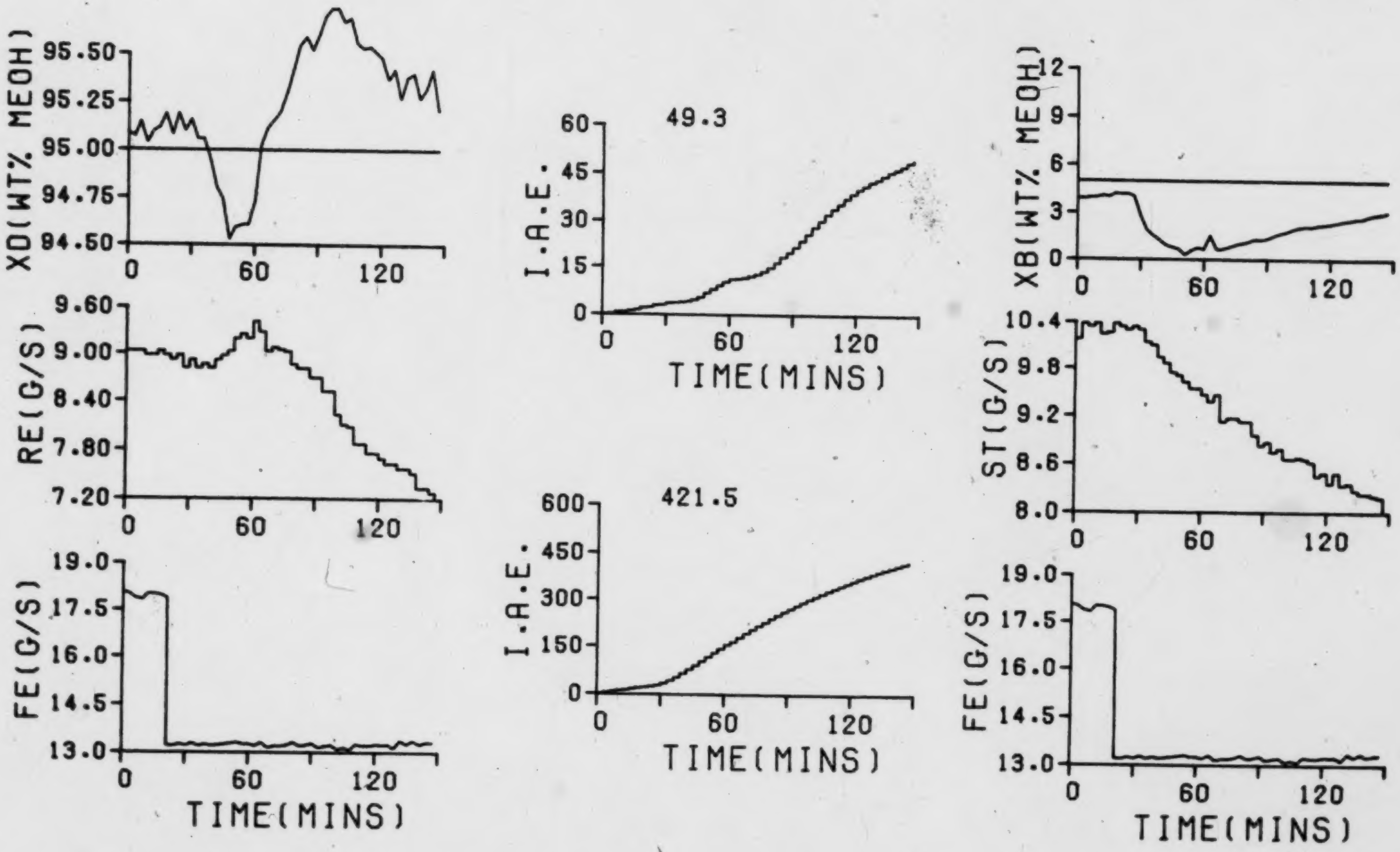

FIGURE 7.3 ML PID Z-N/PID(PB=54.432.TI=499.95.TD=0.)/TS=180.0/
PID(PB=208.345.TI=900.0.TD=225.0)/TS=180.0/

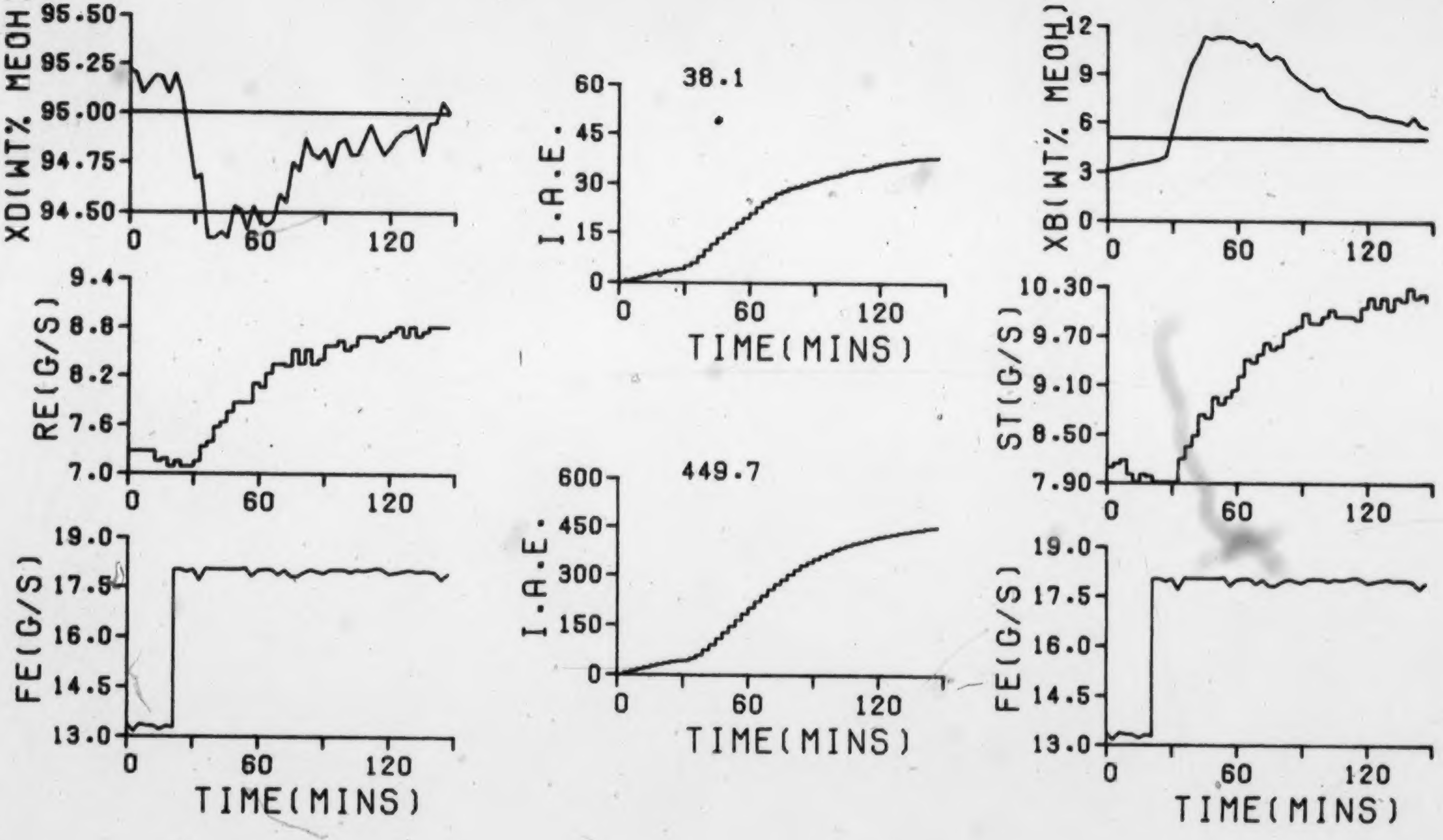

FIGURE 7.4 ML PID Z-N/PID(PB=54.432.TI=499.95.TD=0.)/TS=180.0/
PID(PB=208.345.TI=900.0.TD=225.0)/TS=180.0/

Figure 7.2 presents the response for a decrease in feed flow rate back to the steady state value. The bottom composition response is similar to that shown in Figure 7.1 in that the controller has not returned the bottom composition to the setpoint. For the top composition the initial control response is poor, deviation from the setpoint is sustained as is illustrated by the IAE value of 21.0. The IAE values of 255.9 and 267.7 for the bottom composition indicate similar responses for the increase and decrease in feed rate as displayed in Figures 7.1 and 7.2 respectively.

The column response for a decrease in feed flow rate from the steady state rate is shown in Figure 7.3. This portion of the disturbance displayed an inverse response behavior in top composition for the open loop tests (cf. Figure 5.3). The difficulty in regulation is obvious from the IAE value for the top composition of 49.3, which is over six times the IAE value of the first step in the disturbance. For the bottom composition, the same general pattern of control was obtained. The bottom composition did not return to the setpoint prior to the end of the test. The IAE value for the bottom loop of 421.5 is almost double the previous values. The added difficulty in controlling the bottom composition can be attributed to the interaction from the reflux flow changes in attempting to control the top composition.

The response for an increase in feed flow back to the steady state value results in the performance shown in Figure 7.4. The top composition control behavior is again poor as shown by the IAE value of 38.1, with the bottom composition control equally poor resulting in an IAE value of 449.7.

The general trend of slow response by the controller to a sustained disturbance is evident for all four step changes. For the bottom composition, the delay inherent for the GC analysis has made regulation of the bottom composition difficult. The top composition is difficult to regulate due to the nonlinear nature of the column as was illustrated in Chapter 5.

7.1.2 Control Performance with Constants Calculated using the Cohen-Coon Equations

Table 7.1.2 provides a summary of the IAE performance values for the tests of the control performance of the pilot plant distillation column when subjected to dual composition control with conventional PID controllers using constants calculated with the Cohen-Coon equations. Figures 7.5 through 7.8 present the observed response of the pilot plant distillation column due to the feed rate disturbances introduced during the test. Figure 7.5 shows the responses when the column is subjected to an increase in feed flow rate from its steady state value. The top composition deviates slightly from the target at the onset of the

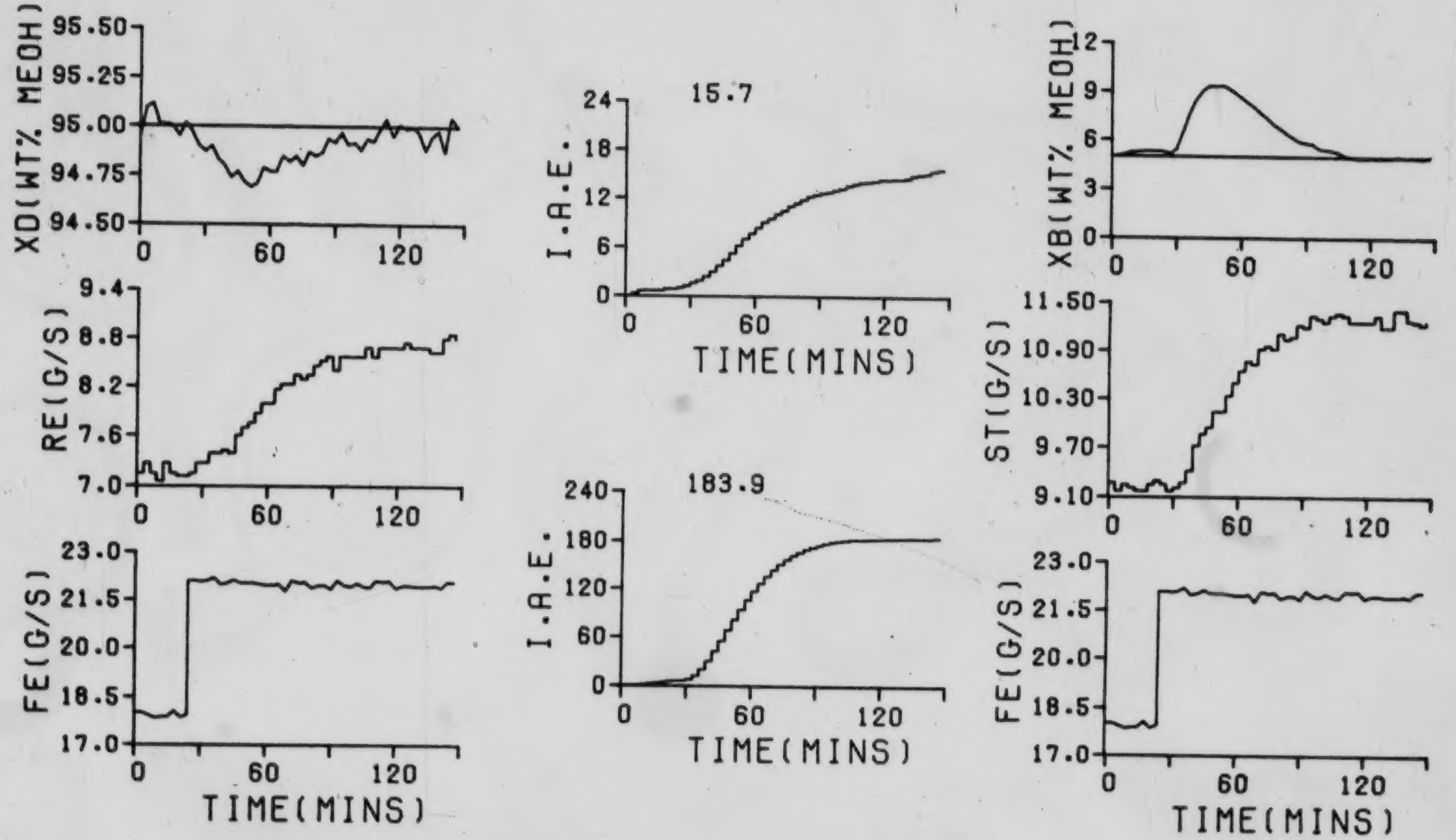

FIGURE 7.5 ML PID 3-C/PID(PB=55.88.TI=215.998.TD=0.0)/TS=180.0/
PID(PB=190.93.TI=422.083.TD=171.851)/TS=180.0/

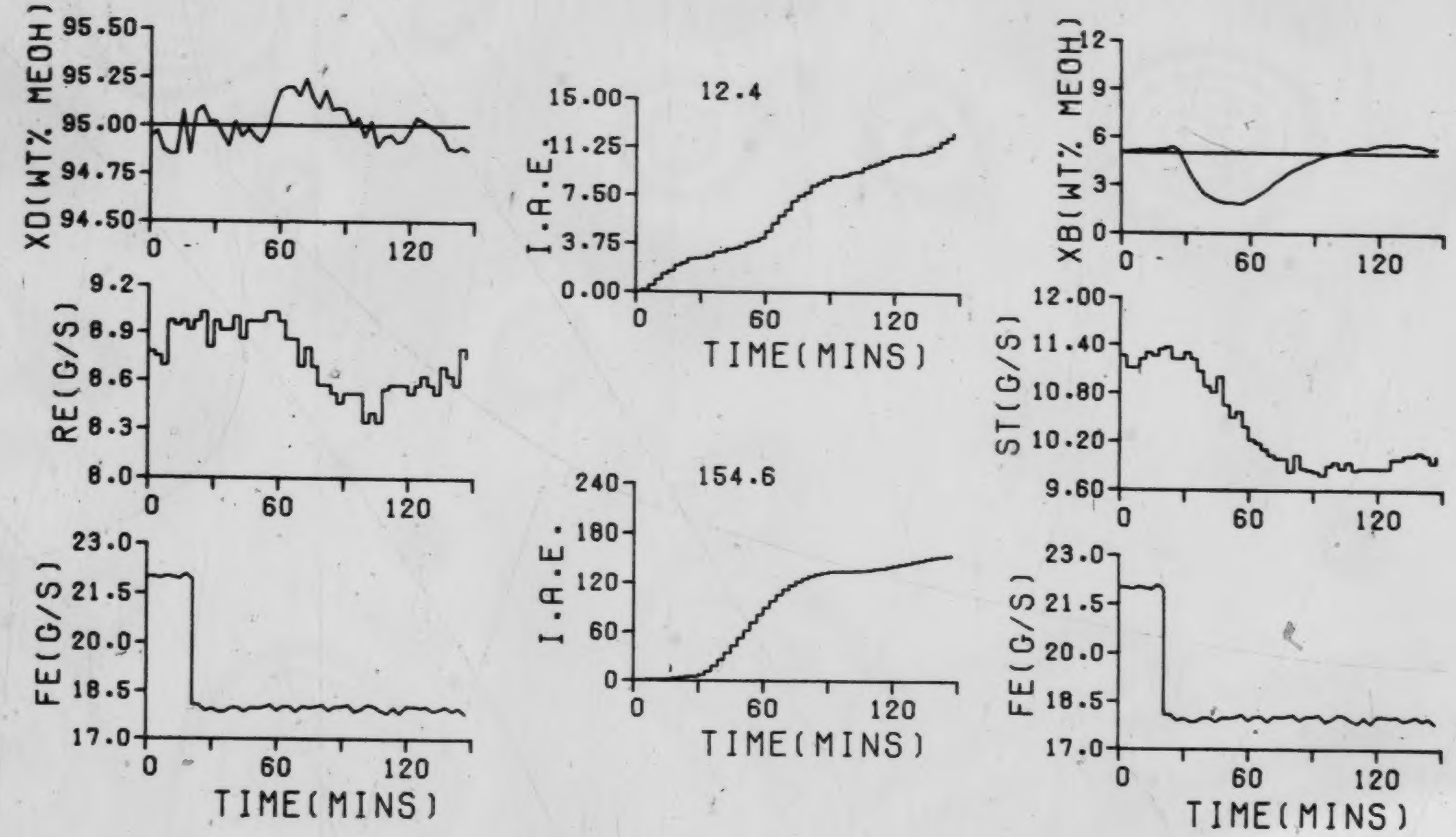

FIGURE 7.6 ML PID 3-C/PID(PB=55.88,TI=215.998,TD=0.0)/TS=180.0/
PID(PB=190.93,TI=422.083,TD=171.851)/TS=180.0/

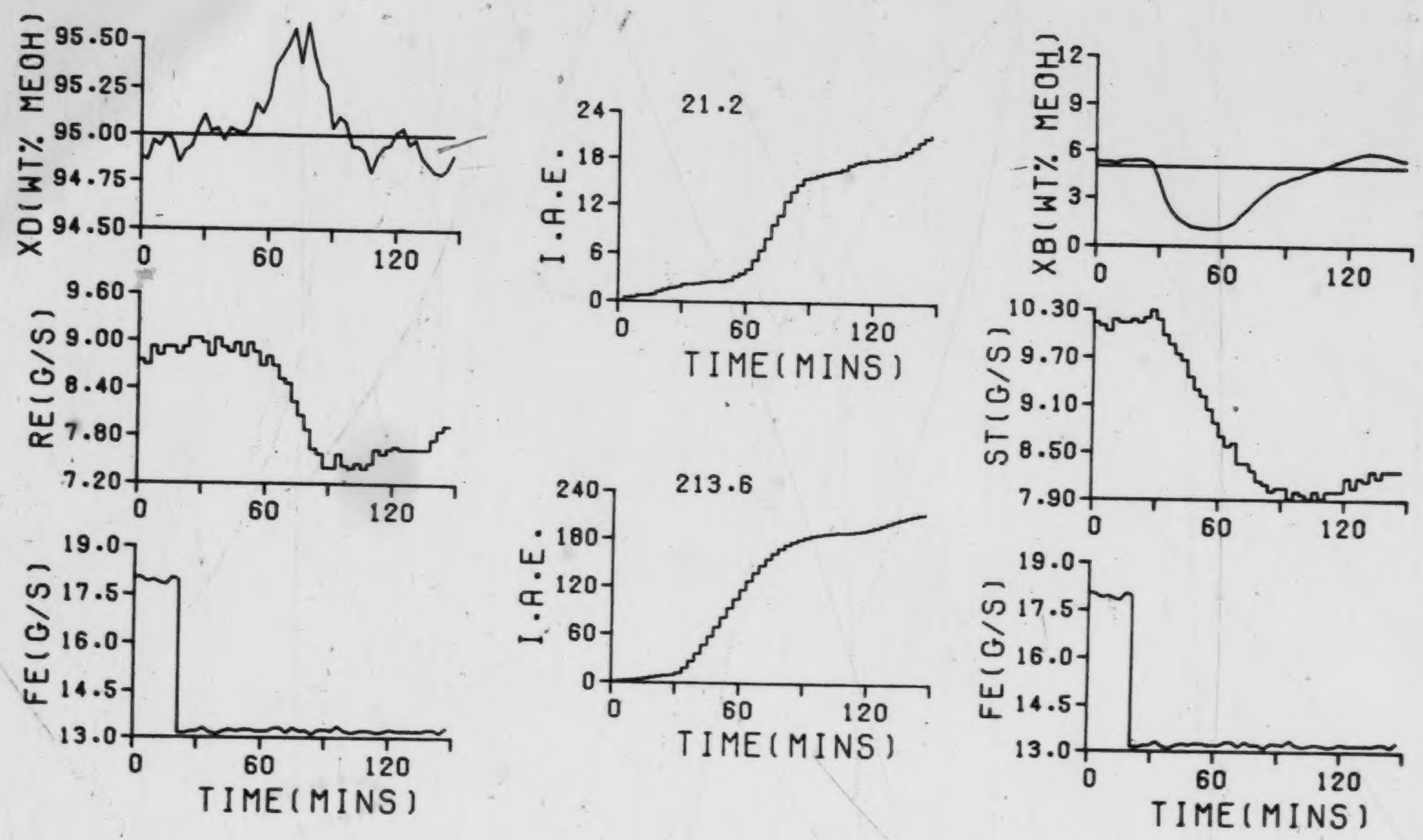

FIGURE 7.7 ML PID 3-C/PID(PB=55.88,TI=215.998,TD=0.0)/TS=180.0/
PID(PB=190.93,TI=422.083,TD=171.851)/TS=180.0/

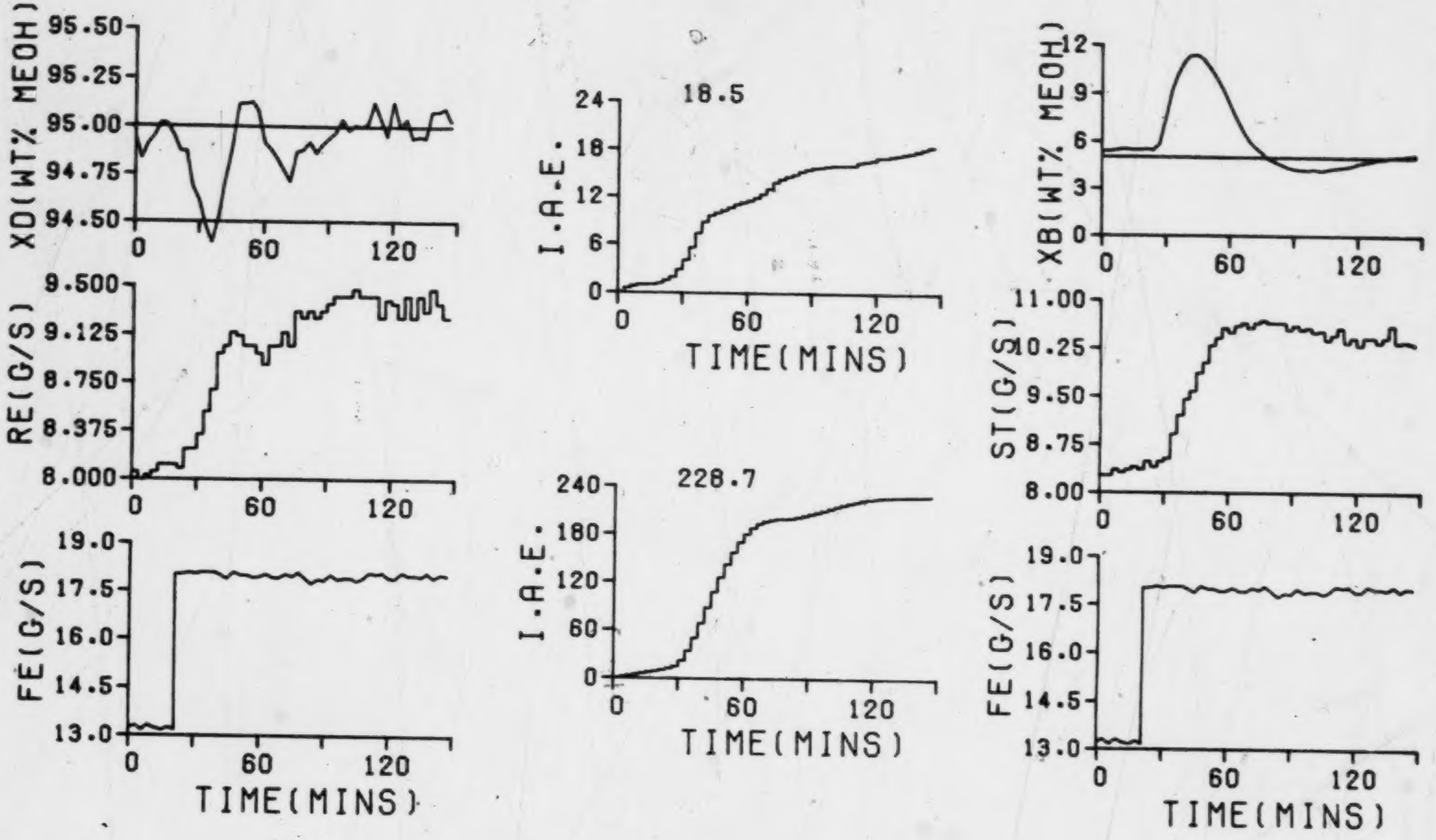

FIGURE 7.8 ML PID 3-C/PID(PB=55.88,TI=215.998,TD=0.0)/TS=180.0/
PID(PB=190.93,TI=422.083,TD=171.851)/TS=180.0/

Table 7.1.2
Multiloop PID Control Performance with Controller Constants Calculated from Cohen-Coon Equations

	IAE Values	
Step	TOP	BOTTOM
increase from steady state	15.7	183.9
decrease to steady state	12.4	154.6
decrease from steady state	21.2	213.6
increase to steady state	18.5	228.7
total	67.8	780.8

disturbance with a resulting IAE value of 15.7. Even under open loop conditions the top composition shows little change for this increase in feed rate, so this deviation is attributed to the interaction from changes in the steam flow resulting from bottom composition control. The bottom composition has returned to the setpoint prior to the completion of the test period of 150 minutes. The response when the feed flow is decreased to its steady state value is shown in Figure 7.6. Better regulation of the top composition is achieved in comparison to the response for the first step change in feed rate, as indicated by the lower IAE value of 12.4. The bottoms composition has returned to the setpoint with only a little overshoot and a corresponding IAE value of 154.6.

Figure 7.7 shows the response for the decrease in feed flow from its steady state. The top composition transient exhibits a large deviation, but the composition returns to the setpoint, resulting in an IAE value of 21.2. The bottom composition displays a similar response compared to the previous feed rate change, but results in a larger IAE value of 213.6, indicative of poorer control performance.

Increasing the feed rate back to its steady state value gives rise to the responses displayed in Figure 7.8. The top composition deviates from its setpoint at the onset of the disturbance, but returns to the setpoint prior to the completion of the test period resulting in an IAE value of 18.5. The bottom composition IAE value of 228.7 is typical of the responses in Figures 7.5 to 7.7 with some overshoot before the composition returns to the setpoint.

7.1.3 Control Performance with Constants Calculated using the Integral of Absolute Error Equations

Table 7.1.3 provides a summary of the IAE performance values for the tests of the control performance of the pilot plant distillation column when subjected to dual composition control with conventional PID controllers using constants calculated from the IAE criterion equations of Miller et al., 1967. The control performance that results using a multiloop PID control strategy with controller settings based on the IAE equations is portrayed by the responses in Figures 7.9 to 7.12. It can be observed from Figure 7.9 which shows the column responses for the increase in feed flow rate from its steady state value that the top composition deviates from the setpoint at the start of the

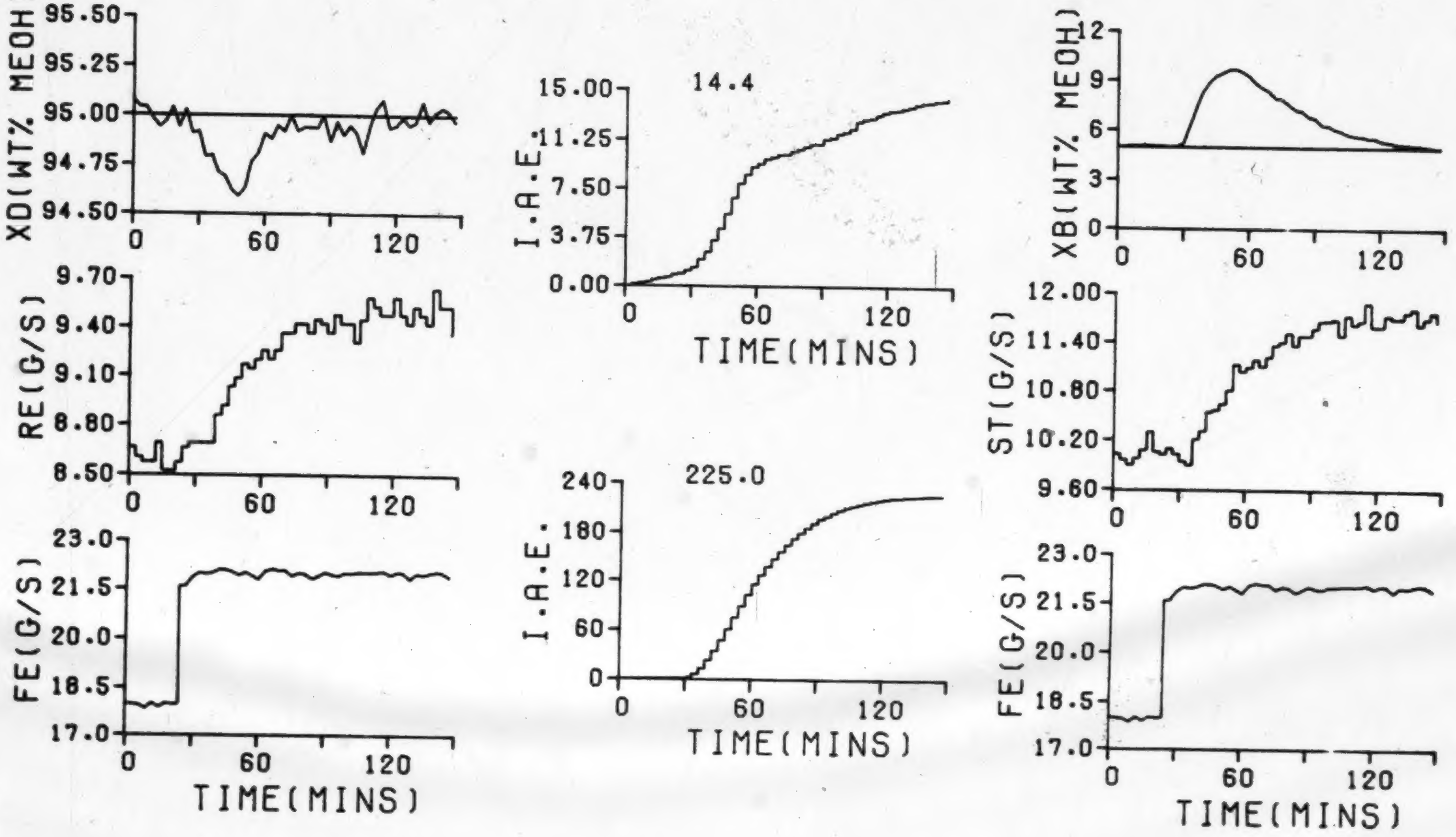

FIGURE 7.9 ML PID IAE/PID(PB=50.525,TI=335.787,TD=0.0)/TS=180.0/
PID(PB=187.135,TI=643.232,TD=191.613)/TS=180.0/

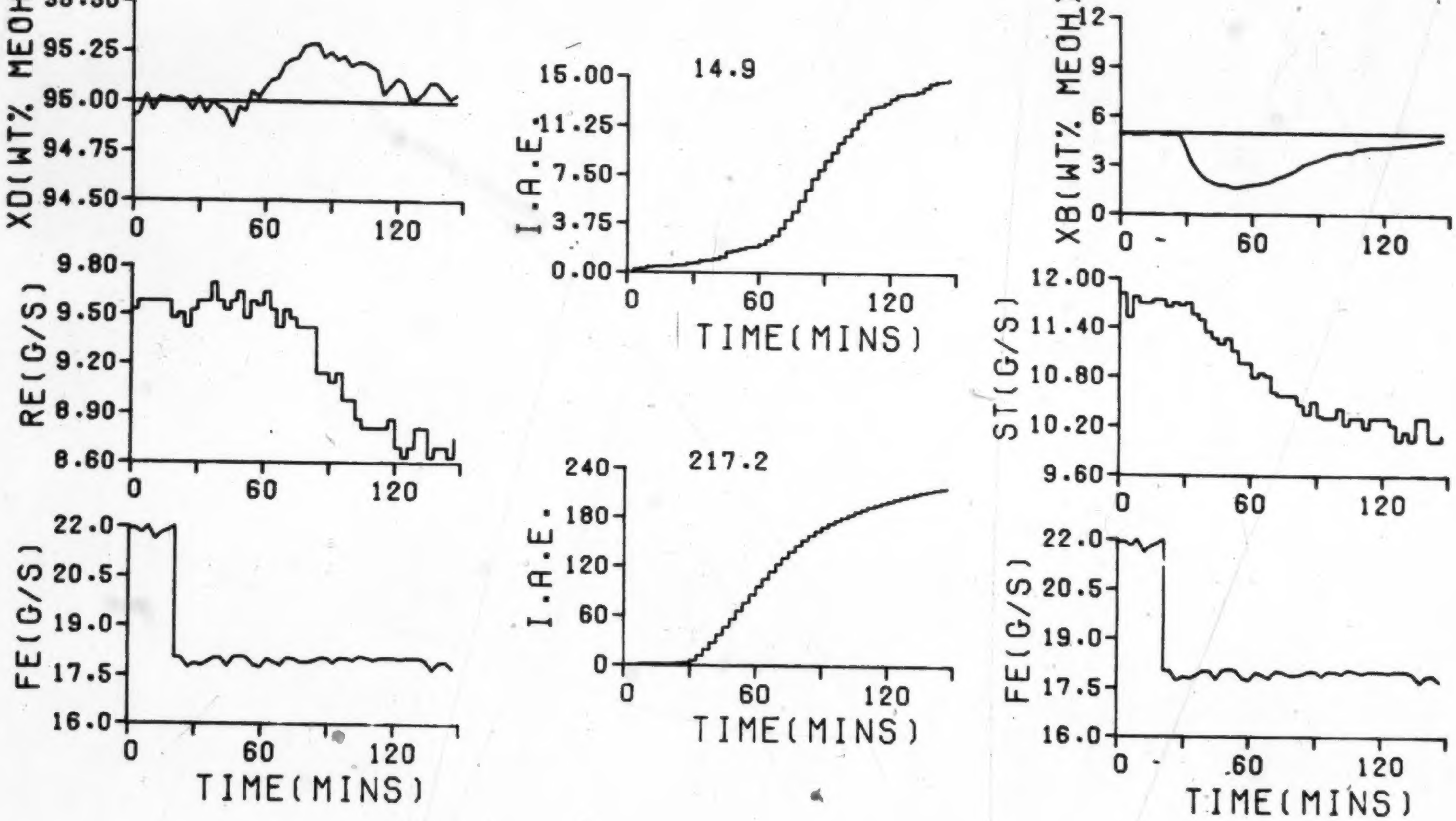

FIGURE 7.10 ML PID IAE/PID(PB=50.525,TI=335.787,TD=0.0)/TS=180.0/
PID(PB=187.135,TI=643.232,TD=191.613)/TS=180.0/

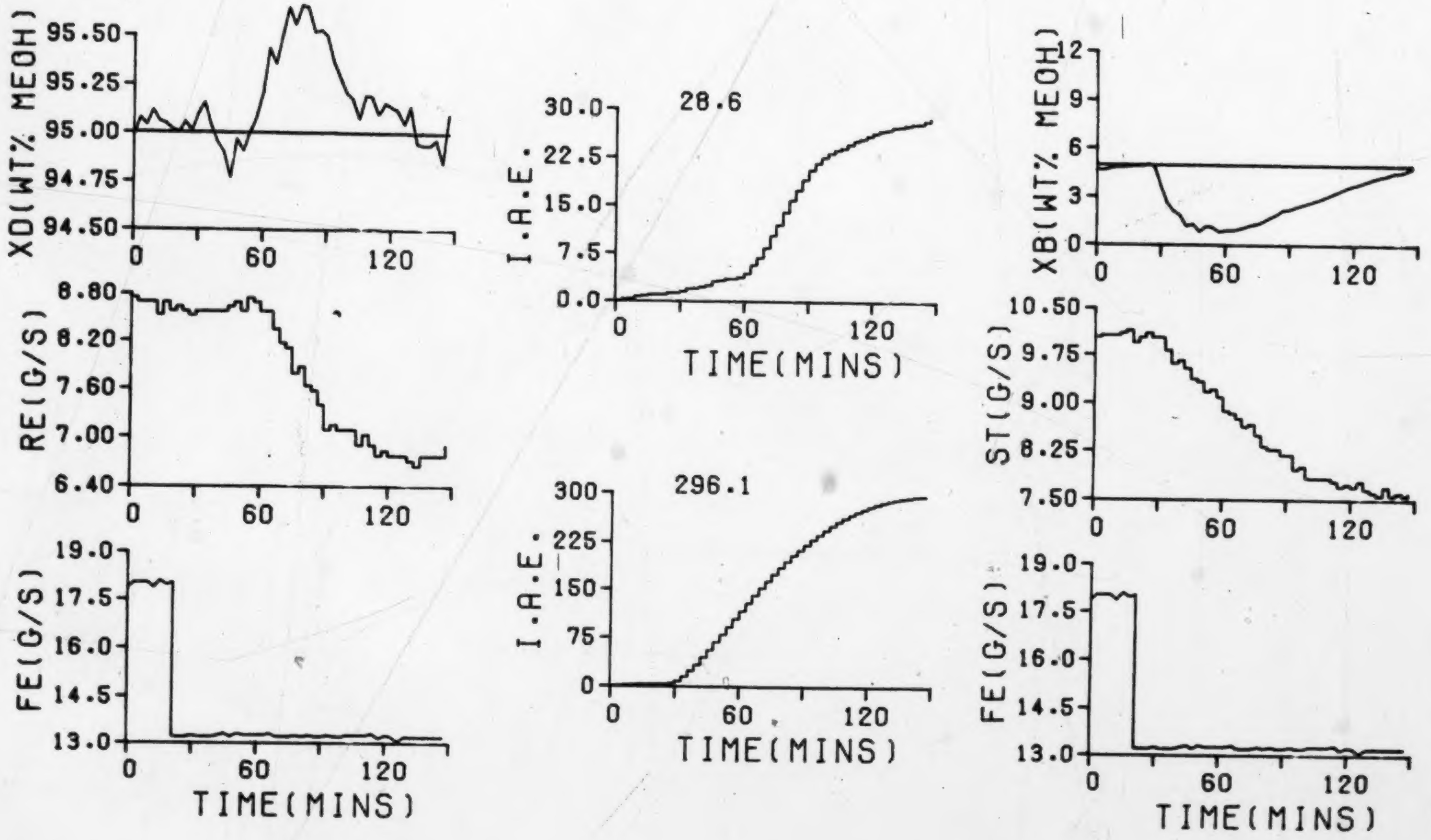

FIGURE 7.11 ML PID IAE/PID(PB=50.525,TI=335.787,TD=0.0)/TS=180.0/
PID(PB=187.135,TI=643.232,TD=191.613)/TS=180.0/

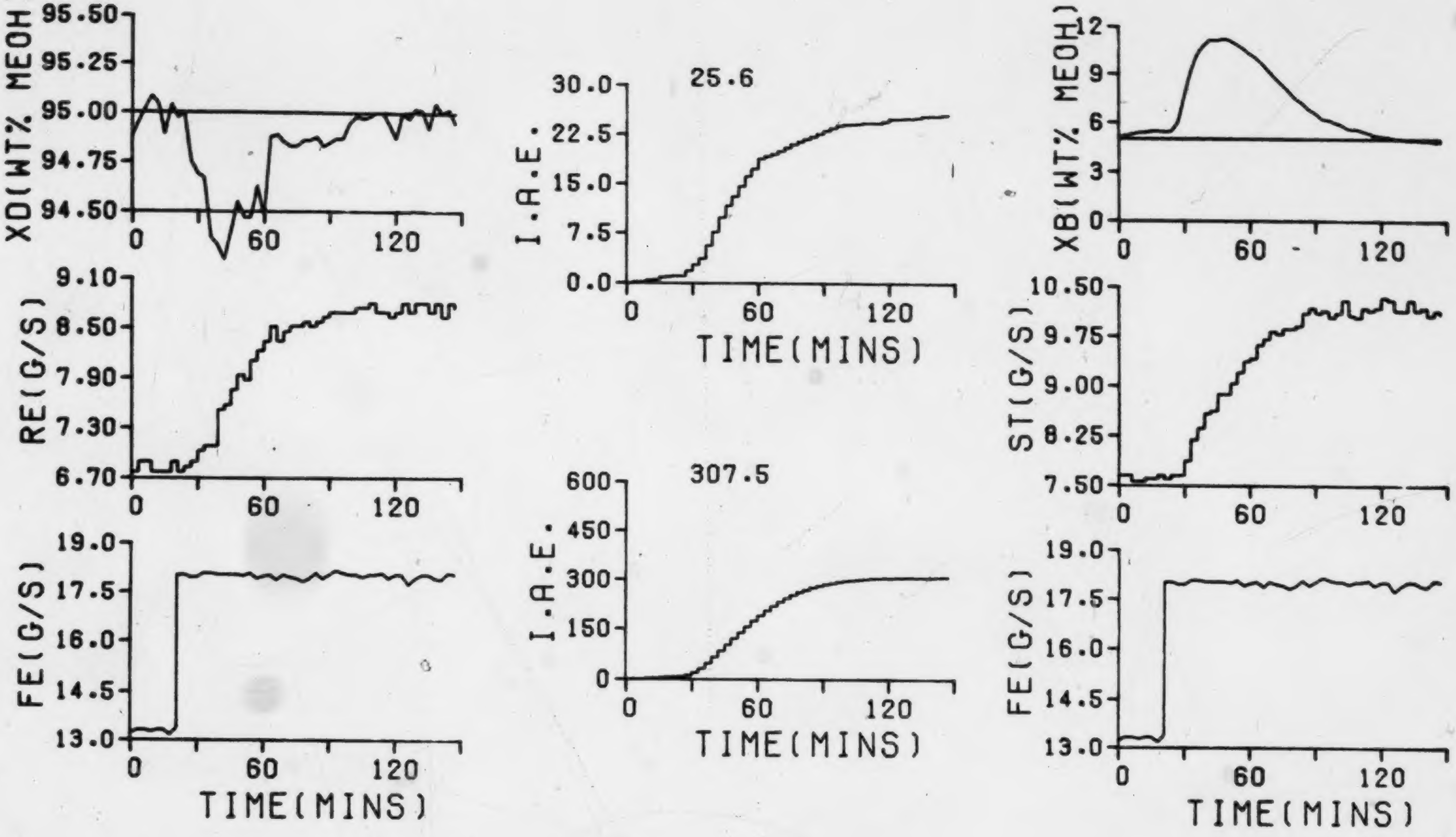

FIGURE 7.12 ML PID IAE/PID(PB=50.525,TI=335.787,TD=0.0)/TS=180.0/
PID(PB=187.135,TI=643.232,TD=191.613)/TS=180.0/

Table 7.1.3
Multiloop PID Control Performance with Controller Constants Calculated from Integral of Absolute Error Equations

	IAE Values	
Step	TOP	BOTTOM
increase from steady state	14.4	225.0
decrease to steady state	14.9	217.2
decrease from steady state	28.6	296.1
increase to steady state	25.6	307.5
total	83.5	1045.8

disturbance but returns with a small IAE value of 14.4. This satisfactory behavior does not result for the bottom loop as the composition deviates by a large amount giving rise to an IAE value of 225.0.

For the decrease in feed flow rate to the steady state value it can be seen from the results in Figure 7.10 that neither the top or bottom composition return to the setpoint by the completion of the test period, resulting in IAE values of 14.9 and 217.2 respectively. The bottom composition returns to the setpoint shortly after the end of the test period as indicated by the initial portion of the responses shown in Figure 7.11 for the decrease in feed rate from its steady state value. This step of the disturbance gave rise to an inverse response characteristic (cf. Figure 5.3), so the large deviation of the top composition from the setpoint which resulted in the large IAE value of 28.6 is to be expected. Despite the large IAE value of 296.1, for the bottom loop, the composition did return to the setpoint prior to the completion of the test period, as did the top composition. When the feed flow rate was increased to its steady state value both the top and bottom compositions did return to their setpoints before the end of the test period, but displayed large deviations from the setpoint, as can be seen from Figure 7.12, giving rise to IAE values of 25.6 and 307.6.

These results for multiloop PID control of the distillation column using controller constants calculated from IAE criterion equations indicate that the control performance is marginally acceptable. The compositions deviate from the setpoint, but eventually do return prior to the completion of the test run. Manipulation of the reflux and steam flows is accomplished smoothly, with rather large changes in operating regions to return to target.

7.1.4 Control Performance with Constants Calculated using the Integral of Time Multiplied by the Absolute Error Equations

Table 7.1.4 provides a summary of the IAE performance values for the tests of the control performance of the pilot plant distillation column when subjected to dual composition control with conventional PID controllers using constants calculated from the ITAE criterion equations of Miller et al., 1967. Column performance for operation under a multiloop PID control strategy with controller settings

Table 7.1.4
Multiloop PID Control Performance with Controller Constants Calculated from Integral of Time Multiplied by the Absolute Error Equations

	IAE Values	
Step	TOP	BOTTOM
increase from steady state	14.9	248.9
decrease to steady state	15.1	243.8
decrease from steady state	18.6	270.5
increase to steady state	37.8	395.0
total	86.4	1158.2

calculated from the ITAE equations is illustrated by the responses in Figures 7.13 to 7.16. As can be seen from the response of the bottom composition for the increase in feed rate presented in Figure 7.13, there is a large deviation from the setpoint with a slow return resulting in an IAE value of 248.9. The top composition response shows similar behavior, but does return to the setpoint. However, considering the nature of the open loop response (cf. Figure 5.3) the composition regulation for this flow change is relatively poor, which is attributed to the large proportional band (low gain) calculated from the ITAE criterion equations used to determine the controller settings.

Figure 7.14 shows that the bottom composition deviates markedly from the setpoint as the feed change is first introduced, but does return to the setpoint, giving rise to

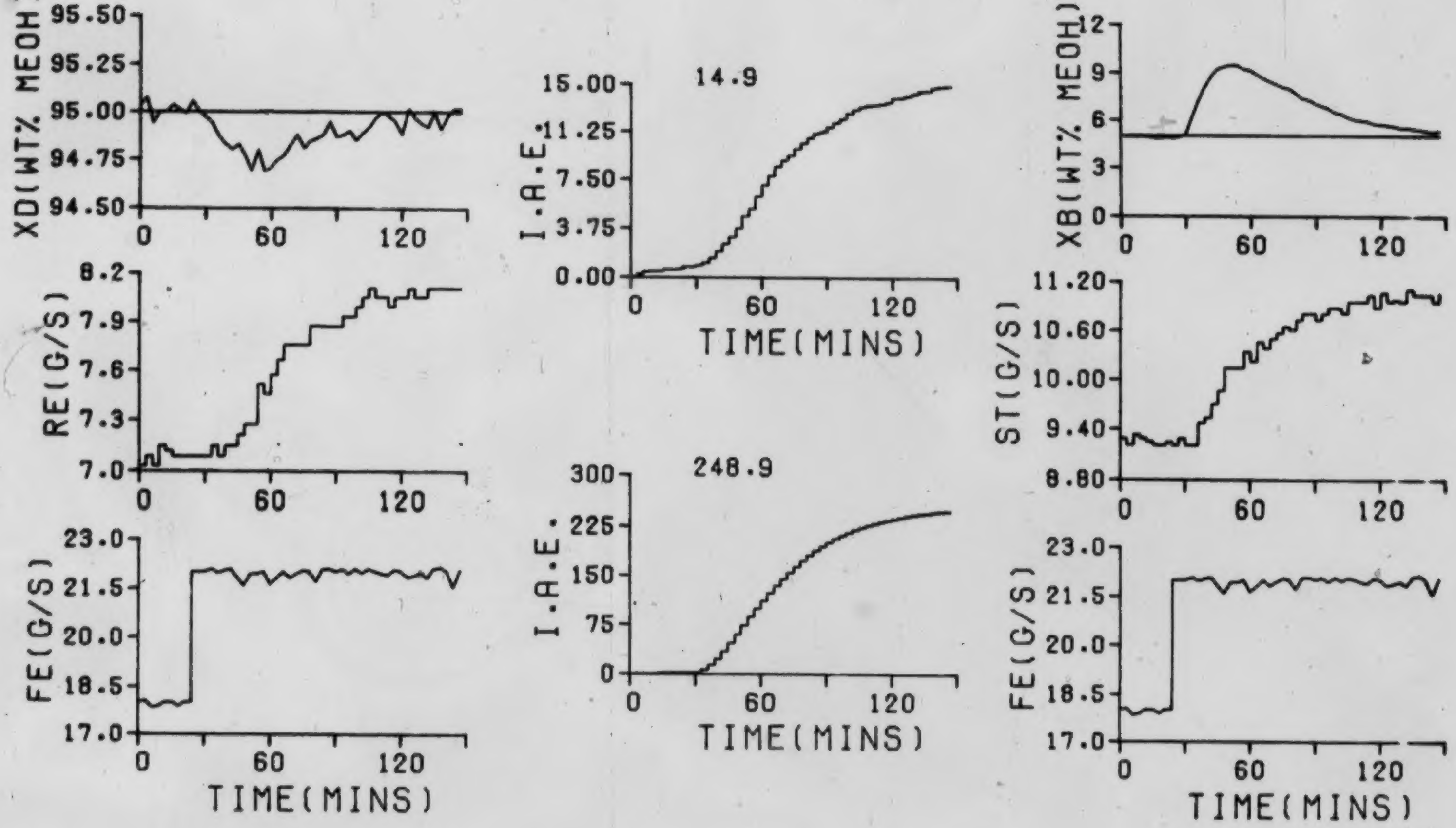

FIGURE 7.13 ML PID ITAE/PID(PB=58.429,TI=311.853,TD=0.0)/TS=180.0/
PID(PB=193.29,TI=670.77,TD=172.23)/TS=180.0/

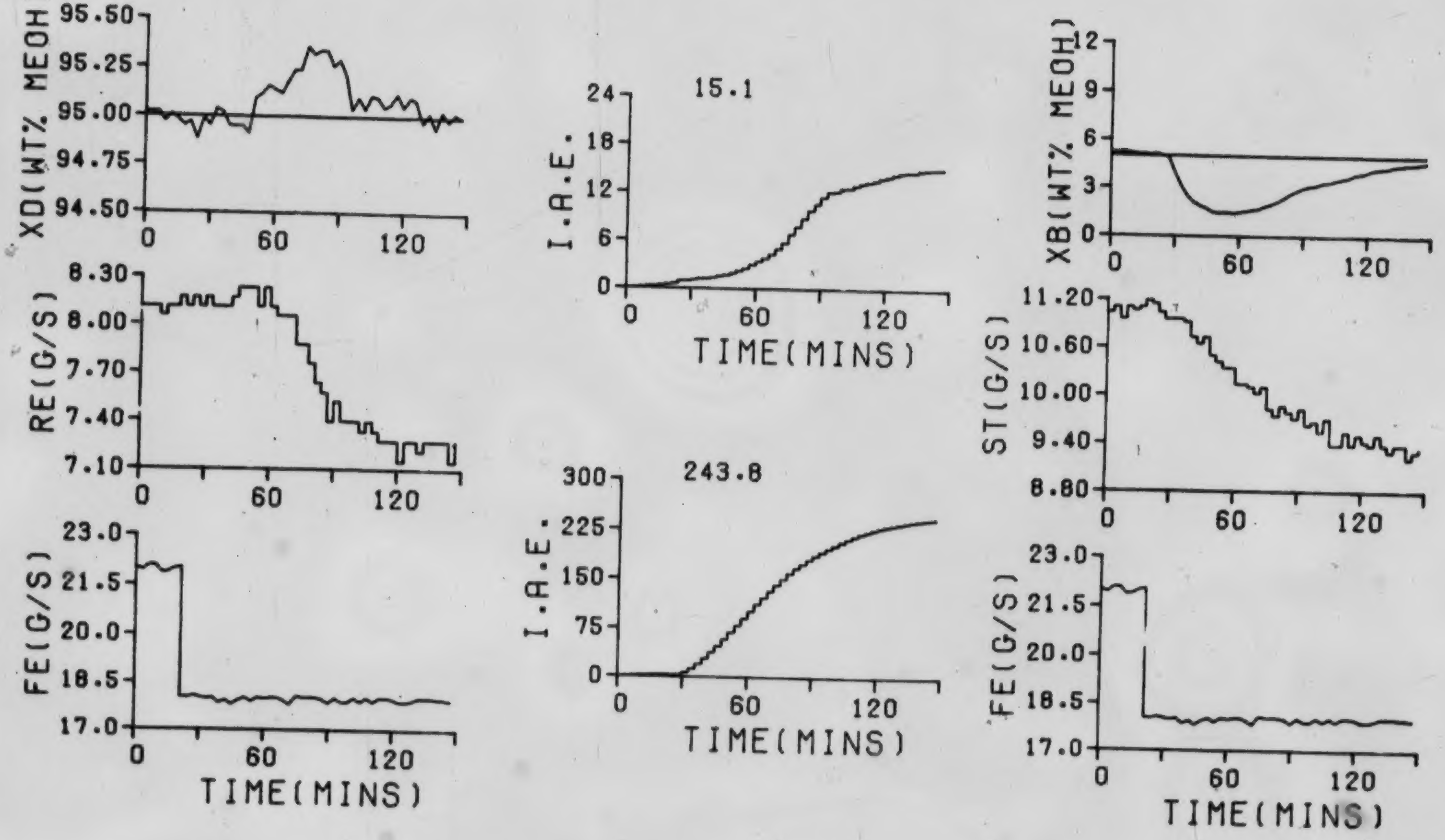

FIGURE 7.14 ML PID ITAE/PID(PB=58.429,TI=311.853,TD=0.0)/TS=180.0/
PID(PB=193.29,TI=670.77,TD=172.23)/TS=180.0/

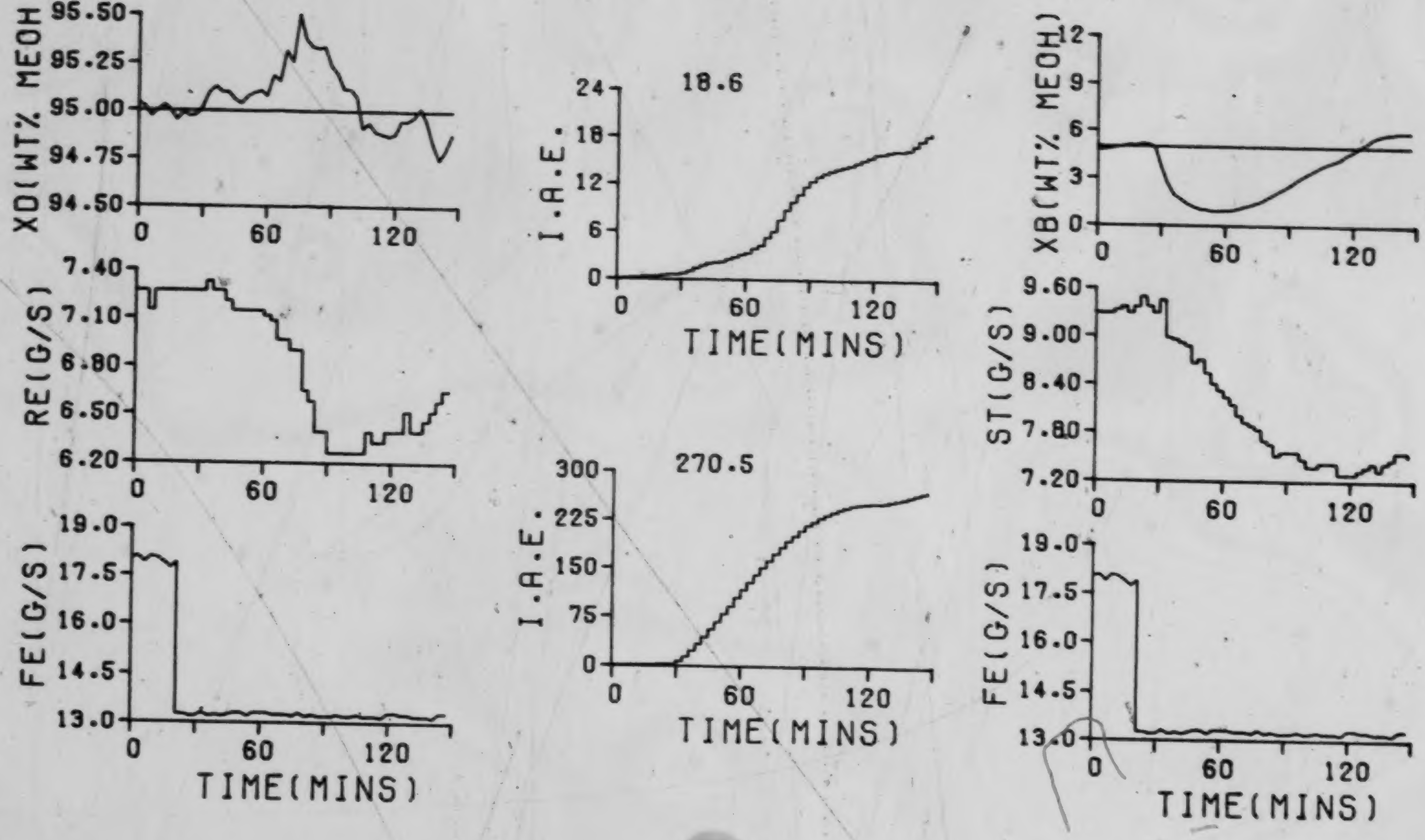

FIGURE 7.15 ML PID ITAE/PID(PB=58.429.TI=311.853.TD=0.0)/TS=180.0/
PID(PB=193.29.TI=670.77.TD=172.23)/TS=180.0/

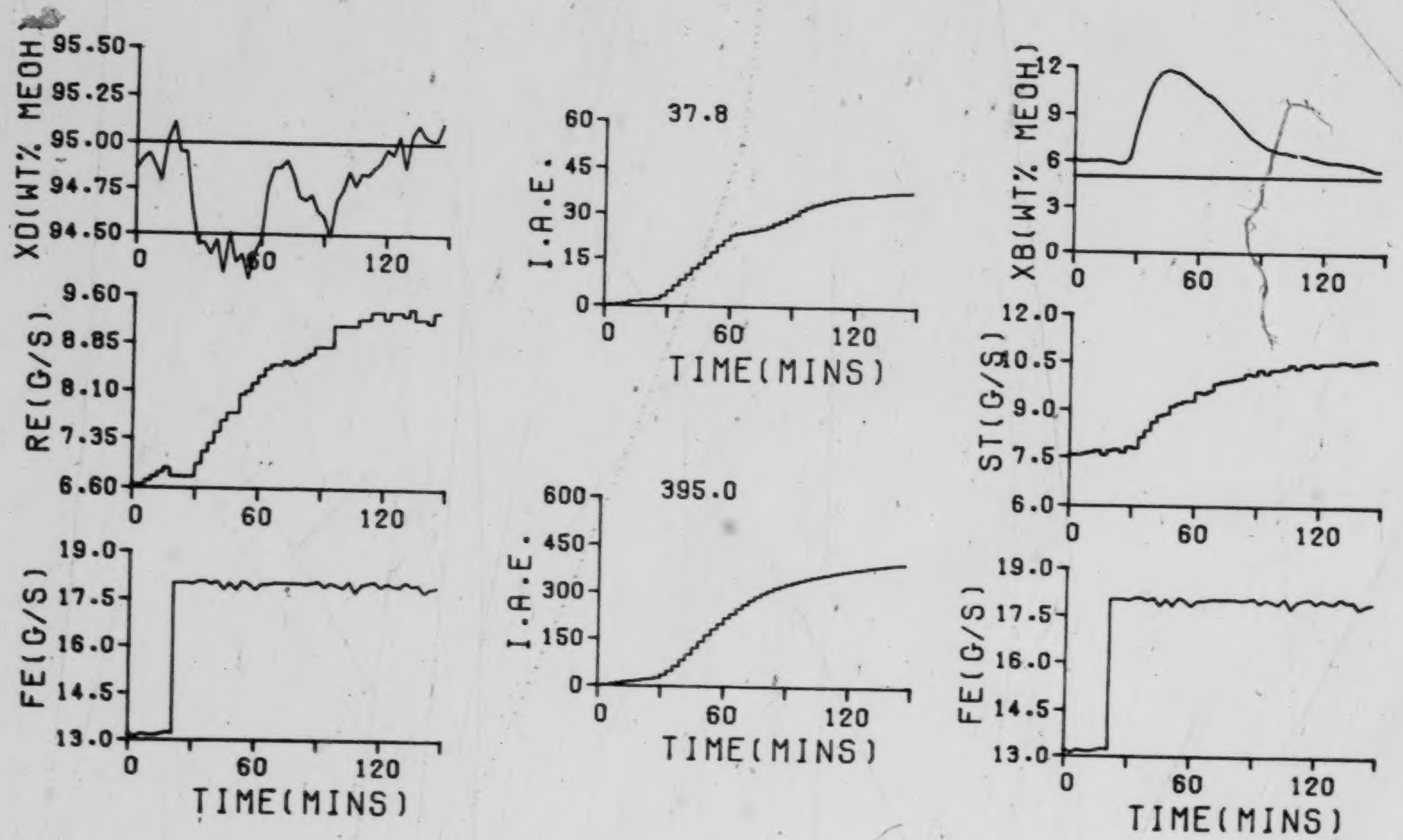

FIGURE 7.16 ML PID ITAE/PID(PB=58.429.TI=311.853.TD=0.0)/TS=180.0/
PID(PB=193.29.TI=670.77.TD=172.23)/TS=180.0/

an IAE value of 243.8. Control behavior of the top composition is similar to that of Figure 7.13, with an IAE value of 15.1.

For the decrease in feed flow from its steady state value, the response of the bottom composition in Figure 7.15 shows that the control is unsatisfactory with an overshoot preventing its return to the setpoint. The top composition response is similar, also not returning to the setpoint before the completion of the test period. For the increase in feed flow rate back to the steady state value, the top composition response exhibits a large and sustained deviation from the setpoint as shown in Figure 7.16, so it is not surprising that the resulting IAE value of 37.8 is higher than observed for the other feed changes. Regulation of bottom composition is unacceptable as the composition remains above the setpoint for the entire duration of the test period.

The testing of multiloop PID control of product compositions with controller settings calculated using the ITAE criterion equations has shown that in general poor regulation results, particularly when compared to the control behavior that resulted using the Cohen-Coon constants. This is considered to be due to the reduced gain and the reduced integral action.

7.1.5 Summary of Column Control Performance Using a Multiloop PID Control Strategy for Calculated Controller Settings

The control performance operating the column under multiloop PID control, as shown by the responses in Figures 7.1 to 7.16, with the controller constants calculated from the various equations (cf. equations 6.6 to 6.8) leads to significantly different behavior. The performance index (IAE value) for each of the individual responses, and the total IAE for each of the four step changes are summarized in Table 7.1.5.

Four parameter selection methods have been presented with respect to the column response when disturbed by identical feed flow patterns. It is evident from the results in Figures 7.5 to 7.8 that better control of the column compositions has been attained by using the Cohen-Coon controller constant selection technique, as compared to the other three methods. Comparison of the column responses in Figures 7.5 to 7.8 with respect to the magnitude of the initial deviations from the setpoint shows that similar values of initial deviations resulted from the Z-N and 3-C selection methods. The improved performance that results using the Cohen-Coon controller settings is attributed to the increased integral action. For the bottom composition control, the reduced derivative action also contributes to the better performance. This tabulation shows that the best overall product composition regulation for the four feed

Table 7.1.5
IAE Values for Multiloop PID Control Based on Calculated Controller Constants

		IAE Values by Method			
Step		Z-N	3-C	IAE	ITAE
increase from SS	top	8.0	15.7	14.4	14.9
	bottom	255.9	183.9	225.0	248.9
decrease to SS	top	21.0	12.4	14.9	15.1
	bottom	267.7	154.6	217.2	243.8
decrease from SS	top	49.3	21.2	28.6	18.6
	bottom	421.5	213.6	296.1	270.5
increase to SS	top	38.1	18.5	25.6	37.8
	bottom	449.7	228.7	307.5	395.0
total	top	116.4	67.8	83.5	86.4
	bottom	1394.8	780.8	1045.8	1158.2
total		1511.2	848.6	1129.3	1244.6

rate disturbances was obtained for controller settings calculated using the Cohen-Coon method. The control performance correlates with the values of the respective controller constants. As can be observed from Tables 6.2 and 6.3, Application of the Cohen-Coon equations results in the largest amount of integral action of any of the four methods. The lower amount of derivative action for the bottom composition controller, calculated using the Cohen-Coon equations was also considered to be a strong factor leading to this method providing the most satisfactory control performance of the four methods used.

7.2 Control of Product Composition Using a Multirate PID Control Strategy

This section presents the results from a series of tests conducted using a sample time of 1.0 minute for the top composition loop to examine the effect of a shorter sample time on column control performance. The sample time for the bottom loop was maintained at 3.0 minutes.

7.2.1 Control Performance With Constants Calculated from the Ziegler-Nichols Equations

Table 7.2.1 provides a summary of the IAE performance values for the tests of the control performance of the pilot plant distillation column when subjected to dual composition control with conventional PID controllers using constants calculated with the Ziegler-Nichols equations. The column performance that resulted using the Ziegler-Nichols equations to calculate controller constants for the four different step changes in feed rate is presented in Figures 7.17 to 7.20. The column responses for an increase in feed flow rate from its steady state value displayed in Figure 7.17 shows that the top composition is virtually unaffected by the feed flow disturbance. The changes in the reflux flow, demanded by the top composition controller have almost completely compensated for the effect of the disturbance on top composition, to yield a very small IAE value of 6.3. The bottom composition response indicates a large, slowly diminishing deviation from the setpoint with the composition

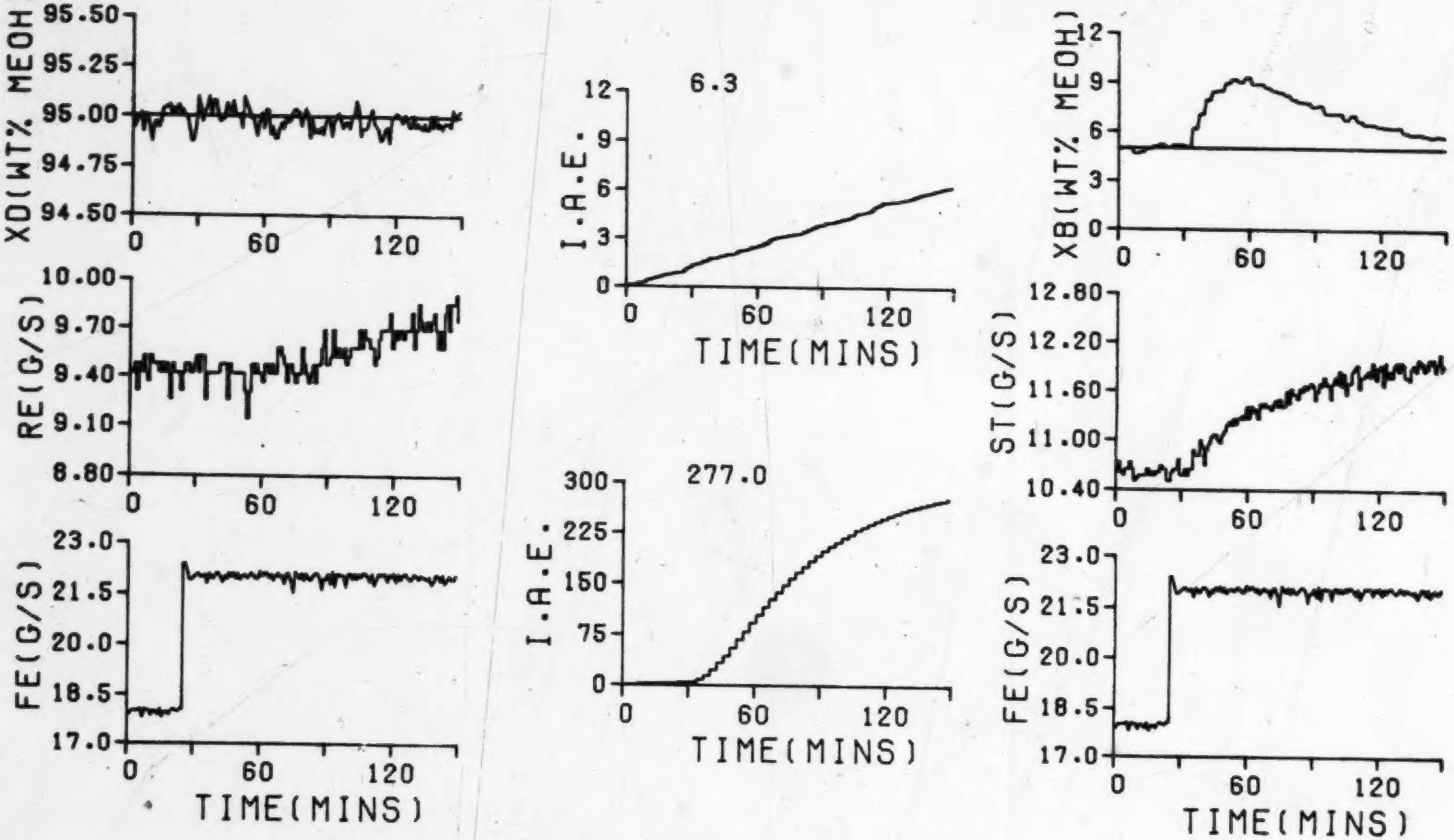

FIGURE 7.17 MR PID Z-N/PID(PB=32.659,TI=299.97,TD=0.0)/TS=60.0/
PID(PB=208.35,TI=900.0,TD=225.0)/TS=180.0/

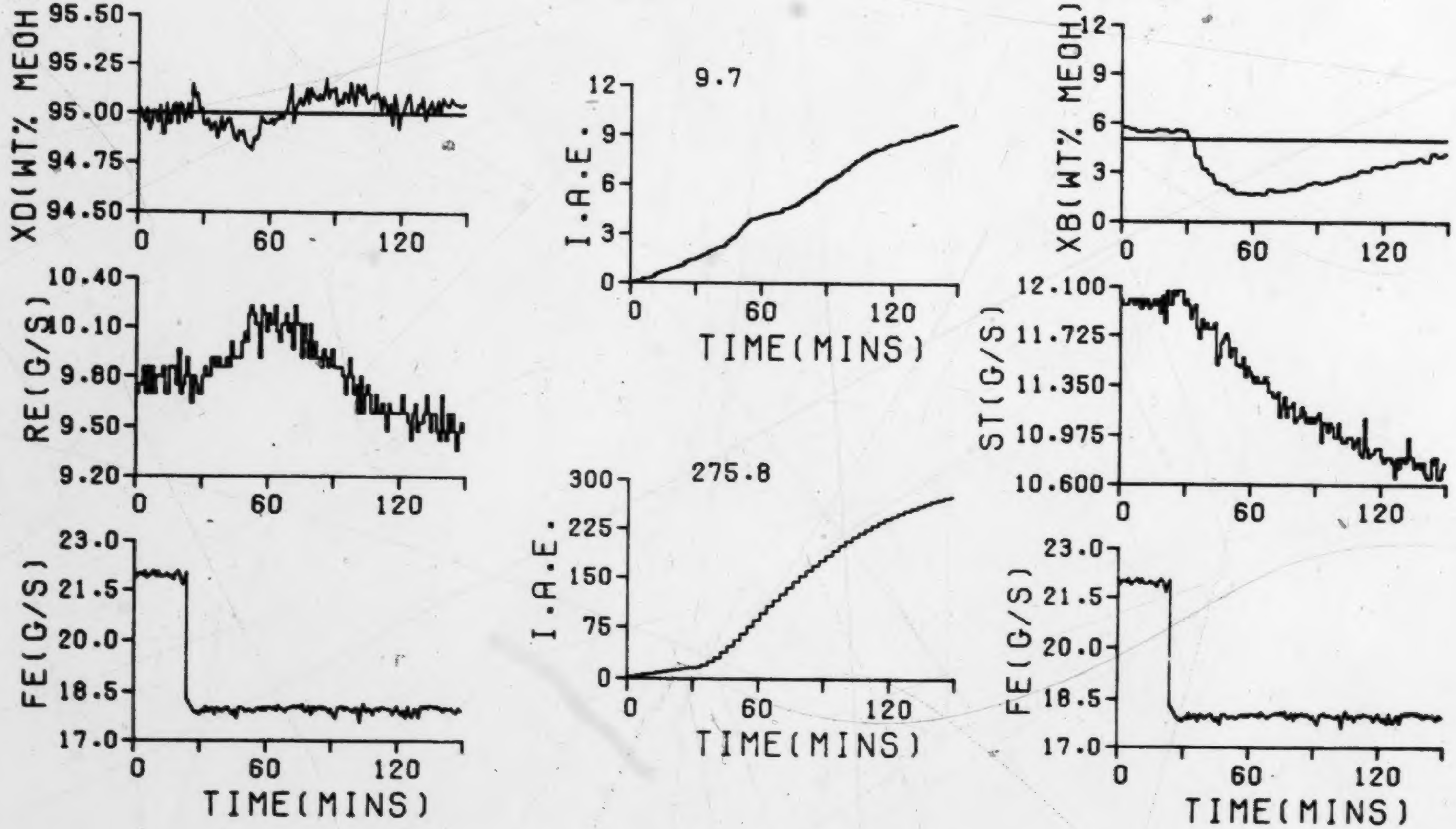

FIGURE 7.18 MR PID Z-N/PID(PB=32.659,TI=299.97,TD=0.0)/TS=60.0/
PID(PB=208.35,TI=900.0,TD=225.0)/TS=180.0/

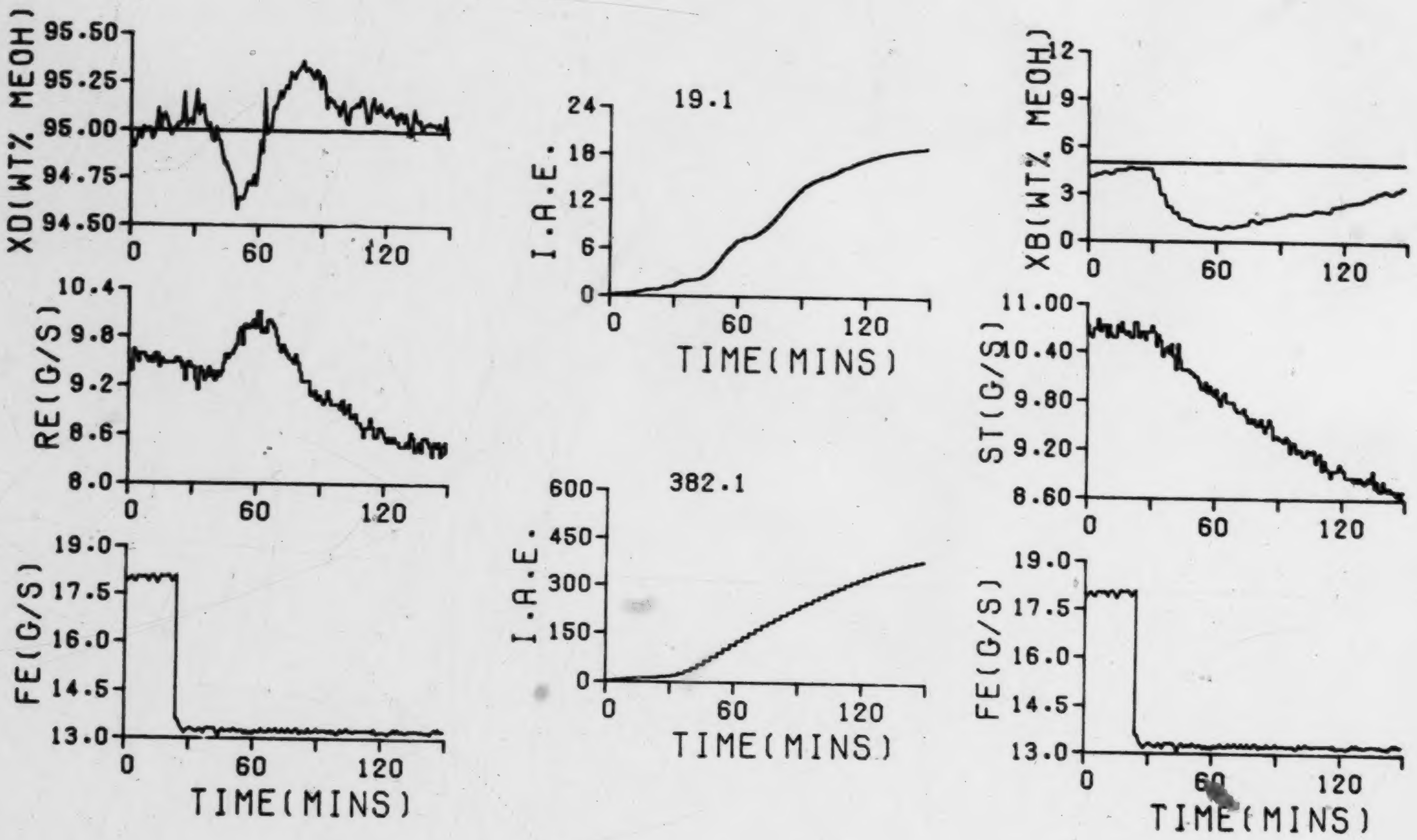

FIGURE 7.19 MR PID Z-N/PID(PB=32.659,TI=299.97,TD=0.0)/TS=60.0/ PID(PB=208.35,TI=900.0,TD=225.0)/TS=180.0/

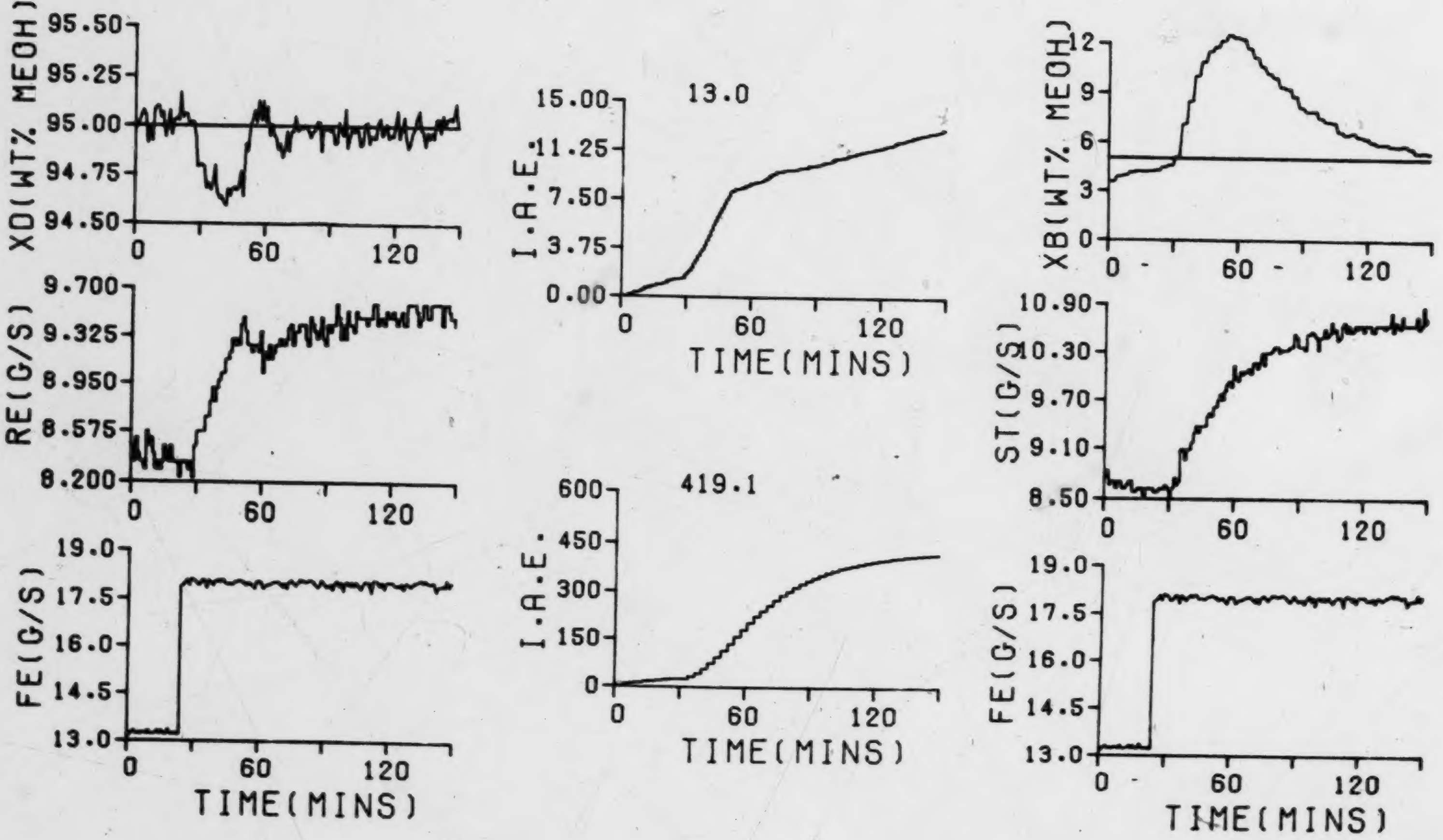

FIGURE 7.20 MR PID Z-N/PID(PB=32.659,TI=299.97,TD=0.0)/TS=60.0/
PID(PB=208.35,TI=900.0,TD=225.0)/TS=180.0/

Table 7.2.1
Multirate PID Control Performance with Controller Constants Calculated from Ziegler-Nichols Equations

	IAE Values	
Step	TOP	BOTTOM
increase from steady state	6.3	277.0
decrease to steady state	9.7	275.8
decrease from steady state	19.1	382.1
increase to steady state	13.0	419.1
total	48.1	1354.0

remaining above the setpoint at the completion of the test period. This sustained deviation from the setpoint assists the top composition controller, since interaction from the steam flow is minimal. The response to a decrease in feed flow rate to its steady state value is presented in Figure 7.18. The top composition regulation shows small deviations, giving rise to a slightly higher IAE value of 9.7. The bottom composition response is virtually a mirror image of that in Figure 7.17, with the bottom composition not returning to the setpoint at the completion of the test period.

For a decrease in feed flow rate from its steady state value the observed column responses are presented in Figure 7.19. This feed disturbance demonstrated an inverse response characteristic in the top composition (cf. Figure 5.3), so it is not surprising that the top composition undergoes a variety of changes, as the controller attempts to compensate for deviations in top composition, yet eventually returns the top composition to the setpoint, whereas the bottom composition remains below the setpoint for the duration of the feed disturbance.

Figure 7.20 shows the response for an increase in feed flow rate to its steady state value. The top composition undergoes a short period of deviation from the setpoint as a result of the feed disturbance, but quickly returns. The bottom composition shows a significant deviation from the setpoint so it is not surprising that the IAE value of 419.1 is higher than for the other feed rate changes. Regulation of the top composition for this change in feed flow is not entirely satisfactory as demonstrated by the large IAE value of 13.0.

7.2.2 Control Performance with Constants Calculated using the Cohen-Coon Equations

Table 7.2.2 provides a summary of the IAE performance values for the tests of the control performance of the pilot plant distillation column when subjected to dual composition control with conventional PID controllers using constants calculated with the Cohen-Coon equations. Figures 7.21 through 7.24 present the responses for control of the distillation column with controller constants based on the Cohen-Coon (3-C) equations. The distillation column control performance resulting from an increase in feed flow rate from its steady state value is presented in Figure 7.21. The

Table 7.2.2
Multirate PID Control Performance with Controller Constants Calculated from Cohen-Coon Equations

	IAE Values	
Step	TOP	BOTTOM
increase from steady state	9.2	196.9
decrease to steady state	8.8	173.9
decrease from steady state	12.6	252.4
increase to steady state	10.8	264.7
total	41.4	887.9

results of open loop tests and previous control performance have indicated that this feed change has little effect on the top composition, yet changes in reflux flow show that the interaction from the steam flow requires the top composition controller to compensate for changes in the steam flow resulting in an IAE value for the top composition control of 9.2. The bottom composition deviates from the setpoint with the onset of the feed change but returns by the completion of the test period yielding an IAE value of 196.9, which is lower than the value of 277.0 achieved using the Ziegler-Nichols equations.

The column performance obtained for a decrease in feed flow rate to its steady state value is shown in Figure 7.22. The top composition control shows slight deviations as a result of the feed disturbance but returns to the setpoint value prior to the completion of the test period. The bottom composition also returns to the setpoint after an initial

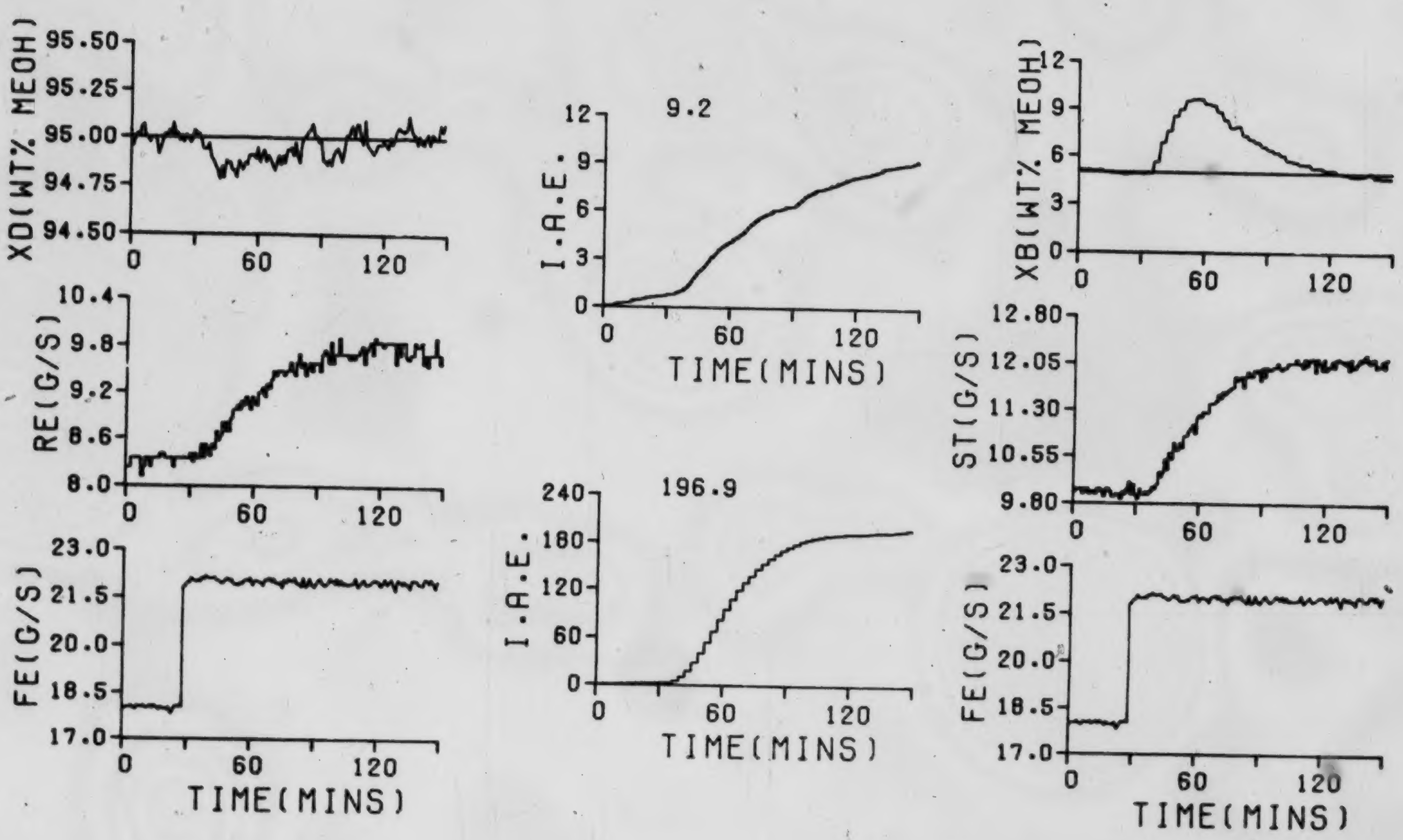

FIGURE 7.21 MR PID 3-C/PID(PB=34.466,TI=160.366,TD=0.0)/TS=60.0/
PID(PB=190.937,TI=422.083,TD=171.851)/TS=180.0/

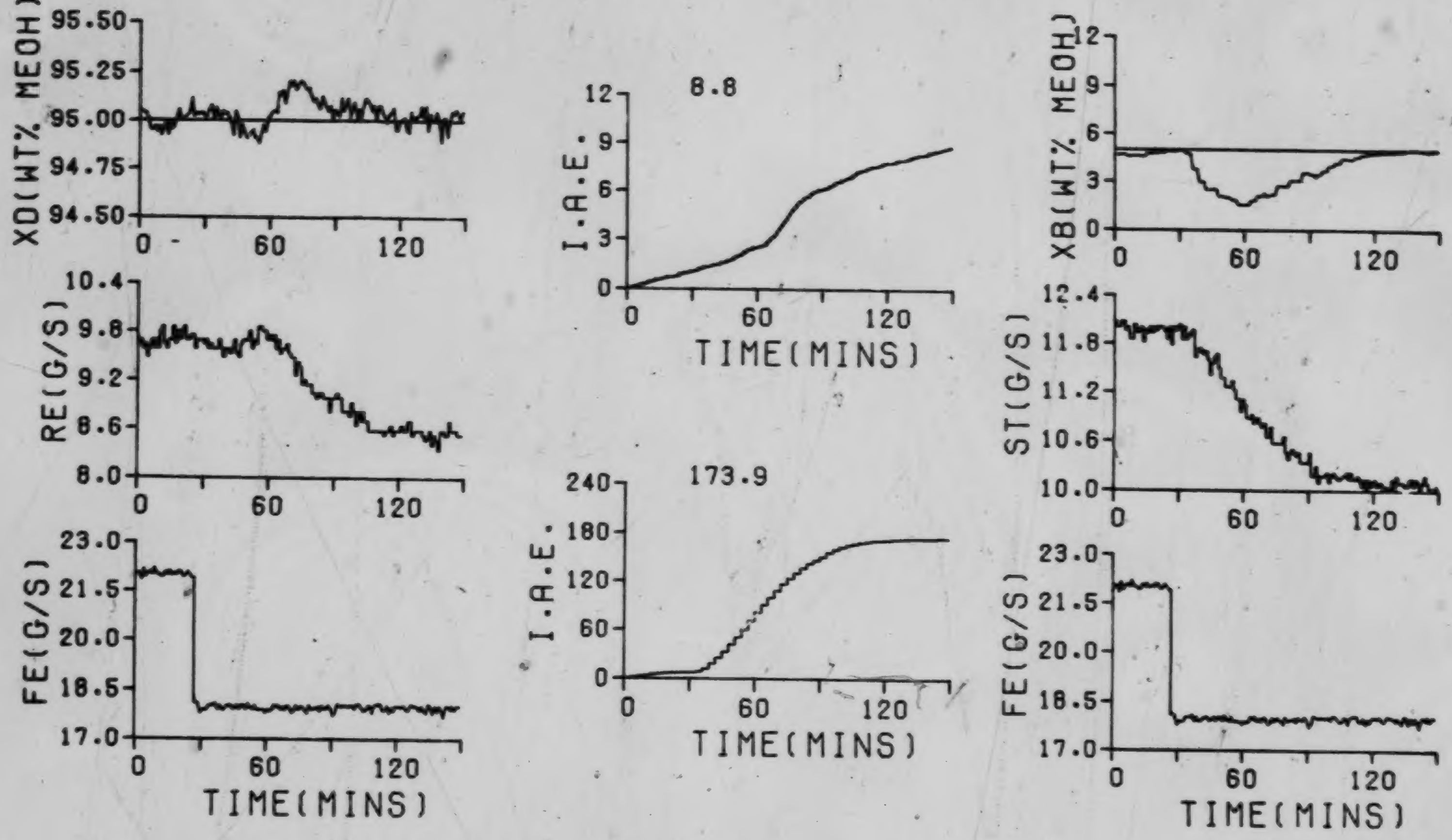

FIGURE 7.22 MR PID 3-C/PID(PB=34.466,TI=160.366,TD=0.0)/TS=60.0/
PID(PB=190.937,TI=422.083,TD=171.851)/TS=180.0/

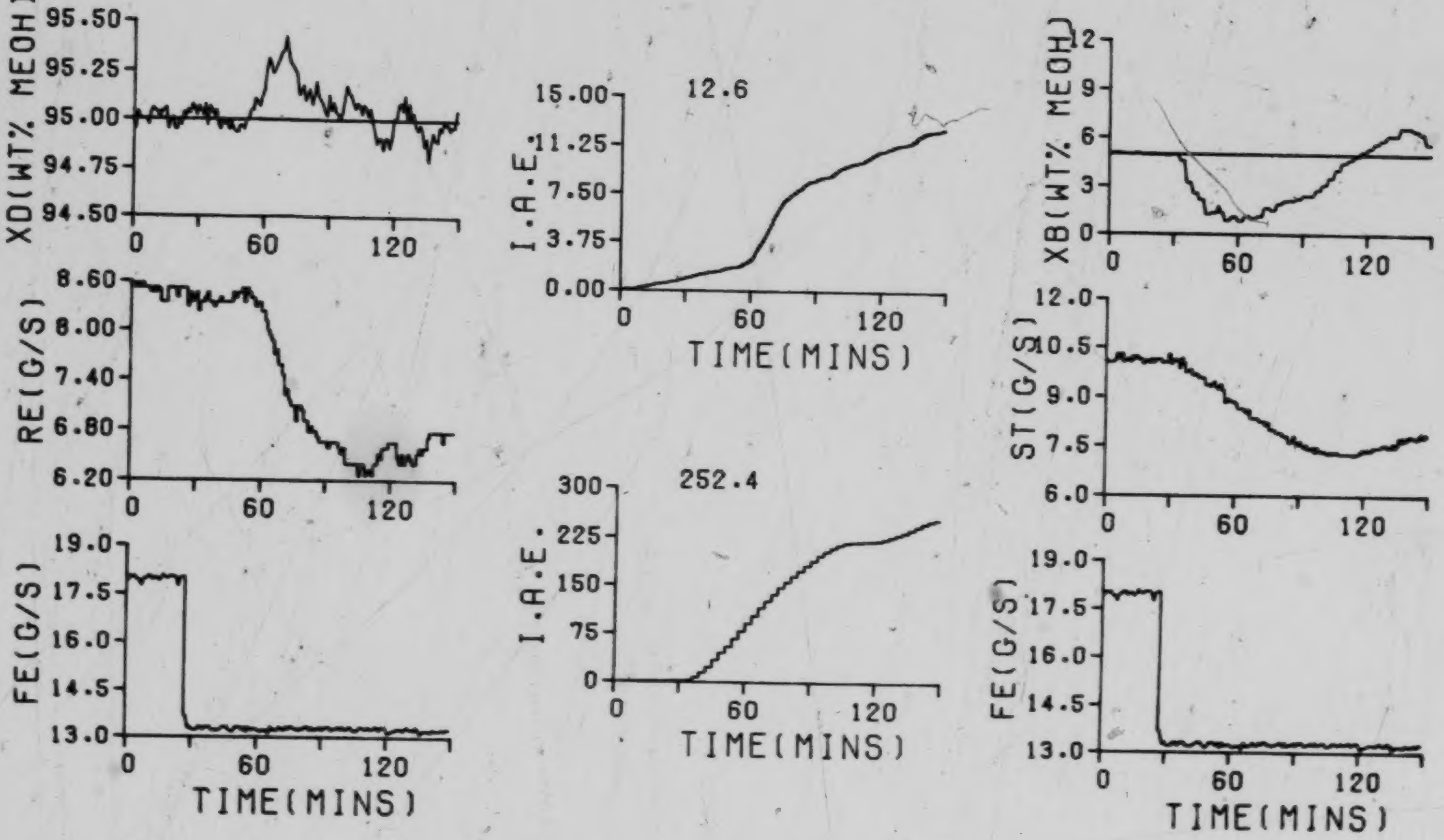

FIGURE 7.23 MR PID 3-C/PID(PB=34.466.TI=160.366.TD=0.0)/TS=60.0/
PID(PB=190.937.TI=422.083.TD=171.851)/TS=180.0/

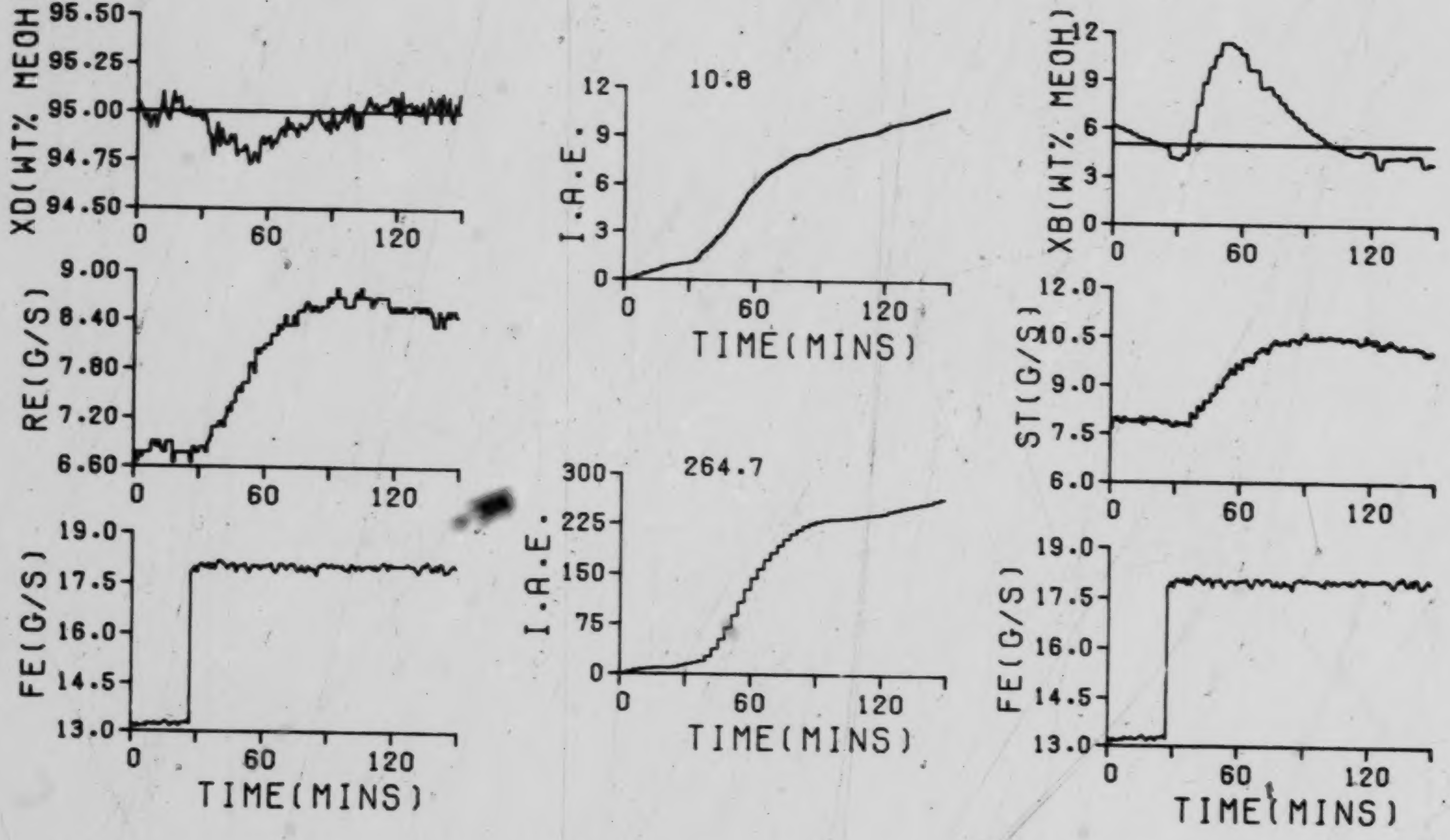

FIGURE 7.24 MR PID 3-C/PID(PB=34.466.TI=160.366.TD=0.0)/TS=60.0/
PID(PB=190.937.TI=422.083.TD=171.851)/TS=180.0/

deviation resulting in IAE values of 8.8 and 173.9, which are lower than those of 9.7 and 275.8 that were obtained for the test performed using the Ziegler-Nichols based controller constants.

Decreasing the feed flow rate from its steady state value, gave rise to the column performance depicted in Figure 7.23. Deviation of the top composition from the setpoint is minimal as a result of the feed disturbance with the composition returning to the setpoint by the completion of the test period, but as can be seen the bottom composition overshoots as it returns to the setpoint resulting in a high IAE value of 252.4. These results demonstrate that top composition regulation with controller settings established by the 3-C method was better than was achieved with the controller constants selected by the Ziegler-Nichols rules.

The control behavior which resulted for an increase in feed flow rate to its steady state value is shown in Figure 7.24. The top composition shows only a minor deviation from the setpoint at the onset of the feed disturbance but the resulting IAE value of 10.8 is higher than for either feed disturbance above the steady state operating condition. Bottom composition exhibits a large deviation from the setpoint, leading to an IAE value of 264.7 higher than for the previous three feed disturbances.

The overall results display a faster return to the setpoint for a given disturbance than was evident for the tests conducted using the Ziegler-Nichols based controller constants.

7.2.3 Control Performance with Constants Calculated using the Integral of Absolute Error Equations

Table 7.2.3 provides a summary of the IAE performance values for the tests of the control performance of the pilot plant distillation column when subjected to dual composition control with conventional PID controllers using constants calculated with the Integral of Absolute Error equations. The column performance which results using multirate sampling for a multiloop PID control strategy with controller constants calculated from the IAE based equations for the four different step changes in the feed flow rate are presented in Figures 7.25 to 7.28. The column response obtained for an increase in feed flow rate from its steady state value is shown in Figure 7.25. The top composition shows only a minor deviation from the setpoint as a result of the feed changes with good regulation of the top composition as indicated by the IAE value of 7.1. The bottom composition regulation is acceptable with a return to the setpoint on completion of the test period.

The top composition exhibits a minor deviation from the setpoint in Figure 7.26, with good regulation of the composition, unlike the control of the bottom composition which remained below the setpoint at the completion of the test period.

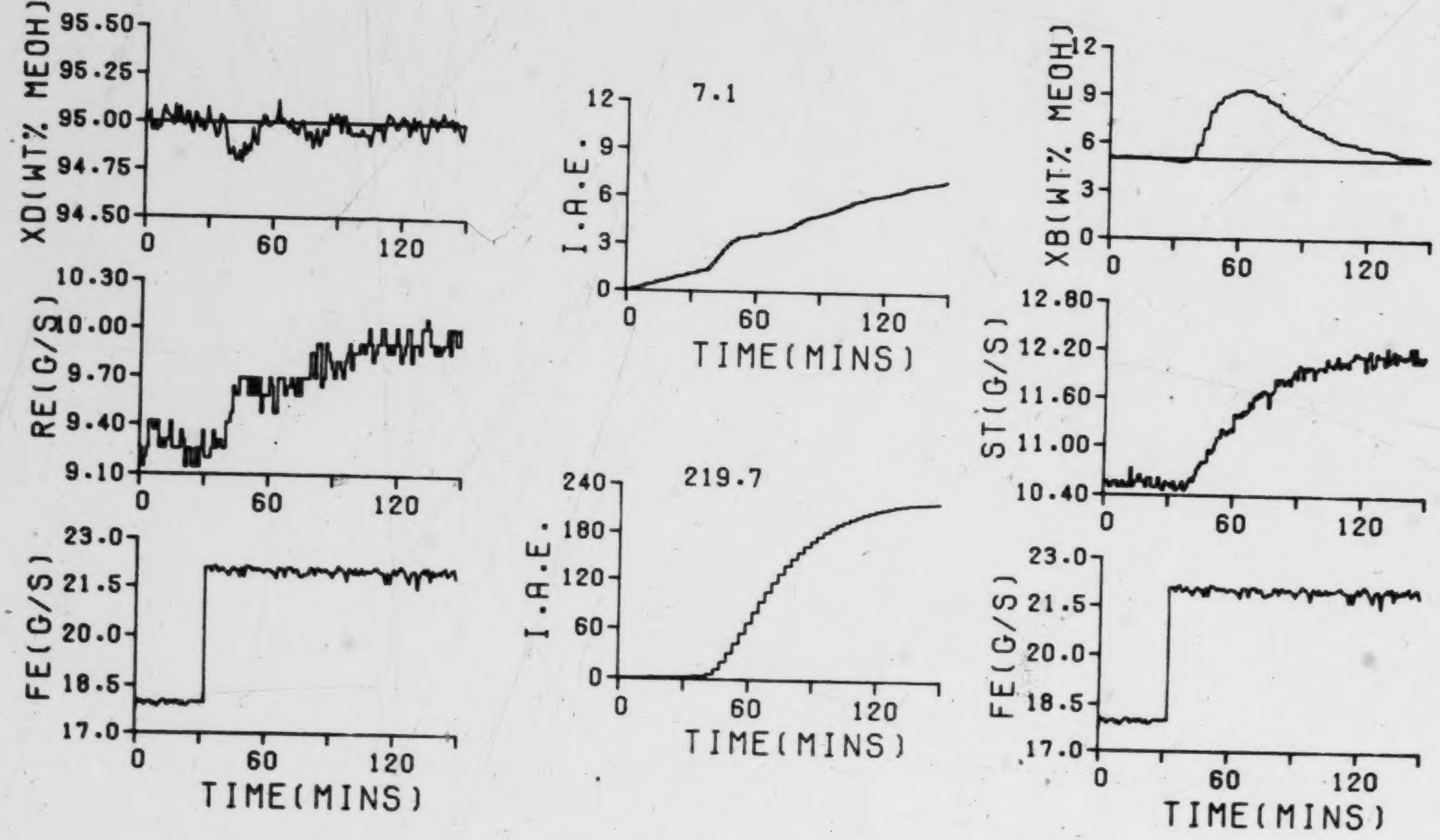

FIGURE 7.25 MR PID IAE/PID(PB=30.533,TI=234.0,TD=0.0)/TS=60.0/
PID(PB=187.135,TI=643.232,TD=191.613)/TS=180.0/

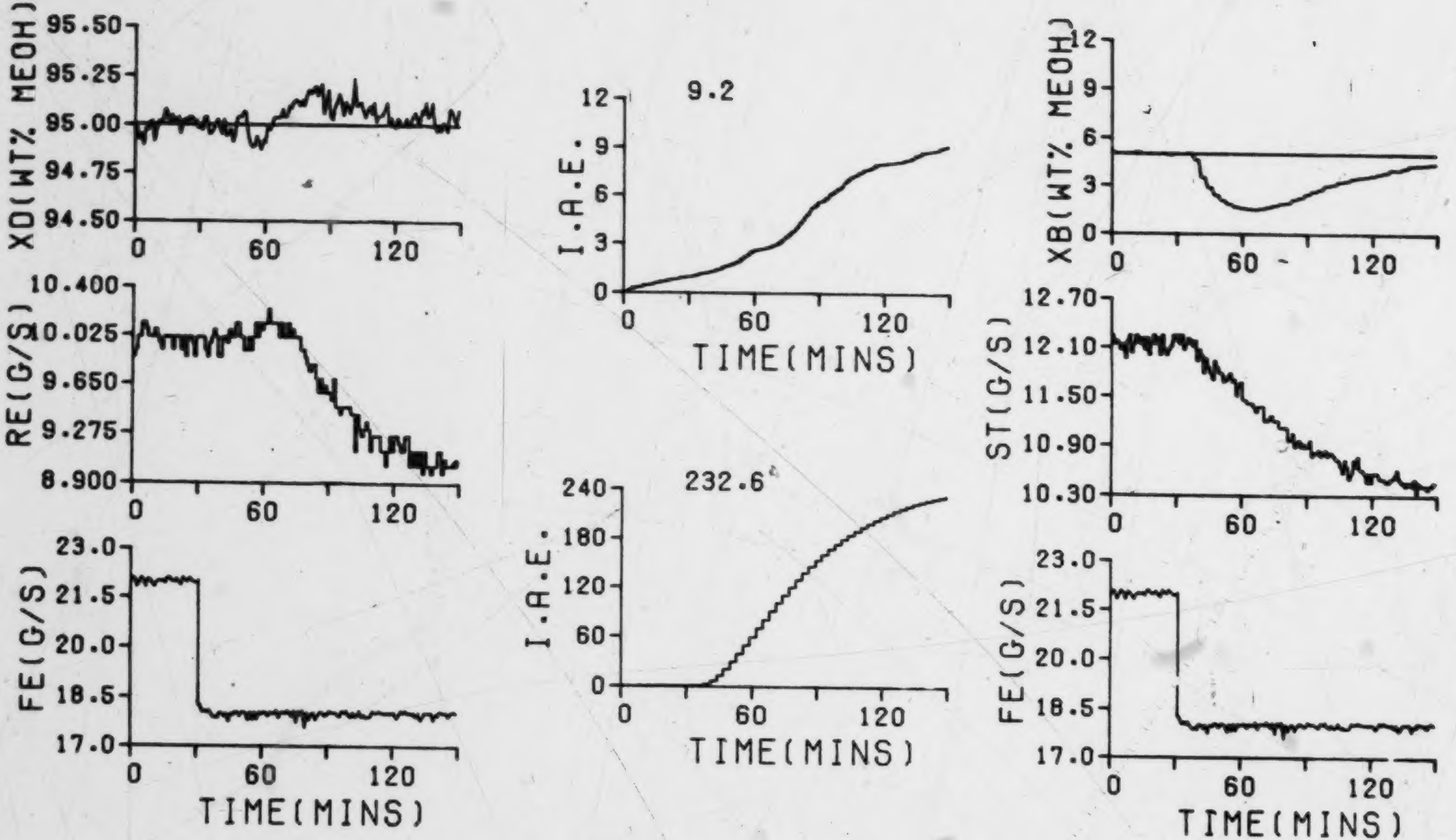

FIGURE 7.26 MR PID IAE/PID(PB=30.533,TI=234.0,TD=0.0)/TS=60.0/
PID(PB=187.135,TI=643.232,TD=191.613)/TS=180.0/

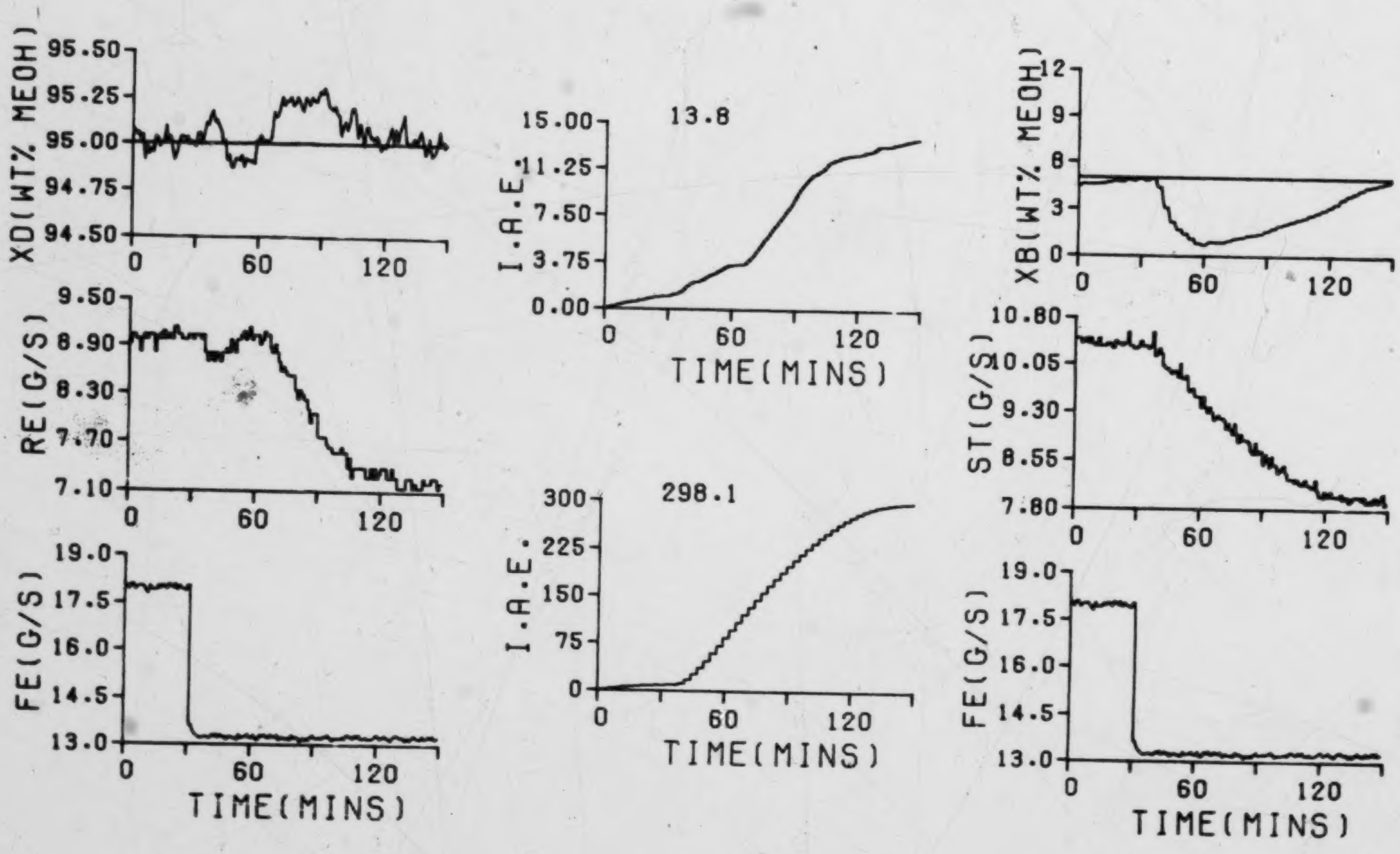

FIGURE 7.27 MR PID IAE/PID(PB=30.533,TI=234.0,TD=0.0)/TS=60.0/
PID(PB=187.135,TI=643.232,TD=191.613)/TS=180.0/

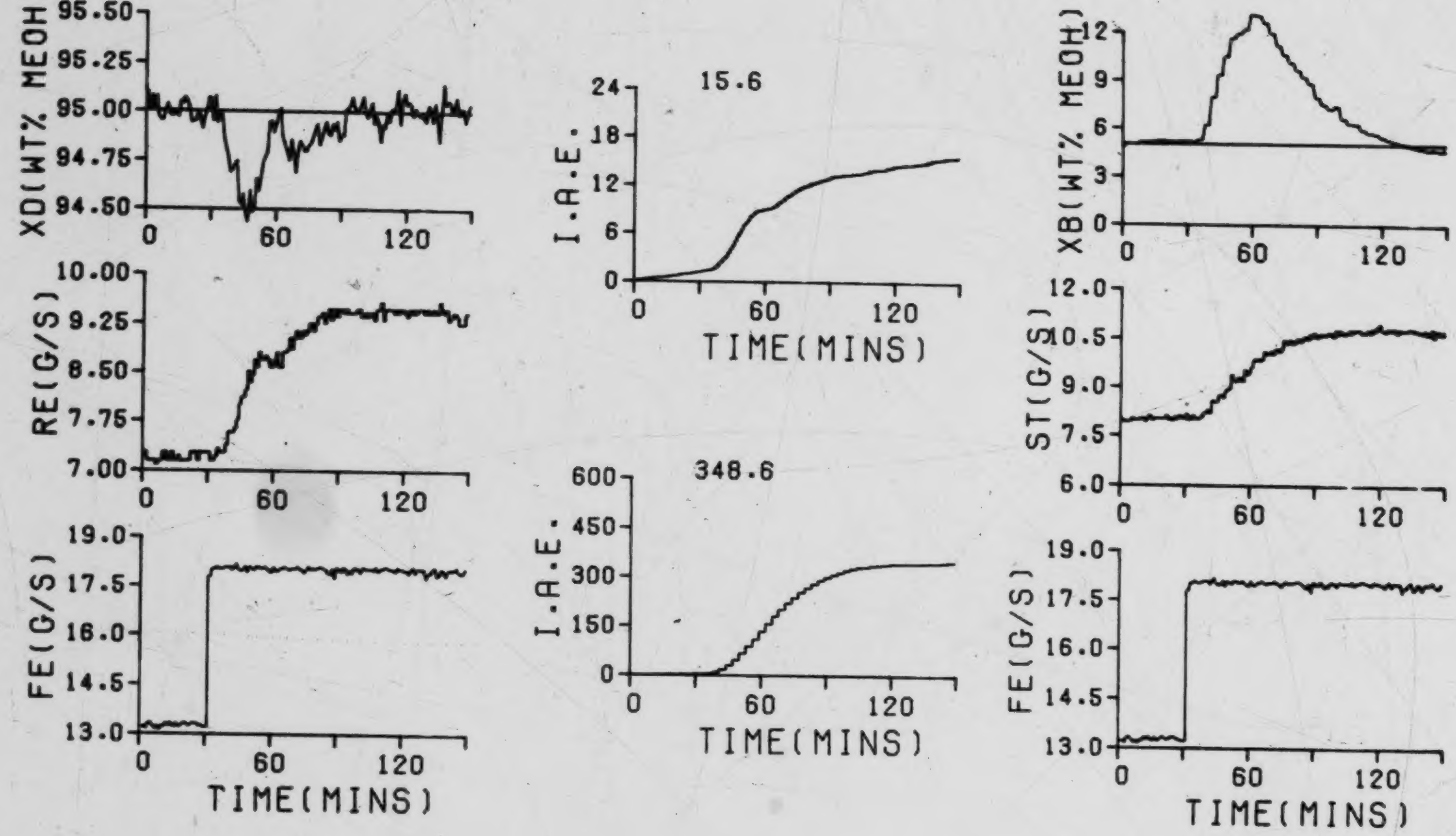

FIGURE 7.28 MR PID IAE/PID(PB=30.533,TI=234.0,TD=0.0)/TS=60.0/
PID(PB=187.135,TI=643.232,TD=191.613)/TS=180.0/

Table 7.2.3
Multirate PID Control Performance with Controller Constants Calculated from Integral of Absolute Error Equations

	IAE Values	
Step	TOP	BOTTOM
increase from steady state	7.1	219.7
decrease to steady state	9.2	232.6
decrease from steady state	13.8	298.1
increase to steady state	15.6	348.6
total	45.7	1099.0

As can be seen from Figure 7.27, the top composition again deviates from the setpoint, but returns to the setpoint prior to the completion of the test. This regulatory performance can be considered satisfactory in view of the inverse response depicted in Figure 5.3, whereas bottom composition control is unacceptable due to the large IAE value of 298.1.

For the increase in feed rate back to its steady state value, as can be observed from Figure 7.28, the top composition slips from the setpoint initially, but returns before the end of the test with an IAE of 15.6. The bottom composition excursion is excessive and unacceptable during the initial portion of the test as the composition reaches a value that is more than double the value of the setpoint, yet the high gain of the controller eventually returns the bottom composition to the setpoint prior to the end of the test period.

7.2.4 Control Performance with Constants Calculated using the Integral of Time Multiplied by the Absolute Error Equations

Table 7.2.4 provides a summary of the IAE performance values for the tests of the control performance of the pilot plant distillation column when subjected to dual composition control with conventional PID controllers using constants calculated with the ITAE criterion equations. The responses of the distillation column using these controller constants for the four feed rate disturbances are presented in Figures 7.29 to 7.32. For the step increase in feed flow rate, as shown in Figure 7.29, the top composition deviates from the setpoint when the feed disturbance is introduced, yet slowly returns to the setpoint with an IAE value of 10.4. Bottom composition control is unsatisfactory due to the sustained deviation from the setpoint for the duration of the step, yielding an IAE value of 279.0. A similar unaccecptable control response is depicted in Figure 7.30 for the disturbance where the feed flow rate is decreased to its steady state value, resulting in a top loop IAE of 12.4, and a bottom loop IAE of 263.0.

The poor response of the distillation column control for a decrease in feed flow from its steady state rate is shown in Figure 7.31. Top composition control barely returns to the setpoint at the completion of the test period, as well bottom composition regulation is equally poor for this change in feed flow.

Table 7.2.4
Multirate PID Control Performance with Controller Constants Calculated from The Integral of Time Multiplied by the Absolute Error Equations

	IAE Values	
Step	TOP	BOTTOM
increase from steady state	10.4	279.0
decrease to steady state	12.4	263.0
decrease from steady state	14.6	351.0
increase to steady state	11.5	295.0
total	48.9	1188.0

The top composition control deviates initially from the setpoint, but returns by the end of the test period, as observed in the response presented in Figure 7.32, with a corresponding IAE value of 11.5. The excessive deviation of bottom composition from the setpoint, coupled with the long period of time required for the bottom composition to return to the setpoint, resulting in an IAE value of 295.0 makes the control performance unacceptable.

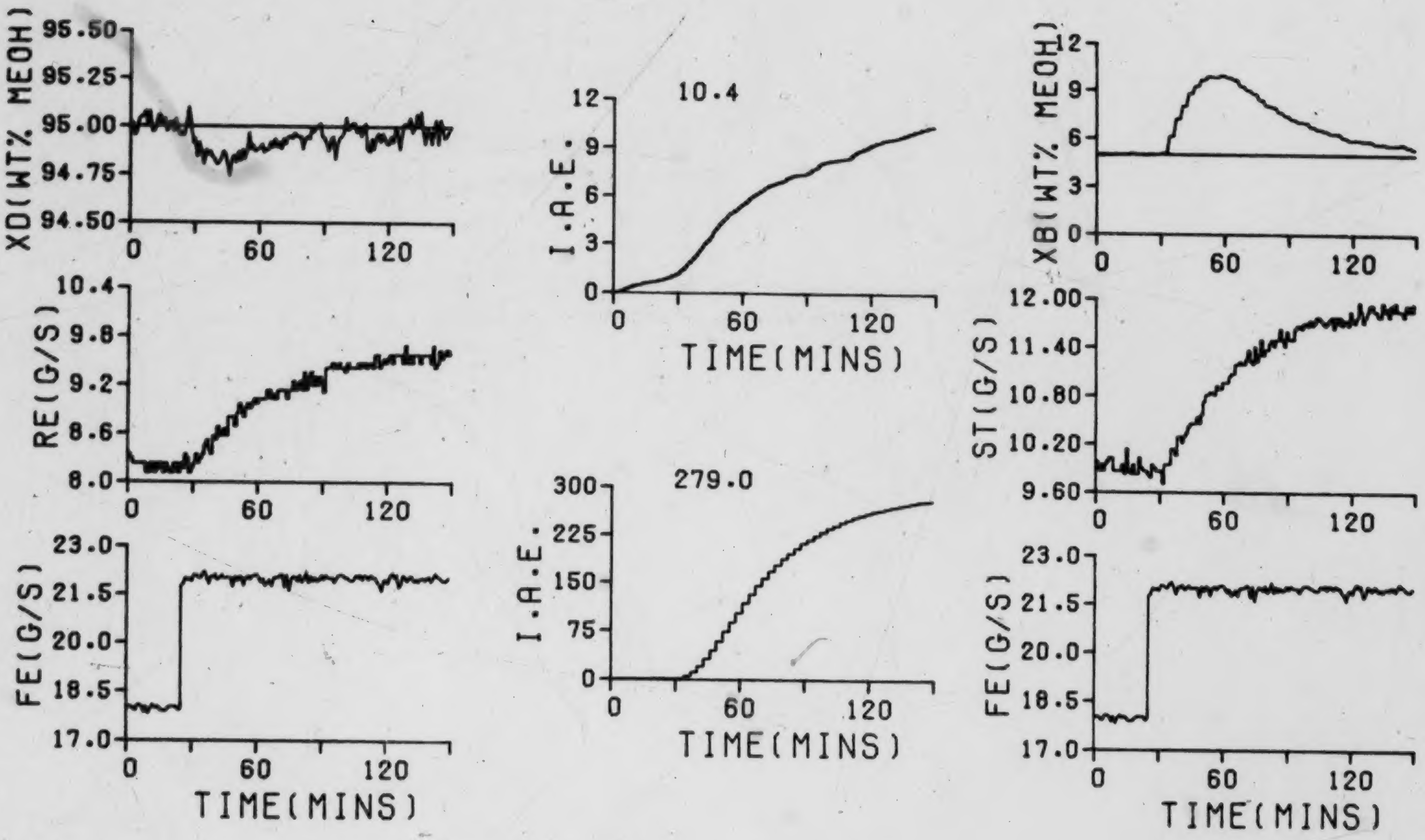

FIGURE 7.29 MR PID ITAE/PID(PB=35.472,TI=220.34,TD=0.0)/TS=60.0/
PID(PB=193.29,TI=670.771,TD=172.227)/TS=180.0/

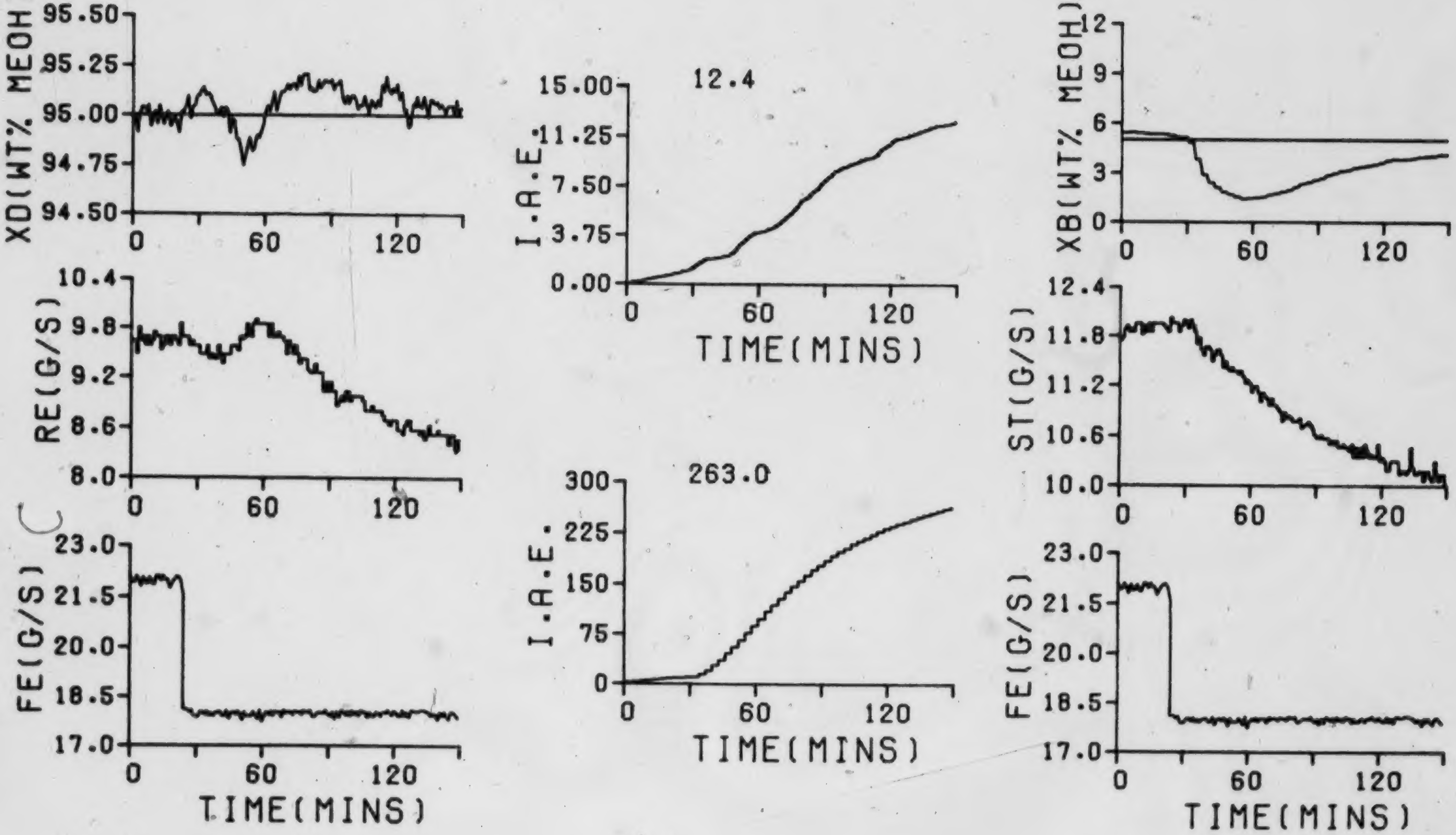

FIGURE 7.30 MR PID ITAE/PID(PB=35.472.TI=220.34.TD=0.0)/TS=60.0/
PID(PB=193.29.TI=670.771.TD=172.227)/TS=180.0/

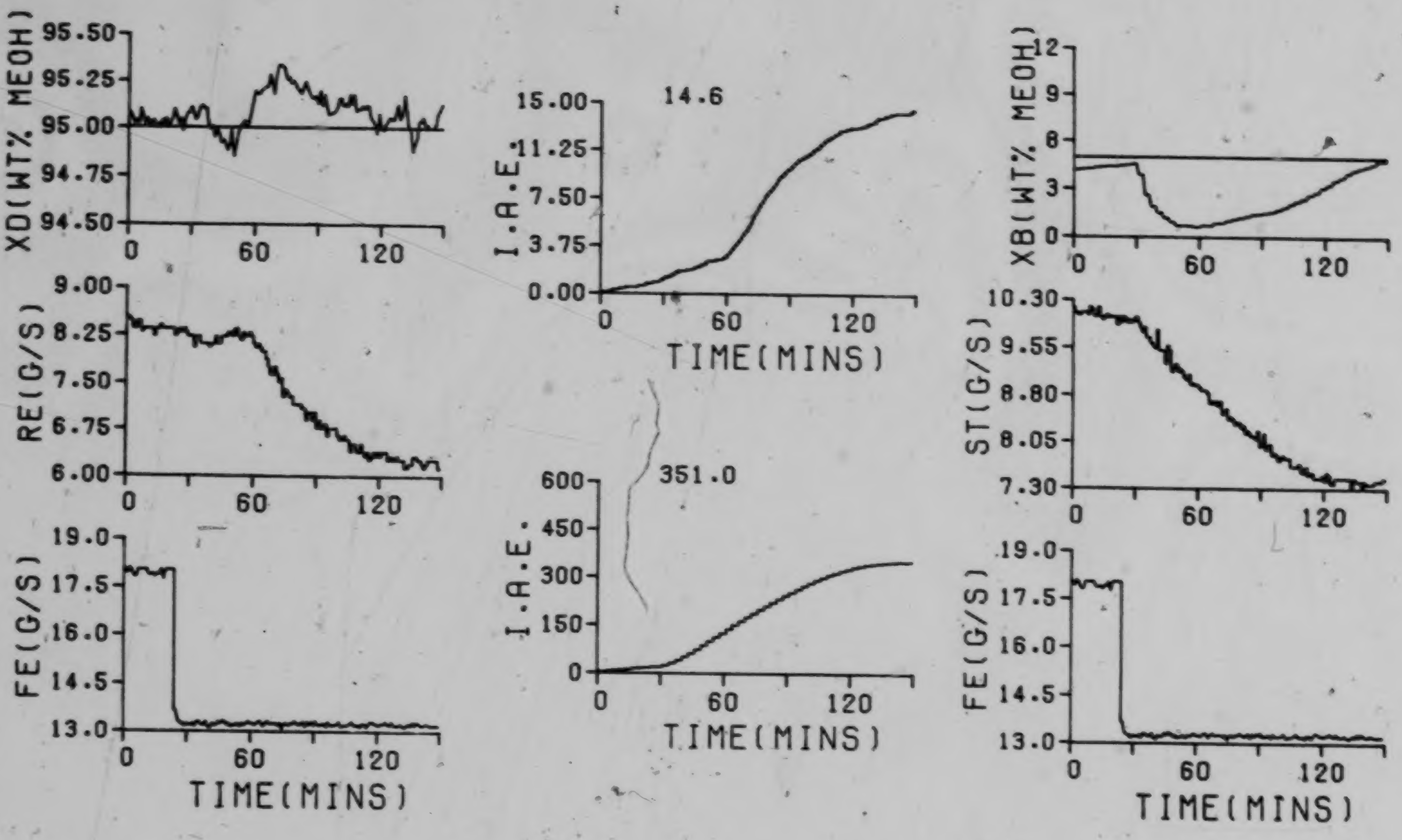

FIGURE 7.31 MR PID ITAE/PID(PB=35.472,TI=220.34,TD=0.0)/TS=60.0/
PID(PB=193.29,TI=670.771,TD=172.227)/TS=180.0/

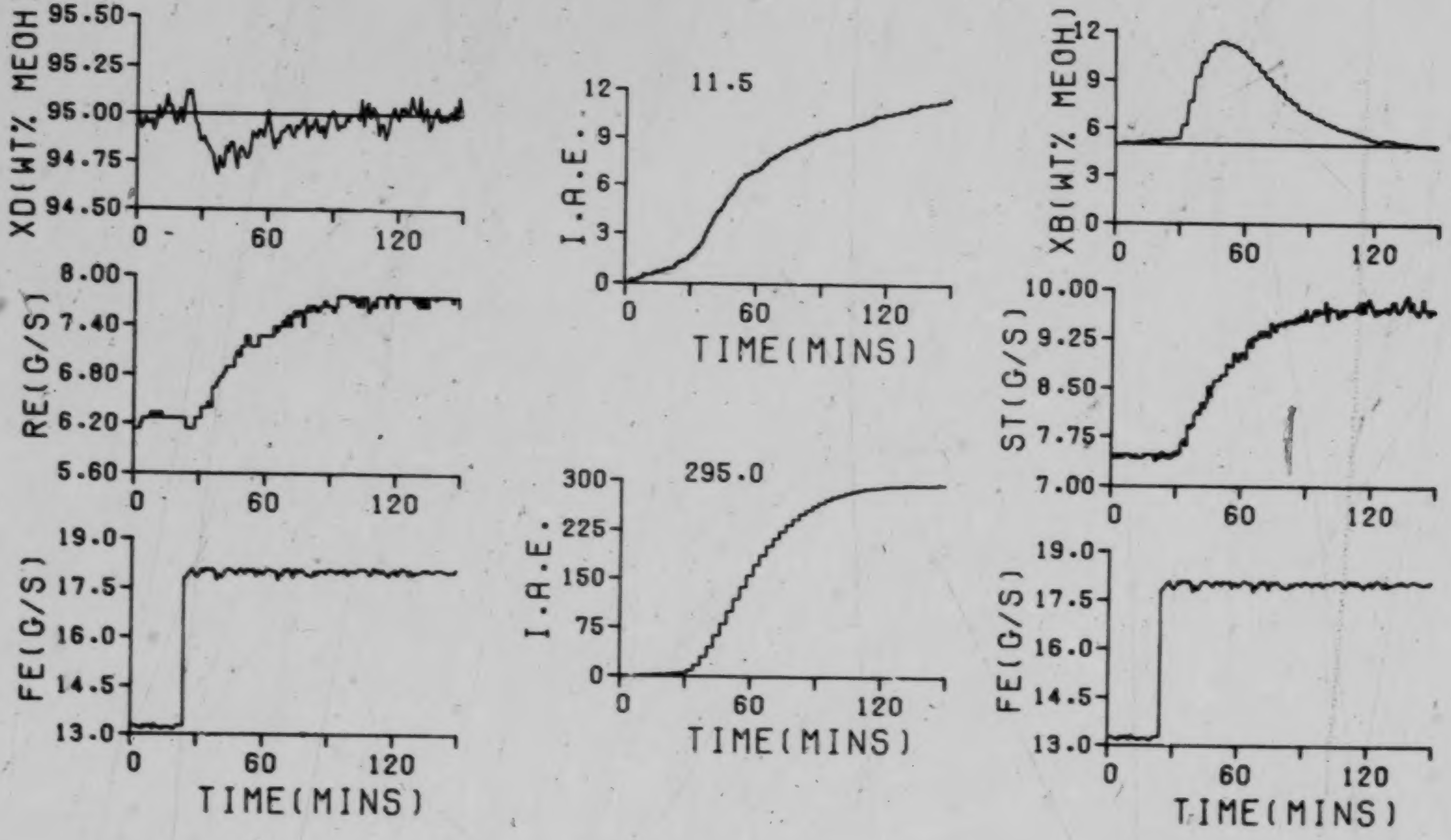

FIGURE 7.32 MR PID ITAE/PID(PB=35.472,TI=220.34,TD=0.0)/TS=60.0/
PID(PB=193.29,TI=670.771,TD=172.227)/TS=180.0/

7.2.5 Summary of Column Control Performance Using a Multiloop PID Control Strategy with Multirate Sampling

The control performance of the distillation column operating under multiloop PID control with multirate sampling, as shown by the responses in Figures 7.17 to 7.32, with controller constants selected from the different equations presented earlier (cf. equations 6.6 to 6.8) caused significantly different control behavior. The IAE performance index for the individual responses and the total IAE for all four step changes are summarized in Table 7.2.5.

As can be seen from the summary of the IAE values given in Table 7.2.5 for multirate sampling with a multiloop PID control strategy, the best overall performance was obtained from the controller constants determined via the Cohen-Coon equations. The IAE values that resulted from the use of Cohen-Coon calculated controller constants are significantly lower than the three other methods, yet all four methods resulted in underdamped control of the compositions. The Cohen-Coon constants presented in Table 6.2 for one minute sampling provide the largest amount of integral action of the four methods, yet the gain associated with the Cohen-Coon method is not the largest. The methods ranked in terms of integral action from largest to smallest are; 3-C, ITAE, IAE and Z-N; in terms of observed overall performance the ranking is 3-C, IAE, ITAE then Z-N. The larger gain of the IAE method improves the performance of the control, even though the intergal constant is less than the ITAE method.

Table 7.2.5
IAE values for Multiloop PID control,with Multirate sampling, based on calculated controller settings

		IAE Values			
Step		Z-N	3-C	IAE	ITAE
increase from SS	top	6.3	9.2	7.1	10.4
	bottom	277.0	196.9	219.7	279.0
decrease to SS	top	9.7	8.8	9.2	12.4
	bottom	275.8	173.9	232.6	263.0
decrease from SS	top	19.1	12.6	13.8	14.6
	bottom	382.1	252.4	298.1	351.0
increase to SS	top	13.0	10.8	15.6	11.5
	bottom	419.1	264.7	348.6	295.0
total		1402.1	929.3	1144.7	1236.9

Obviously the best blend of gain and reset action was provided by the Cohen-Coon equations, as substantiated in the observed control performance.

7.2.6 The Effect of Multirate Sampling On Control Performance Using a Multiloop PID Control Strategy

Table 7.2.6 summarizes the IAE totals for the top and bottom composition response for multiloop and multirate PID control.

The tabulation clearly indicates that the top composition regulation improved with the use of a one minute sample interval. The same controller constants were used for the bottom composition control for both multiloop and

Table 7.2.6
Comparison of Single rate and Multirate sampling PID control

IAE Totals by Method

Top Totals	Z-N	3-C	IAE	ITAE
Multiloop	116.4	67.8	83.5	86.4
Multirate	48.1	41.4	45.7	48.9
Bottom Totals	**Z-N**	**3-C**	**IAE**	**ITAE**
Multiloop	1394.8	780.8	1045.8	1158.2
Multirate	1354.0	887.9	1099.9	1188.0

multirate control. This improvement in top composition regulation reduces the effectiveness of the bottom composition controller due to the increased interaction resulting from the improved control of top composition by larger changes in the reflux flow at each sample instant. This is illustrated by the totals of the IAE values for the bottom loop, in all but one case the totals were higher for multirate control. In the case of the Ziegler-Nichols control, bottom composition control was so poor in the single sample rate case that the improvement in top composition regulation has very little effect on the bottom composition. The largest reduction in performance occurred with the Cohen-Coon method, a 14% reduction in bottom composition regulation occurred for a corresponding increase in the top composition regulation of 39%. Use of controller constants established from the Cohen-Coon method provided the most satisfactory regulation of top and bottom composition for both the single rate and multirate sampling tests.

The responses showed that for bottom composition control, the initial deviation of the composition from the setpoint, were of the same magnitude for the corresponding steps of the disturbance. Therefore, any comparison of the control effectiveness of the different controller constants should be judged on the rate at which the composition returns to the setpoint and the amount of oscillation or overshoot which results during the response. This initial deviation cannot be removed by employing only a feedback control strategy. Feedforward action could be introduced in order to compensate for this disturbance, but this would require a feed flow rate measurement as well as additional tuning and more information in the form of transfer functions relating the feed disturbance to the individual compositions. These test results of the control performance that can be achieved using conventional feedback PID control shows its limitations in dual composition control. It is difficult to compensate for the interaction of the manipulated variables, steam and reflux flow rates, especially when the interaction varies in magnitude depending on the type of disturbance. This very fact has been the driving force for multivariable control strategies for many years. Once a feedforward control strategy has been implemented, several other factors come to light; how does one tune the parameters, set the model if model based or even account for disturbances other than those which are now measured. These questions should become easier to answer after the presentation of the multivariable and multirate self-tuning control results.

7.3 Control of Product Composition Using a Multivariable Self-Tuning Controller Strategy

This section presents responses for control of top and bottom composition of the pilot scale distillation column using the multivariable self-tuning control algorithm. The parameters for Q weighting used for the controller are tabulated in Tables 6.4 and 6.5. The sample and control interval used for these tests was 3.0 minutes, as governed by the GC sample time described in Chapter 4. The number of controller parameters and the polynomials used are specified in Chapter 6. Feedforward disturbance compensation was implemented with the use of three L parameters for both top and bottom controllers. For this portion of the study the feedforward compensation was implemented by use of the prediction error as the feedforward term to the observation vector:

$$Y(t) - Y^{*}(t|t-k_{11}) \qquad (7.1)$$

This form of estimated feedforward compensation has been applied with the self-tuning controller, since no additional sensors and no additional information is required from the process.

For this study the forgetting factor (exponential discounting factor) used in the identification algorithm is $\rho_1 = 0.998$. The initial controller parameters for the identification algorithm were set at zero, with the diagonal of the covariance matrix initialized at 1000I. In order to identify the controller parameters, the column was first operated under manual control, at an operating point different from that of the steady state which the tests would be conducted. The column was then switched over to PID control and brought to steady state operation with controller parameter identification in progress. After completion of approxiamtely 100 control and sampling intervals, the diagonal elements of the covariance matrix were examined. Control of the column was transferred to the self-tuning controller, with the Q weighting parameters set to conservative default values, when the magnitude of the largest element of the diagonal became less than or equal to unity.

The magnitude of the diagonal elements of the covariance matrix indicates the confidence in the value of the parameters being identified. The smaller the value of the diagonal elements the more confidence is perceived in the parameter estimates. With the distillation column operating under the control of the self-tuning controller and at the desired steady state, the Q weighting parameters to be studied were entered into the control program from the terminal keyboard and the column operated at steady state for a minimum of 5 hours prior to the commencement of any testing. This proceedure was followed to ensure that the Q weighting parameters selected for study were capable of maintaining steady state operation, as well as ensuring that the column is not in a transient period at the beginning of a test.

7.3.1 Control Performance with Q Weighting Constants Determined With The Ziegler-Nichols Equations

Table 7.3.1 provides a summary of the IAE performance values for the tests of the self-tuning control performance of the pilot plant distillation column when subjected to dual composition control with multivariable self-tuning control using Q weighting constants calculated with the Ziegler-Nichols equations. The distillation column performance obtained while operating under multivariable self-tuning control with Q weighting parameters determined by the Ziegler-Nichols method are presented in Figures 7.33 to 7.36. The top composition, as can be seen in Figure 7.33, deviates slightly from its setpoint but returns quickly with

Table 7.3.1
Multivariable Self-Tuning Control Performance with Q Weighting Constants Calculated from Ziegler-Nichols Equations

	IAE Values	
Step	TOP	BOTTOM
increase from steady state	8.5	97.3
decrease to steady state	12.0	88.0
decrease from steady state	28.2	119.0
increase to steady state	19.4	93.0
total	68.1	397.3

a resulting IAE value of 8.5, whereas the bottom composition deviates slightly but returns quickly, with an IAE value of 97.3, which is significantly lower than the IAE value of 255.9 that resulted for the same feed disturbance with the column operating under the multiloop PID control strategy.

As can be seen from the values in Table 7.3.1 the composition regulation for the step change in feed rate to steady state was acceptable, as can be observed from the response displayed in Figure 7.34. The bottom composition regulation is good, characterized by a quick return to the setpoint, with some minor overshoot and an IAE value of 88.0, which is superior to that obtained with the corresponding multiloop PID response of 267.7.

The distillation column responses obtained for a decrease in feed flow rate from its steady state rate are shown in Figure 7.35. The top composition deviates from the

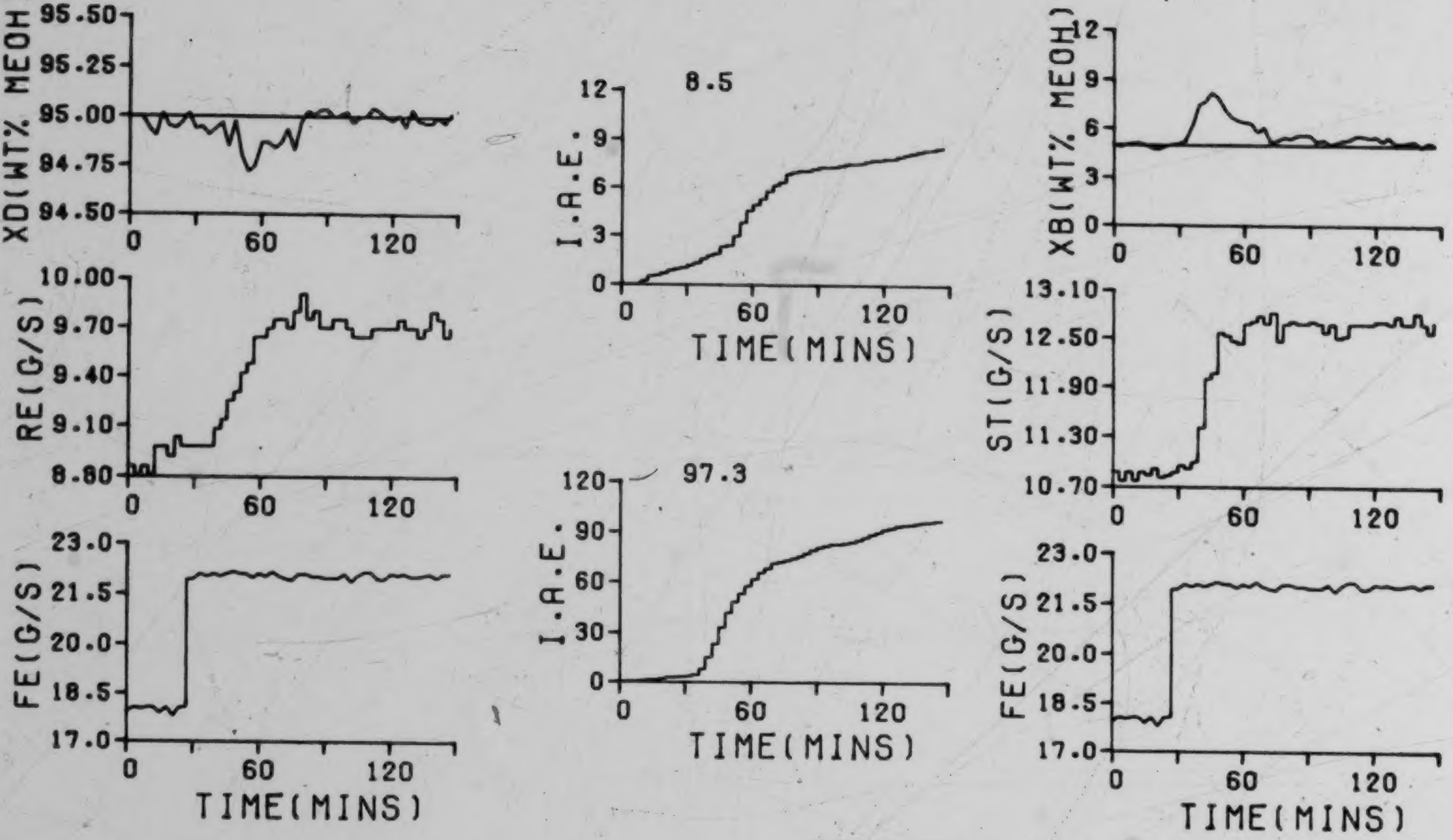

FIGURE 7.33 MV ST ZN/Q(PB=32.659,TI=299.97,TD=0.0)/TS=180.0/4.3.3.0.4/
Q(PB=55.539,TI=299.97,TD=0.0)/TS=180.0/5.3.3.0.6/

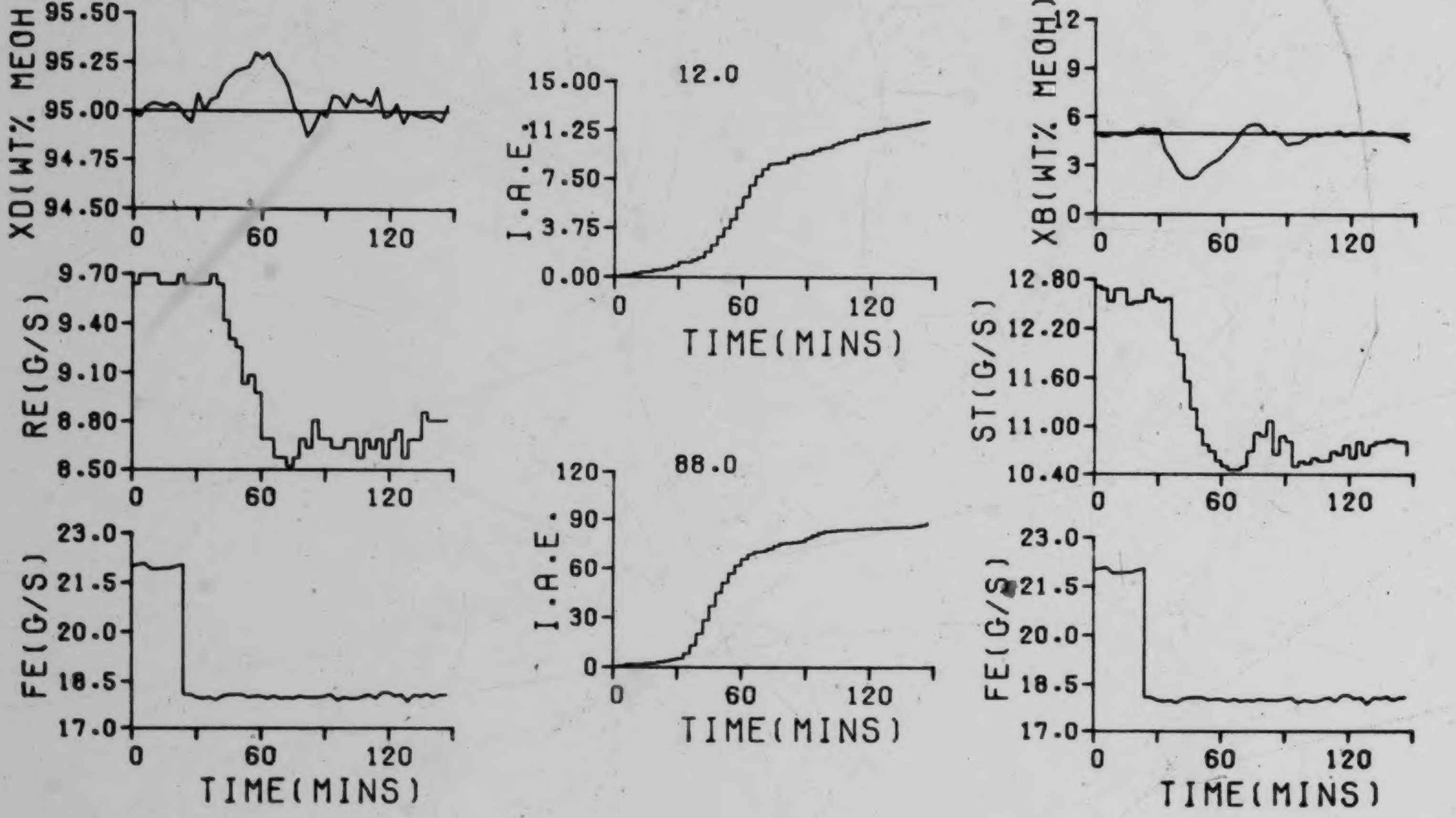

FIGURE 7.34 MV ST Z-N/Q(PB=32.659.TI=299.97.TD=0.0)/TS=180.0/4.3.3.0.4/
Q(PB=55.539.TI=299.97.TD=0.0)/TS=180.0/5.3.3.0.6/

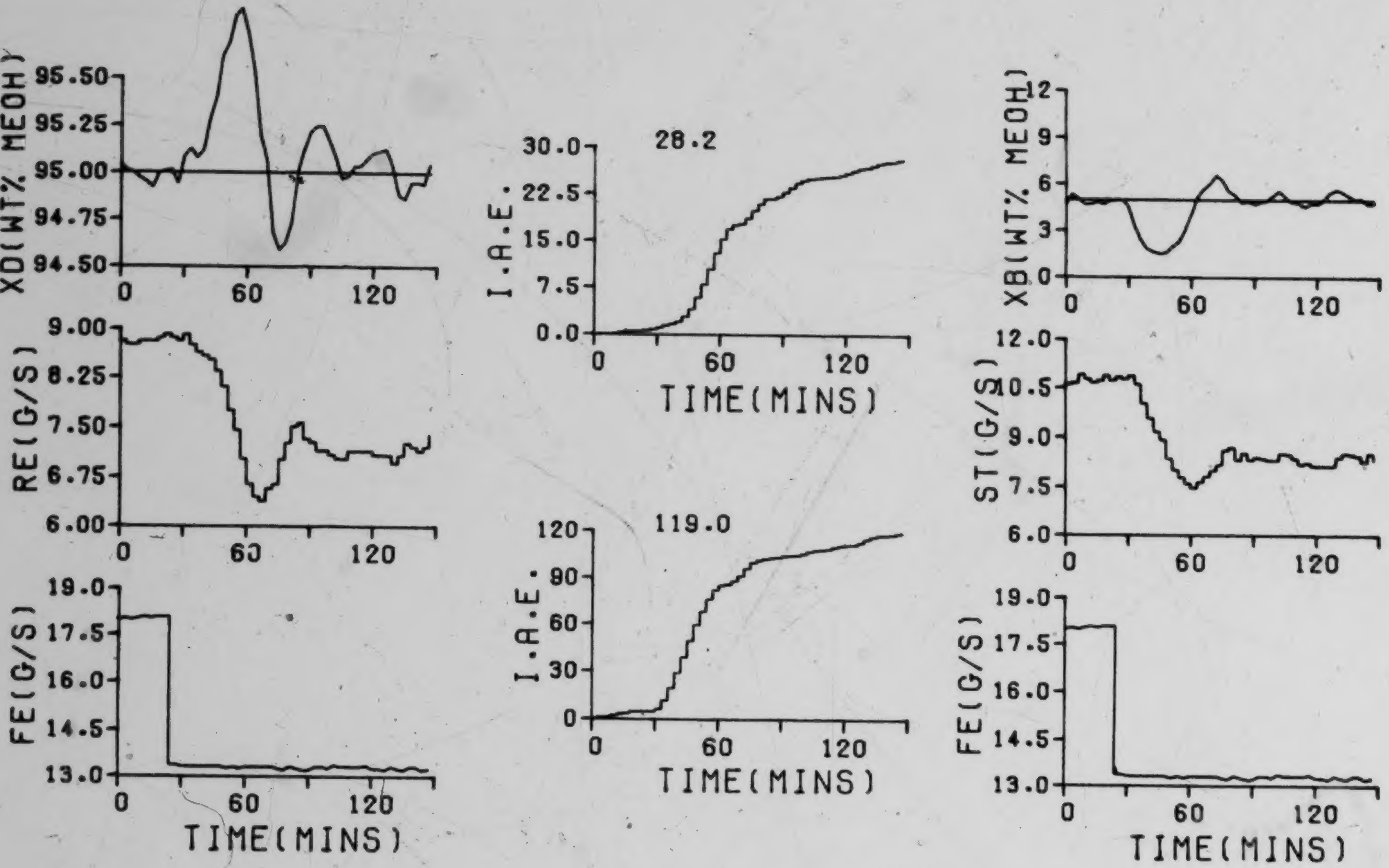

FIGURE 7.35 MV ST Z-N/Q(PB=32.659,TI=299.97,TD=0.0)/TS=180.0/4.3.3.0.4/
Q(PB=55.539,TI=299.97,TD=0.0)/TS=180.0/5.3.3.0.6/

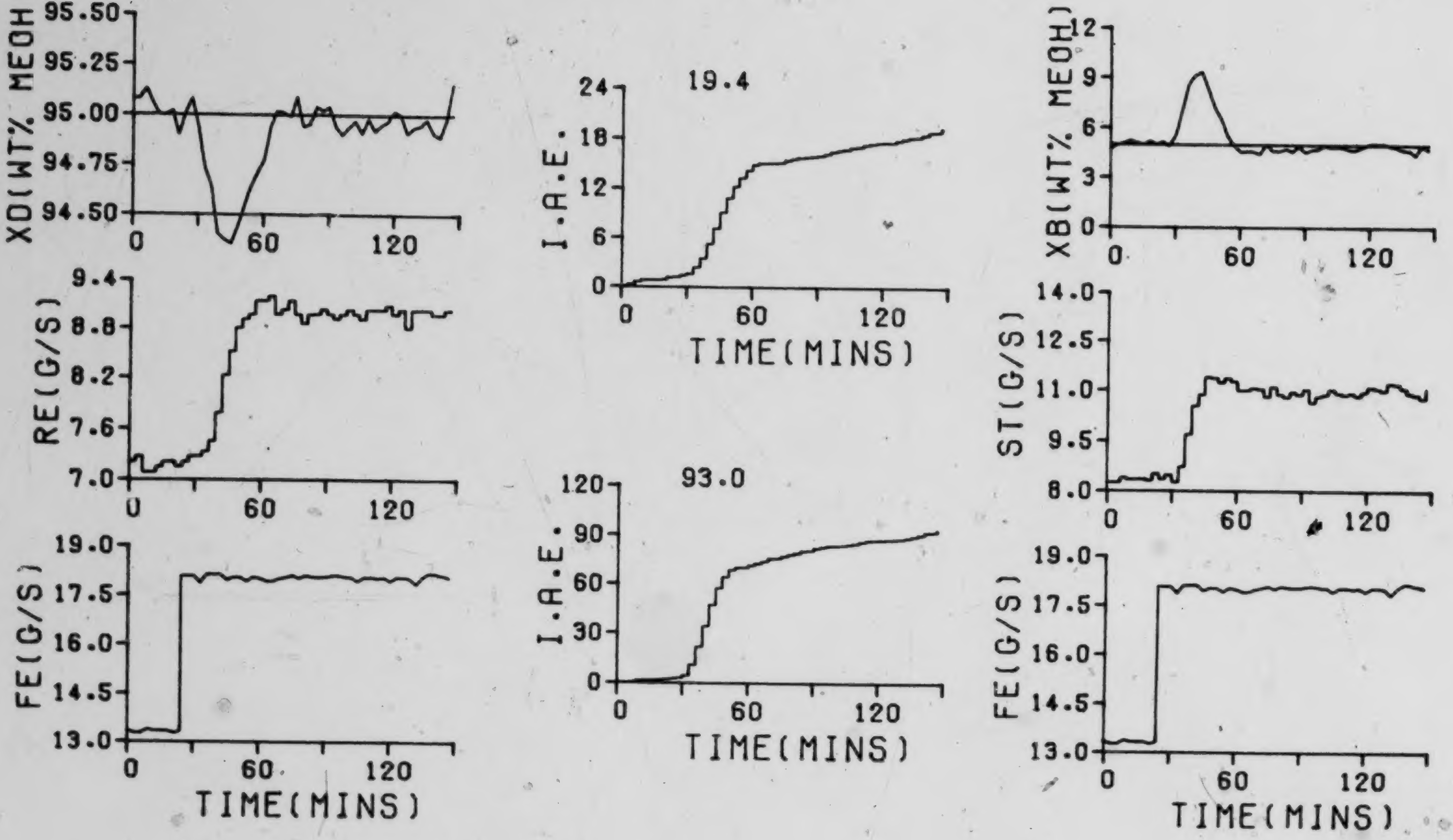

FIGURE 7.36 MV ST Z-N/Q(PB=32.659.TI=299.97.TD=0.0)/TS=180.0/4.3.3.0.4/
Q(PB=55.539.TI=299.97.TD=0.0)/TS=180.0/5.3.3.0.6/

setpoint by a large amount, yet eventually returns to the setpoint. Despite the fact that the column is difficult to regulate due to the inverse behavior noted in the open loop tests (cf. Figure 5.3) for this feed disturbance, the resulting IAE value of 28.2 was nearly one half the IAE value for control using the multiloop PID control strategy. As can be observed, bottom composition deviates from its setpoint at the initiation of the feed disturbance, but returns well before the completion of the test period, resulting in an IAE value of 119.0 compared to 421.5 for the corresponding multiloop PID control strategy test.

Figure 7.36 shows the distillation column response for the increase in feed flow back to its steady state rate. The top composition low IAE value of 19.4 is in sharp contrast to the value of 38.1 for the corresponding multiloop PID test. The improvement in bottom composition control is even more marked with the composition returning to the setpoint with little or no overshoot, resulting in an IAE value of 93.0, which is less than one quarter of the equivalent multiloop PID IAE value of 449.7.

The responses of the distillation column operating under the multivariable self-tuning controller with Q weighting parameters based on the Ziegler-Nichols method, show a quick response and a return to the setpoint with little overshoot. The IAE values are lower, for all four step disturbances, than those that resulted using a multiloop PID control strategy with the controller constants based on the same Ziegler-Nichols rules.

7.3.2 Control Performance With Q Weighting Constants Determined By The Cohen-Coon Equations

Table 7.3.2 provides a summary of the IAE performance values for the tests of the self-tuning control performance of the pilot plant distillation column when subjected to dual composition control with multivariable self-tuning control using Q weighting constants calculated with the Cohen-Coon equations. Figures 7.37 through 7.40 show the distillation column response after being subjected to the four different feed flow disturbances employing the multivariable self-tuning control with Q weighting constants calculated using the Cohen-Coon (3-C) method. As can be seen from the composition responses in Figures 7.37 and 7.38, for feed disturbances above the steady state value, satisfactory control is achieved. Comparison of these results with those obtained using the multiloop PID strategy shows that the use of the self-tuning control strategy has provided a significant improvement in control performance. However for the feed rate disturbances below the steady state value, the composition responses in Figures 7.39 and 7.40 show that satisfactory control of bottom composition is achieved but this is not the case for top composition. As can be seen for the feed flow rate decrease, the top composition shows a marked deviation from the setpoint, resulting in an IAE value of 19.5, nearly as large as the 21.2 value for the

Table 7.3.2
Multivariable Self-Tuning Control Performance with Q
Weighting Constants Calculated from Cohen-Coon Equations

	IAE Values	
Step	TOP	BOTTOM
increase from steady state	7.6	61.4
decrease to steady state	8.7	72.8
decrease from steady state	19.5	93.3
increase to steady state	13.5	86.2
total	49.3	313.7

multillop PID control strategy.

Although the top composition also shows a marked deviation from the setpoint, for an increase in the feed flow rate back to its steady state value, the resulting IAE value of 13.5 does represent a suitable improvement over the IAE of 18.5 that resulted for the control of the column using the multiloop PID strategy.

7.3.3 Control Performance With Q Weighting Constants Calculated from the Integral of Absolute Error Equations

Table 7.3.3 provides a summary of the IAE performance values for the tests of the self-tuning control performance of the pilot plant distillation column when under dual composition control with multivariable self-tuning control using Q weighting constants calculated with the IAE criterion equations. The distillation column responses, for

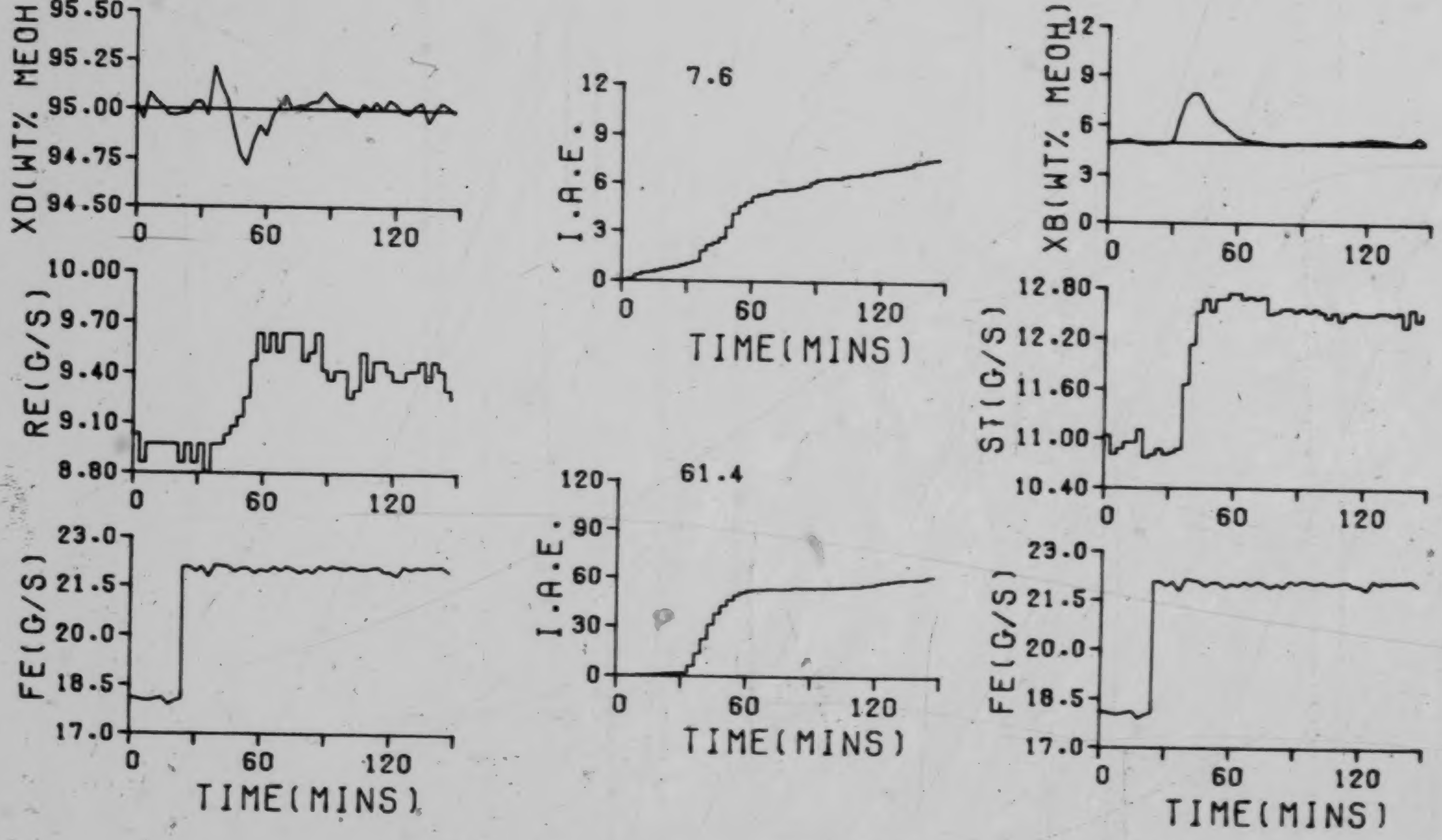

FIGURE 7.37 MV ST 3-C/Q(PB=34.466.TI=160.366.TD=0.0)/TS=180.0/4.3.3.0.4/
Q(PB=61.718.TI=238.3.TD=0.0)/TS=180.0/5.3.3.0.6/

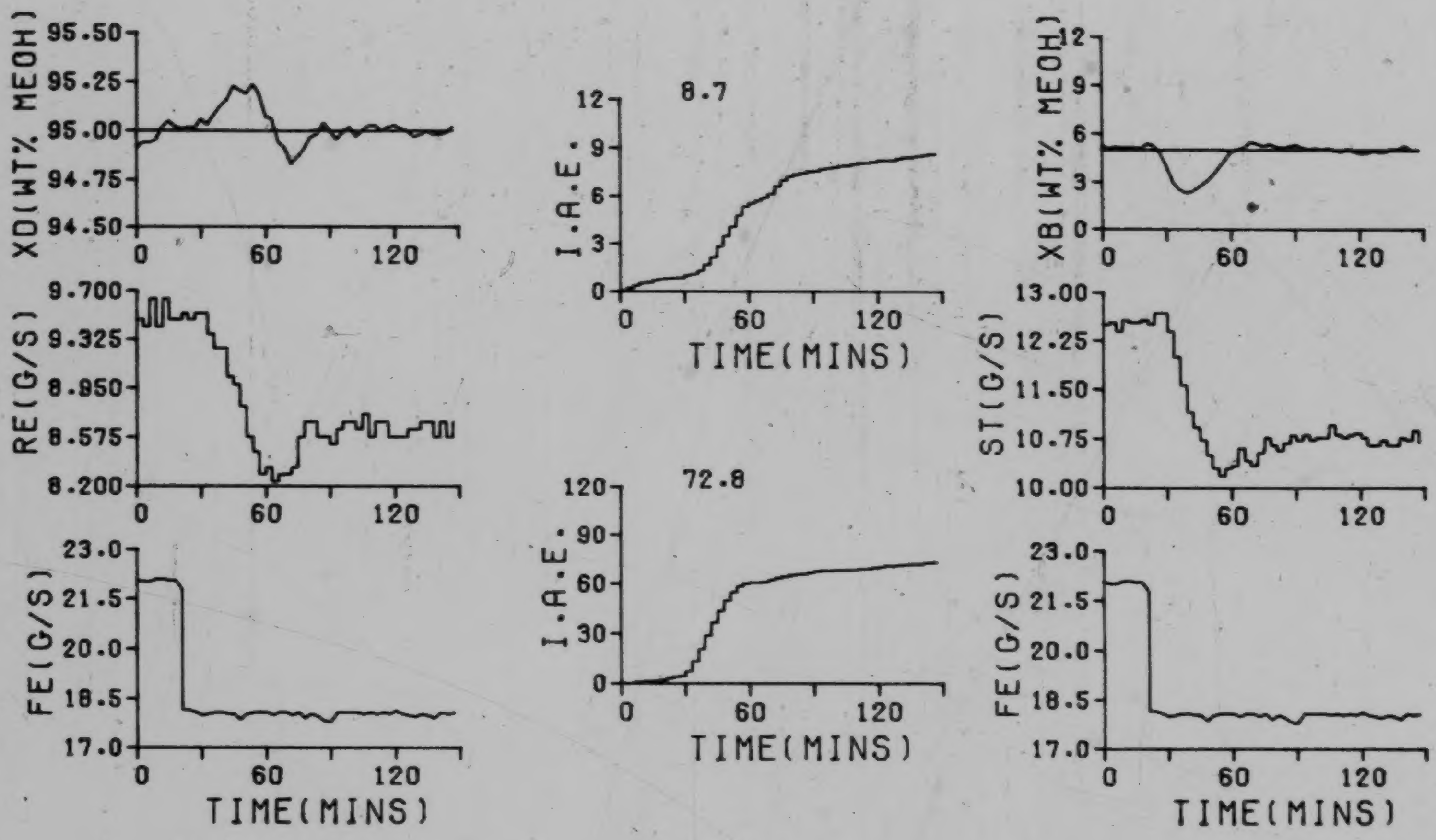

FIGURE 7.38 MV ST 3-C/Q(PB=34.466,TI=160.366,TD=0.0)/TS=180.0/4.3.3.0.4/
Q(PB=61.718,TI=238.3,TD=0.0)/TS=180.0/5.3.3.0.6/

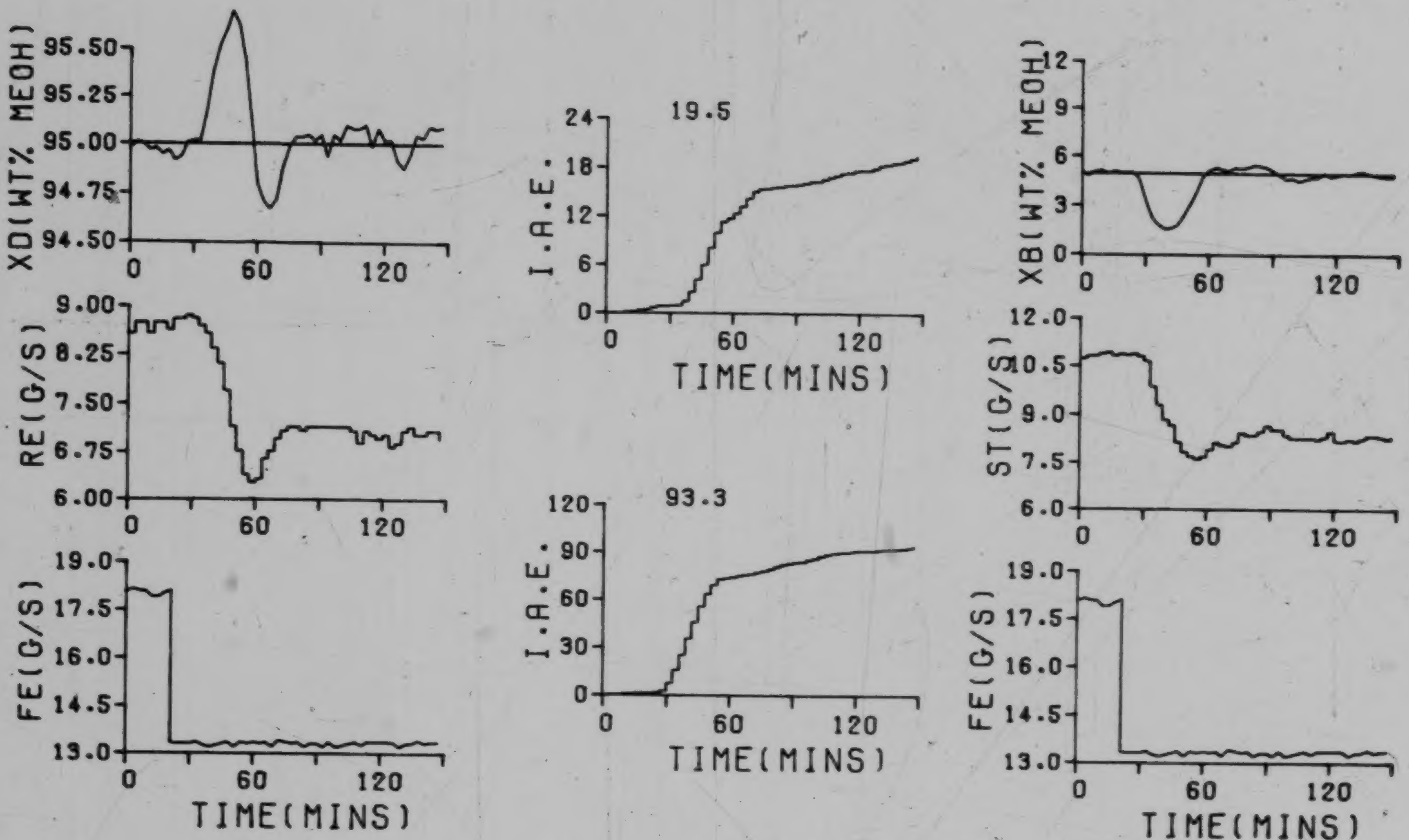

FIGURE 7.39 MV ST 3-C/Q(PB=34.466,TI=160.366,TD=0.0)/TS=180.0/4.3.3.0.4/
Q(PB=61.718,TI=238.3,TD=0.0)/TS=180.0/5.3.3.0.6/

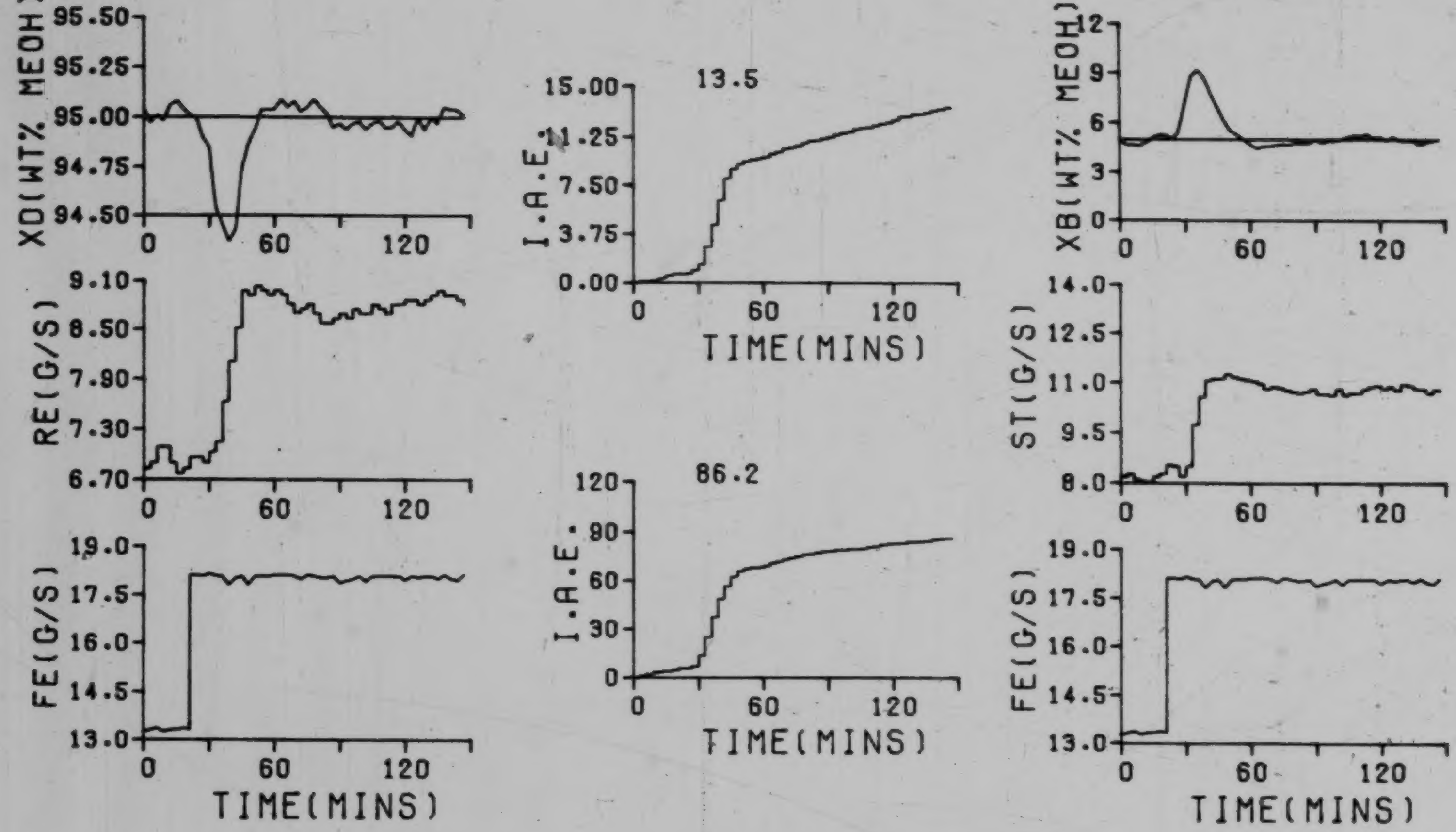

FIGURE 7.40 MV ST 3-C/G(PB=34.466,TI=160.366,TD=0.0)/TS=180.0/4,3,3,0,4/
G(PB=61.718,TI=238.3,TD=0.0)/TS=180.0/5,3,3,0,6/

Table 7.3.3
Multivariable Self-Tuning Control Performance with Q Weighting Constants Calculated from Integral of Absolute Error Equations

	IAE Values	
Step	TOP	BOTTOM
increase from steady state	12.5	80.6
decrease to steady state	12.9	78.6
decrease from steady state	24.4	97.8
increase to steady state	17.5	77.6
total	67.3	334.6

the four feed rate disturbances with the column operated under multivariable self-tuning control with the Q weighting parameters fixed on the basis of the integral of absolute error criterion are presented in Figures 7.41 to 7.44. Figure 7.41 presents the distillation column response to an increase in feed flow rate from its steady state value. Comparison of these results with those achieved using the multiloop PID control strategy (cf. Figures 7.9 to 7.12) show that the use of the self-tuning control has only lead to a marginal improvement in top composition control from 83.5 to 67.3. This is in sharp contrast to the significantly improved bottoms composition control which has reduced the total IAE value for all four step tests from 1045.8 to 334.6.

These results show that multivariable self-tuning control of the column with the Q weighting parameters

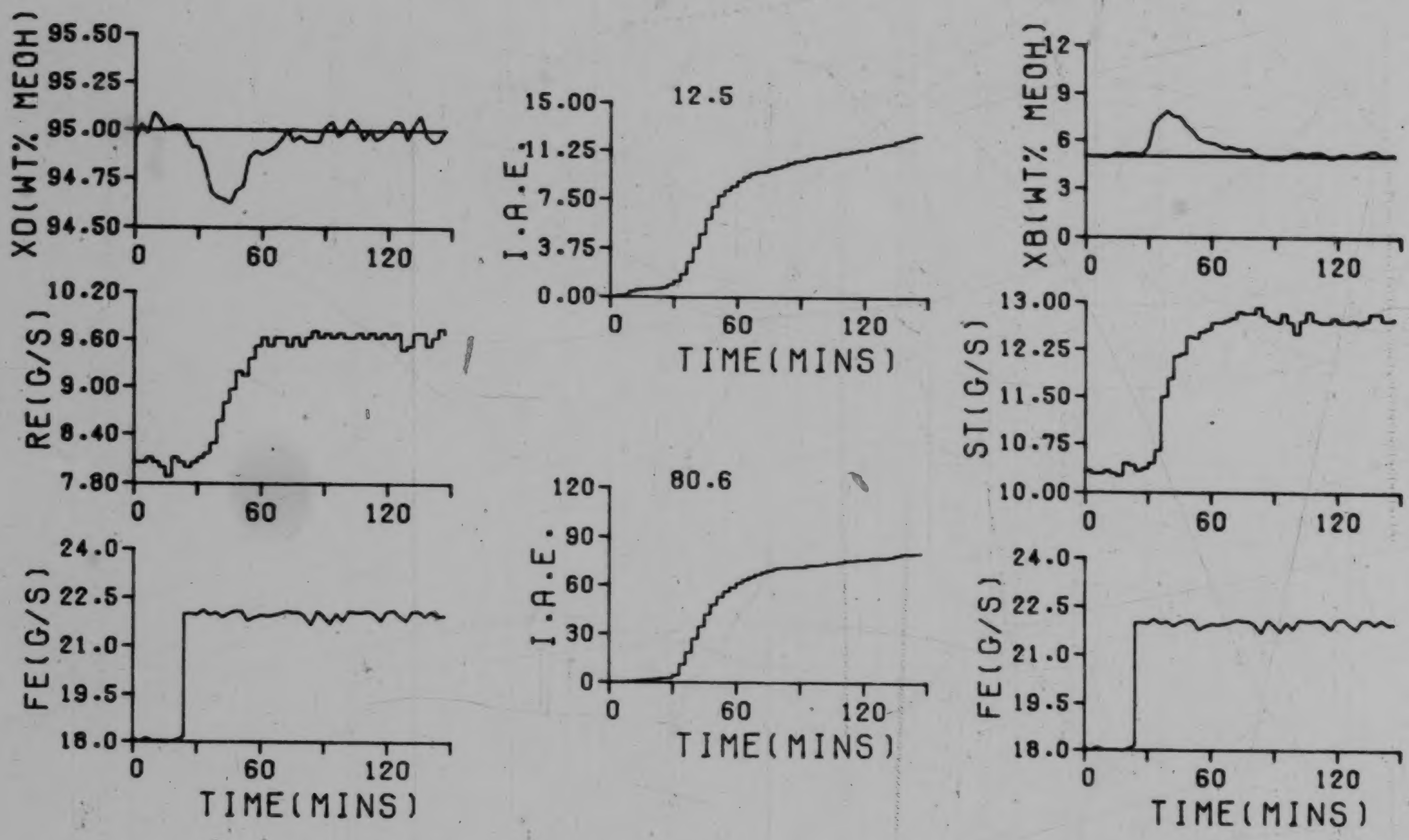

FIGURE 7.41 MV ST IAE/Q(PB=30.533,TI=234.0,TD=0.0)/TS=180.0/4.3.3.0.4/
Q(PB=52.636,TI=309.085,TD=0.0)/TS=180.0/5.3.3.0.6/

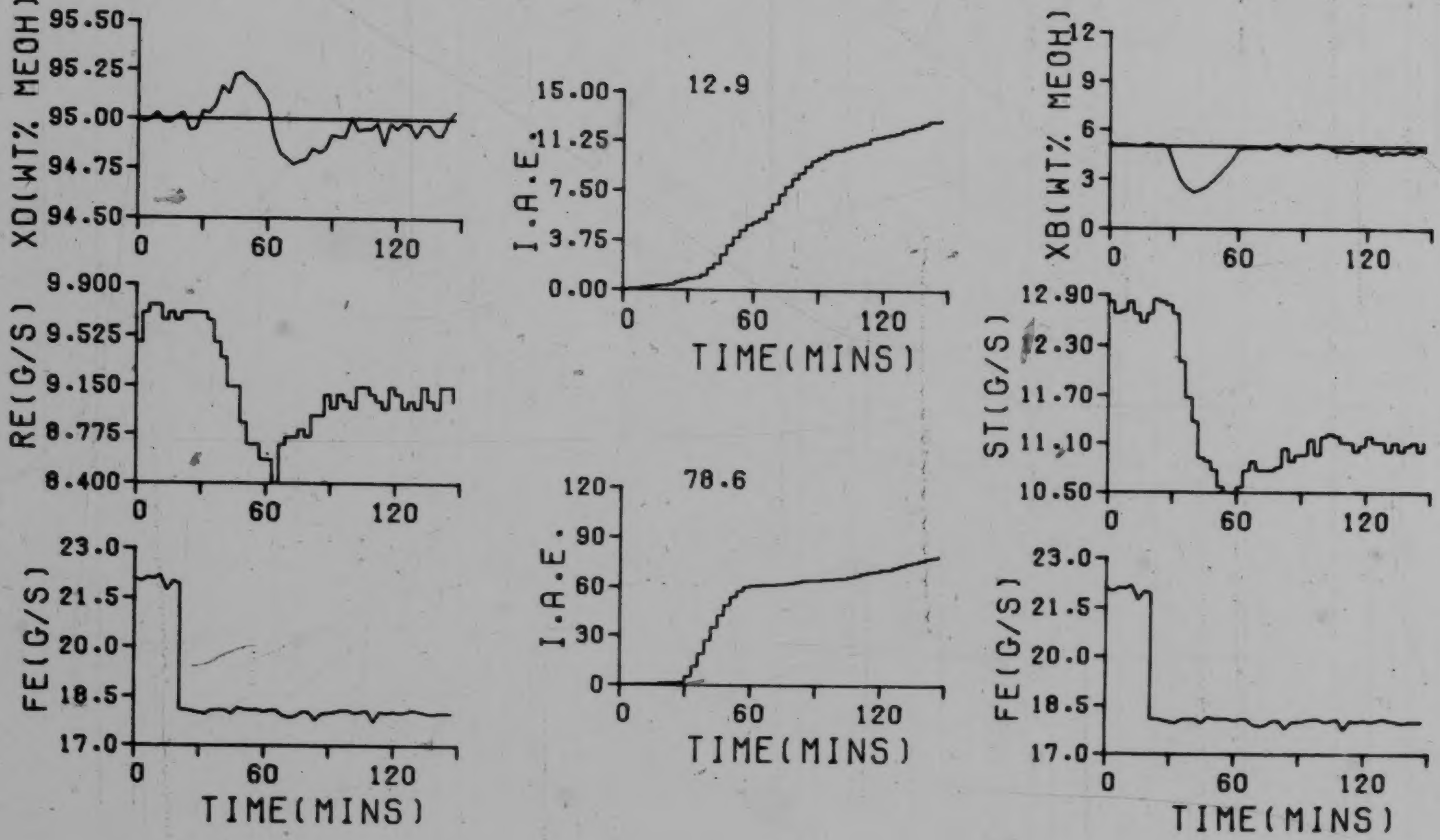

FIGURE 7.42 MV ST IAE/Q(PB=30.533,TI=234.0,TD=0.0)/TS=180.0/4.3.3.0.4/
Q(PB=52.636,TI=309.085,TD=0.0)/TS=180.0/5.3.3.0.6/

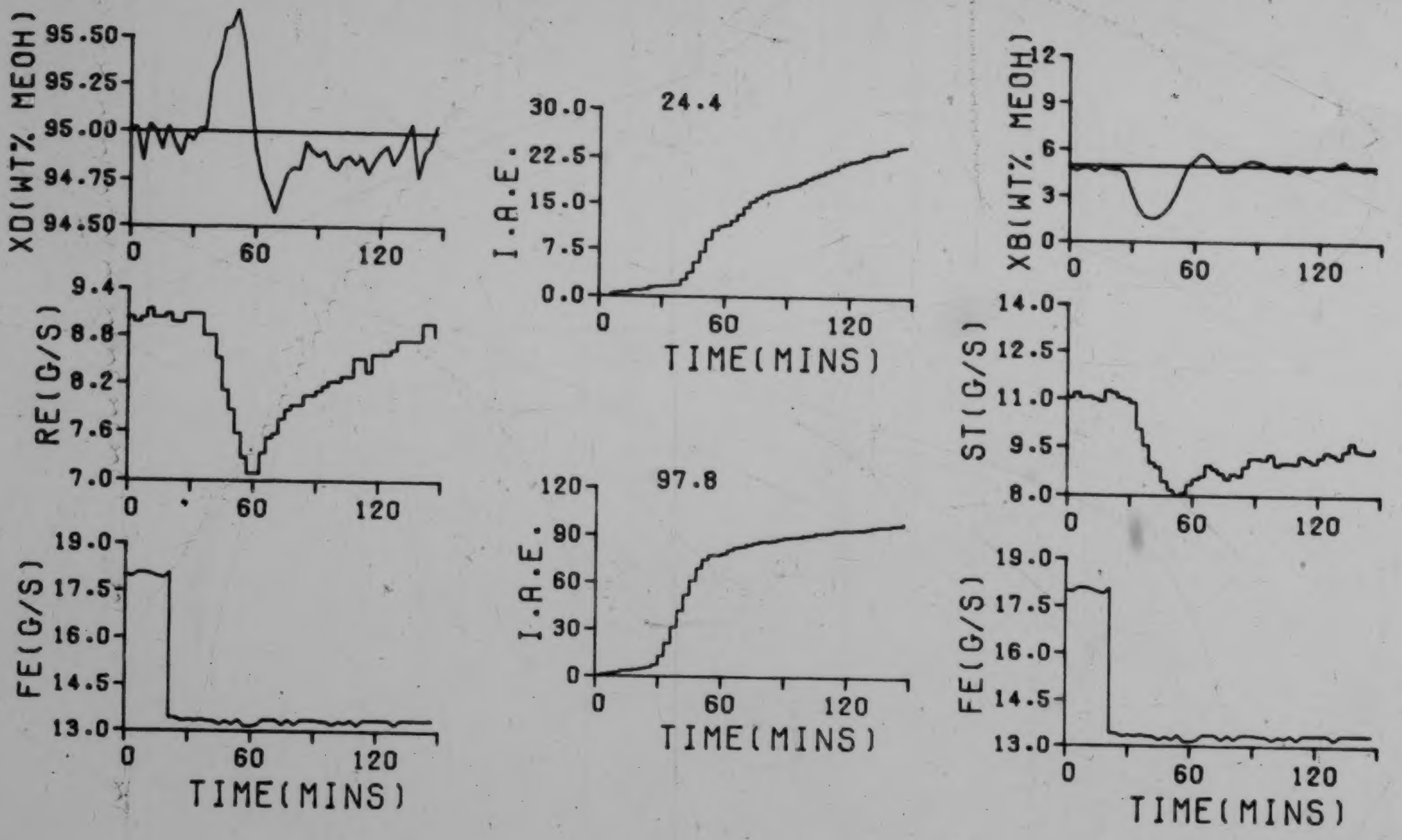

FIGURE 7.43 MV ST IAE/Q(PB=30.533,TI=234.0,TD=0.0)/TS=180.0/4.3.3.0.4/
Q(PB=52.636,TI=309.085,TD=0.0)/TS=180.0/5.3.3.0.6/

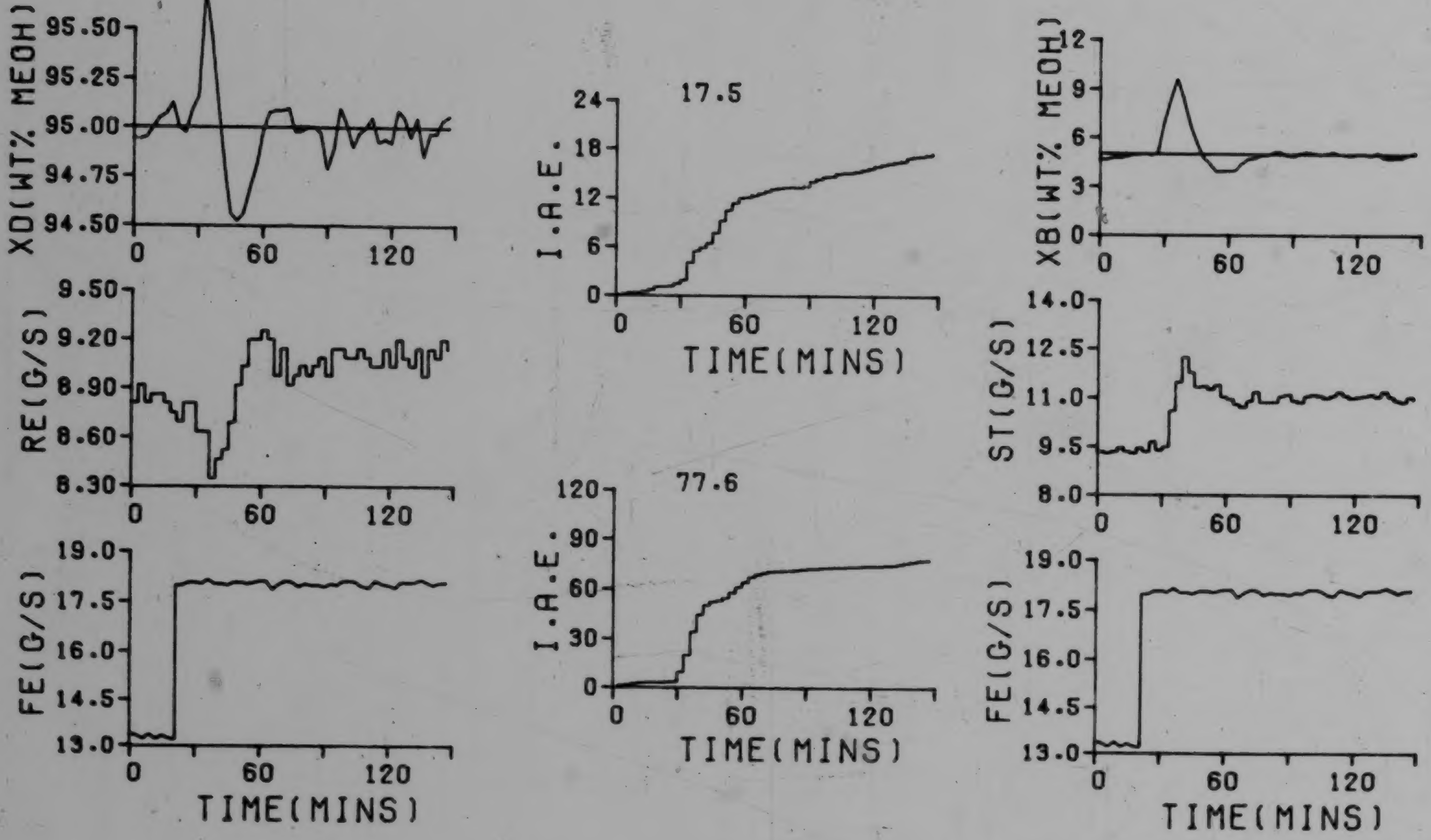

FIGURE 7.44 MV ST IAE/Q(PB=30.533,TI=234.0,TD=0.0)/TS=180.0/4.3.3.0.4/
Q(PB=52.636,TI=309.085,TD=0.0)/TS=180.0/5.3.3.0.6/

established by the integral of absolute error method, provide acceptable regulation of the top composition, and excellent bottom composition control.

7.3.4 Control Performance With Q Weighting Constants Calculated from the Integral of Time Multiplied by the Absolute Error Equations

Table 7.3.4 provides a summary of the IAE performance values for the tests of the self-tuning control performance of the pilot plant distillation column when operating with multivariable self-tuning control using Q weighting constants calculated with the ITAE criterion equations. The control behavior results obtained for the distillation column subjected to the feed rate changes when operated under multivariable self-tuning control with the Q weighting parameters calculated on the basis on the integral of time multiplied by the absolute error criterion are presented in Figures 7.45 to 7.48. Comparison of the results in Figures 7.45 and 7.46 with those in Figures 7.13 and 7.14 show that self-tuning control has reduced the top composition IAE values by nearly one third. However just as observed for the other tests of the self-tuning controller, use of this strategy has significantly improved regulation of bottom composition. The results in Figures 7.13 and 7.14 versus those in Figures 7.45 and 7.46 show that the IAE value has been decreased by a factor of four. Similar improvements can also be observed by comparing the results in Figures 7.47

Table 7.3.4
Multivariable Self-Tuning Control Performance with Q Weighting Constants Calculated from the Integral of Time Multiplied by the Absolute Error Equations

	IAE Values	
Step	TOP	BOTTOM
increase from steady state	10.0	78.5
decrease to steady state	11.7	82.6
decrease from steady state	23.3	105.2
increase to steady state	17.9	83.1
total	62.9	349.4

and 7.48 with those in Figures 7.15 and 7.16. A substantial improvement in composition control is evident when the IAE totals from Table 7.1.4 are compared with the results in Table 7.3.4, IAE totals for the top composition are reduced from 86.4 to 62.9, with bottom composition IAE totals reduced even further from 1158.2 to 349.4.

7.3.5 Comparison of The Effect of The Method of Selecting The Self-Tuning Controller Q Weighting Parameters on Column Performance

The IAE performance index for top and bottom composition responses from all the test results of Figures 7.33 to 7.48 and the total IAE for each of the four different step changes in feed rate are summarized in Table 7.3.5. Examination of these values reveals that for all four flow rate disturbances, the best control of top composition

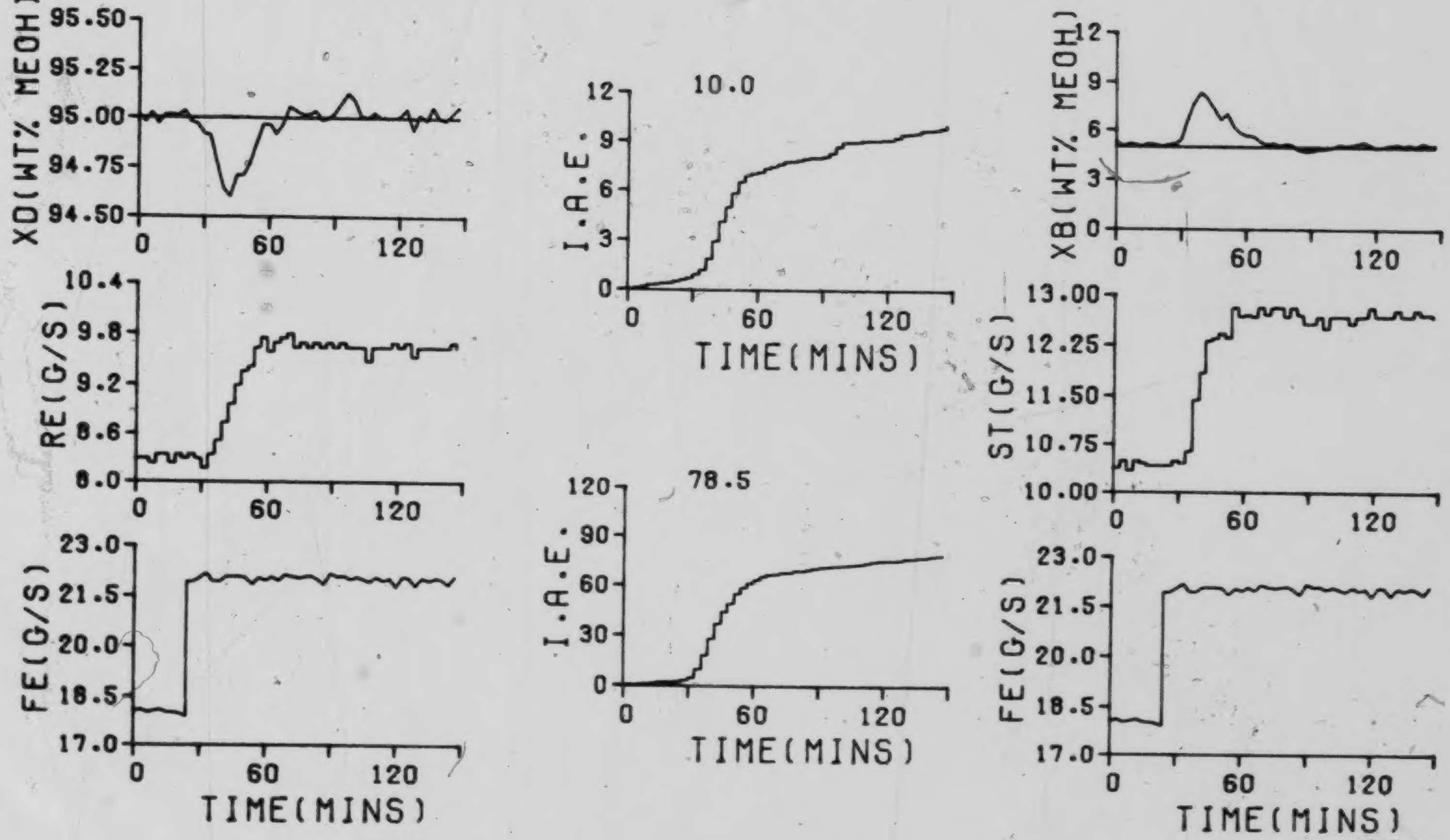

FIGURE 7.45 MV ST ITAE/Q(PB=35.472,TI=220.34,TD=0.0)/TS=180.0/4.3.3.0.4/
Q(PB=61.676,TI=298.602,TD=0.0)/TS=180.0/5.3.3.0.6/

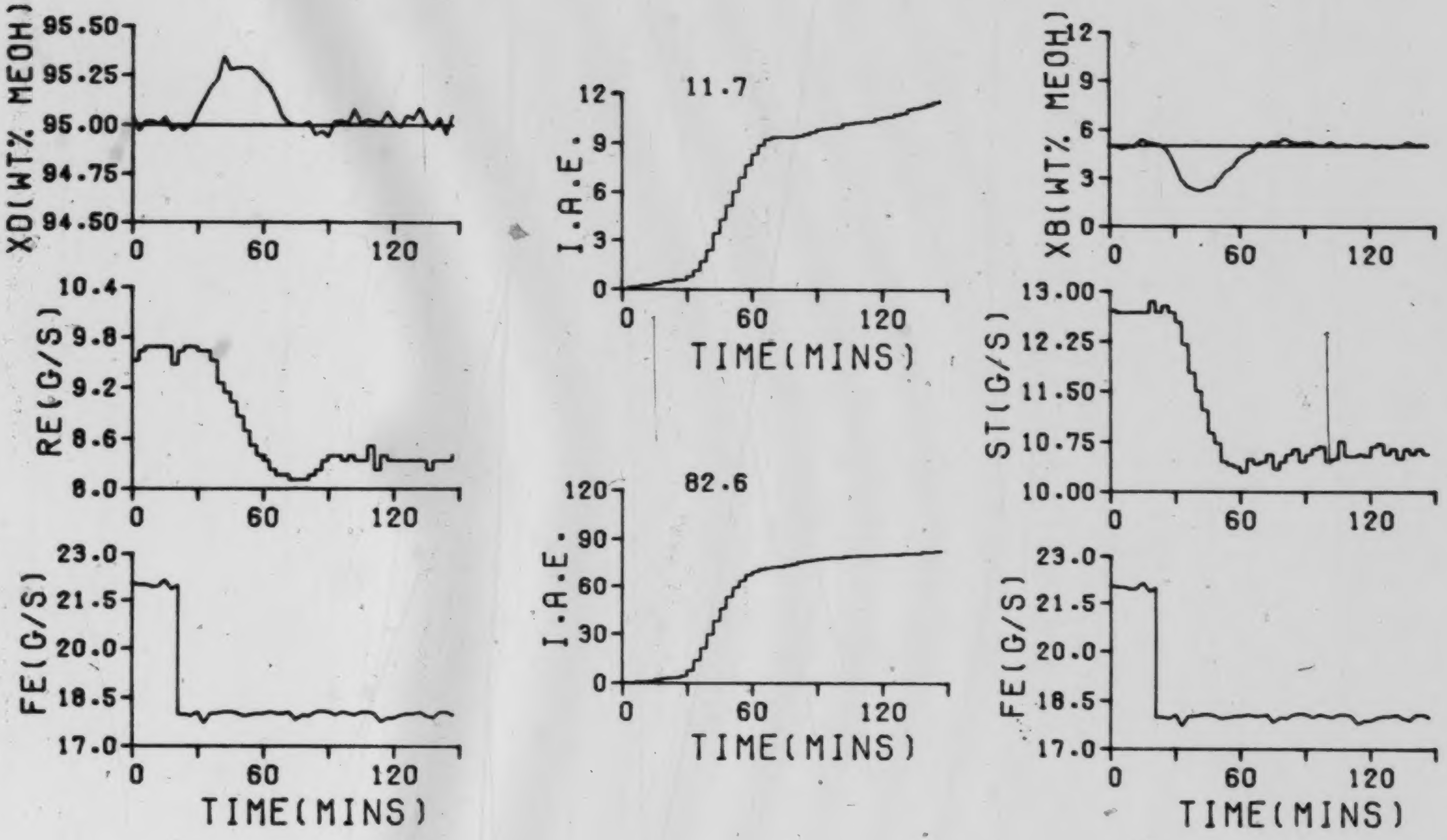

FIGURE 7.46 MV ST ITAE/Q(PB=35.472,TI=220.34,TD=0.0)/TS=180.0/4.3.3.0.4/
Q(PB=61.676,TI=298.602,TD=0.0)/TS=180.0/5.3.3.0.6/

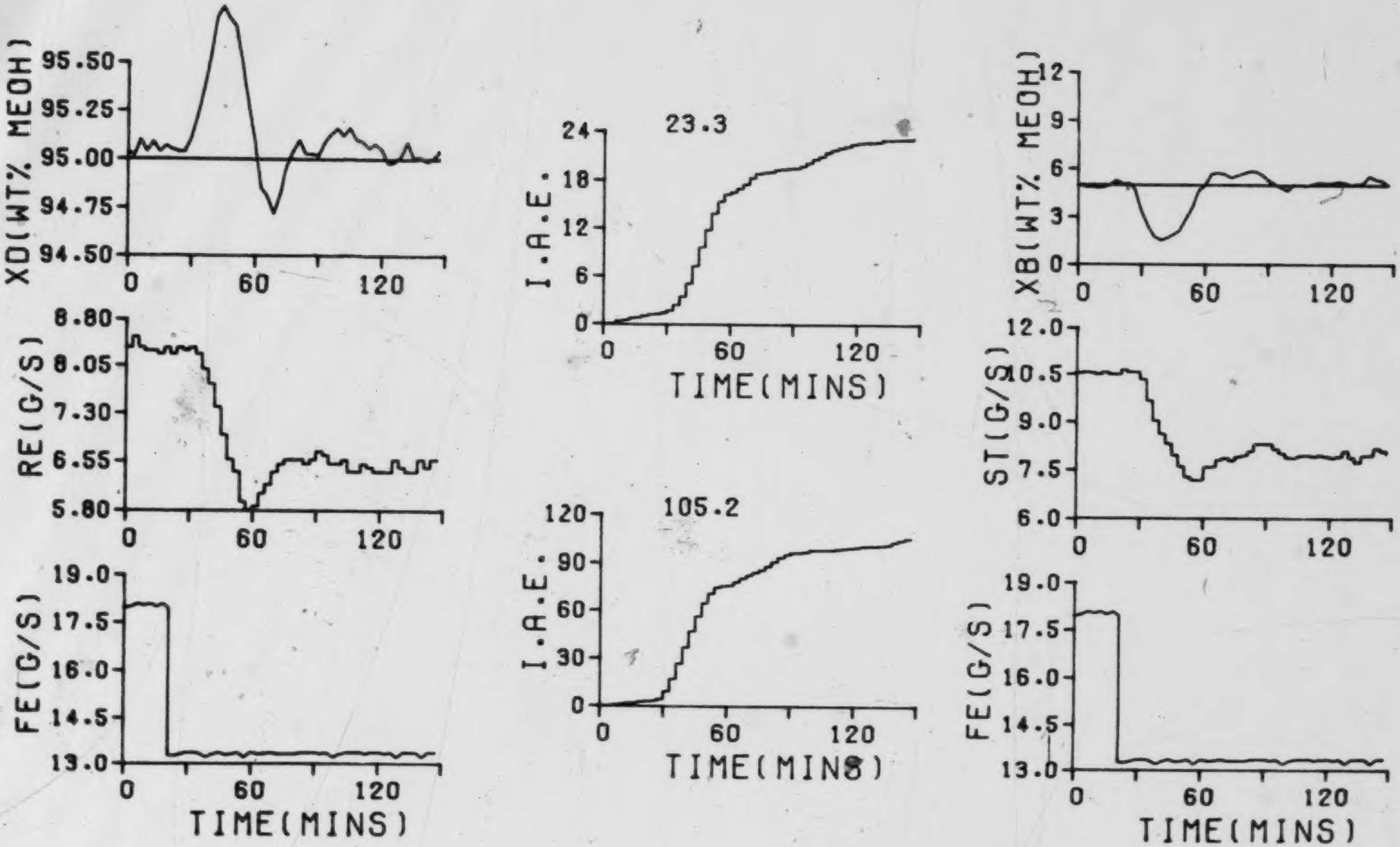

FIGURE 7.47 MV ST ITAE/Q(PB=35.472,TI=220.34,TD=0.0)/TS=180.0/4.3.3.0.4/
Q(PB=61.676,TI=298.602,TD=0.0)/TS=180.0/5.3.3.0.6/

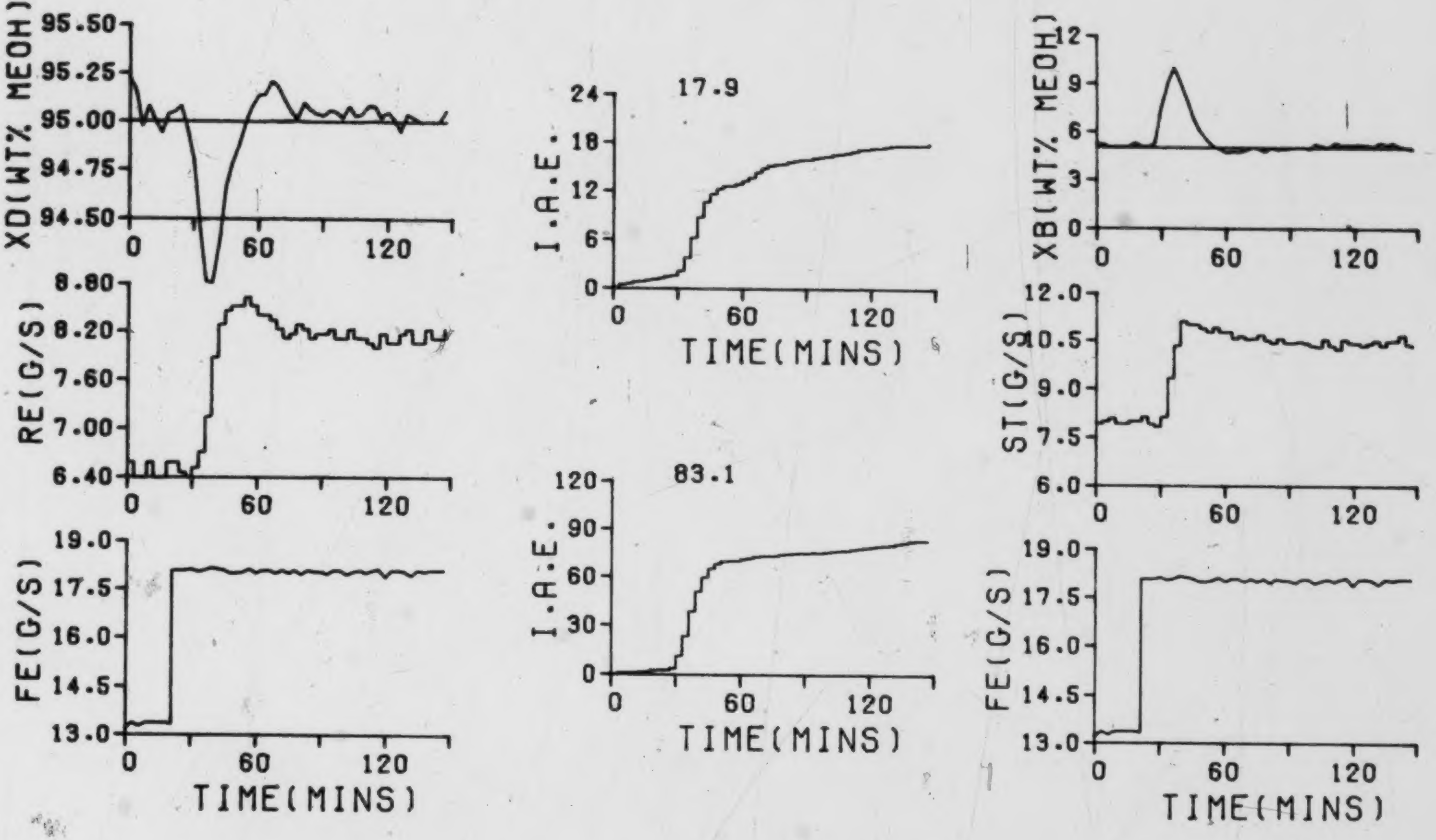

FIGURE 7.48 MV ST ITAE/Q(PB=35.472,TI=220.34,TD=0.0)/TS=180.0/4.3.3.0.4/
Q(PB=61.676,TI=298.602,TD=0.0)/TS=180.0/5.3.3.0.6/

Table 7.3.5
IAE values for the Multivariable Self-Tuning Control
Responses for initial parameter values

		IAE Totals by Method			
Step	loop	Z-N	3-C	IAE	ITAE
increase from SS	top	8.5	7.6	12.5	10.0
	bottom	97.3	61.4	80.6	78.5
decrease to SS	top	12.0	8.7	12.9	11.7
	bottom	88.0	72.8	78.6	82.6
decrease from SS	top	28.2	19.5	24.4	23.3
	bottom	119.0	93.3	97.8	105.2
increase to SS	top	19.4	13.5	17.5	17.9
	bottom	93.0	86.2	77.6	83.1
total		465.4	363.0	401.9	412.3

is achieved using the Cohen-Coon method of selecting the Q weighting parameters for the self-tuning controllers. Furthermore, only for one feed disturbance did this method of selecting the Q weighting parameters not provide the best control of the bottom composition. It is therefore not surprising as shown by the total IAE value for top and bottom composition, for the four different feed rate disturbances, that the Cohen-Coon method of selecting the Q weighting parameters provides the best control performance. It is very important to note that even though use of the Ziegler-Nichols rules for selecting the Q weighting parameters results in the poorest control performance for this series of tests, the IAE value does represent a substantial improvement in column control behavior when compared with the IAE value of 1511.2 obtained using the Ziegler-Nichols rules for selecting the controller constants for the multiloop PID control strategy tests (cf Table 7.1.5). The initial deviation of the bottom composition from the setpoint resulting from the feed flow rate disturbance occurred for these tests of the multivariable self-tuning controller just as for the tests of the multiloop PID strategy. The magnitude of the deviations have been reduced for this series of tests by including estimated feedforward compensation in the control algorithm (cf. equation 7.1). However, to reduce (and possibly eliminate) this deviation, direct feedforward compensation would be required.

7.4 Evaluation of Multivariable Self-Tuning Control Using Multirate Sampling for Column Control

Just as for the series of tests of the multiloop PID control strategy using multirate sampling, this series of tests was undertaken to evaluate control behavior using multirate sampling for the multivariable self-tuning control strategy. The studies were performed with a top composition sample time of 1.0 minute and a bottom composition sample time of 3.0 minutes.

The multirate form of the self-tuning control algorithm, because of its inherent decoupling action requires the identification of interaction polynomials. With the top composition control accomplished at 60.0 second intervals, there are three control actions for the top loop for every control calculation of the bottom loop controller. This now requires the determination of the inputs to the observation vector which will determine the G_{ij} polynomial. For this study the input for the bottom loop interaction polynomial G_{21} was set to be the average of the last three control actions including the control action at time t.

$$u_1(t-k_{12}) = \sum_{i=0}^{2} \frac{u_1(t-i)}{3} \qquad (7.2)$$

Equation 7.2 provides the inputs required to formulate the observation vector given by equation 3.70 for the bottom controller identification [Nazer, 1981; Tham 1985] with $u_j(t-k_{ij})$ replaced by $u_1(t-k_{12})$ from equation 7.2. The current control action, at time t can be used in the identification algorithm since, the value is not required for calculations until the delay k_{12} has occurred.

7.4.1 Control Performance with Q Weighting Constants Calculated With The Ziegler-Nichols Equations

Table 7.4.1 provides a summary of the IAE values for the tests of the self-tuning control performance of the pilot plant distillation column when subjected to feed disturbances while under control using the multirate self-tuning control algorithm employing Q weighting

Table 7.4.1
Multirate Self-Tuning Control Performance with Q Weighting Constants Calculated with Ziegler-Nichols Equations

	IAE Values	
Step	TOP	BOTTOM
increase from steady state	8.3	116.1
decrease to steady state	17.1	72.6
decrease from steady state	13.2	109.6
increase to steady state	18.8	70.3
total	57.4	368.6

constants calculated with the Ziegler-Nichols equations. The control behavior of the distillation column for all four feed disturbances using the multirate self-tuning control strategy with Q weighting parameters based on the Ziegler-Nichols rules is shown in Figures 7.49 through 7.52. For the increase in feed flow rate from its steady state value the top composition only deviates from the setpoint for the initial period of the disturbance as can be seen from the response in Figure 7.49. The changes in the reflux flow rate indicate a large amount of interaction from the steam flow.

Figure 7.50 presents the results of the distillation column control performance for a decrease in feed flow to its steady state value. It can be seen that the top composition IAE value of 17.1, resulting from the oscillations is more than double the value for the previous test when the feed rate was increased. Examination of the

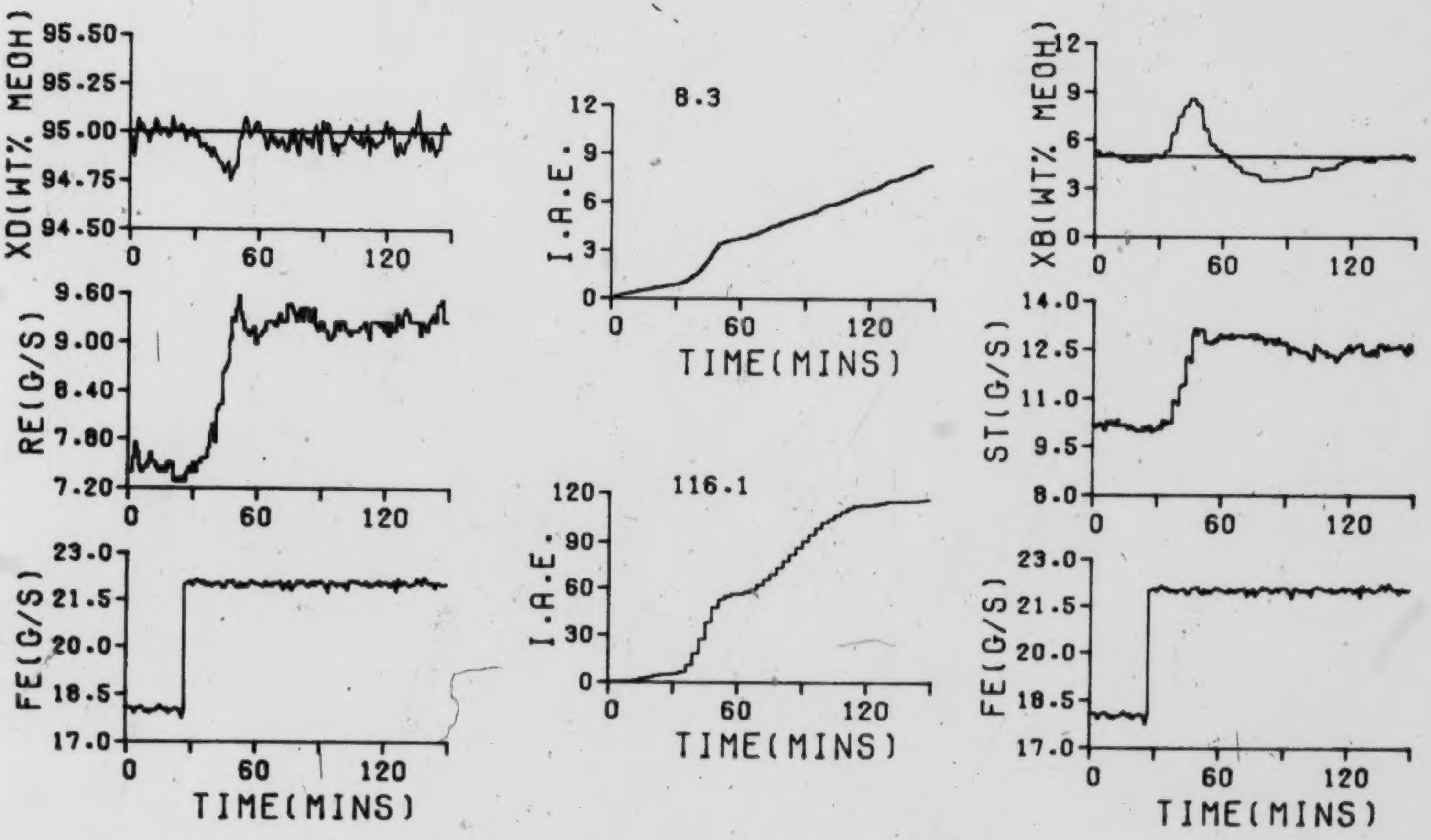

FIGURE 7.49 MR ST Z-N/Q(PB=10.886,TI=99.99,TD=0.0)/TS=60.0/4.3.3.0.4/
Q(PB=55.559,TI=299.97,TD=0.0)/TS=180.0/5.3.3.0.6/

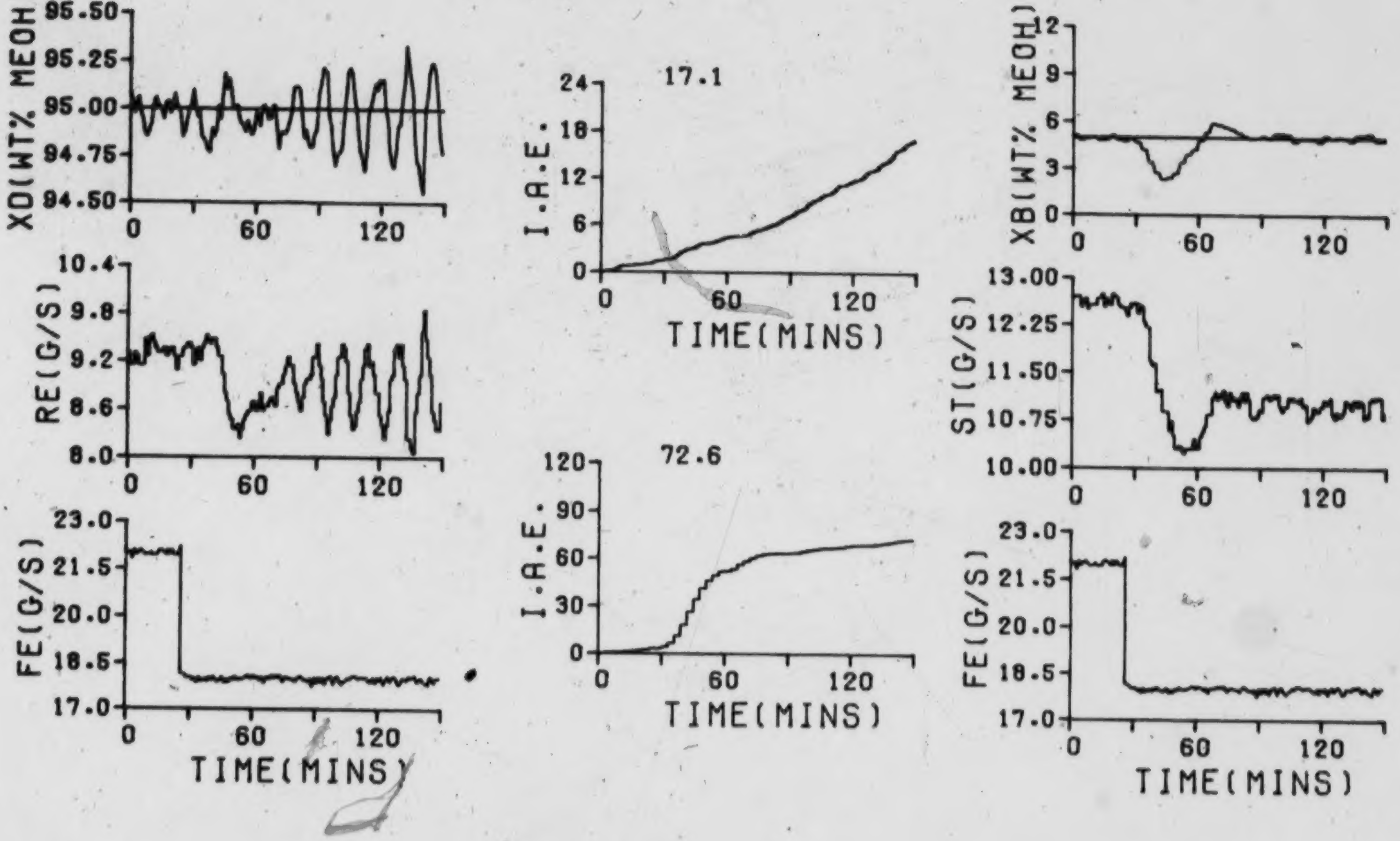

FIGURE 7.50 MR ST Z-N/Q(PB=10.886,TI=99.99,TD=0.0)/TS=60.0/4.3.3.0.4/
Q(PB=55.559,TI=299.97,TD=0.0)/TS=180.0/5.3.3.0.6/

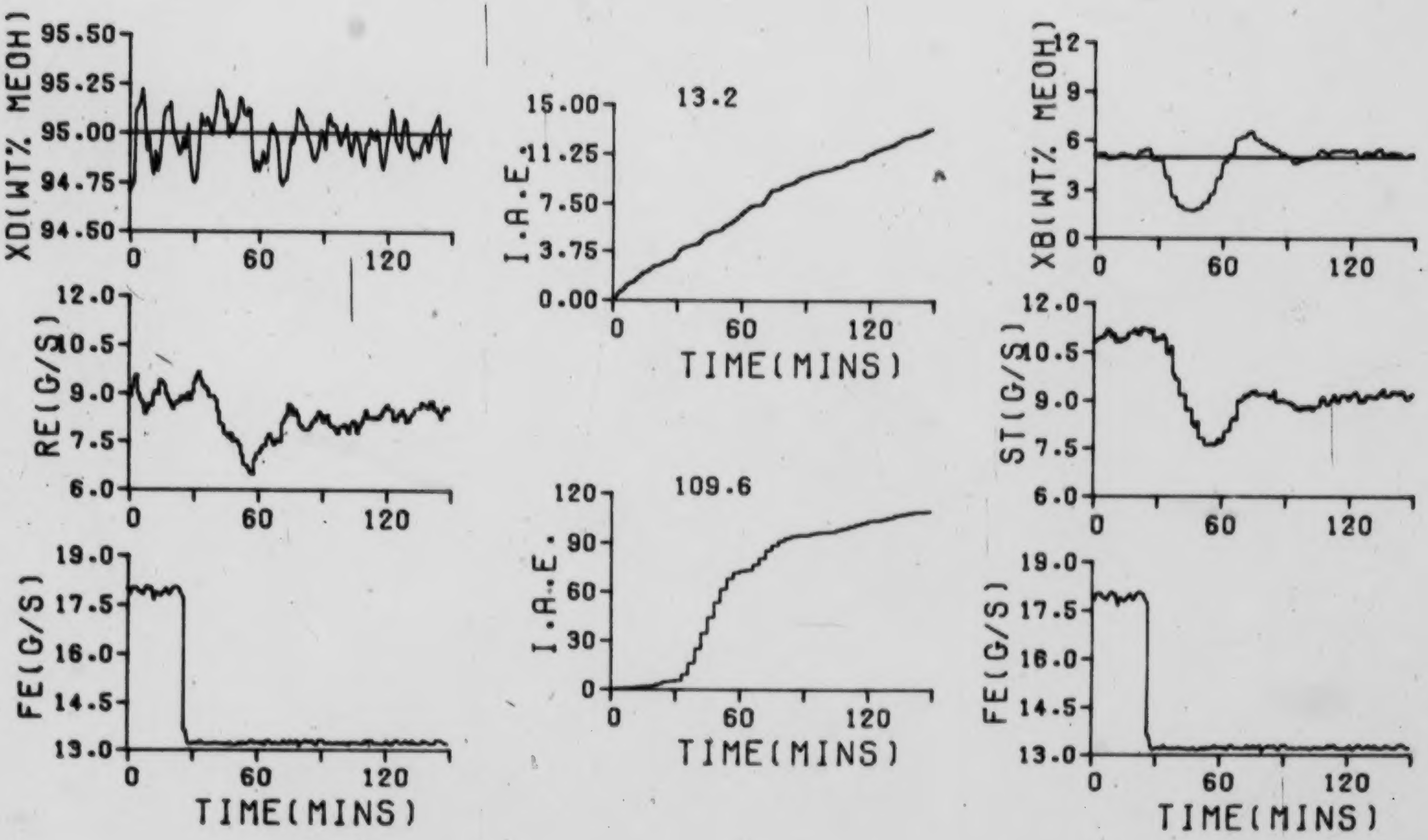

FIGURE 7.51 MR ST Z-N/Q(PB=10.886,TI=99.99,TD=0.0)/TS=60.0/4.3.3.0.4/
Q(PB=55.559,TI=299.97,TD=0.0)/TS=180.0/5.3.3.0.6/

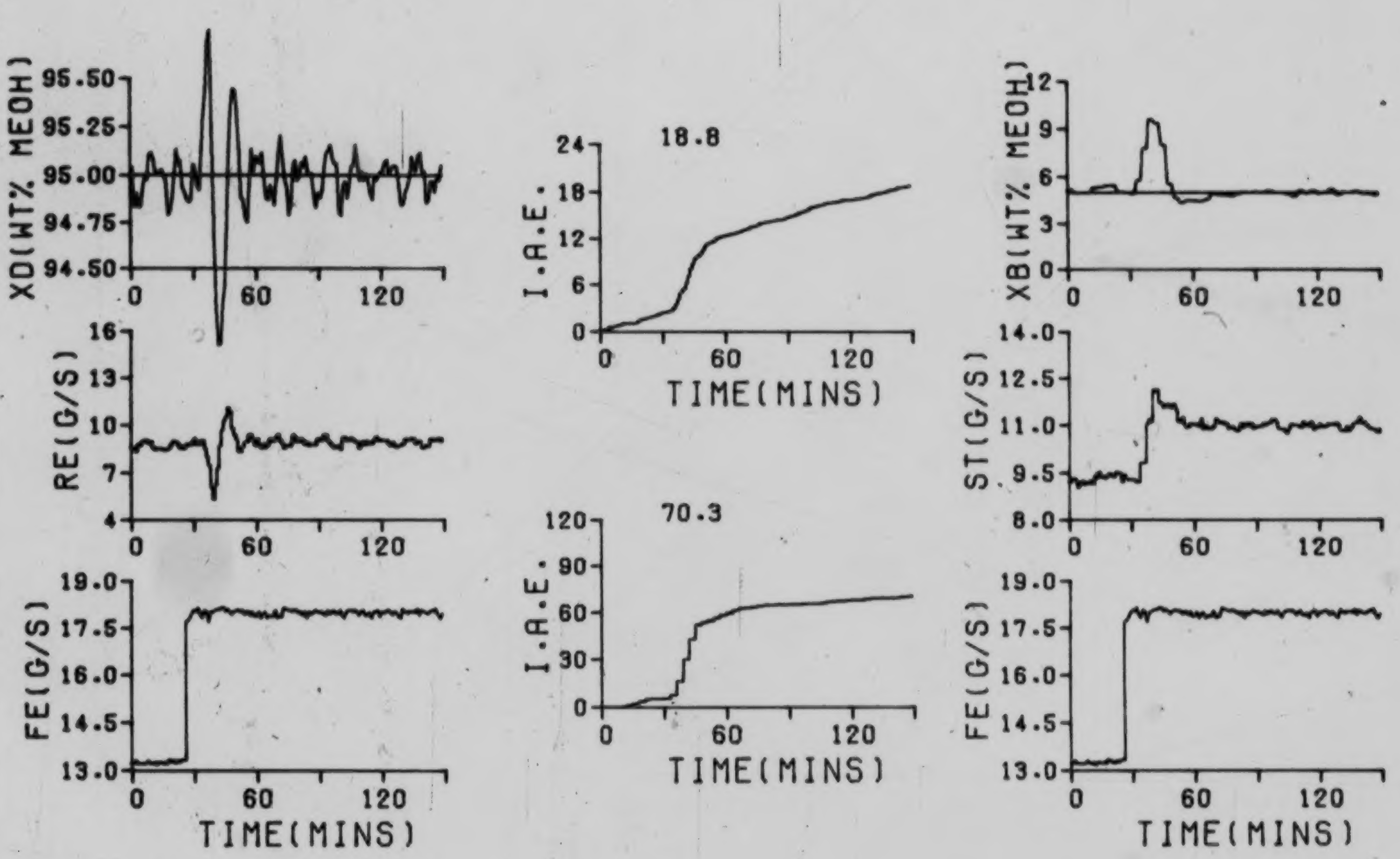

FIGURE 7.52 MR ST Z-N/Q(PB=10.886.TI=99.99.TD=0.0)/TS=60.0/4.3.3.0.4/
Q(PB=55.559.TI=299.97.TD=0.0)/TS=180.0/5.3.3.0.6/

first portion of Figure 7.51 shows that the oscillations which appeared in Figure 7.50 to be increasing in magnitude did decrease prior to the next feed change. This oscillatory behavior was attributed to the combination of high gain and large amount of integral action in the Q weighting parameters. Bottom composition control is very satisfactory showing only an initial deviation from the setpoint followed by a small overshoot when returning to the setpoint resulting in an IAE value of only 72.6.

Regulation of the top composition for a decrease in feed flow from its steady state seems to be unaffected by the inverse dynamic response characteristics that seemed to affect control performance in the previous tests of other algorithms as can be observed from Figure 7.51.

As for the previous tests, when feed flow is increased back to its steady state value, control of top composition has been shown to be difficult which is borne out by the results presented in Figure 7.52. This is reflected by the high IAE value of 18.8 caused by the rapid changes in steam flow. The sharp increase in top composition may also be caused by some interaction from the condenser level control loop.

Comparison of the results of the four tests using multirate sampling with Q weighting parameters selected by the Ziegler-Nichols rules, with those using a single sample interval of 3.0 minutes shows that there has only been a marginal improvement in the control behavior.

7.4.2 Control Performance with Q Weighting Constants Calculated by the Cohen-Coon Equations

Table 7.4.2 provides a summary of the IAE values for the tests of the self-tuning control performance of the pilot plant distillation column when subjected to feed disturbances while under multirate self-tuning control using Q weighting constants in the control algorithm which were calculated with the Cohen-Coon equations. The column performance for the four feed flow changes is displayed in Figures 7.53 through 7.56. Comparing the composition responses and IAE values given in Figure 7.53 with those in Figure 7.37 reveals that use of multirate rather than single rate sampling has not improved the control behavior. This is attributed to the large amount of integral action which tends to lead to oscillatory responses.

Comparison of the composition responses in Figures 7.54 to 7.56 with those in Figures 7.38 to 7.40 shows that for the other three feed flow rate disturbances, that regulation of top composition has improved by the use of multirate sampling. This is not the case for the control of the bottom composition as the IAE values that resulted from the tests using the multirate sampling form of the algorithm (cf. Figures 7.53 to 7.56, Table 7.4.2) were all higher than when only single rate sampling was employed (cf. Figures 7.37 to 7.40, Table 7.3.2).

The column composition responses using multirate self-tuning control for Q weighting parameters based on the

Table 7.4.2
Multirate Self-Tuning Control Performance with Q Weighting Constants Calculated with Cohen-Coon Equations

	IAE Values	
Step	TOP	BOTTOM
increase from steady state	10.0	85.7
decrease to steady state	7.8	85.5
decrease from steady state	15.1	139.5
increase to steady state	9.3	95.1
total	42.2	405.8

Cohen-Coon equations tend to be characterized by a quick return of the composition to the setpoint followed by overshoot. This response pattern is attributed to the high integral action provided by the Q weighting parameters.

7.4.3 Control Performance with Q Weighting Constants Calculated By Integral of Absolute Error Equations

Table 7.4.3 provides a summary of the IAE values for the tests of the self-tuning control performance of the pilot plant distillation column when subjected to feed disturbances while under multirate self-tuning control with Q weighting constants calculated from the IAE criterion equations. The control behavior that resulted using these Q weighting parameters is displayed in Figures 7.57 through 7.60. As can be seen by comparing the top composition responses in Figures 7.41 to 7.44 with those in Figures 7.57 to 7.60, it can be observed that the use of the multirate

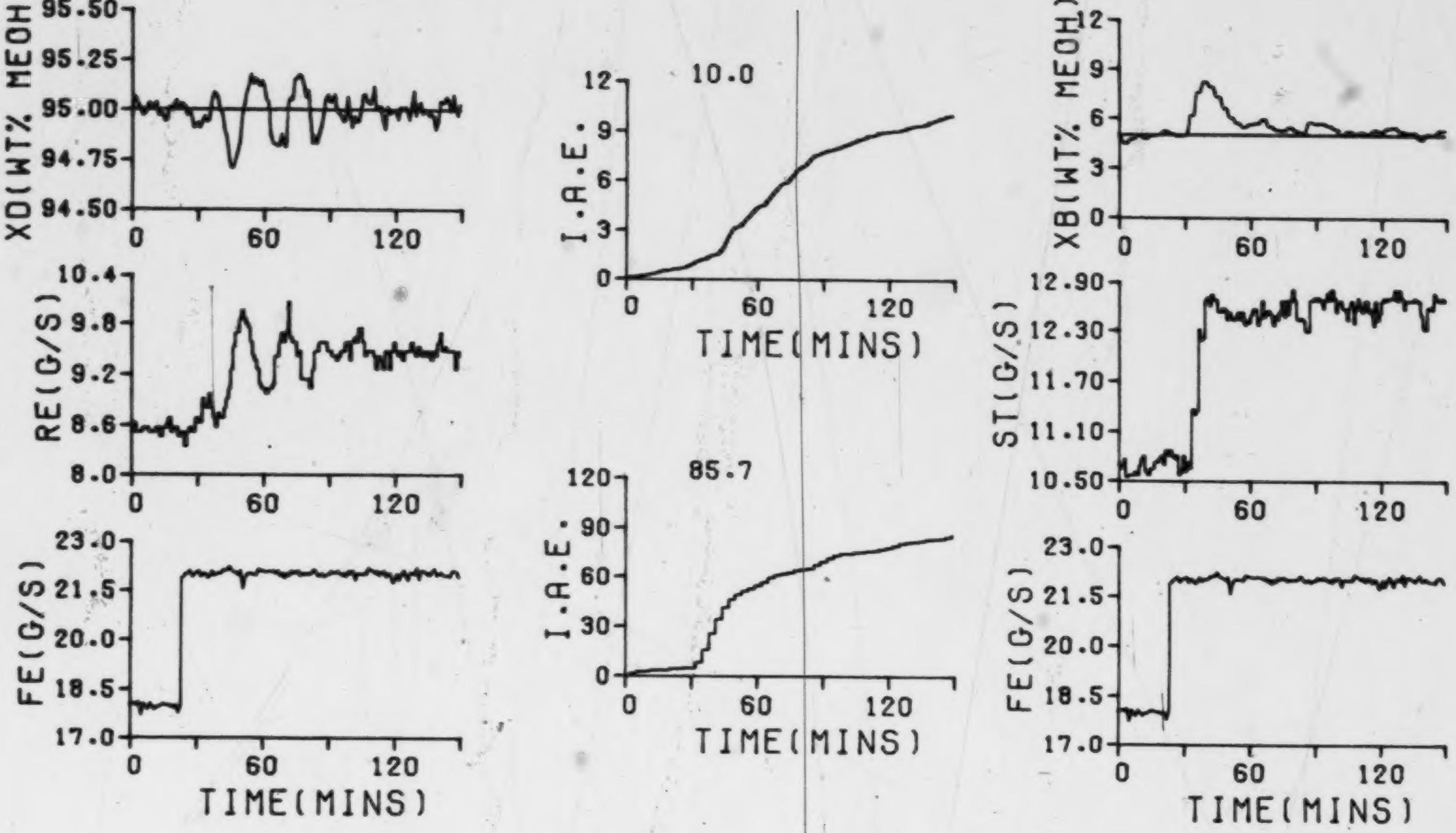

FIGURE 7.53 MR ST 3-C/Q(PB=12.191,TI=84.518,TD=0.0)/TS=60.0/4,3,3,0,4/
Q(PB=61.718,TI=238.3,TD=0.0)/TS=180.0/5,3,3,0,6/

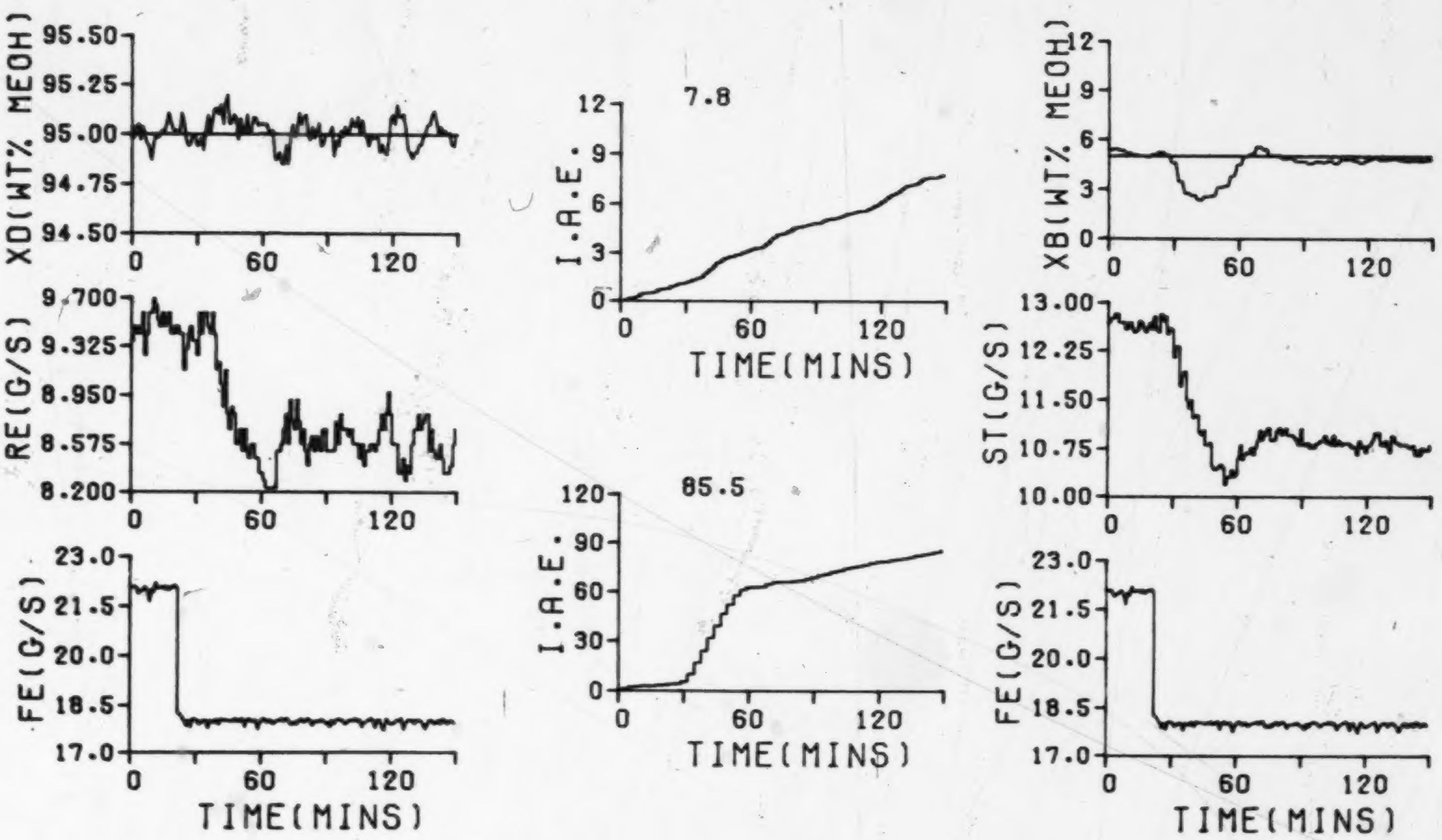

FIGURE 7.54 MR ST 3-C/Q(PB=12.191.TI=84.518.TD=0.0)/TS=60.0/4.3.3.0.4/
Q(PB=61.718.TI=238.3.TD=0.0)/TS=180.0/5.3.3.0.6/

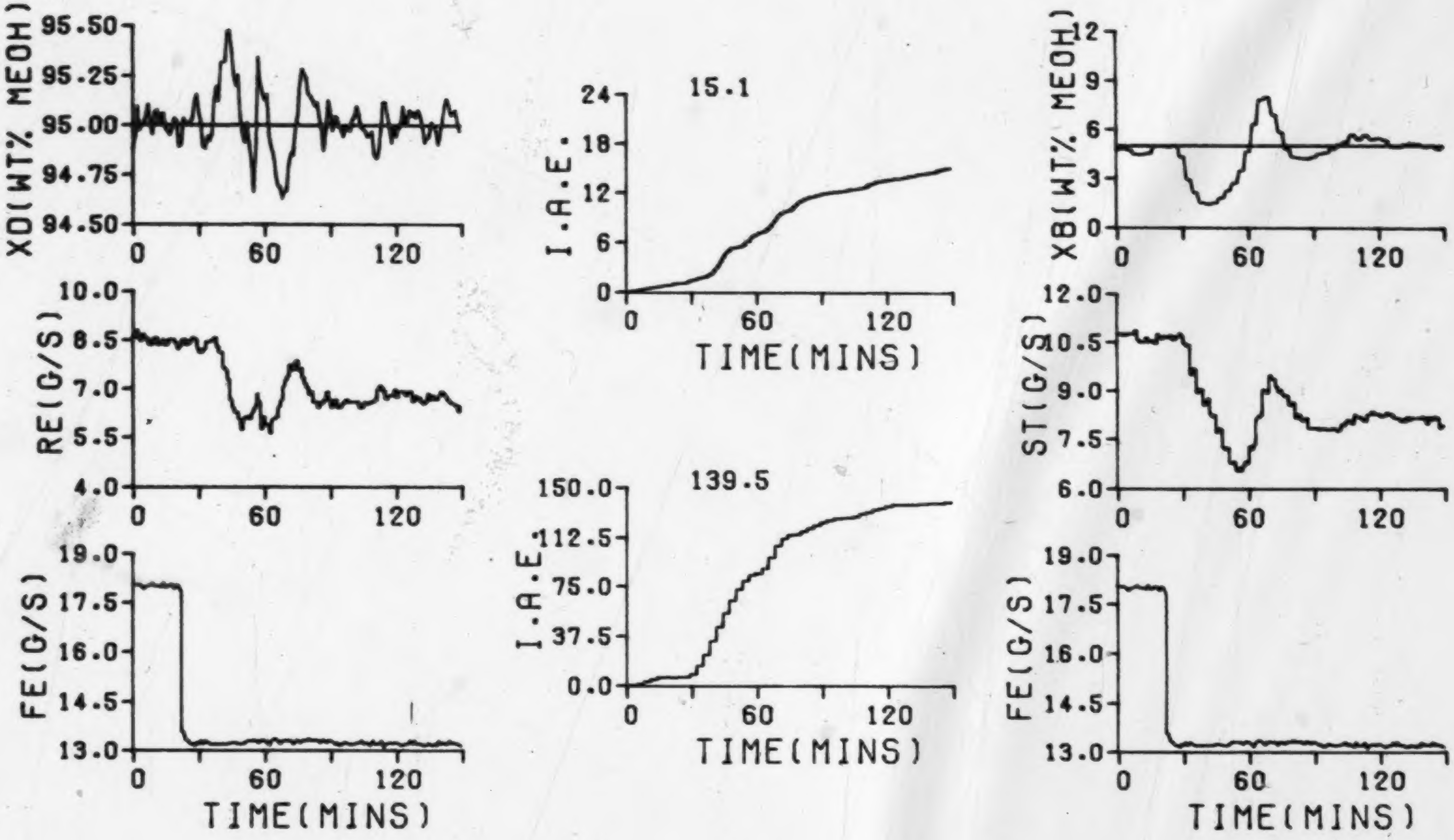

FIGURE 7.55 MR ST 3-C/Q)PB=12.191.TI=84.518.TD=0.0)/TS=60.0/4.3.3.0.4/
Q(PB=61.718.TI=238.3.TD=0.0)/TS=180.0/5.3.3.0.6/

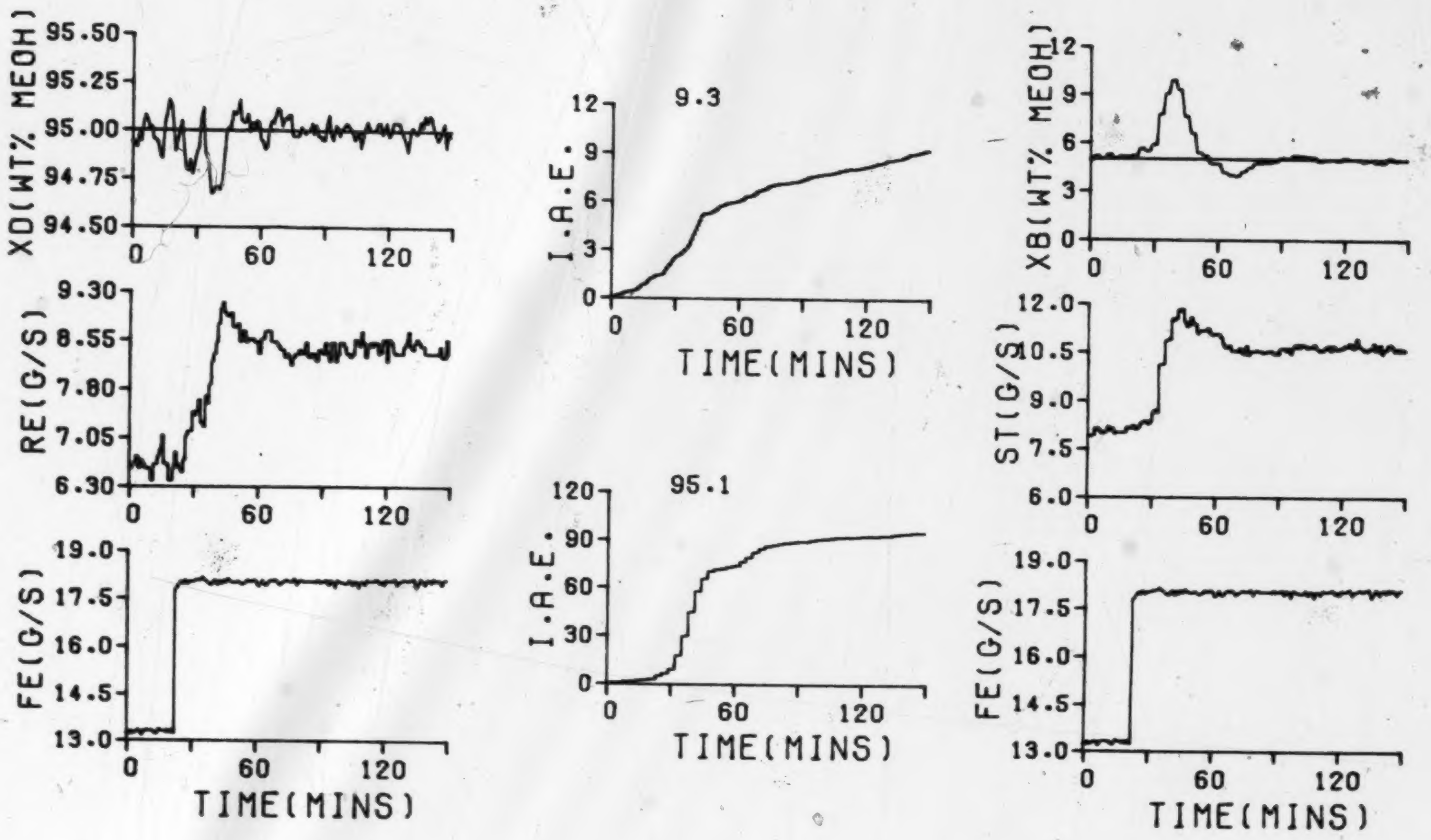

FIGURE 7.56 MR ST 3-C/Q(PB=12.191.TI=84.518.TD=0.0)/TS=60.0/4.3.3.0.4/
Q(PB=61.718.TI=238.3.TD=0.0)/TS=180.0/5.3.3.0.6/

Table 7.4.3
Multirate Self-Tuning Control Performance with Q Weighting Constants Calculated with Integral of Absolute Error Equations

	IAE Values	
Step	TOP	BOTTOM
increase from steady state	6.0	78.3
decrease to steady state	5.6	65.4
decrease from steady state	8.8	116.0
increase to steady state	9.2	97.2
total	29.6	356.9

sampling form of the algorithm has reduced the IAE value by at least 50%. Analysis of the IAE values for the bottom composition responses in Tables 7.3.3 with those in Table 7.4.3 reveals that multirate sampling leads to a marginal reduction in the IAE value for the feed rate changes above the steady state rate but not for the other feed rate changes. The IAE value for the step decrease in feed rate from the steady state rate has increased from 97.8 to 116.0 and for the step back to the steady state, the increase is from 77.6 to 97.2. In general, both the top and bottom compositions return quickly to their setpoints after the onset of the disturbance with little overshoot.

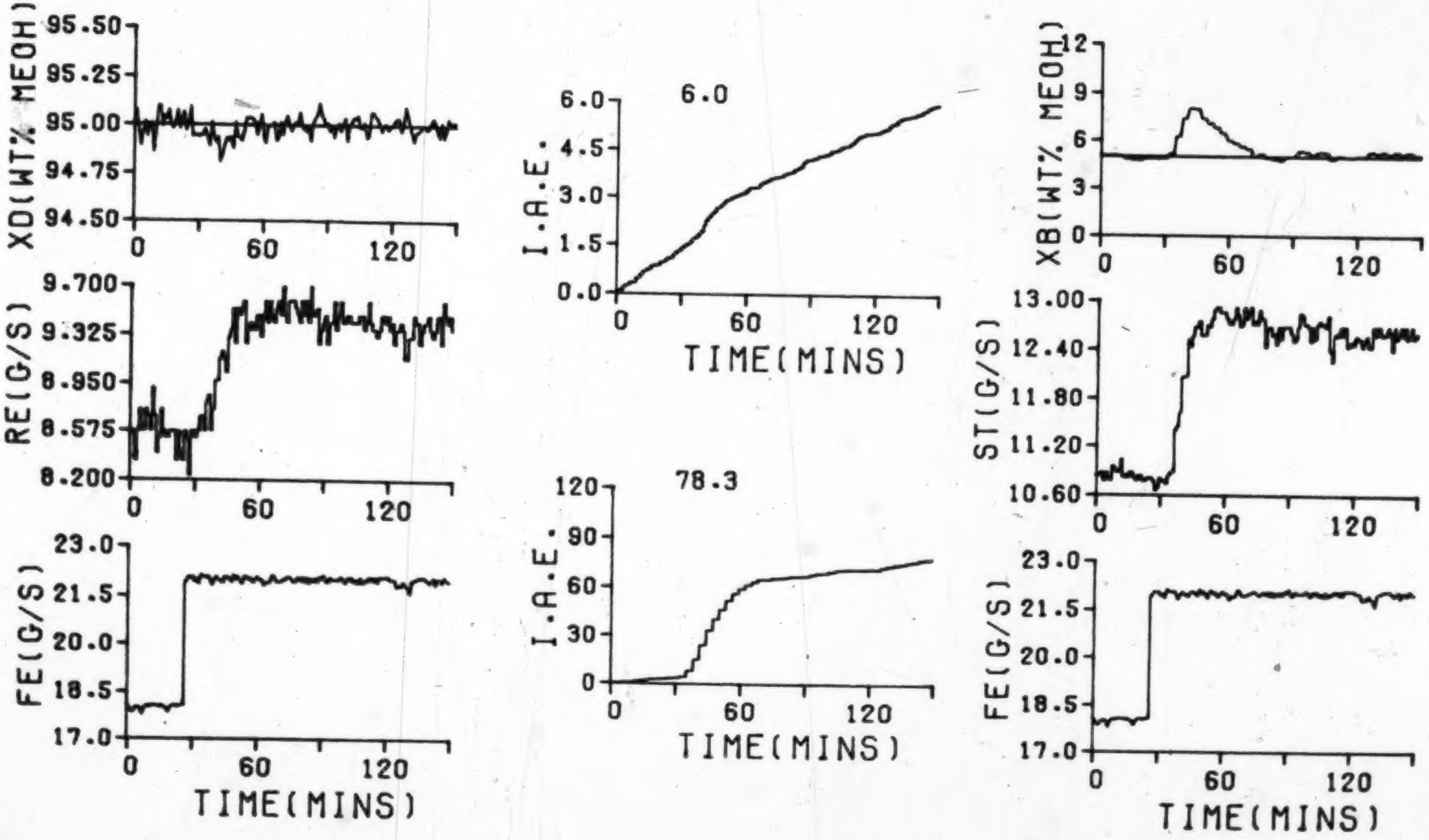

FIGURE 7.57 MR ST IAE/Q(PB=10.335,TI=107.62,TD=0.0)/TS=60.0/4.3.3.0.4/
Q(PB=52.636,TI=309.085,TD=0.0)/TS=180.0/5.3.3.0.6/

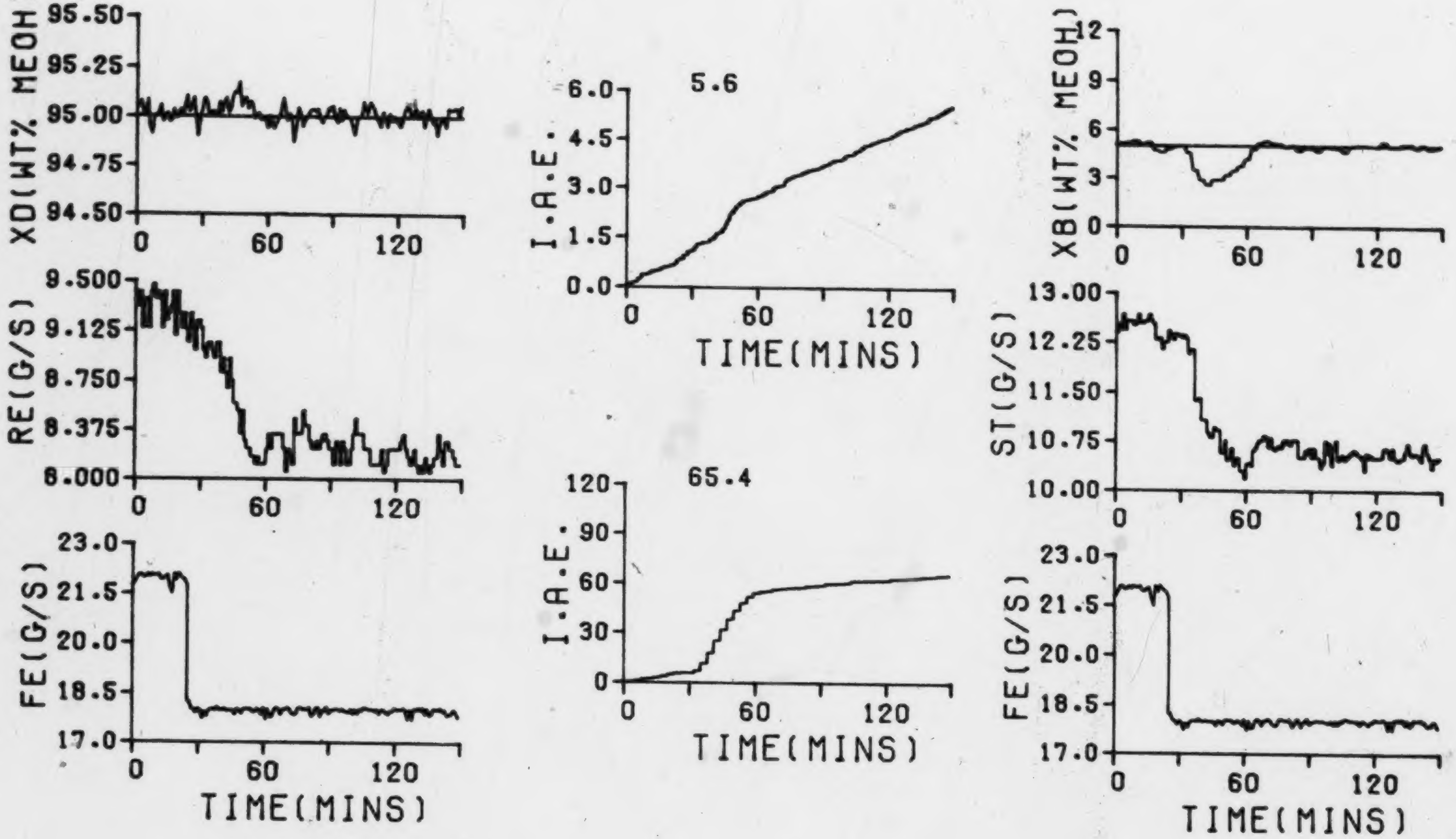

FIGURE 7.58 MR ST IAE/Q(PB=10.335,TI=107.62,TD=0.0)/TS=60.0/4.3.3.0.4/
Q(PB=52.636,TI=309.085,TD=0.0)/TS=180.0/5.3.3.0.6/

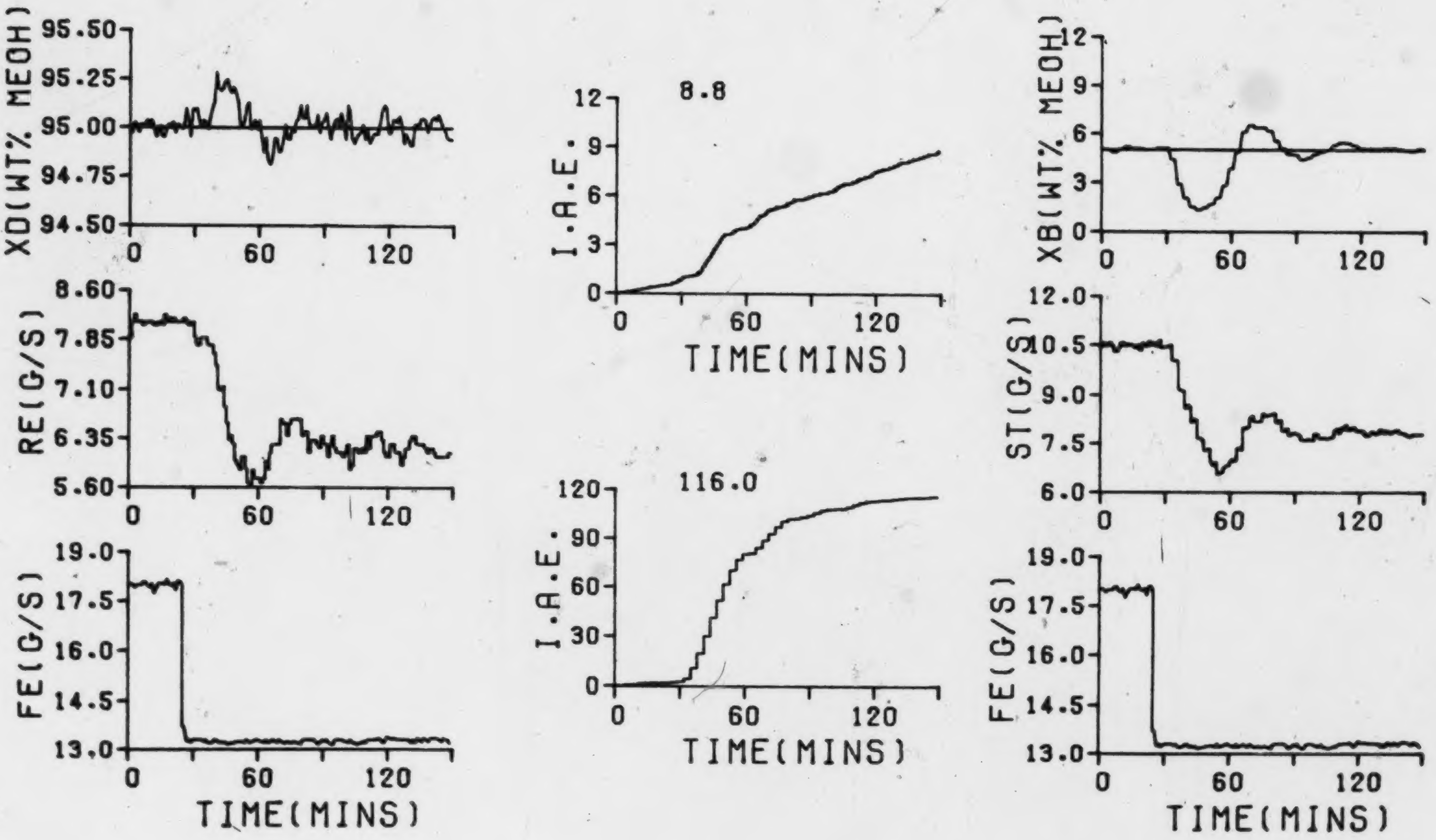

FIGURE 7.59 MR ST IAE/Q(PB=10.335,TI=107.62,TD=0.0)/TS=60.0/4.3.3.0.4/
Q(PB=52.636,TI=309.085,TD=0.0)/TS=180.0/5.3.3.0.6/

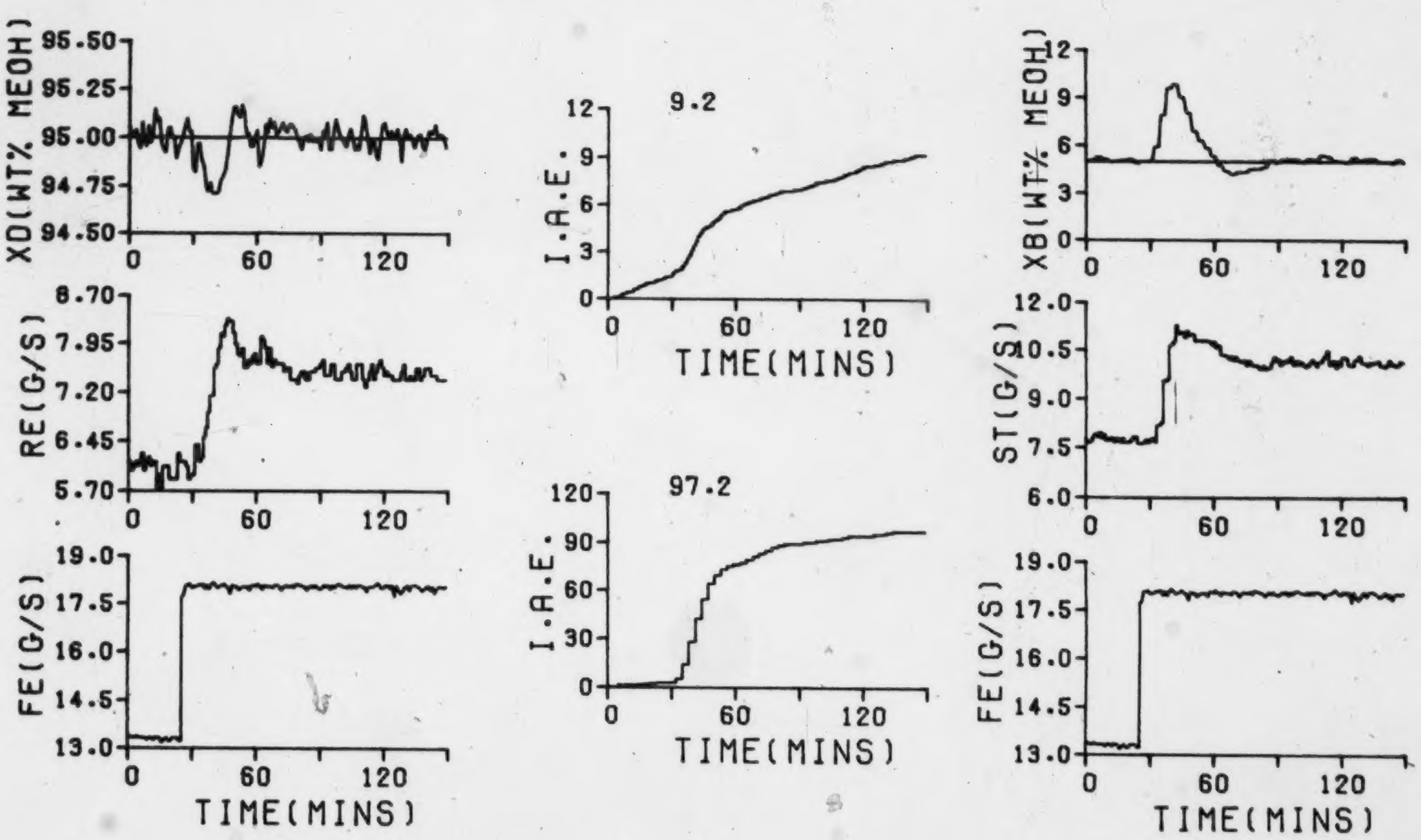

FIGURE 7.60 MR ST IAE/Q(PB=10.335,TI=107.62,TD=0.0)/TS=60.0/4,3,3,0,4/
Q(PB=52.636,TI=309.085,TD=0.0)/TS=180.0/5,3,3,0,6/

7.4.4 Control Performance With Q Weighting Constants Calculated from the Integral of Time Multiplied by the Absolute Error Equation

Table 7.4.4 provides a summary of the IAE values for the tests of the self-tuning control performance of the pilot plant distillation column when subjected to feed disturbances while under control with the multirate self-tuning control using Q weighting constants calculated with the integral of time multiplied by the absolute error equations.

Table 7.4.4
Multirate Self-Tuning Control Performance with Q Weighting Constants Calculated with the Integral of Time Multiplied by the Absolute Error Equations

	IAE Values	
Step	TOP	BOTTOM
increase from steady state	8.5	69.9
decrease to steady state	6.0	85.9
decrease from steady state	8.7	121.7
increase to steady state	11.1	102.5
total	34.3	380.0

The distillation column control performance is shown graphically in Figures 7.61 through 7.64. Comparison of the IAE values for the control of top composition for this series of tests with those of the previous set for the Q weighting parameters based on the IAE equations shows that the overall performance is very similar. However, the effect

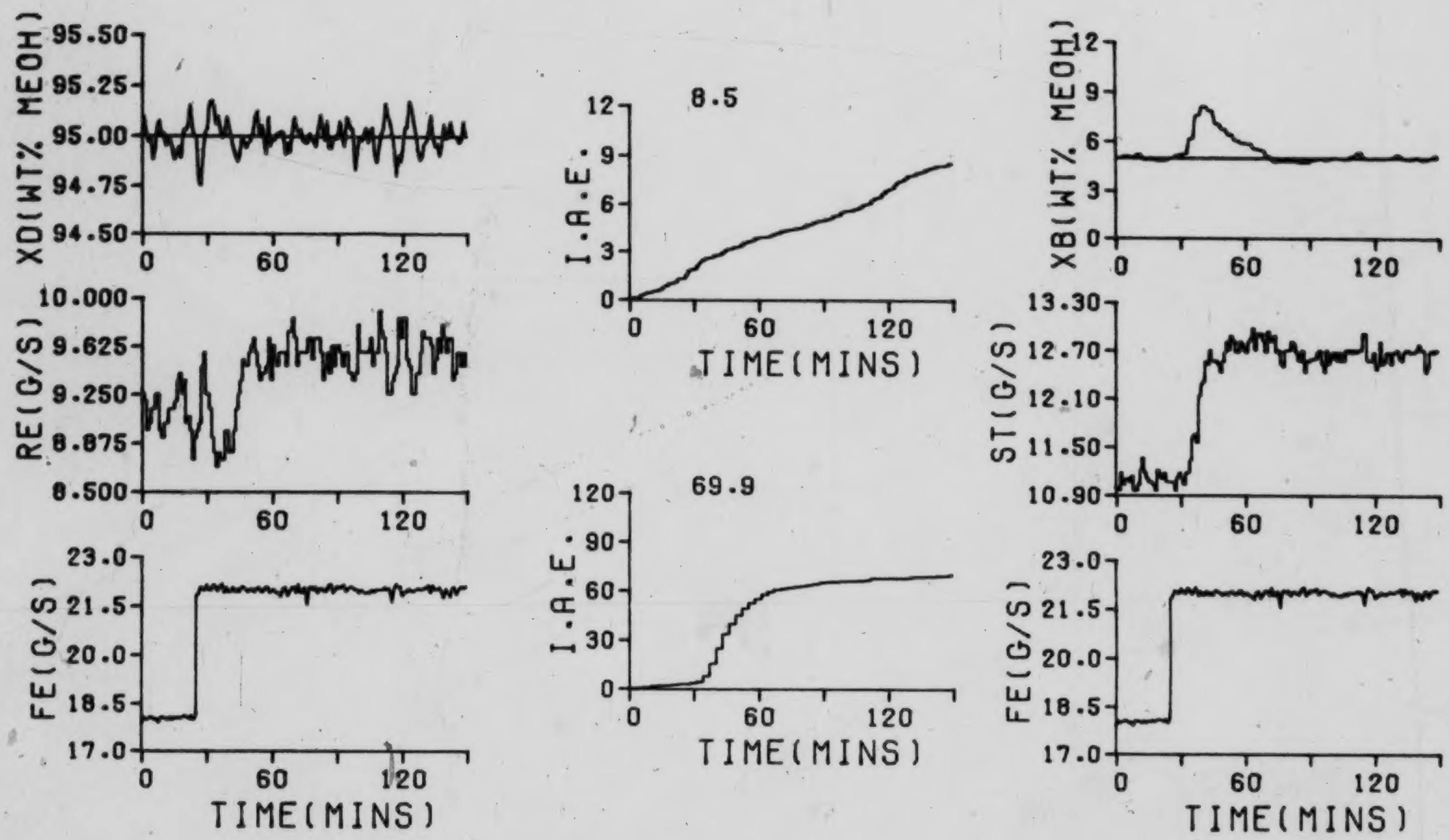

FIGURE 7.61 MR ST ITAE/Q(PB=12.126,TI=104.388,TD=0.0)/TS=60.0/4.3.3.0.4/
Q(PB=61.676,TI=298.602,TD=0.0)/TS=180.0/5.3.3.0.6/

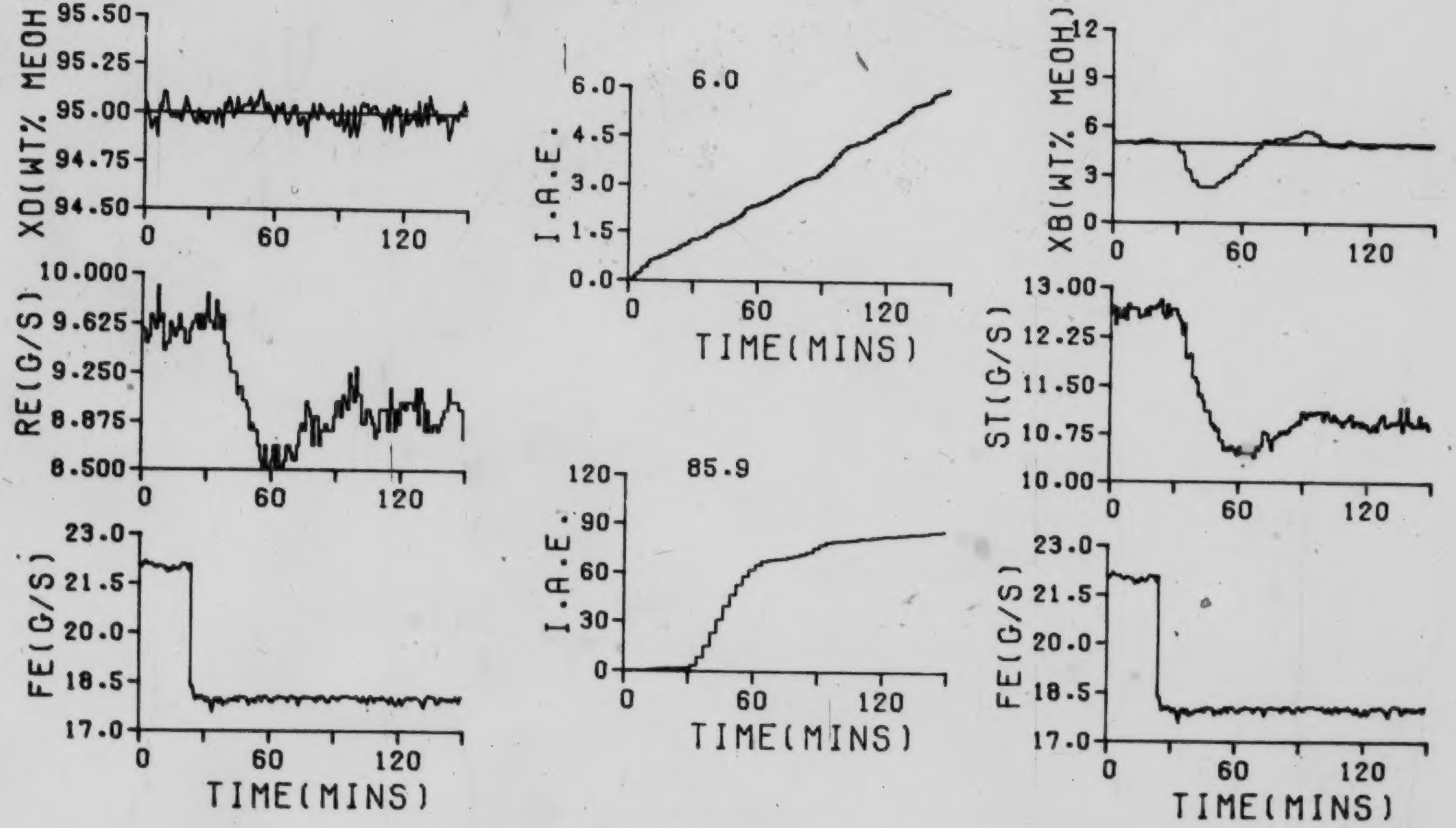

FIGURE 7.62 MR ST ITAE/Q(PB=12.126.TI=104.388.TD=0.0)/TS=60.0/4.3.3.0.4/
Q(PB=61.676.TI=298.602.TD=0.0)/TS=180.0/5.3.3.0.6/

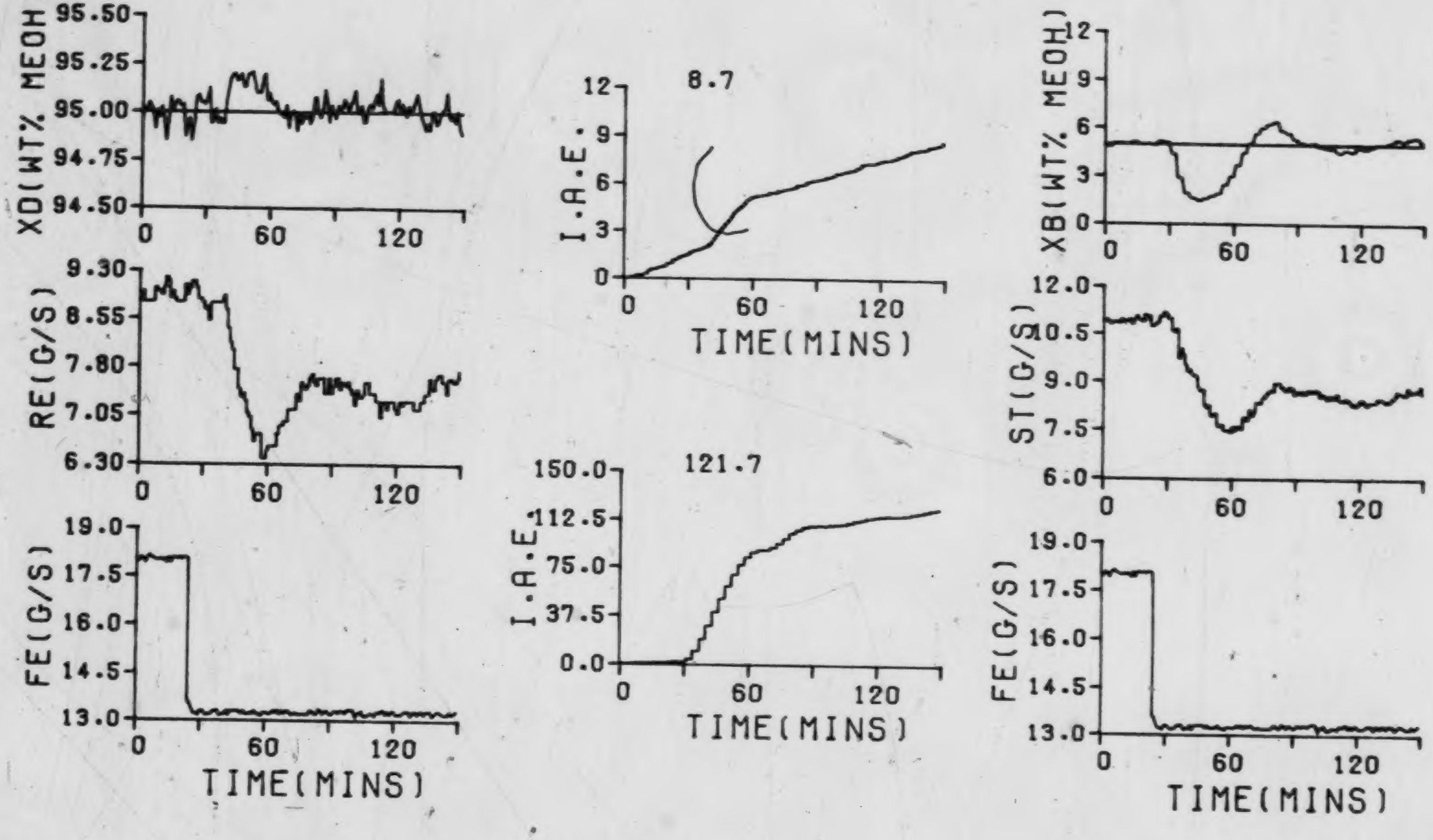

FIGURE 7.63 MR´ST ITAE/Q(PB=12.126,TI=104.388,TD=0.0)/TS=60.0/4.3.3.0.4/
Q(PB=61.676,TI=298.602,TD=0.0)/TS=180.0/5.3.3.0.6/

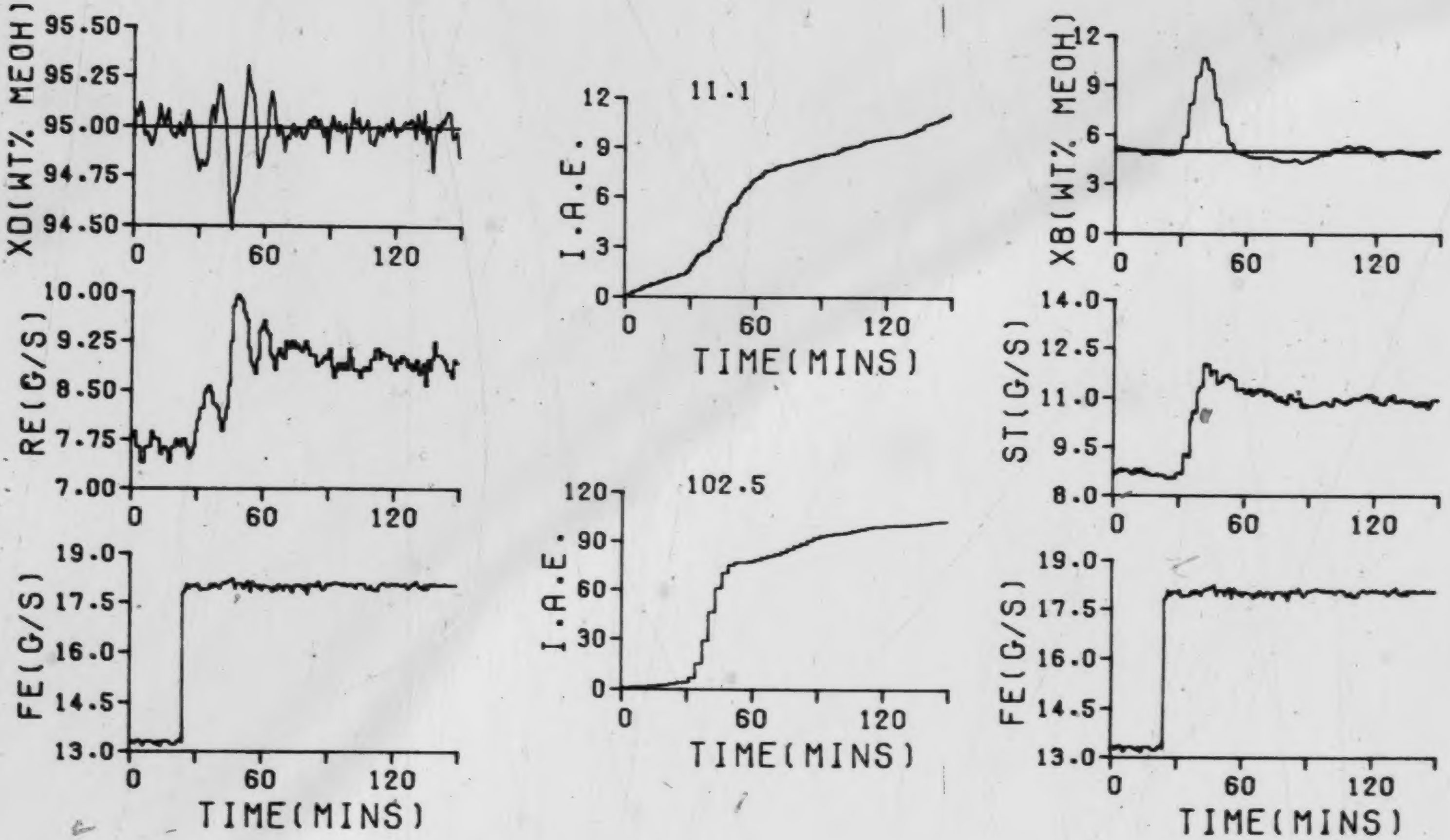

FIGURE 7.64 MR ST ITAE/Q(PB=12.126,TI=104.388,TD=0.0)/TS=60.0/4,3,3,0,4/
Q(PB=61.676,TI=298.602,TD=0.0)/TS=180.0/5,3,3,0,6/

of multirate sampling on improving the performnace as measured by the IAE values is not as marked as with the case using the IAE equation based Q weighting parameters. In the case of the control of the bottom composition, only for the case of the step increase in feed rate from the steady state value did multirate sampling reduce the IAE value (cf. Figure 7.45 and 7.61). For the other three feed disturbances, use of Q weighting parameters calculated from the ITAE equations, with the multirate sampling form of the algorithm, has resulted in a deterioration of control performance. This deterioration in bottom control performance is at the expense of top composition control improvement and increased interaction (cf. Table 7.3.4 and Table 7.4.4).

7.4.5 Comparison of The Effect on Control Performance of The Method of Selecting the Self-Tuning Controller Q Weighting Parameters Using The Multirate Algorithm

The IAE values for the test results presented in Figures 7.49 through 7.64 are summarized in Table 7.4.5. As can be seen from the tabulation, the best overall control performance was obtained with the Q weighting parameters calculated using the IAE equations, followed by the ITAE, Ziegler-Nichols and Cohen-Coon methods, in that order. The initial deviations in the bottom composition from the setpoint are smaller in magnitude than that provided from the multirate PID control performance. This is in contrast to the test results obtained with the single rate sampling algorithm that showed that the best overall control behavior using Q weighting parameters based on the Cohen-Coon equations.

Table 7.4.5
IAE Values for Multirate Self-Tuning Control Based on Calculated Q Weighting Parameters

IAE		IAE Values by Method			
		Z-N	3-C	IAE	ITAE
increase from SS	top	8.3	10.0	6.0	8.5
	bottom	116.1	85.7	78.3	69.9
decrease to SS	top	17.1	7.8	5.6	6.0
	bottom	72.6	85.5	65.4	85.9
decrease from SS	top	13.2	15.1	8.8	8.7
	bottom	109.6	139.5	116.0	121.7
increase to SS	top	18.8	9.3	9.2	11.1
	bottom	70.3	95.1	97.2	102.5
total		426.0	448.8	386.5	414.3

7.4.6 Effect On Control Performance of Using The Multirate Sampling Form of The Self-Tuning Control Algorithm

The combined IAE values for top and bottom composition for the single rate and multirate sampling tests of the self-tuning control for all four tests are summarized in Table 7.4.6.

Careful examination of the results presented in Table 7.4.6 indicates that for top composition regulation, multirate self-tuning control provides the lowest combined IAE value regardless of the method used to select the Q weighting parameters. As can be seen, the lowest value resulted when the parameters were calculated using the IAE equations. In the case of the bottom composition, only for

Table 7.4.6
Combined IAE Values for Single and Multirate Sampling
Self-Tuning Control: Effect of Q weighting Parameter
Combined IAE Values

	IAE Totals by Method			
Top Composition	Z-N	3-C	IAE	ITAE
Multivariable	68.1	49.3	67.3	62.9
Multirate	57.4	42.2	29.6	34.3
Bottom Composition	Z-N	3-C	IAE	ITAE
Multivariable	397.3	313.7	334.6	349.4
Multirate	368.6	405.8	356.9	380.0

the use of the Ziegler-Nichols rules was the multirate sampling advantageous in terms of the combined IAE values that resulted. This was also the case for the comparison between the control performance of conventional PID control using single and multirate sampling (cf. Table 7.2.6). This reduction in performance, in terms of the combined IAE values, is apparently due to the increased interaction from the top composition loop because of the shorter sample interval and improved top loop performance. Examination of the information in Table 7.4.6 shows that the combined IAE totals for the top composition control using Q weighting parameters calculated by either of the two integral minimization methods provided the largest improvement in regulation and caused the least degradation in bottom composition regulation in the transition from multivariable control to multirate control.

7.5 Comparison of The Control Performance Achieved Using Multiloop Conventional PID and Multivariable Self-Tuning Control

As has been presented, each control strategy was tested using four different step disturbances in feed flow rate. Four different methods for selecting PID controller constants and for specifying the Q weighting parameters of the control penalty of the self-tuning controller cost function were studied. The results of these tests are summarized in Table 7.5.1. The test results showed that for top composition PID control a sample time of one minute, resulted in improved regulation of the top composition when compared to the results obtained using a three minute control interval, illustrated by the range of values expressed in Table 7.5.1. The variation of IAE values for the control of the top composition using PID control decreases significantly when a one minute control interval is employed. For multiloop control the top composition IAE results range from 67.8 to 116.4, and is reduced to 41.4 to 48.9 with multirate control (cf. Table 7.5.1). The average improvement in regulation for the top composition is 92.4%, which provides substantiation for the application of

Table 7.5.1
Comparison of Controller Performance Bewteen Conventional PID versus Self-Tuning Control For Both Single Rate and Multirate Sampling Using Four Parameter Selection Methods

		IAE Totals by Method			
PID Response		Z-N	3-C	IAE	ITAE
Multiloop	top	116.4	67.8	83.5	86.4
	bottom	1394.8	780.8	1045.8	1158.2
	total	1511.2	848.6	1129.3	1244.6
Multirate	top	48.1	41.4	45.7	48.9
	bottom	1354.0	887.9	1099.0	1188.0
	total	1402.1	929.3	1144.7	1236.9
Self-Tuning Response		Z-N	3-C	IAE	ITAE
Multivariable	top	68.1	49.3	67.3	62.9
	bottom	397.3	313.7	334.6	349.4
	total	465.4	363.0	401.9	412.3
Multirate	top	57.4	42.2	29.6	34.3
	bottom	368.6	405.8	356.9	380.0
	total	426.0	448.0	386.5	414.3

multirate control. For the bottom composition regulation, the GC analyzer sample time restriction of three minutes does not allow a shorter sample and control interval to be tested. The IAE values for the bottom composition regulation vary between 780.8 to 1394.8 for multiloop PID control, whereas the range of IAE values is reduced to 887.9 to 1354.0 for multirate control. The individual increases in the IAE values are primarily due to the interaction from the improved top composition control. The overall increase in IAE performance based on the four methods is a reduction in bottom composition control performance of only 3.4%. The overall economics of the individual situations will dictate whether the control enhancements to multirate control are deemed necessary.

Examination of the results in Table 7.5.1 show that although top composition control has not improved, in applying multivariable self-tuning control, when compared with multirate sampling of the PID control strategy, bottom composition control improved immensely with the implementation of the multivariable self-tuning control algorithm. This improvement in bottom composition regulation can be credited to the dead time compensation capabilities of the self-tuning controller algorithm, along with the decoupling nature inherent within the formulation of the algorithm. The multirate self-tuning control algorithm provided improved control of the top composition for three out of the four different methods used for selecting controller parameters, indicating that self-tuning control does provide an advantage in controlling processes without dead time.

Self-tuning control with Q weighting parameters chosen with standard open loop response techniques yield superior control performance of the pilot plant distillation column when subjected to feed disturbances when compared to conventional PID control using the same techniques to establish controller constants. Multirate sampling for column control improves the regulation of the top composition loop with minimal reduction in control performance of the bottom composition loop for both PID and self-tuning control studies.

7.6 Column Control Behavior Using Tuned Controller Settings For PID And Self-Tuning Strategies

From the test results that have been presented, it is obvious that control of the distillation column is affected by the choice of the PID controller settings and the Q weighting parameters of the self-tuning controllers. This section will present the results achieved using tuned PID controller settings, and Q weighting parameters for the self-tuning controllers for the same ±25% disturbances in feed flow rate as used for the previous tests. In most cases approximately 12 different combinations of controller constants and Q weighting parameters were tested to establish favorable values in terms of the resulting IAE values. To check that the values represented well tuned PID control and Q weighting self-tuning control, parameters of the controllers were adjusted slightly and the tests repeated. When changes resulted in higher IAE values, the results were deemed to have been obtained using "well tuned" controller constants and Q weighting parameters.

7.6.1 Performance Using a Tuned Multiloop PID Control Strategy

Table 7.6.1 provides a comparison of the IAE values for the tests of the multiloop PID control performance of the pilot plant distillation column when subjected to feed

Table 7.6.1
Control Performance of Multiloop PID Control With Tuned Controller Constants

	IAE Values			
	Tuned		3-C	
Step	TOP	BOTTOM	TOP	BOTTOM
increase from SS	8.0	99.0	15.7	183.9
decrease to SS	7.9	117.9	12.4	154.6
decrease from SS	10.6	161.3	21.2	213.6
increase to SS	9.3	134.0	18.5	228.7
total	35.8	512.2	67.8	780.8

disturbances using tuned controller constants and the best response from calculated controller constants. The control performance that was achieved using a multiloop PID control strategy when the constants of the controllers were adjusted experimentally, is illustrated by the responses presented in Figures 7.65 to 7.68. The significant improvement in the control behavior shown by these results can be readily appreciated from the IAE values presented in Table 7.6.1. The Cohen-Coon IAE values were selected for comparison since it was this set of calculated controller constants, of the four different methods tested that produced the most satisfactory control performance (cf. Table 7.5.1). It can be seen that tuning of the PID controller constants, starting from constants calculated using the Cohen-Coon equations, has resulted in a large percentage reduction in the IAE values. Comparison of the IAE values for tuned

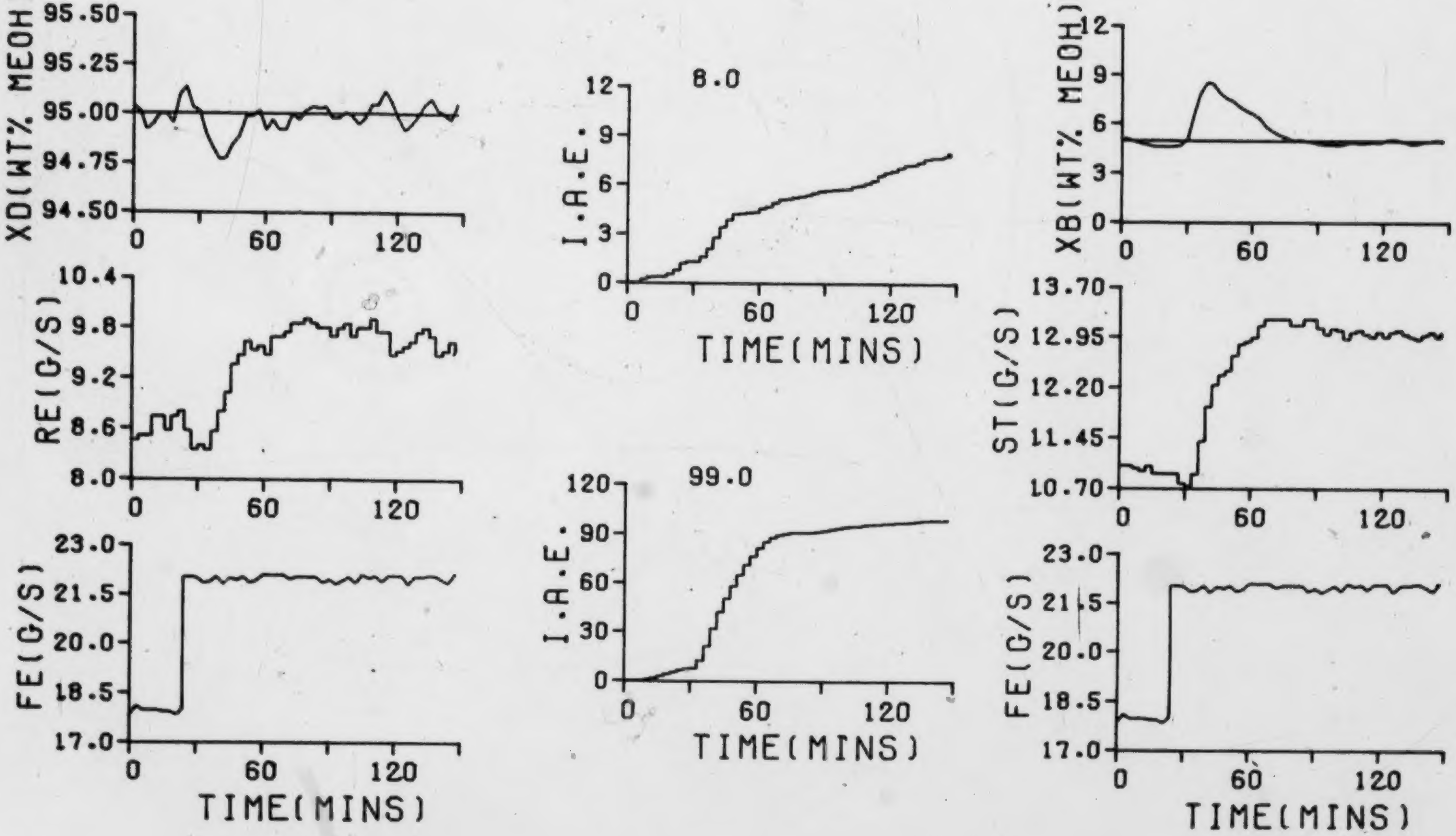

FIGURE 7.65 ML PID/PID(PB=20.0,TI=175.0,TD=0.0)/TS=180.0/
PID(PB=70.0,TI=450.0,TD=110.0)/TS=180.0/

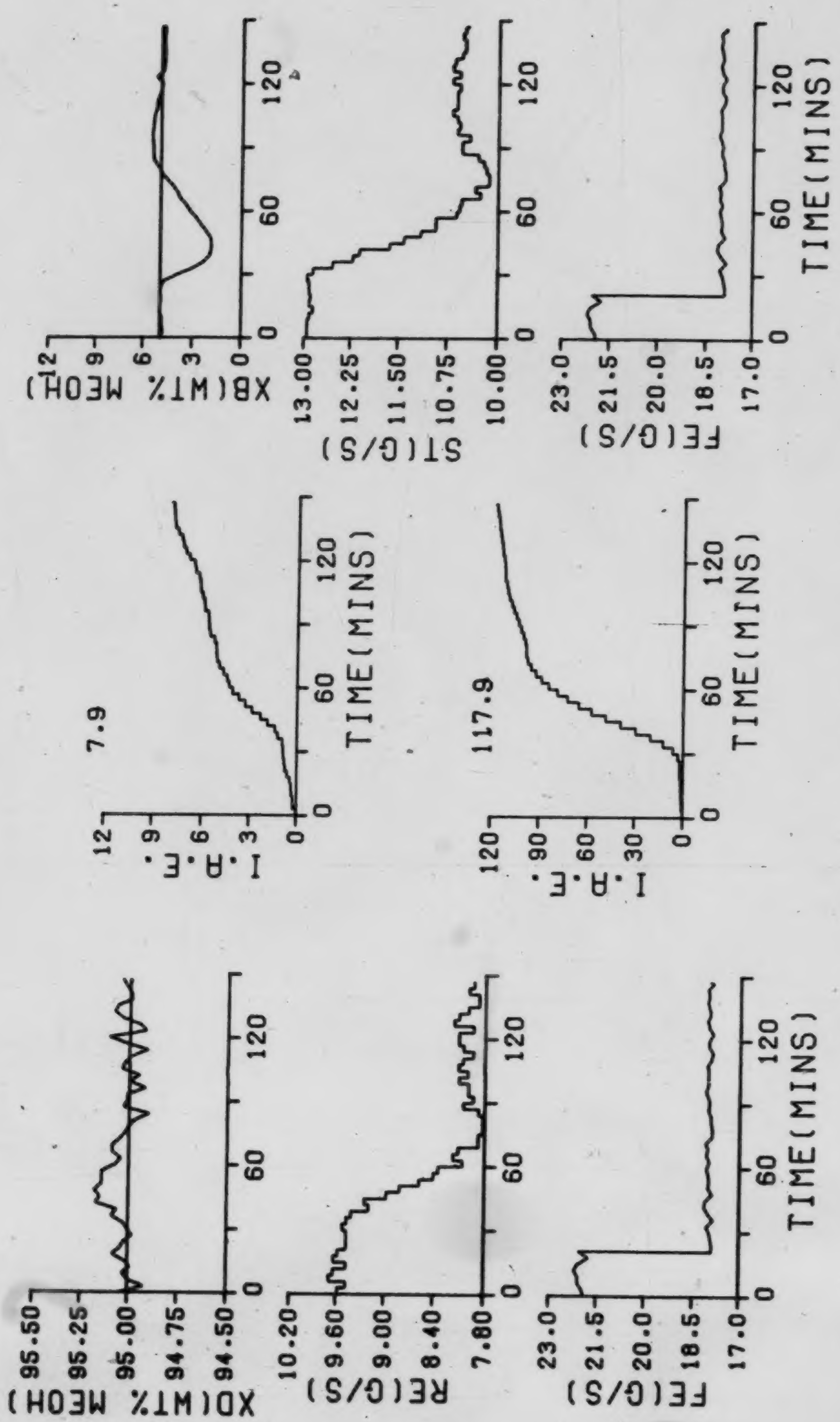

FIGURE 7.66 ML PID/PID(PB=20.0,TI=175.0,TD=0.0)/TS=180.0/
PID(PB=70.0,TI=450.0,TD=110.0)/TS=180.0/

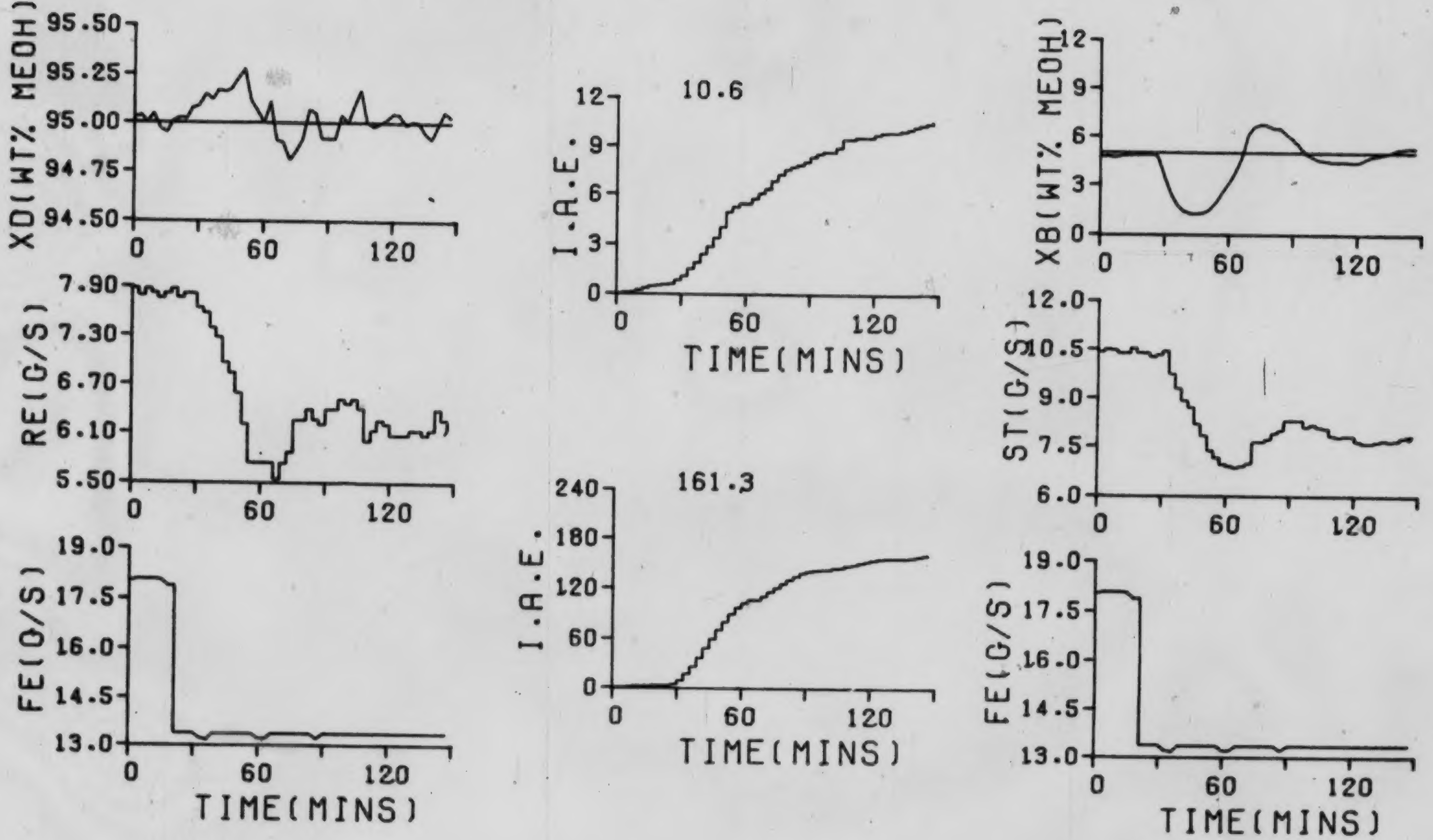

FIGURE 7.67 ML PID/PID(PB=20.0,TI=175.0,TD=0.0)/TS=180.0/
PID(PB=70.0,TI=450.0,TD=110.0)/TS=180.0/

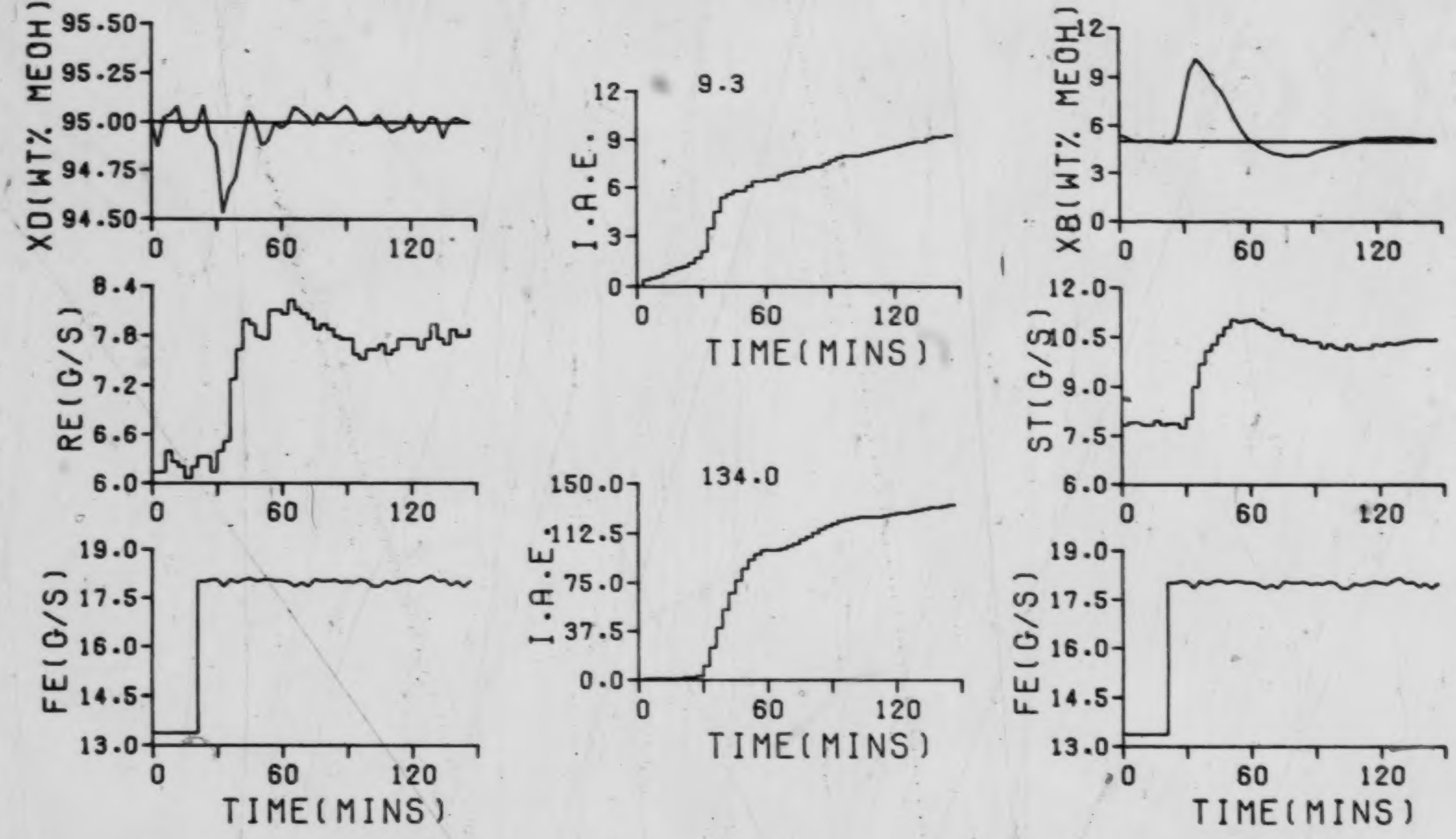

FIGURE 7.68 ML PID(PID(PB=20.0,TI=175.0,TD=0.0)/TS=180.0/
PID(PB=70.0,TI=450.0,TD=110.0)/TS=180.0/

settings with the values achieved in the previous set of tests using other calculated controller constant values illustrates the marked improvement in control behavior that can be achieved by "controller tuning".

Comparison of the tuned PID controller constants with those established by the different calculation methods shows that the improved performance was achieved due to larger gains (smaller proportional bands), more integral action for both loops as well as reduced derivative action for the bottom loop. Despite the extensive program of tuning controller constants the bottom composition consistently exhibited large deviations from the setpoint at the onset of each disturbance. These large deviations result because of the time delay associated with the bottom composition analysis, and the inability of conventional PID controllers to compensate for this time delay.

7.6.2 Performance Using a Tuned PID Control Strategy With Multirate Sampling

In order to further study the effect on control performance of reducing the sampling and control interval of the top composition control loop from 3.0 minutes to 1.0 minute, tests were performed for each of the same feed disturbances for tuned controller settings. The results of these tests, with controller constants selected by monitoring the IAE values are shown in Figures 7.69 through 7.72. To appreciate the control behavior that was achieved

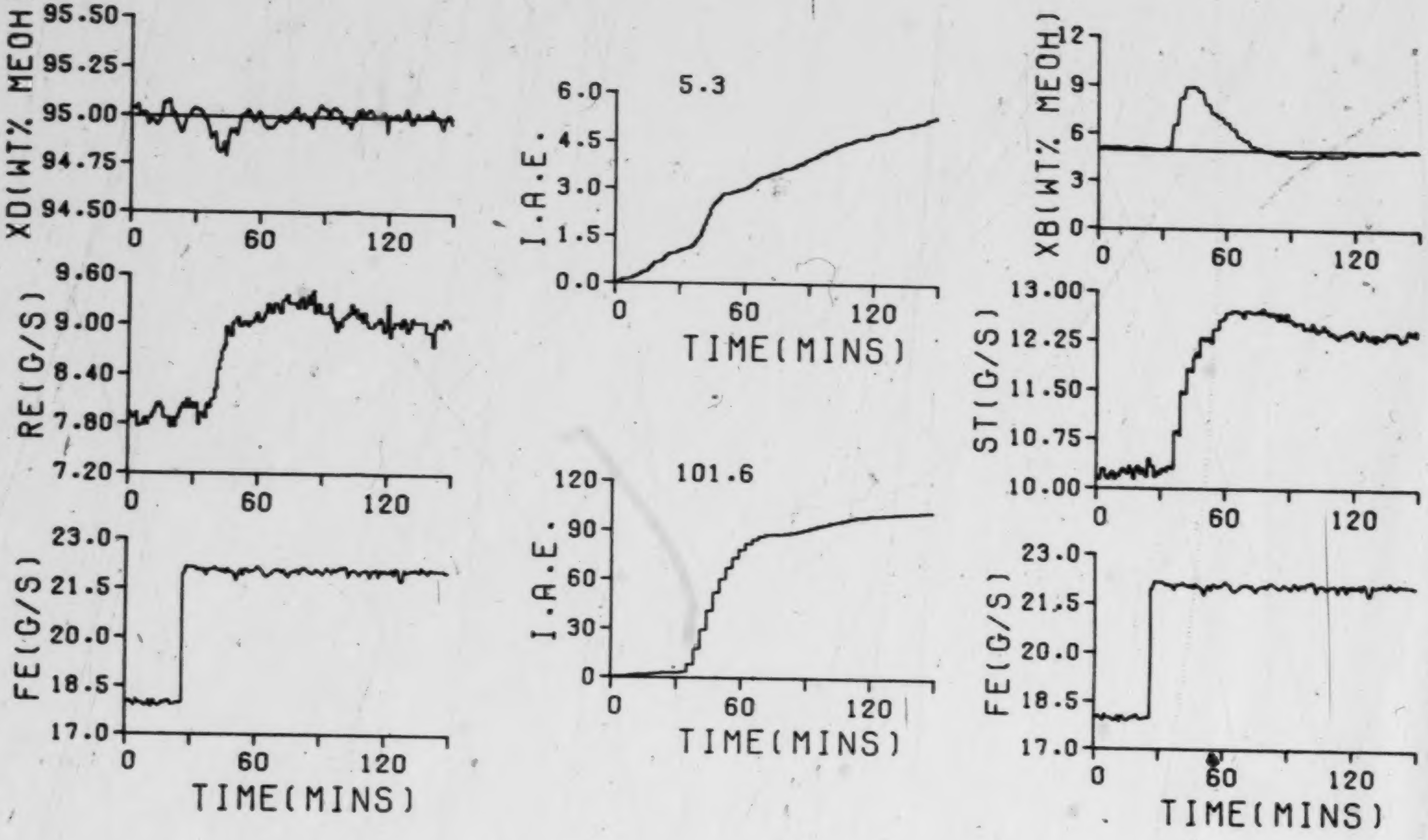

FIGURE 7.69 MR PID/PID(PB=20.0,TI=100.0,TD=30.0)/TS=60.0/
PID(PB=70.0,TI=450.0,TD=110.0)/TS=180.0/

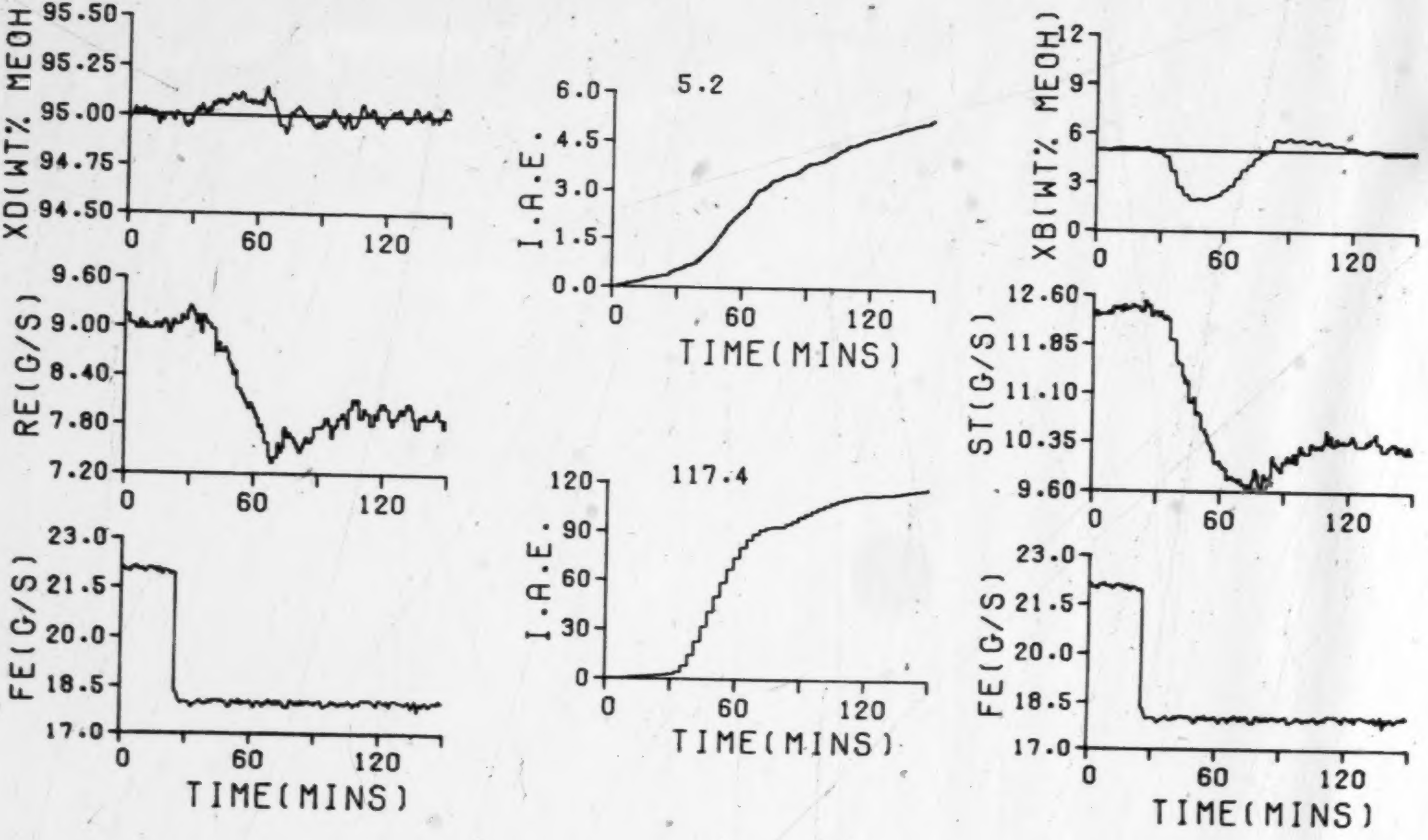

FIGURE 7.70 MR PID/PID(PB=20.0,TI=100.0,TD=30.0)/TS=60.0/
PID(PB=70.0,TI=450.0,TD=110.0)/TS=180.0/

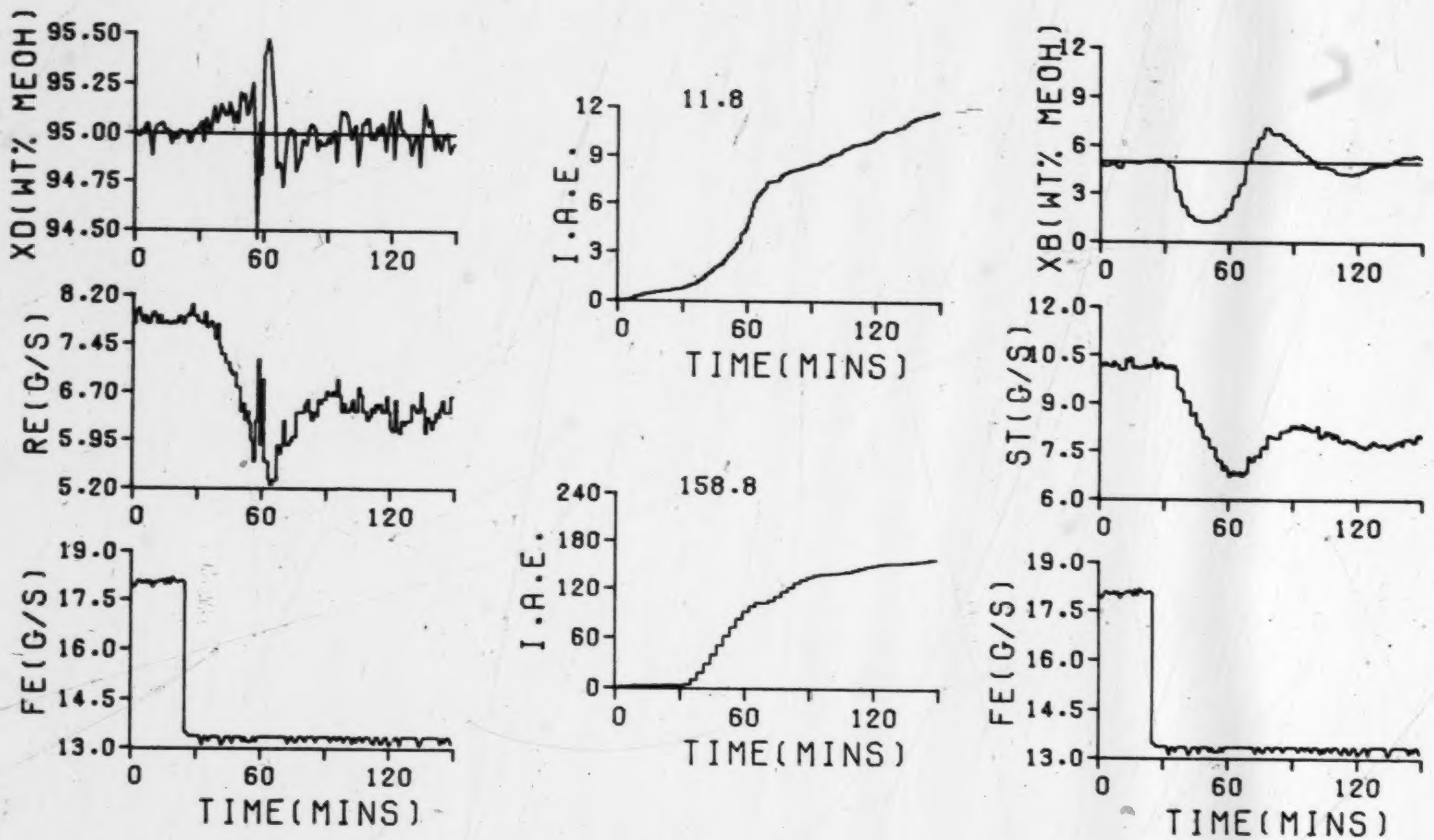

FIGURE 7.71 MR PID/PID(PB=20.0,TI=100.0,TD=30.0)/TS=60.0/
PID(PB=70.0,TI=450.0,TD=110.0)/TS=180.0/

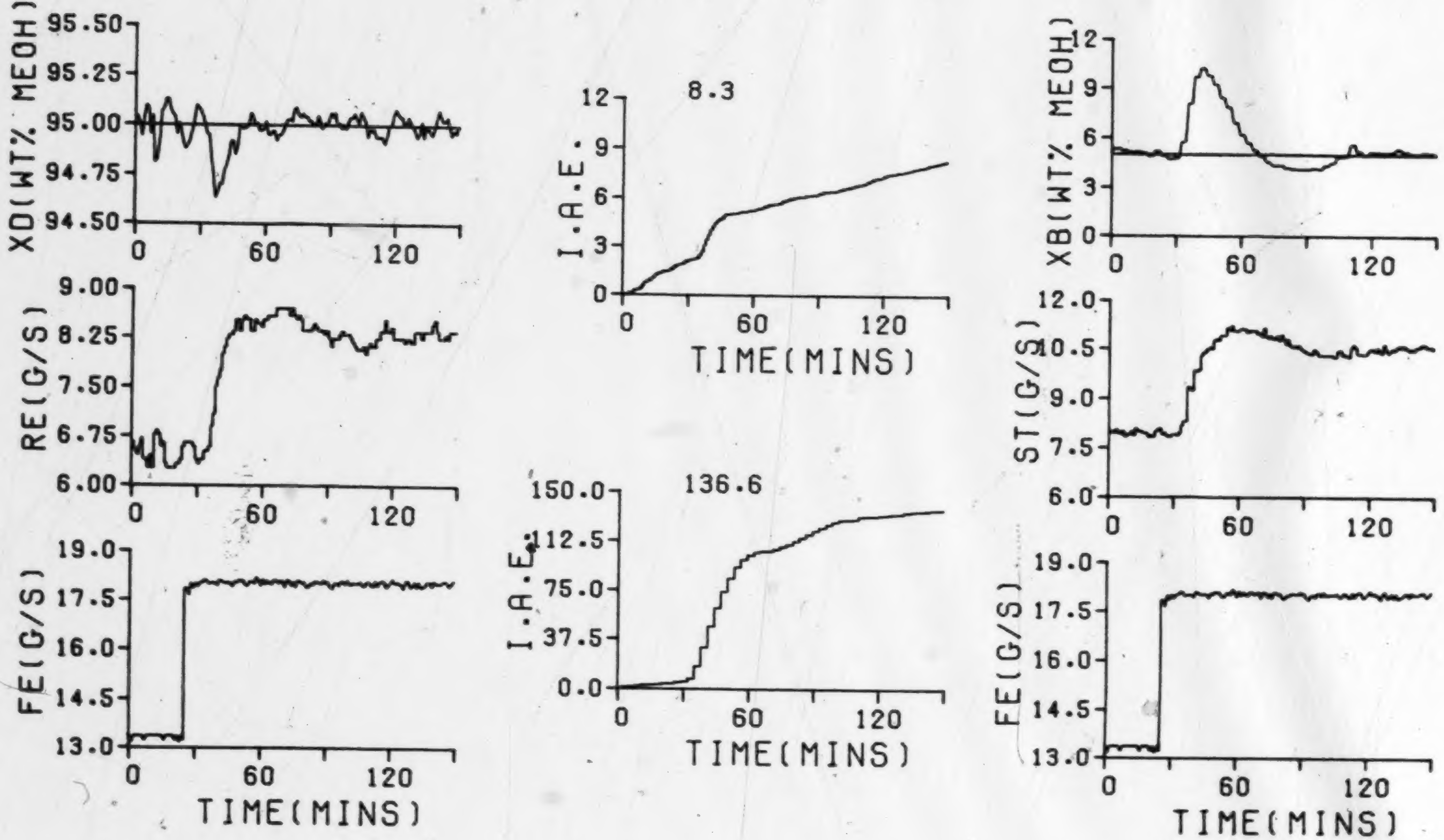

FIGURE 7.72 MR PID/PID(PB=20.0,TI=100.0,TD=30.0)/TS=60.0/
PID(PB=70.0,TI=450.0,TD=110.0)/TS=180.0/

by tuning the controller constants, it is appropriate to consider the best behavior that was achieved using calculated controller settings. For ease of comparison the IAE values that resulted using the Cohen-Coon based equations to generate the controller constants and those from this series of tests are presented in Table 7.6.2. As was the case for the previous series of tests, starting from the Cohen-Coon calculated controller constants, adjustment of the constants reduced the IAE value for both top and bottom composition control for all four feed rate disturbances. In order to examine the effect of a reduced sampling interval for top composition on performance, the corresponding IAE values in Table 7.6.2 need to be compared with those in Table 7.6.1. Comparison of the IAE values obtained using tuned controller constants shows that for top composition, except for the step decrease in feed rate that the short sample and control interval has improved the control performance even for well tuned control.

As might be expected, comparison of the corresponding IAE values shows that no improvement in the regulation of bottom composition resulted from the use of the 1.0 minute sample and control interval for the top composition loop. Therefore it is not surprising that a comparison of all of the responses in Figures 7.69 to 7.72 with those in Figures 7.65 to 7.68 shows that the only noticeable difference is the tighter control of the top composition that was achieved using multirate sampling.

Table 7.6.2
Control Performance of Multirate Sampling PID Control With Tuned Controller Constants

	IAE Values			
	Tuned		3-C	
Step	TOP	BOTTOM	TOP	BOTTOM
increase from SS	5.3	101.6	9.2	196.9
decrease to SS	5.2	117.4	8.8	173.9
decrease from SS	11.8	158.8	12.6	252.4
increase to SS	8.3	136.6	10.8	264.7
total	30.6	514.4	41.4	887.9

7.6.3 Multivariable Self-Tuning Column Control Behavior Using Tuned Q Weighting Parameters

The responses that resulted with the distillation column operated under multivariable self-tuning control using tuned Q weighting parameters for the four different feed disturbances are presented in Figures 7.73 through 7.76.

Assessment of the control behavior, as expressed by the magnitude of the IAE values, shows that use of tuned Q weighting parameters versus calculated Q weighting parameters has a very limited effect on control performance as can be seen from the results summarized in Table 7.6.3. These results must be compared against the multivariable self-tuning control performance observed with the use of the Q weighting parameters calculated using the Cohen-Coon equations. As can be seen from Table 7.5.1 the Cohen-Coon

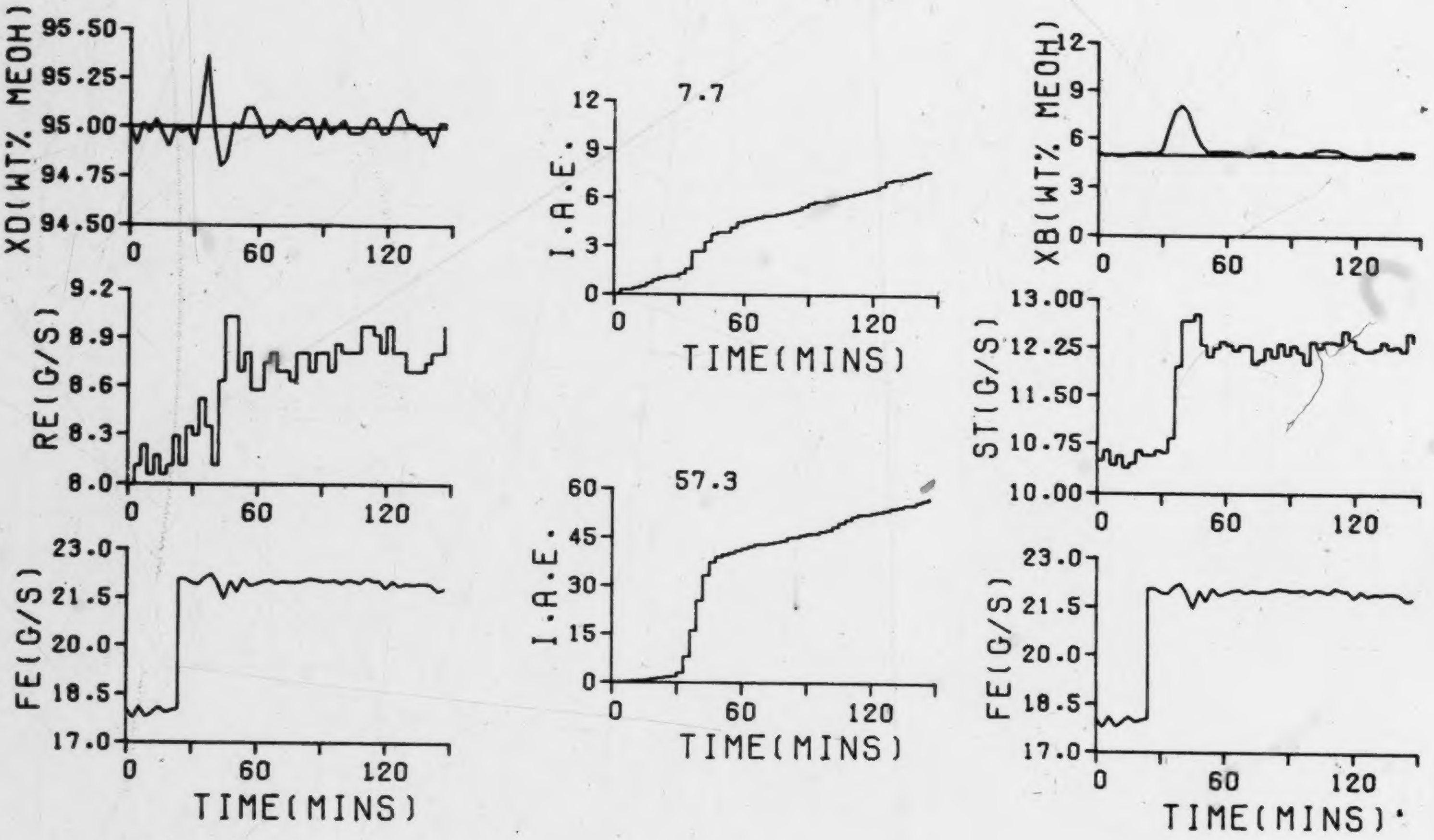

FIGURE 7.73 MV ST/Q(PB=15.0,TI=80.0,TD=0.0)/TS=180.0/4.3,3.0,4/
Q(PB=50.0,TI=150.0,TD=0.0)/TS=180.0/5.3,3.0,6/

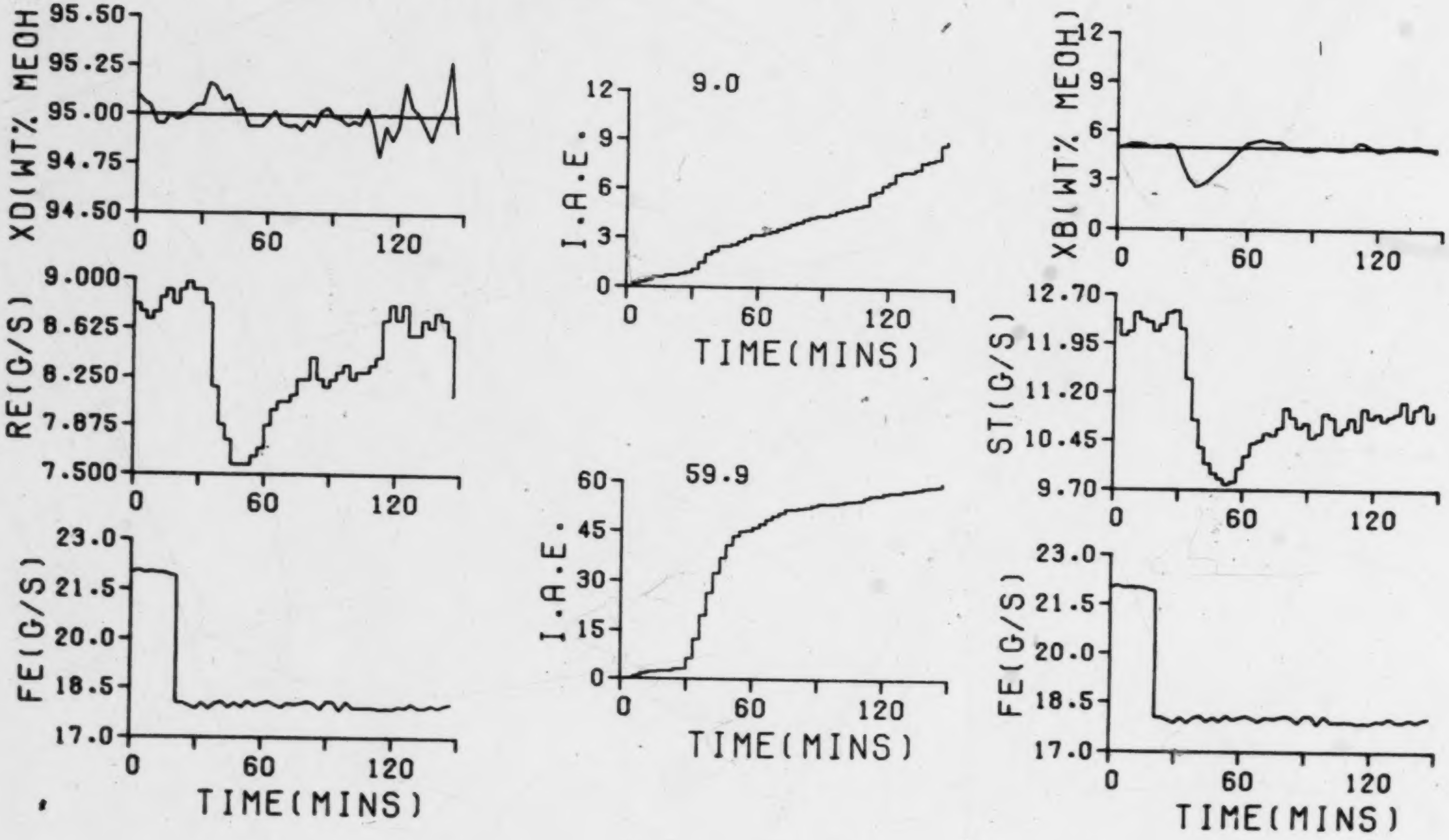

FIGURE 7.74 MV ST/Q(PB=15.0.TI=80.0.TD=0.0)/TS=180.0/4.3.3.0.4/
Q(PB=50.0.TI=150.0.TD=0.0)/TS=180.0/5.3.3.0.6/

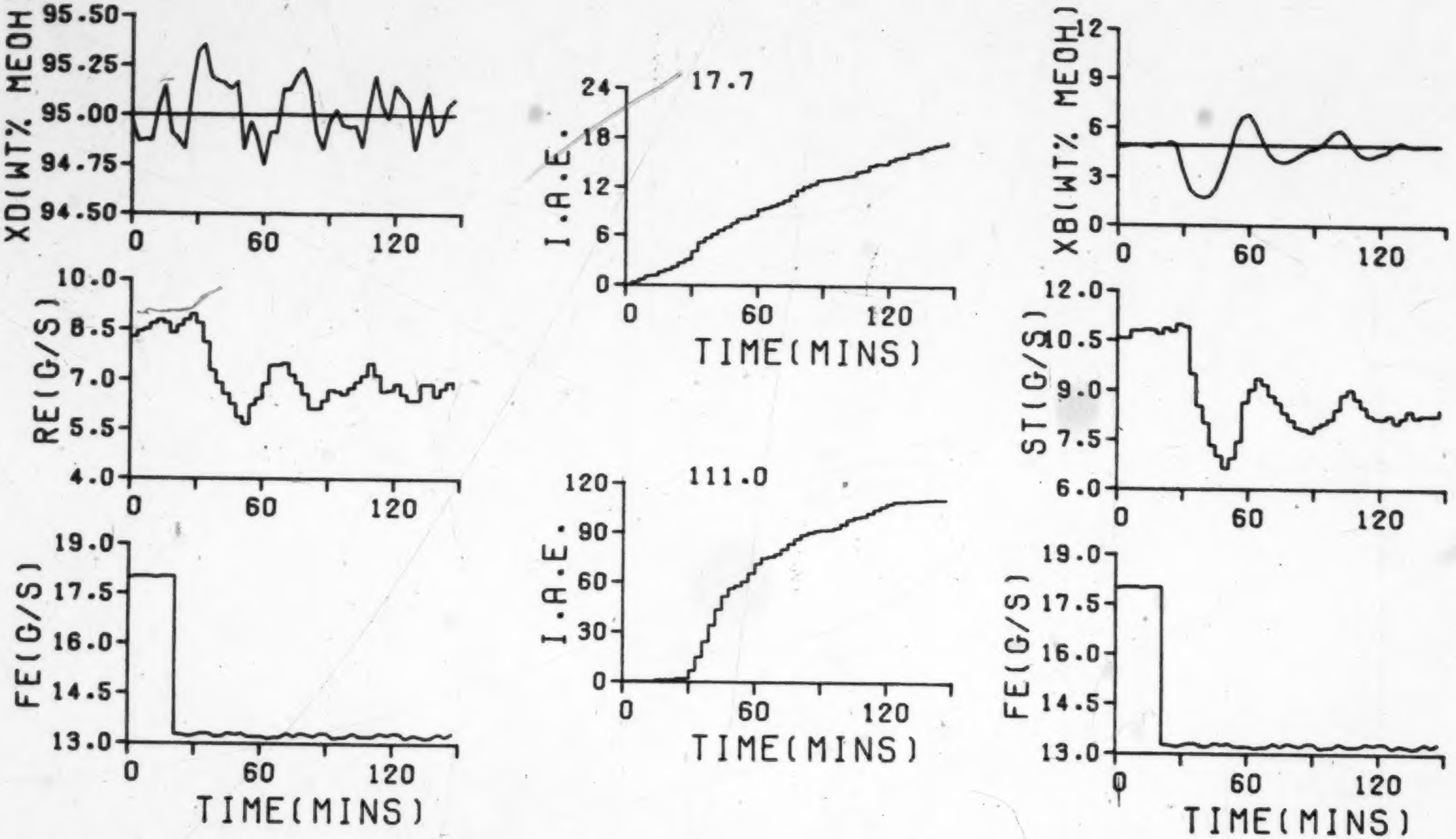

FIGURE 7.75 MV ST/Q(PB=15.0,TI=80.0,TD=0.0)/TS=180.0/4.3.3.0.4/
Q(PB=50.0,TI=150.0,TD=0.0)/TS=180.0/5.3.3.0.6/

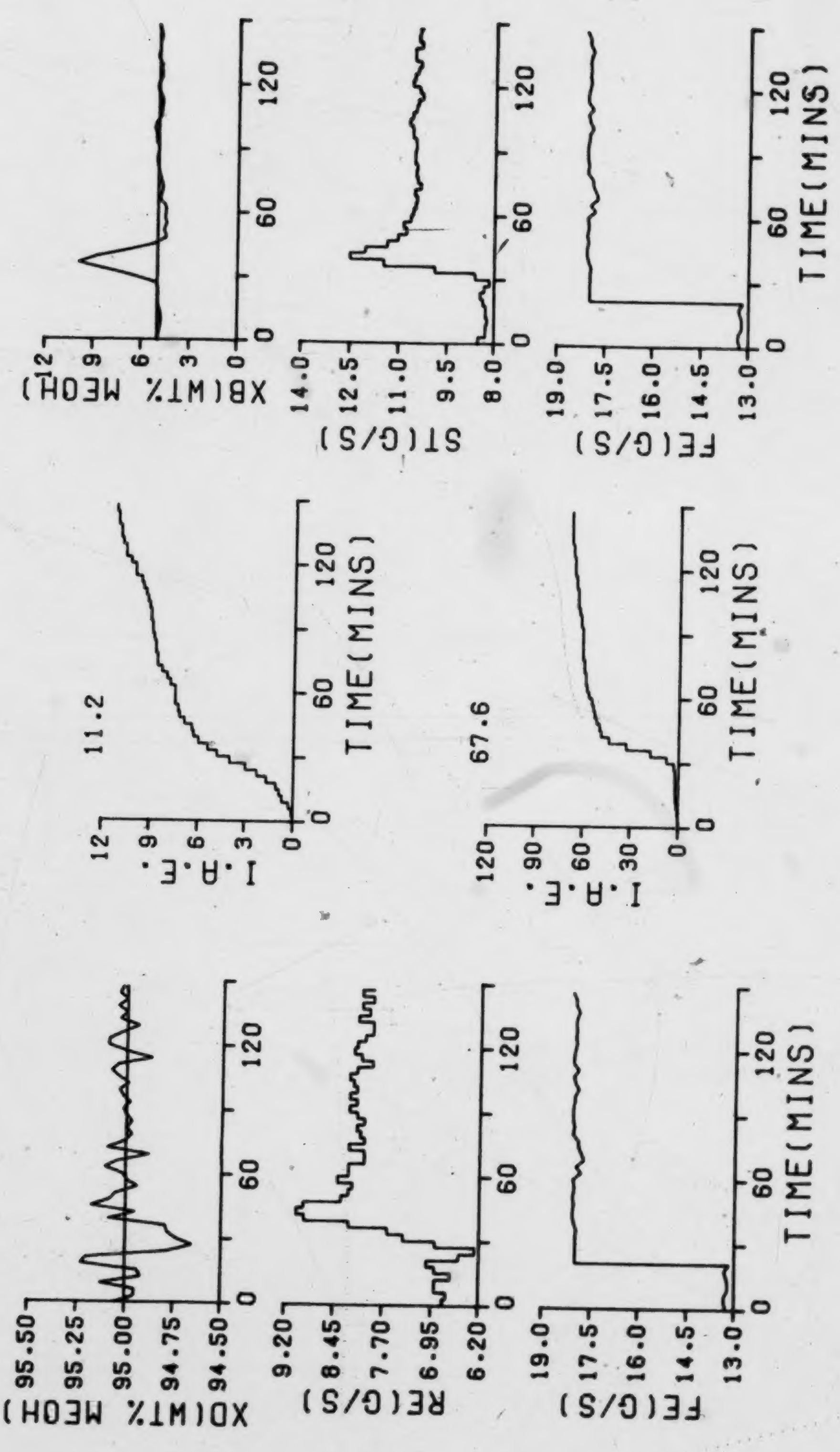

FIGURE 7.76 MV ST/Q(PB=15.0.TI=80.0.TD=0.0)/TS=180.0/4.3.3.0.4/
Q(PB=50.0.TI=150.0.TD=0.0)/TS=180.0/5.3.3.0.6/

Table 7.6.3
Multivariable Self-Tuning Control Performance with Tuned Q Weighting Constants

	IAE Values			
	Tuned		3-C	
Step	TOP	BOTTOM	TOP	BOTTOM
increase from SS	7.7	57.3	7.6	61.4
decrease to SS	9.0	59.9	8.7	72.8
decrease from SS	17.7	111.0	19.5	93.3
increase to SS	11.2	67.6	13.5	86.2
total	45.6	295.8	49.3	313.7

response provided the lowest overall total IAE response of the four methods tested. These results show that regulation of the bottom composition has improved for three out of the four feed rate changes, with the step change exhibiting the inverse response (cf. Figure 5.3) providing the greatest difficulty in composition control. In the case of top composition regulation, only the two cases where feed rates are below steady state conditions do the composition regulations show any improvement. The two conditions where feed rates are above steady state rates show minimal reduction in performance, since they were already very well regulated responses it would indeed be difficult to improve. Comparison of the results in Table 7.6.3 with those given in Table 7.6.1, for the multiloop PID control strategy, reveals that for control of the bottom composition the multivariable self-tuning controller with tuned Q weighting parameters outperforms the multiloop PID controllers, but just the opposite situation exists for the top composition regulation. The improvement in bottom composition regulation has resulted in a significant amount of interaction that influences top composition control.

7.6.4 Control Performance Using Multirate Self-Tuning Controller With Tuned Q Weighting Parameters

The results presented in Figures 7.77 through 7.80 show the column responses obtained using the multivariable self-tuning controller with multirate sampling when the Q weighting parameters were established by tuning. The IAE values that resulted from this set of tests are summarized in Table 7.6.4, as are the IAE values from the series of tests using the multivariable self-tuning controller with multirate sampling when the Q weighting parameters were determined by the IAE equations. As can be seen from the IAE values, regulation of bottom composition for all four feed flow rate disturbances was improved by tuning, but this was not the case for the top composition. This same pattern of behavior, considered to be caused by the interaction of the steam acting as a disturbance to the top composition control loop, was also observed for the multivariable self-tuning tests (cf. Table 7.6.3).

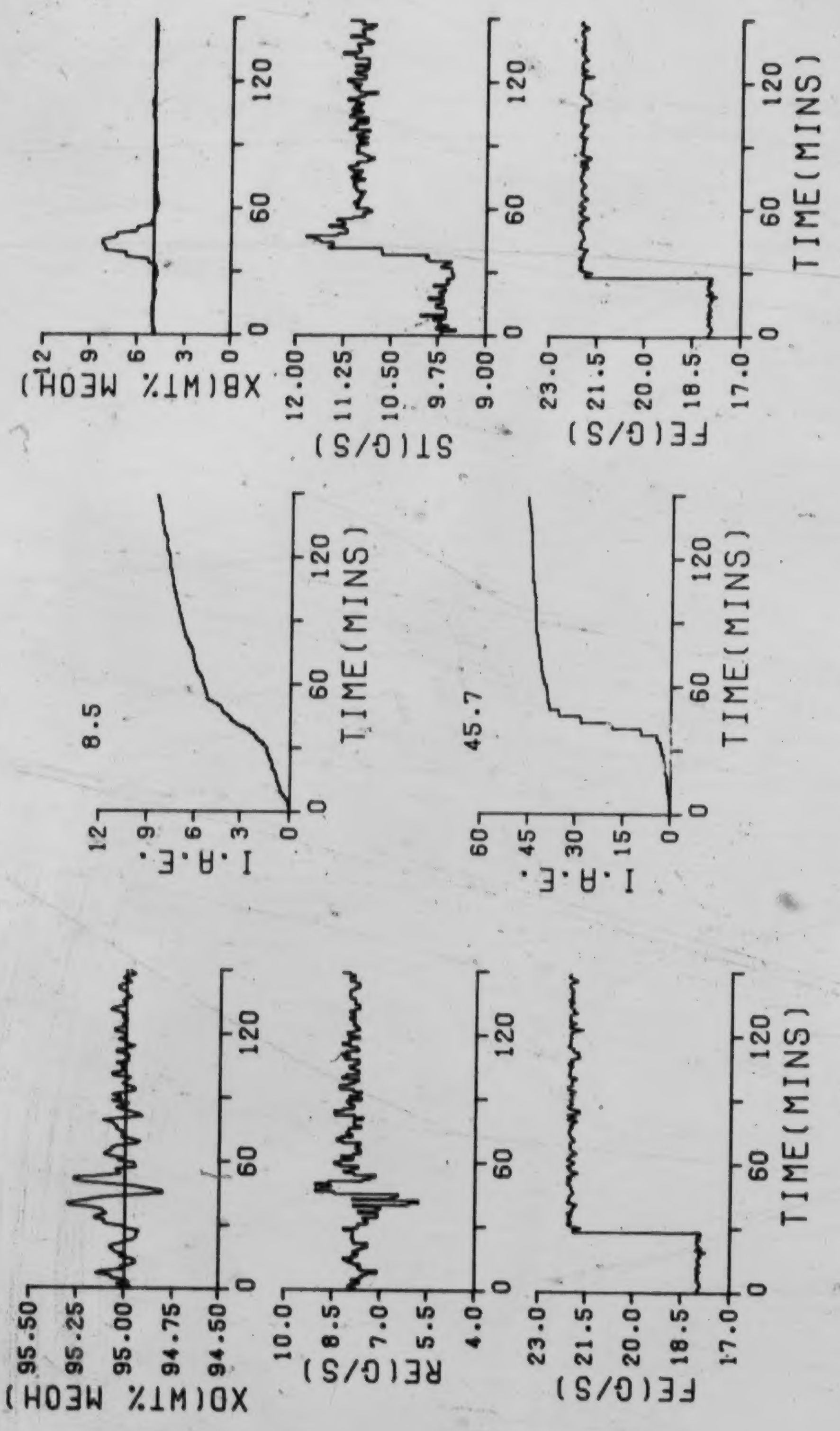

FIGURE 7.77 MR ST/Q(PB=5.2,TI=107.6,TD=0.0)/TS=60.0/4,3,3,0,4/
Q(PB=50.0,TI=150.0,TD=0.0)/TS=180.0/5,3,3,0,6/

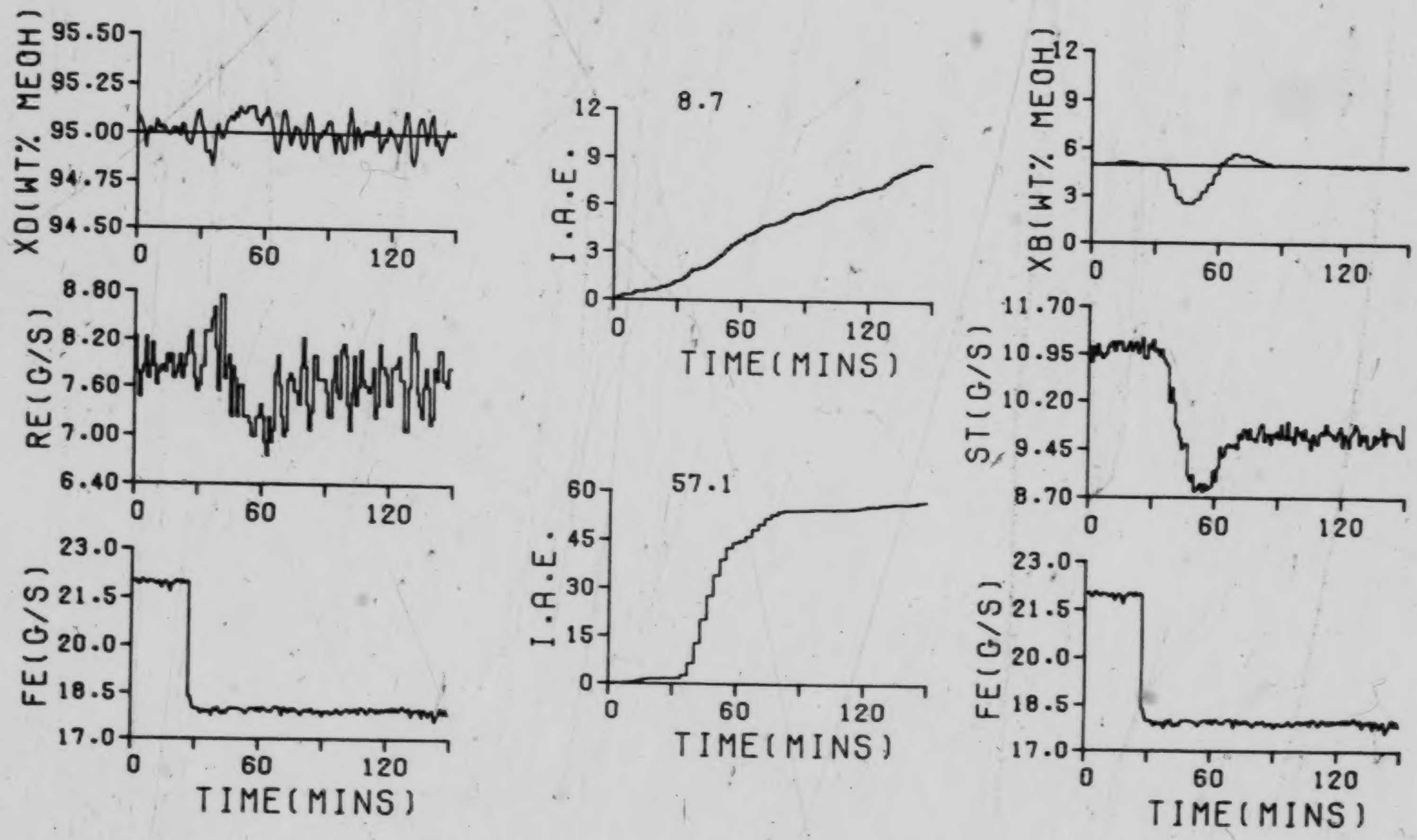

FIGURE 7.78 MR ST/Q(PB=5.2.TI=107.6.TD=0.0)/TS=60.0/4.3.3.0.4/
Q(PB=50.0.TI=150.0.TD=0.0)/TS=180.0/5.3.3.0.6/

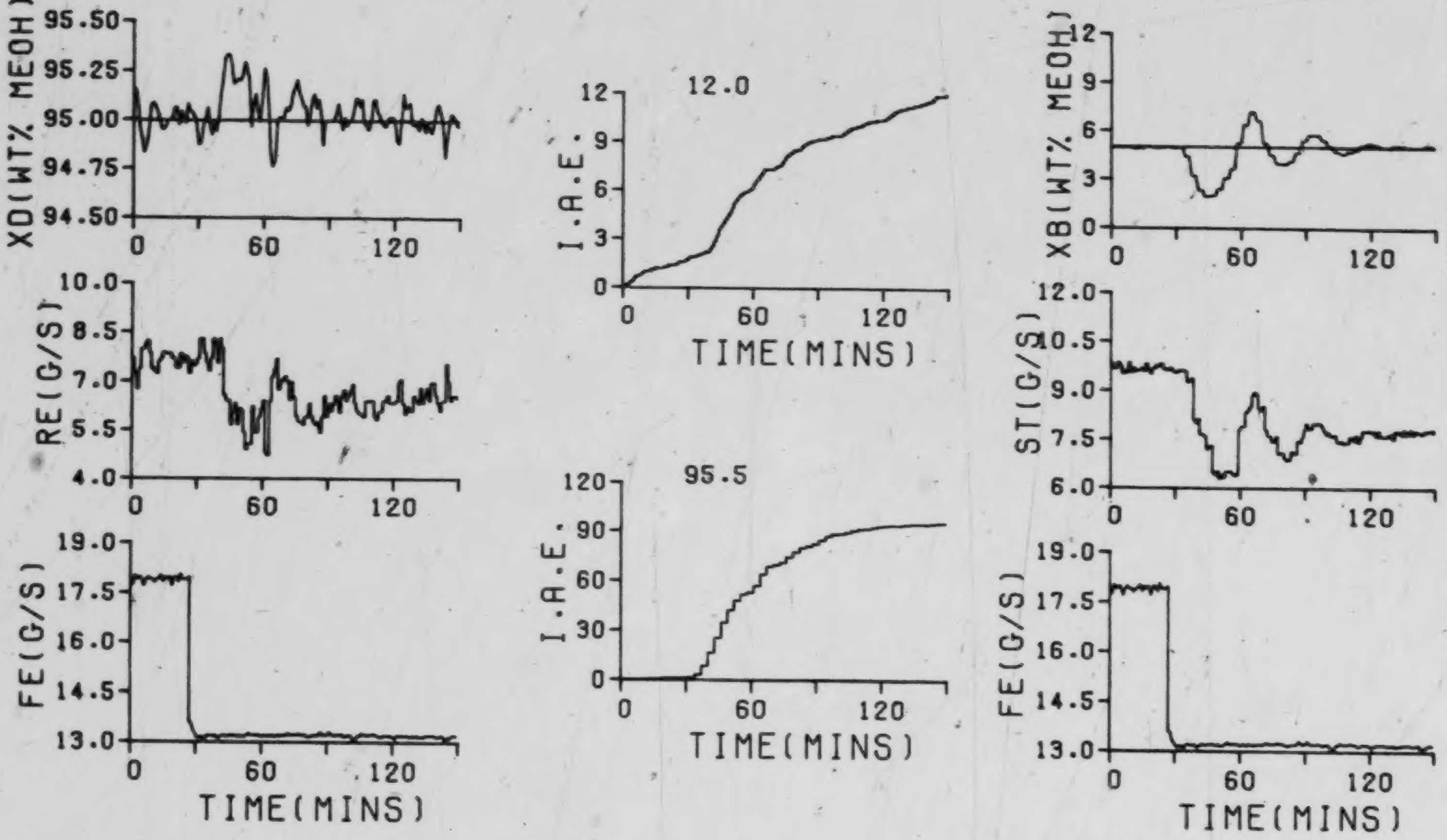

FIGURE 7.79 MR ST/Q(PB=5.2,TI=107.6,TD=0.0)/TS=60.0/4.3.3.0.4/
Q(PB=50.0,TI=150.0,TD=0.0)/TS=180.0/5.3.3.0.6/

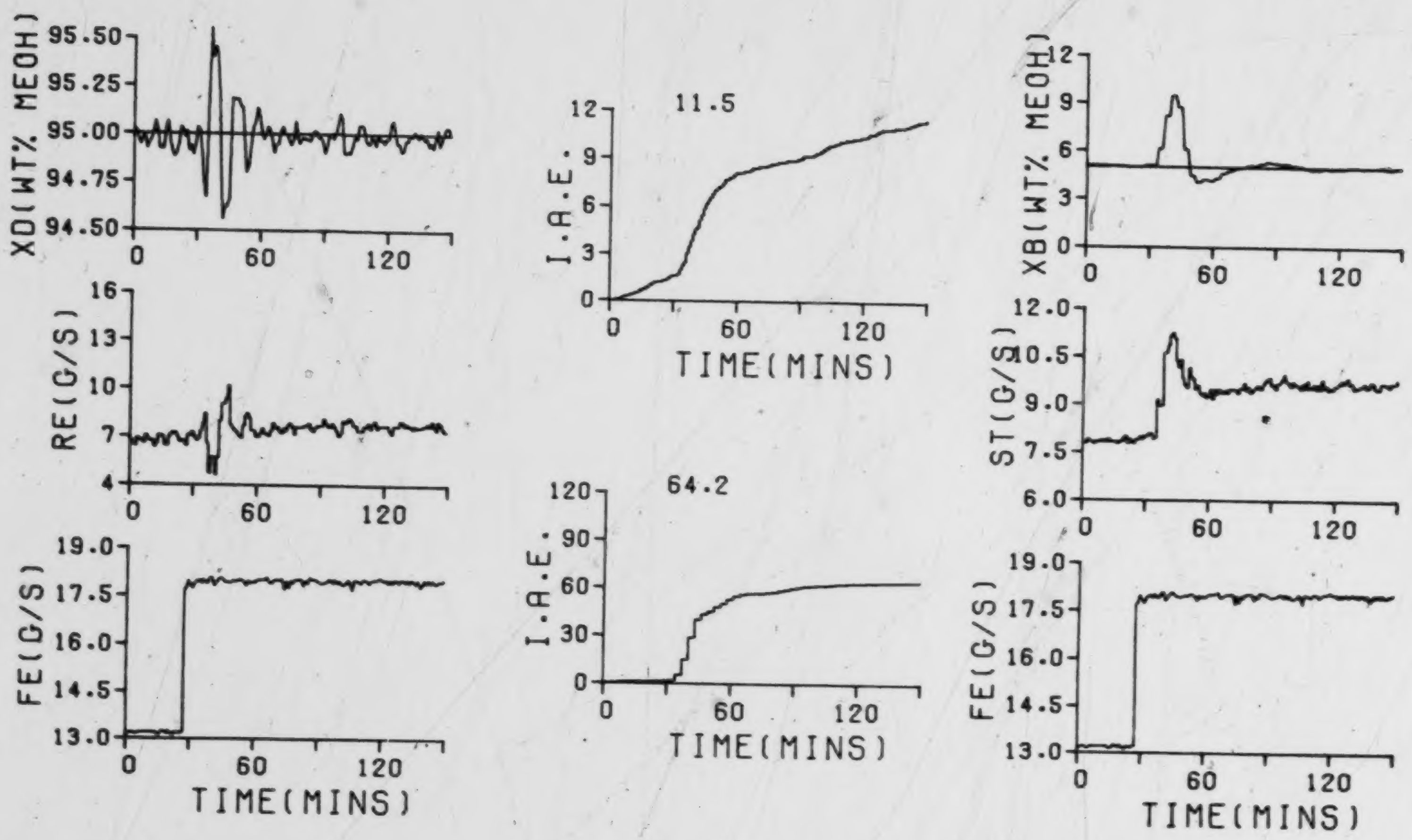

FIGURE 7.80 MR ST/Q(PB=5.2,TI=107.6,TD=0.0)/TS=60.0/4.3.3.0.4/
Q(PB=50.0,TI=150.0,TD=0.0)/TS=180.0/5.3.3.0.6/

Table 7.6.4
Multirate Self-Tuning Control Performance with Tuned Q
Weighting Constants

	IAE Values			
	Tuned		IAE	
Step	TOP	BOTTOM	TOP	BOTTOM
increase from SS	8.5	45.7	6.0	78.3
decrease to SS	8.7	57.1	5.6	65.4
decrease from SS	12.0	95.5	8.8	116.0
increase to SS	11.5	64.2	9.2	97.2
total	40.7	262.5	29.6	356.9

7.6.5 Comparison of Tuned Controller Performance

As can be seen from the IAE values summarized in Tables 7.6.5 and 7.6.6 for multiloop PID control of the column using single rate sampling an improvement of 35.4% has been achieved by tuning of the PID controller constants. For multirate sampling using the PID control strategy, an improvement of 41.4% was obtained by tuning the controller constants. It is worthwhile to observe that the total IAE values for operating the column using a multiloop PID control strategy for single and multirate sampling were virtually identical. However it must be stressed that a substantial amount of time and effort had to be expended due to the large number of trial runs which were performed to arrive at the final controller settings. The total IAE values with the column operating under multivariable self-tuning control show that smaller improvements were

Table 7.6.5
Comparison of Tuned Controller Performance

		IAE Total by Control Strategy			
Sampling		Single Rate		Multirate	
Step		PID	STC	PID	STC
increase from SS	top	8.0	7.7	5.3	8.5
	bottom	99.0	57.3	101.6	45.7
decrease to SS	top	7.9	9.0	5.2	8.7
	bottom	117.9	59.9	117.4	57.1
decrease from SS	top	10.6	17.7	11.8	12.0
	bottom	161.3	111.0	158.8	95.5
increase to SS	top	9.3	11.2	8.3	11.5
	bottom	134.0	67.6	136.6	64.2
total		548.0	341.4	545.0	303.2

Table 7.6.6
Comparison of Tuned Controller Performance and That Obtained With Calculated Constants

	IAE Total by Control Strategy			
Sampling	Single Rate		Multirate	
	PID	STC	PID	STC
Tuned IAE Total	548.0	341.4	545.0	303.2
IAE total	848.6	363.0	929.3	386.5
percent improvement	35.4%	6.0%	41.4%	21.6%
Method	3-C	3-C	3-C	IAE

realized by adjustment of the Q weighting parameters than for adjustment of the PID controller settings.

A further comparison of control performance of the two different strategies showing the IAE values for each composition as well as the total values is presented in Table 7.6.7. This summary shows that the best top composition control was obtained using the multiloop PID control strategy with multirate sampling. The IAE values show that use of multirate self-tuning control clearly provides superior bottom composition regulation, but this superior performance has resulted in increased interaction with the top composition control which causes degradation in the control of top composition compared with that achieved with the PID control strategy.

Since the results have shown that for multirate sampling only a marginal improvement in control performance is obtained using the multivariable self-tuning control strategy with tuned Q weighting parameters versus calculated values, it is appropriate to compare the IAE values achieved using calculated Q weighting parameters versus these values that resulted using tuned PID controllers with the multiloop strategy. These values for the two sets of tests are summarized in Table 7.6.8. Based on tabulations provided in Tables 7.6.7 and 7.6.8 we can conclude that the multirate sampling form of the self-tuning control algorithm provides superior control when compared with the best performance that can be achieved using a multiloop PID control strategy.

Table 7.6.7
Total and Individual Product Composition IAE Values for PID and STC Control Using Tuned Controller Settings

	Controller Method			
	ML PID	MV ST	MR PID	MR ST
top response	35.8	45.6	30.6	40.7
Bottom response	512.2	295.8	514.4	262.5
IAE Total	548.0	341.4	545.0	303.2

Table 7.6.8
Comparison of Tuned PID Control With Self-Tuning Control Using Calculated Q Weighting Constants

		Control Strategy	
Step	\composition	PID	STC *
increase from SS	top	5.3	6.0
	bottom	101.6	78.3
decrease to SS	top	5.2	5.6
	bottom	117.4	65.4
decrease from SS	top	11.8	8.8
	bottom	158.8	116.0
increase to SS	top	8.3	9.2
	bottom	136.6	97.2
Total IAE for top Composition		30.6	29.6
Total IAE for Bottom Composition		514.4	356.9
Total IAE Value		545.0	386.5

* Q weighting parameters based on the IAE criterion equations (cf. Table 7.5.1)

7.7 Effect On Column Control Performance Using Measured Feedforward Compensation with Multivariable Self-Tuning Control

In all the previous tests of control performance, the self-tuning controller employed estimated feedforward compensation (cf. equation 7.1). For this series of tests: the disturbance, i.e. feed flow rate, is measured and used as the input value of the observation vector. The same Q weighting parameters as determined from the tuned performance results were employed to obtain the column responses shown in Figures 7.81 through 7.84. These results, obtained using the single rate sampling form of the algorithm show that excellent control of the bottom composition was achieved. To further appreciate the improved control that results from using direct measurement of the feed disturbance, the IAE values of both composition responses displayed in Figures 7.81 to 7.84 are summarized in Table 7.7.1 as are the IAE values that were obtained using an estimate of the feedforward disturbance for both tuned and calculated Q weighting parameters.

As can be seen from the tabulation, we can conclude that measurement versus estimation of the feed disturbance for feedforward compensation improves the regulatory performance of the self-tuning controller. In terms of individual loop performance, the IAE values in Table 7.7.1 show that for bottom composition the measured feedforward compensation tests result in the lowest IAE values. These

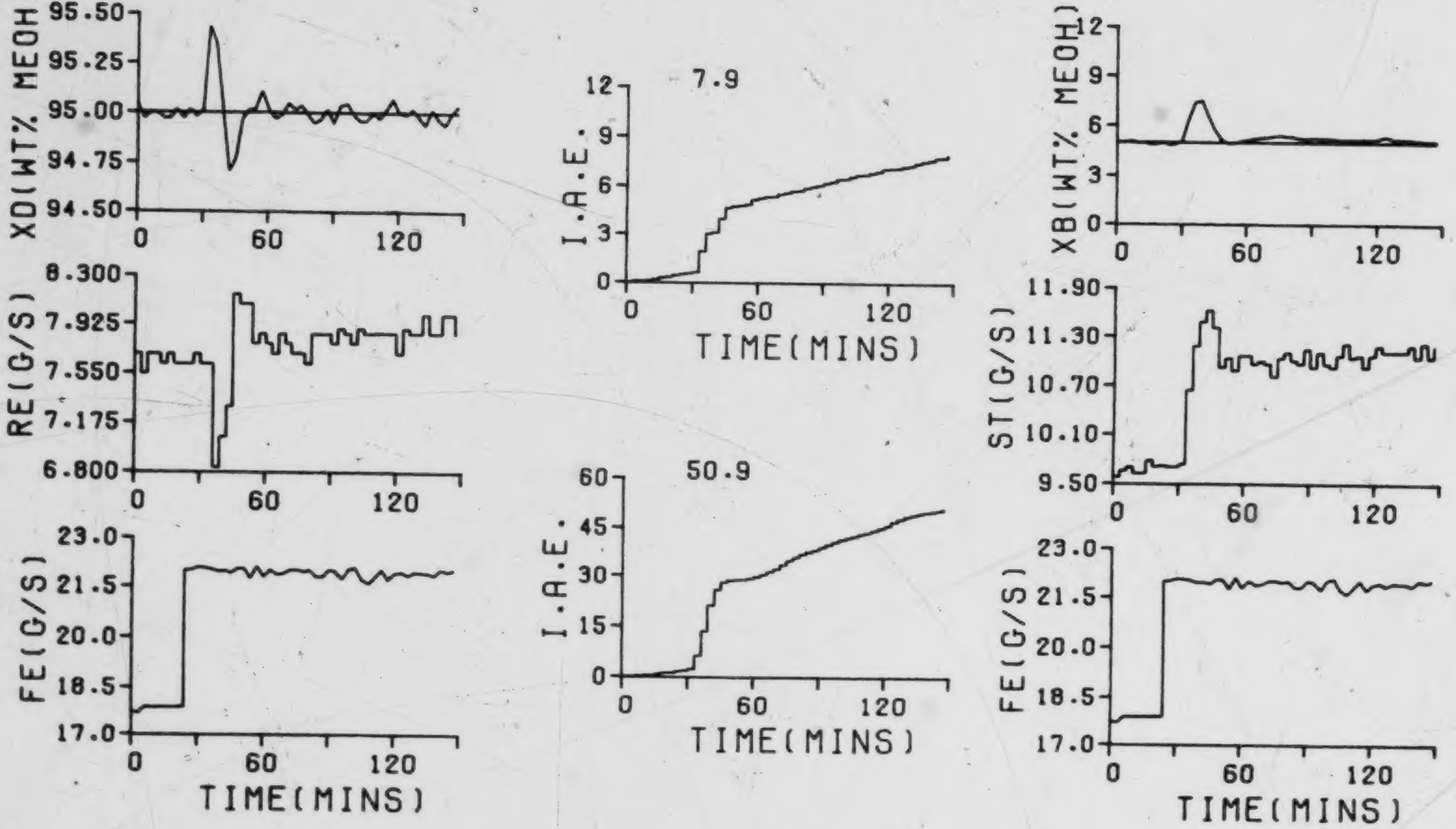

FIGURE 7.81 MV ST MFF/Q(PB=15.0,TI=80.0,TD=0.0)/TS=180.0/4.3.3.0.4/
Q(PB=50.0,TI=150.0,TD=0.0)/TS=180.0/5.3.3.0.6/

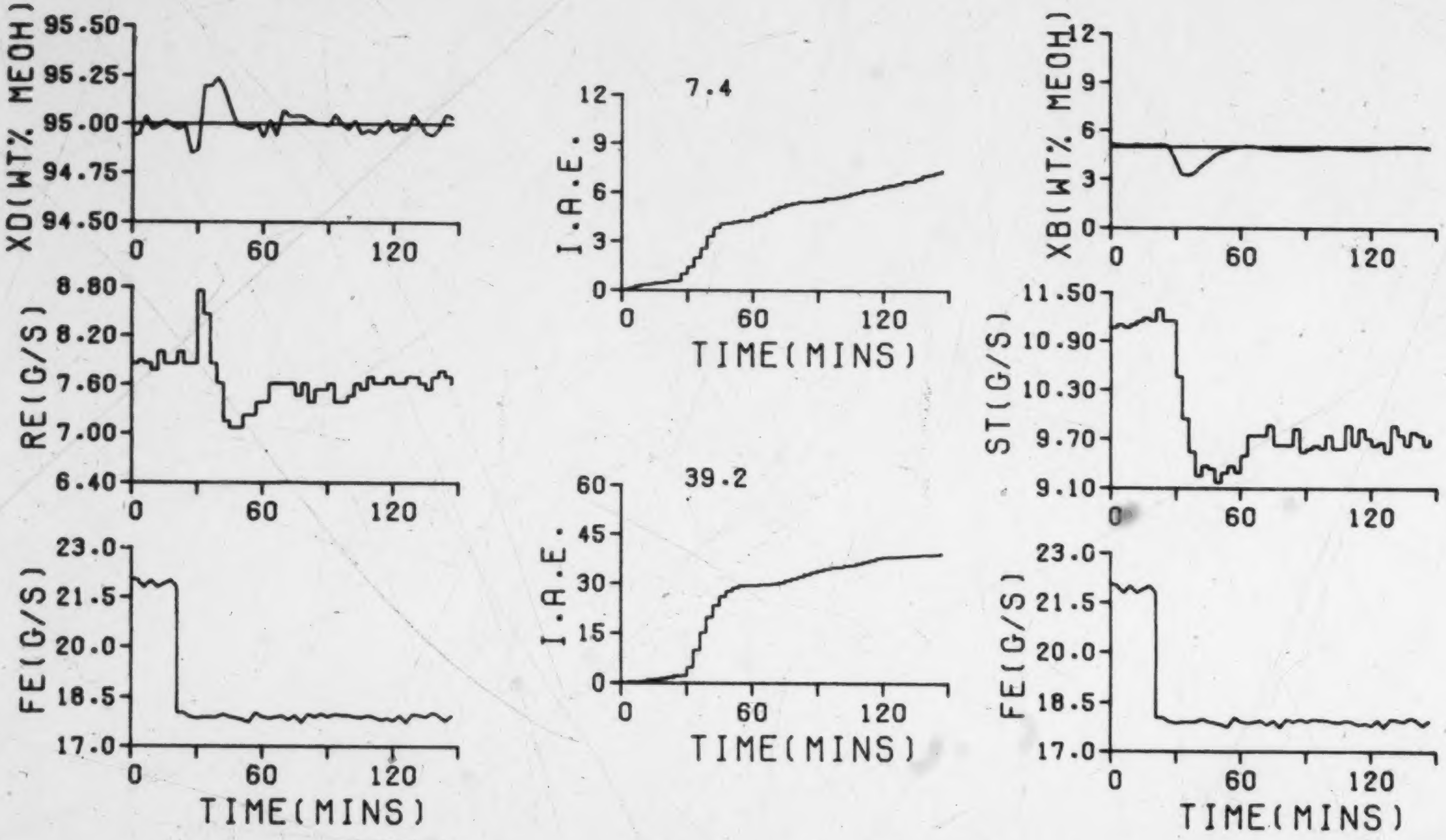

FIGURE 7.82 MV ST MFF/Q(PB=15.0,TI=80.0,TD=0.0)/TS=180.0/4.3.3.0.4/
Q(PB=50.0,TI=150.0,TD=0.0)/TS=180.0/5.3.3.0.6/

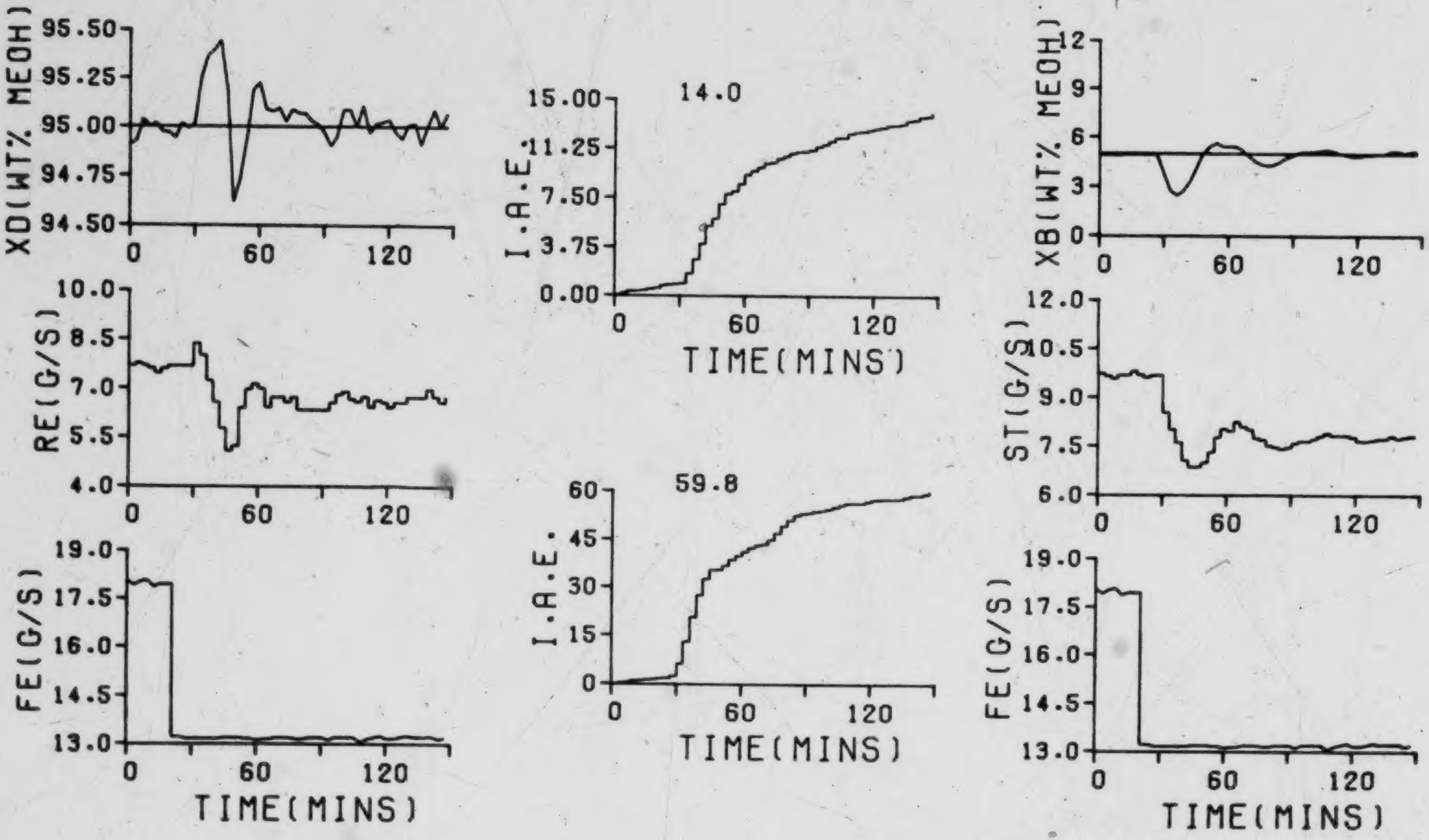

FIGURE 7.83 MV ST MFF/Q(PB=15.0.TI=80.0.TD=0.0)/TS=180.0/4.3.3.0.4/
Q(PB=50.0.TI=150.0.TD=0.0)/TS=180.0/5.3.3.0.6/

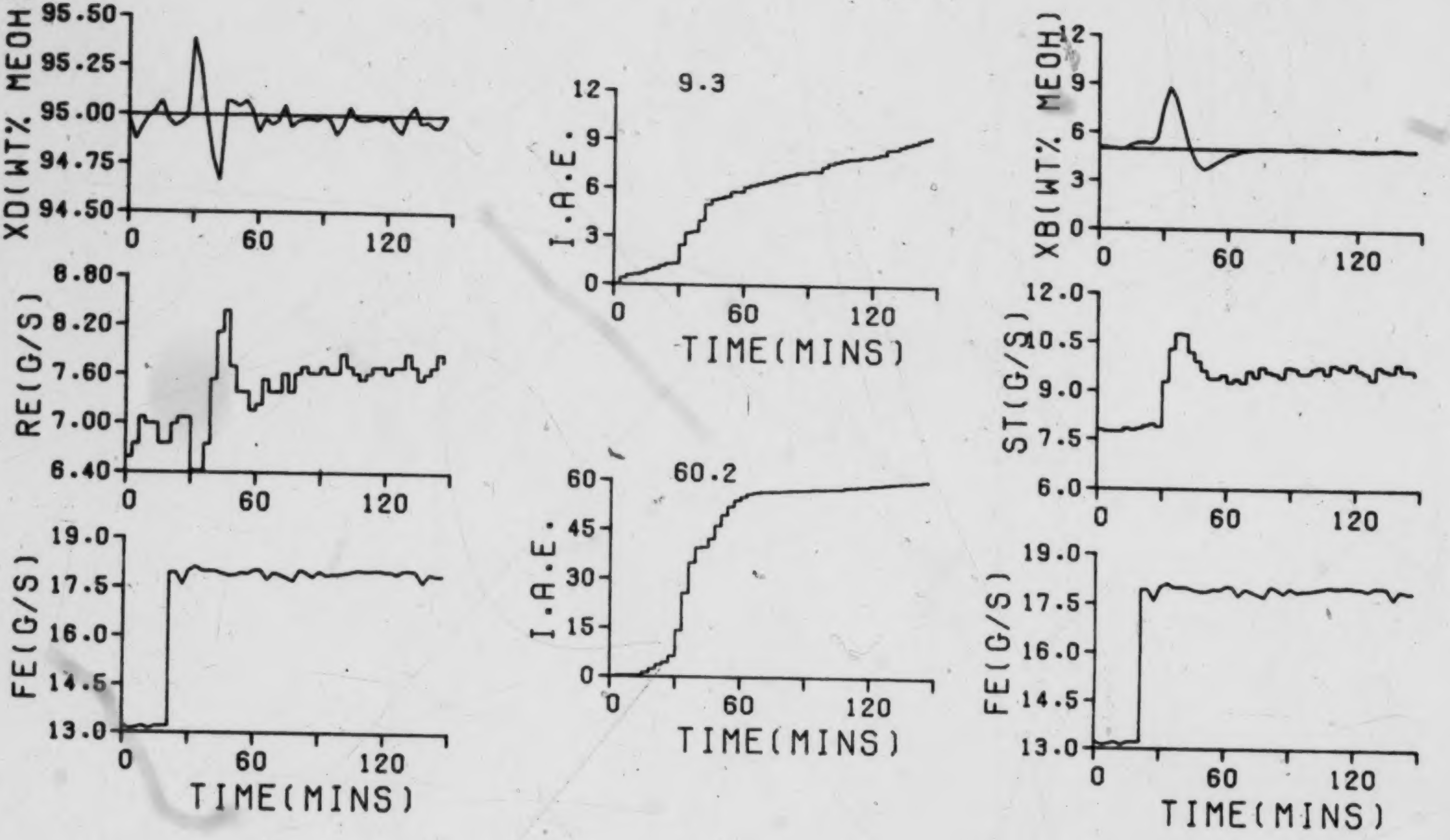

FIGURE 7.84 MV ST MFF/Q(PB=15.0,TI=80.0,TD=0.0)/TS=180.0/4.3.3.0.4/
Q(PB=50.0,TI=150.0,TD=0.0)/TS=180.0/5.3.3.0.6/

Table 7.7.1
Comparison of Multivariable Self-Tuning Controller
Performance IAE Values

		Estimated Feedforward Compensation		Measured Disturbance
step	loop	Calculated Constants	Tuned Constants	Tuned Constants
increase from SS	top	7.6	7.7	7.9
	bottom	61.4	57.3	50.9
decrease to SS	top	8.7	9.0	7.4
	bottom	72.8	59.9	39.2
decrease from SS	top	19.5	17.7	14.0
	bottom	93.3	111.0	59.8
increase to SS	top	13.5	11.2	9.3
	bottom	86.2	67.6	60.2
Top loop IAE Total		49.3	45.6	38.6
Bottom loop IAE Total		313.7	295.8	210.1
Total		363.0	341.4	248.7

results also show that for feed flow rate disturbances below steady state that regulation is more difficult. This is due to the inverse response and nonlinear characteristics that characterize the column dynamics for these disturbances. The larger IAE values relate directly to the oscillatory return of the bottom composition to the setpoint for the step decrease from the steady state value while for the step return to the normal feed rate the composition response has shown that overshoot accompanies the return of the composition to the setpoint.

Tuning of the Q weighting parameters to reduce integral action and gain should improve the regulatory control for these disturbances.

As the responses in Figures 7.81 to 7.84 show the bottom composition, as for the previous tests, undergoes a deviation from the setpoint at the onset of the disturbance for each of the four flow rate changes, but the magnitude of the initial deviation has been reduced, indicating that measured feedforward compensation is more effective than use of estimated feedforward action to minimize any initial deviation from the setpoint for feed disturbances.

To further assess the improvement in control behavior that results by using measured feedforward compensation, a series of tests of the multivariable self-tuning control strategy were performed using multirate sampling. With the top composition sampled on a 1.0 minute cycle, with the bottom composition sampled at the 3.0 minute interval. The column responses that resulted for the four feed rate disturbances using tuned Q weighting parameters are presented in Figures 7.85 to 7.88.

The effective decoupling action provided by the self-tuning controller is clearly shown in Figure 7.85 by sharp bottom composition control action (large steam rate increase) to compensate for the disturbance, that is accompanied by the rapid short duration decrease in reflux flow (top composition control action) resulting in improved

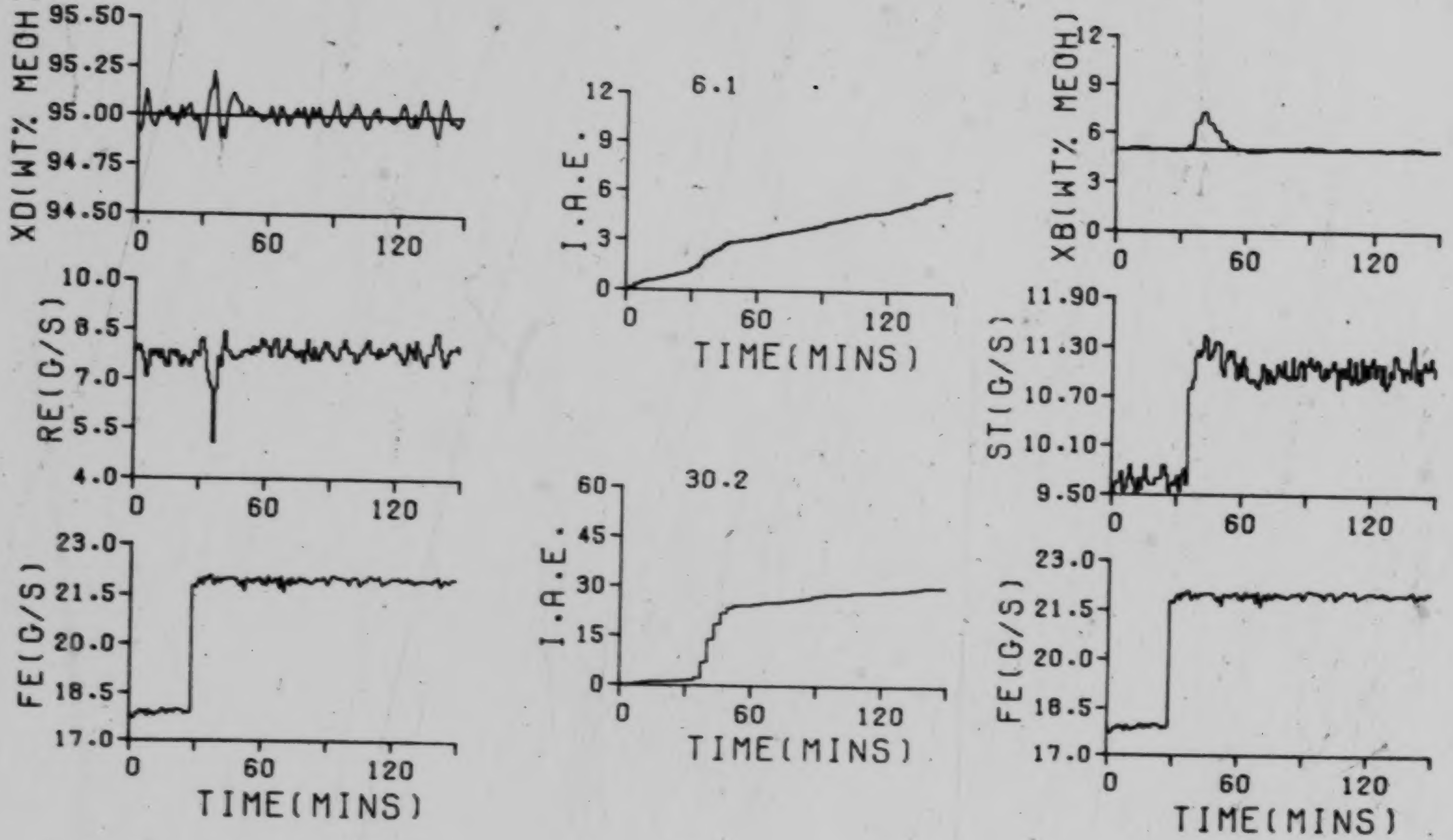

FIGURE 7.85 MR ST MFF/Q(PB=5.2.TI=107.6.TD=0.0)/TS=60.0/4.3.3.0.4/
Q(PB=50.0.TI=150.0.TD=0.0)/TS=180.0/5.3.3.0.6/

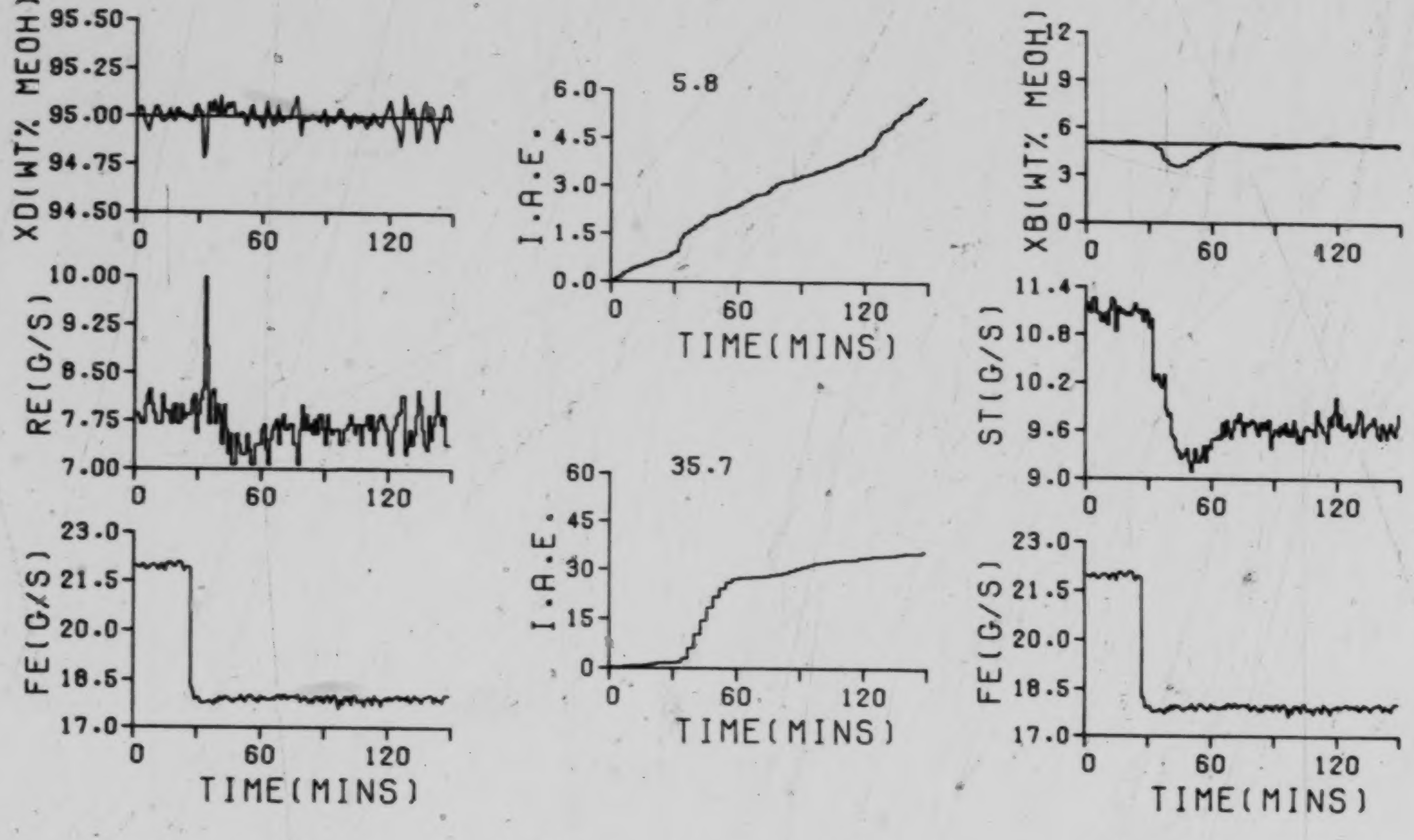

FIGURE 7.86 MR ST MFF/Q(PB=5.2,TI=107.6,TD=0.0)/TS=60.0/4.3.3.0.4/
Q(PB=50.0,TI=150.0,TD=0.0)/TS=180.0/5.3.3.0.6/

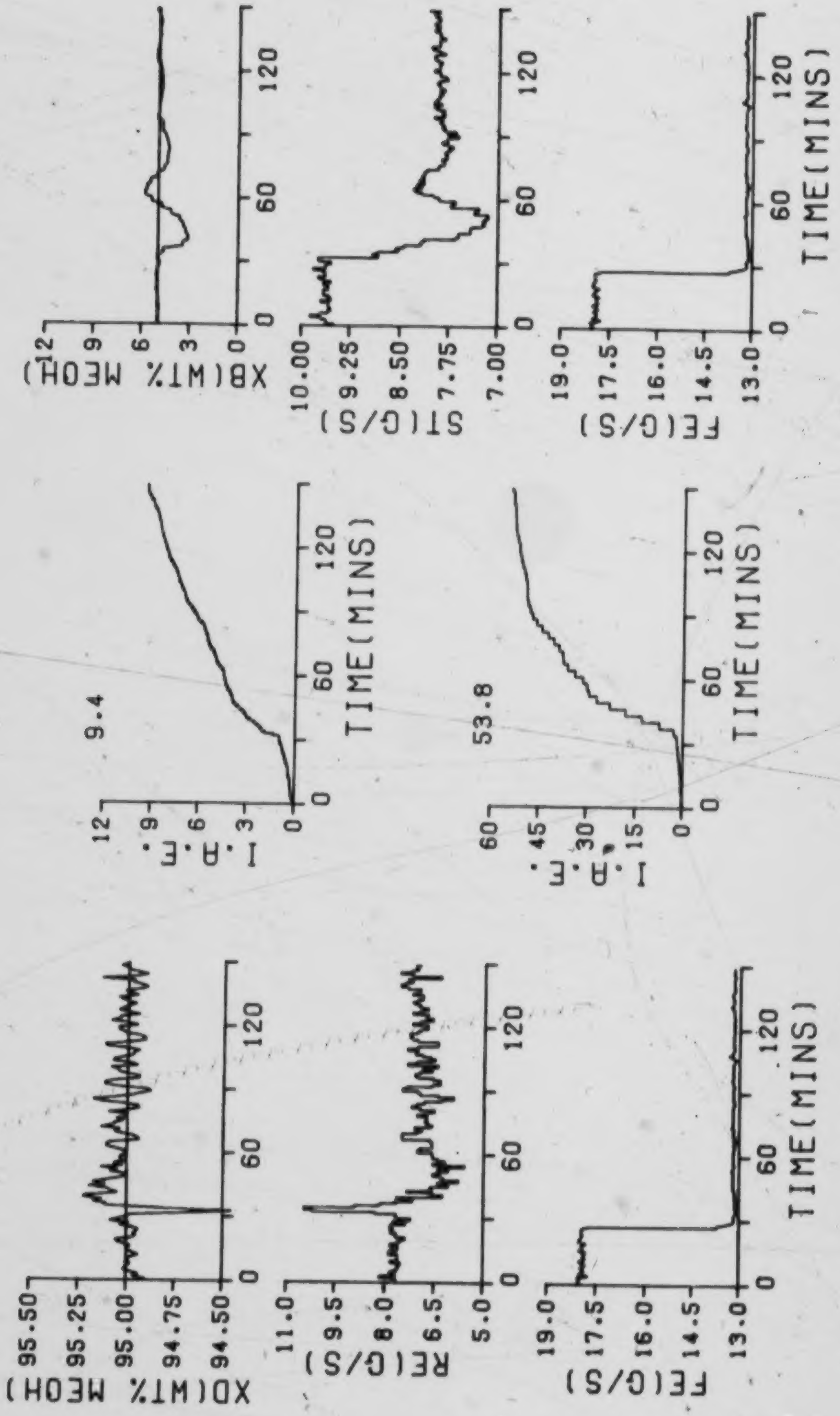

FIGURE 7.87 MR ST MFF/Q(PB=5.2,TI=107.6,TD=0.0)/TS=60.0/4.3.3.0.4/
Q(PB=50.0,TI=150.0,TD=0.0)/TS=180.0/5.3.3.0.6/

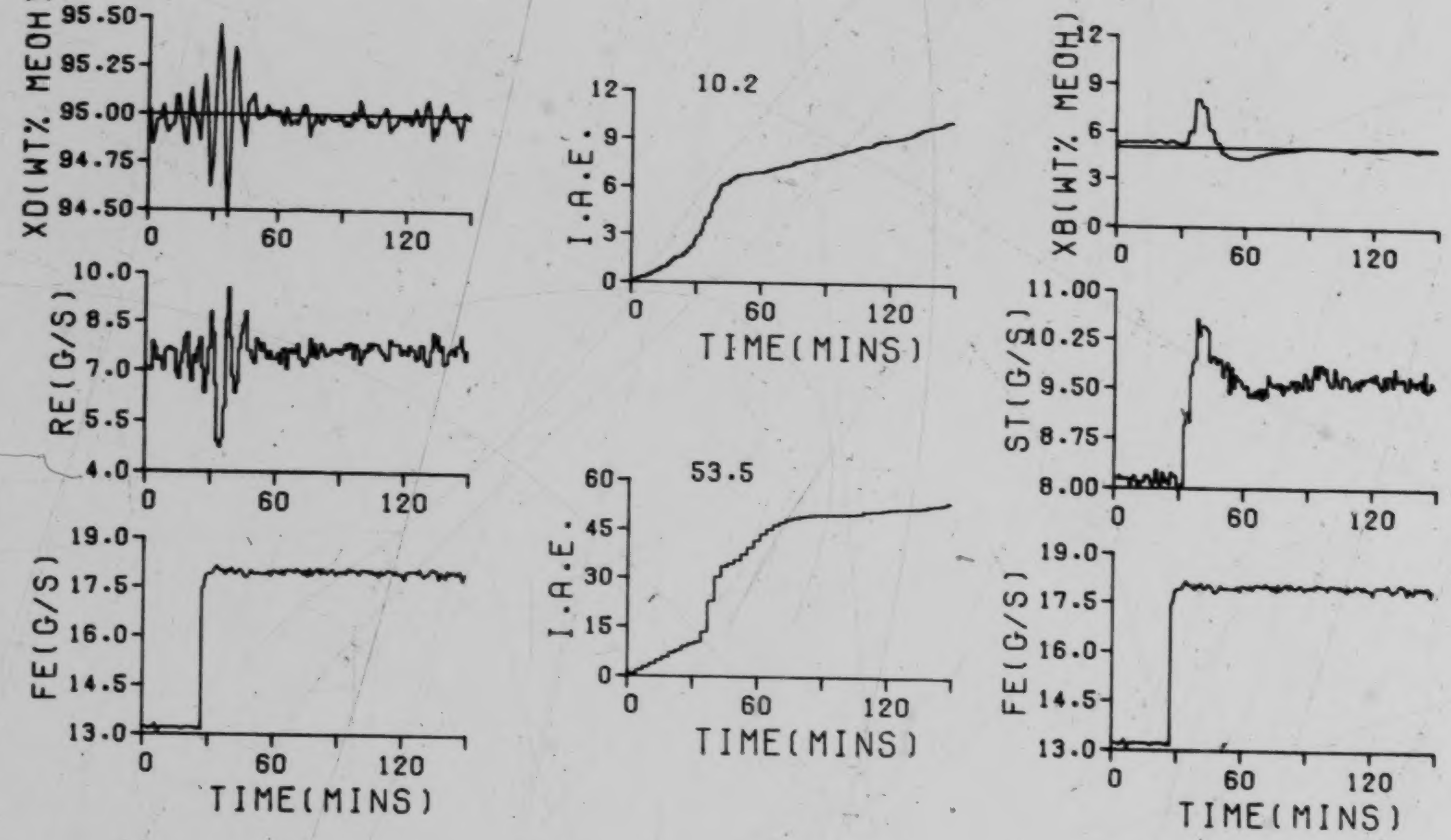

FIGURE 7.88 MR ST MFF/Q(PB=5.2,TI=107.6,TD=0.0)/TS=60.0/4.3.3.0.4/
Q(PB=50.0,TI=150.0,TD=0.0)/TS=180.0/5.3.3.0.6/

top and bottom composition regulation. This decoupling action is also evident from the responses for the other feed rate disturbances.

The effectiveness of the measured feed rate disturbances for applying feedforward action is clearly shown by the IAE values summarized in Table 7.7.2. This tabulation which shows the IAE values for the estimated feedforward action versus feedforward action based on the measured feed disturbance for tuned Q weighting, also contains the IAE values obtained using calculated Q weightings. Although no tests were conducted using the calculated Q weighting with measurement of the feed rate disturbance, it is to be expected that the total IAE value would decrease from the 386.5 value but likely not fall below the 204.7 value.

7.8 Column Performance Using The K-Incremental Form of the Self-Tuning Controller

In Chapter 3 the extension of the basic algorithm to provide k-incremental self-tuning control was presented. This section presents results obtained using measured feedforward compensation for both single rate and multirate sampling with the Q weighting parameters of both controllers set at the tuned values used in the previous tests. The distillation column responses provided in Figures 7.89 through 7.92 document the performance achieved using the K-incremental form of the algorithm with no adjustment of

Table 7.7.2
Comparison of Multirate Self-Tuning Controller Performance

IAE Values				
		Estimated Feedforward Compensation		Measured Disturbance
step	loop	Calculated Constants	Tuned Constants	Tuned Constants
increase from SS	top	6.0	8.5	6.1
	bottom	78.3	45.7	30.2
decrease to SS	top	5.6	8.7	5.8
	bottom	65.4	57.1	35.7
decrease from SS	top	8.4	12.0	9.4
	bottom	116.0	95.5	53.8
increase to SS	top	9.2	11.5	10.2
	bottom	97.2	64.5	53.5
Top loop IAE Total		29.2	40.7	31.5
Bottom loop IAE Total		356.9	262.8	173.2
Total		386.5	303.2	204.7

the Q weighting. Regulation of the column product composition has improved by use of the k-incremental form of the multivariable self-tuning controller as shown by the individual composition IAE values as well as the total values presented in Table 7.8.1. For all four feed rate disturbances, the IAE value for the control of top composition was reduced by use of the k-incremental algorithm, but for bottom composition the control action

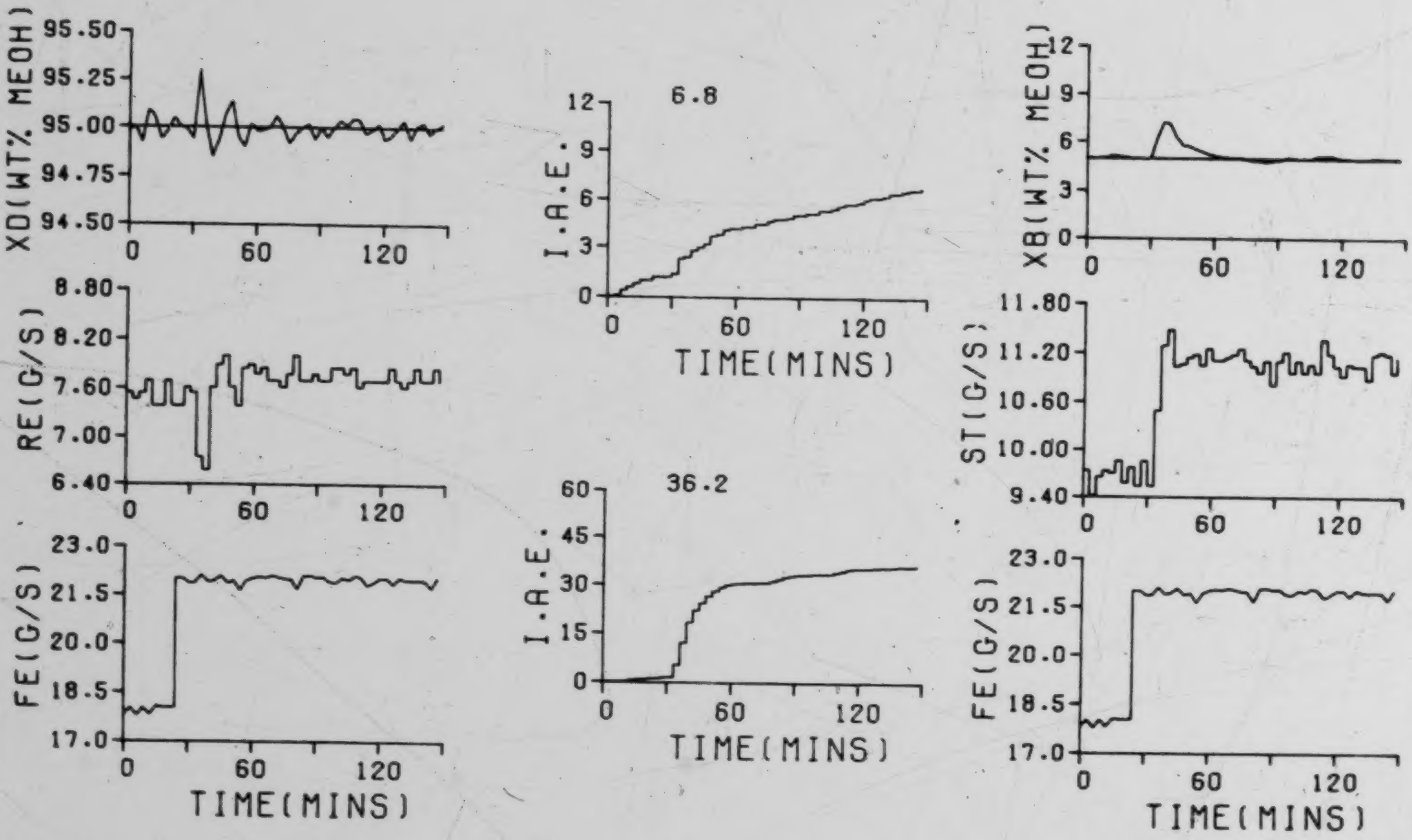

FIGURE 7.89 MV KINC ST MFF/Q(PB=15.0,TI=80.0,TD=0.0)/TS=180.0/4.3.3.0.4/
Q(PB=40.0,TI=150.0,TD=0.0)/TS=180.0/5.3.3.0.6/

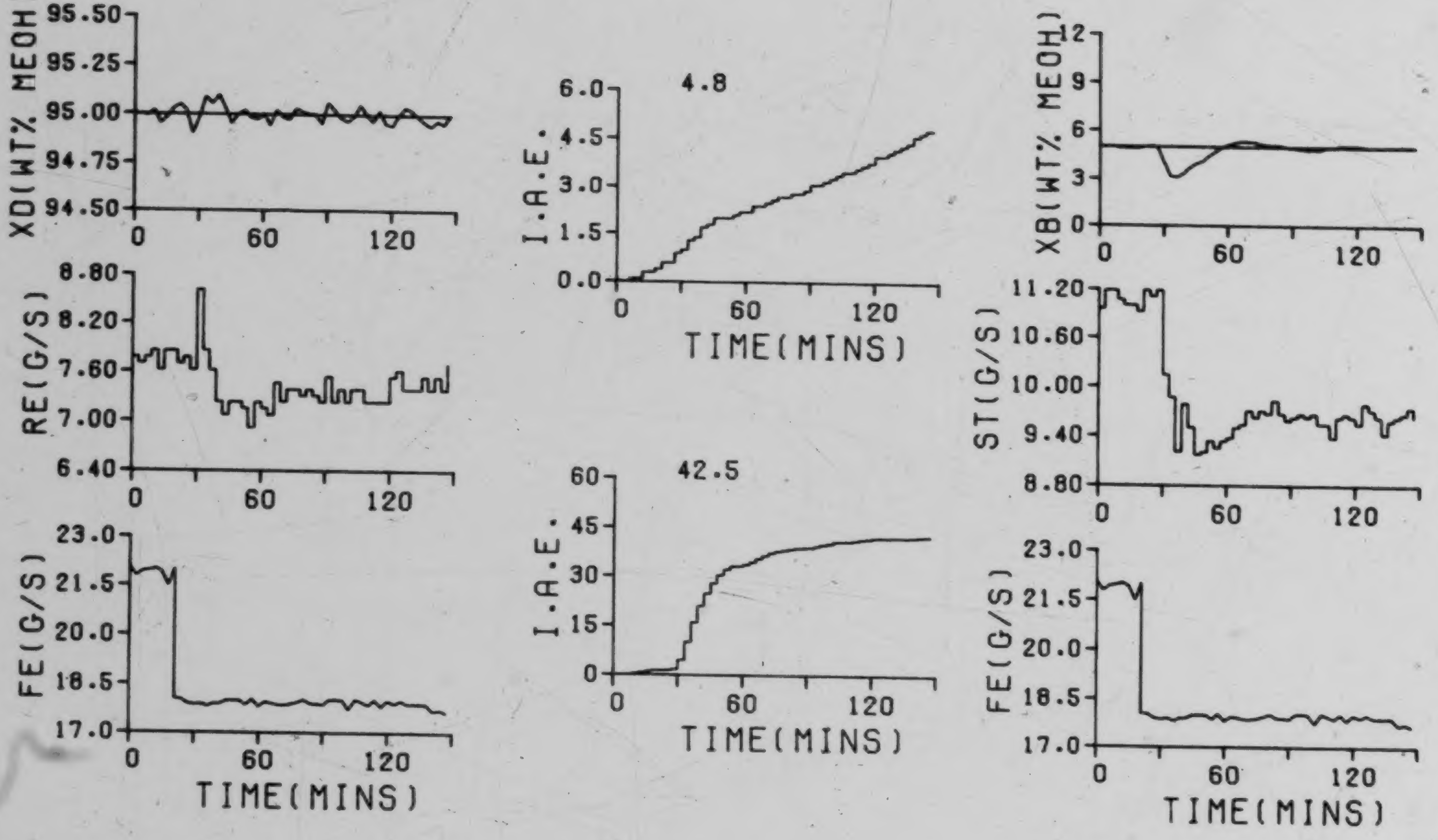

FIGURE 7.90 MV KINC ST MFF/Q(PB=15.0,TI=80.0,TD=0.0)/TS=180.0/4.3.3.0.4/
Q(PB=40.0,TI=150.0,TD=0.0)/TS=180.0/5.3.3.0.6/

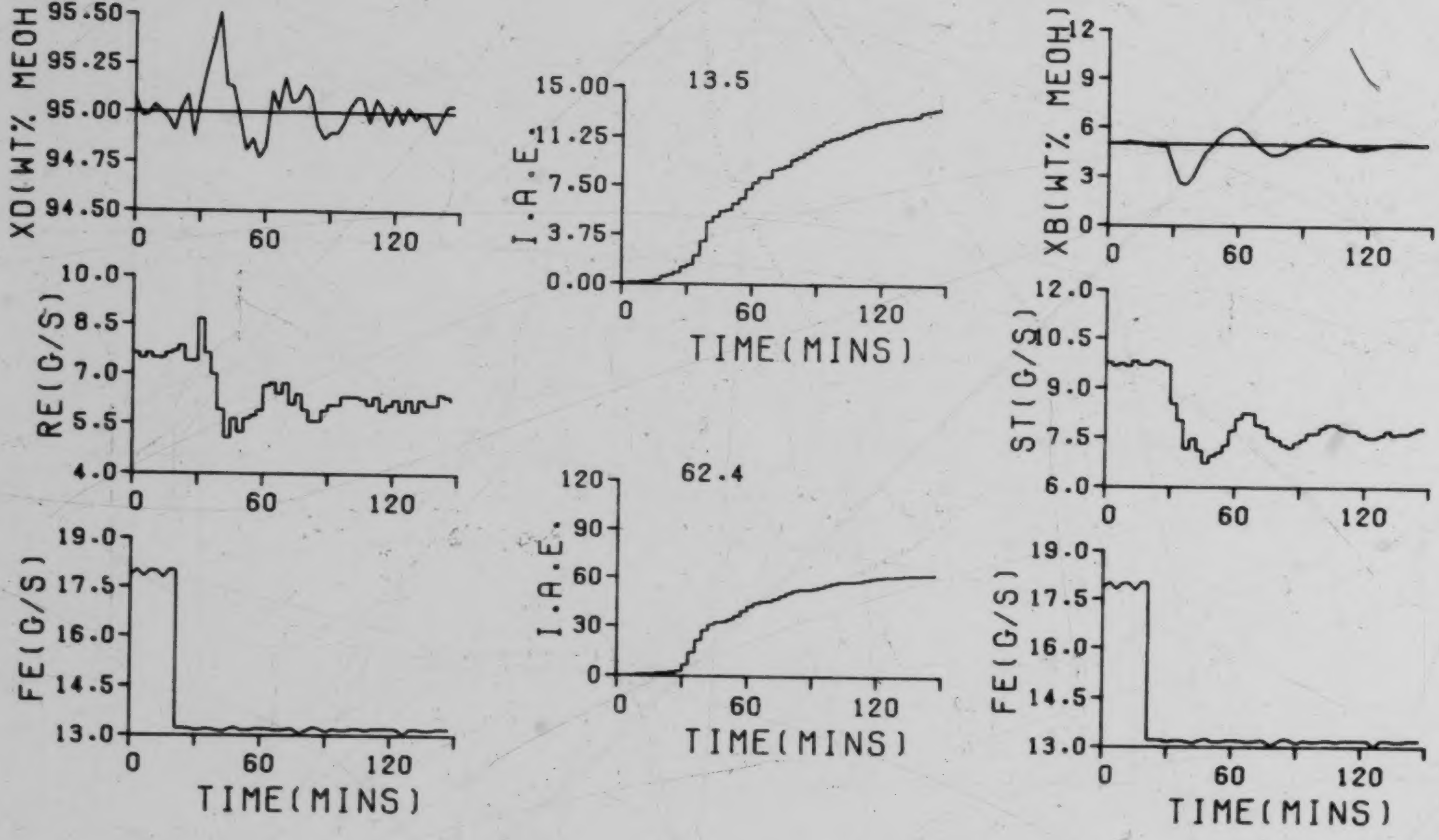

FIGURE 7.91 MV KINC ST. MFF/Q(PB=15.0.TI=80.0.TD=0.0)/TD=180.0/4.3.3.0.4/
Q(PB=40.0.TI=150.0.TD=0.0)/TS=180.0/5.3.3.0.6/

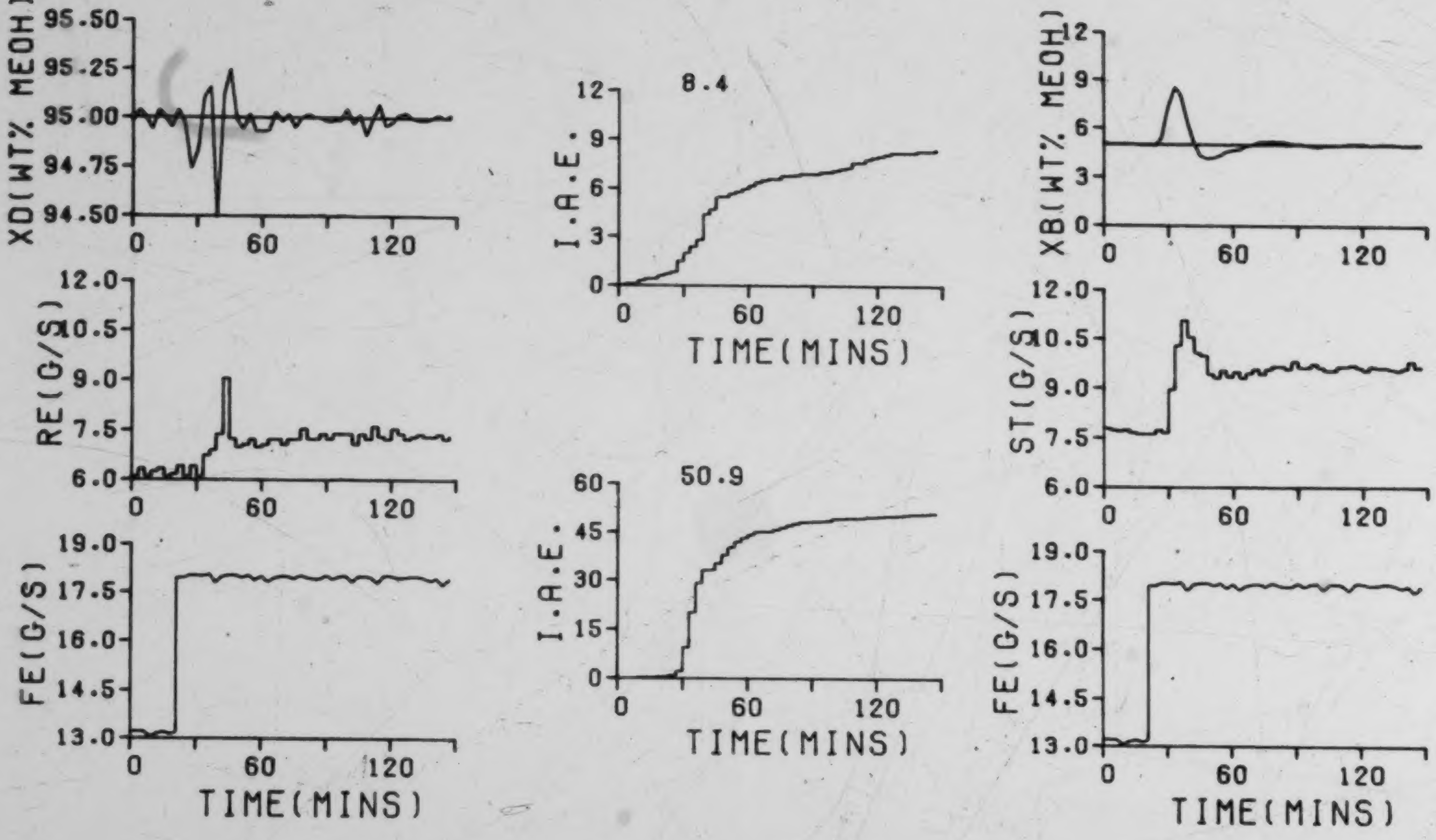

FIGURE 7.92 MV KINC ST MFF/Q(PB=15.0,TI=80.0,TD=0.0)/TS=180.0/4,3,3,0,4/
Q(PB=40.0,TI=150.0,TD=0.0)/TS=180.0/5,3,3,0,6/

Table 7.8.1
Column Performance Using Multivariable K-Incremental Self-Tuning Control With Tuned Q Weighting Constants

	IAE Values	
Step	TOP	BOTTOM
increase from steady state	6.8	36.2
decrease to steady state	4.8	42.5
decrease from steady state	13.5	62.4
increase to steady state	8.4	50.9
total	33.5	192.0

produced a lower IAE value for only two of the four disturbances.

To further demonstrate the performance of the k-incremental form of the algorithm, the self-tuning controller was employed under multirate sampling with the tuned Q weighting parameters unchanged from those used in the previous multirate tests. The control behavior that resulted by employing multirate sampling with the k-incremental self-tuning controller is displayed by the responses in Figures 7.93 to 7.96. Just as was the case for the single sample rate series of tests, use of the k-incremental form of the algorithm has improved the regulation of the top composition as shown by the IAE values tabulated in Table 7.8.2. However, this improvement has caused a degradation in the control of the bottom composition for all four feed disturbances. It is worthy of note that for the changes in feed rate, below the normal

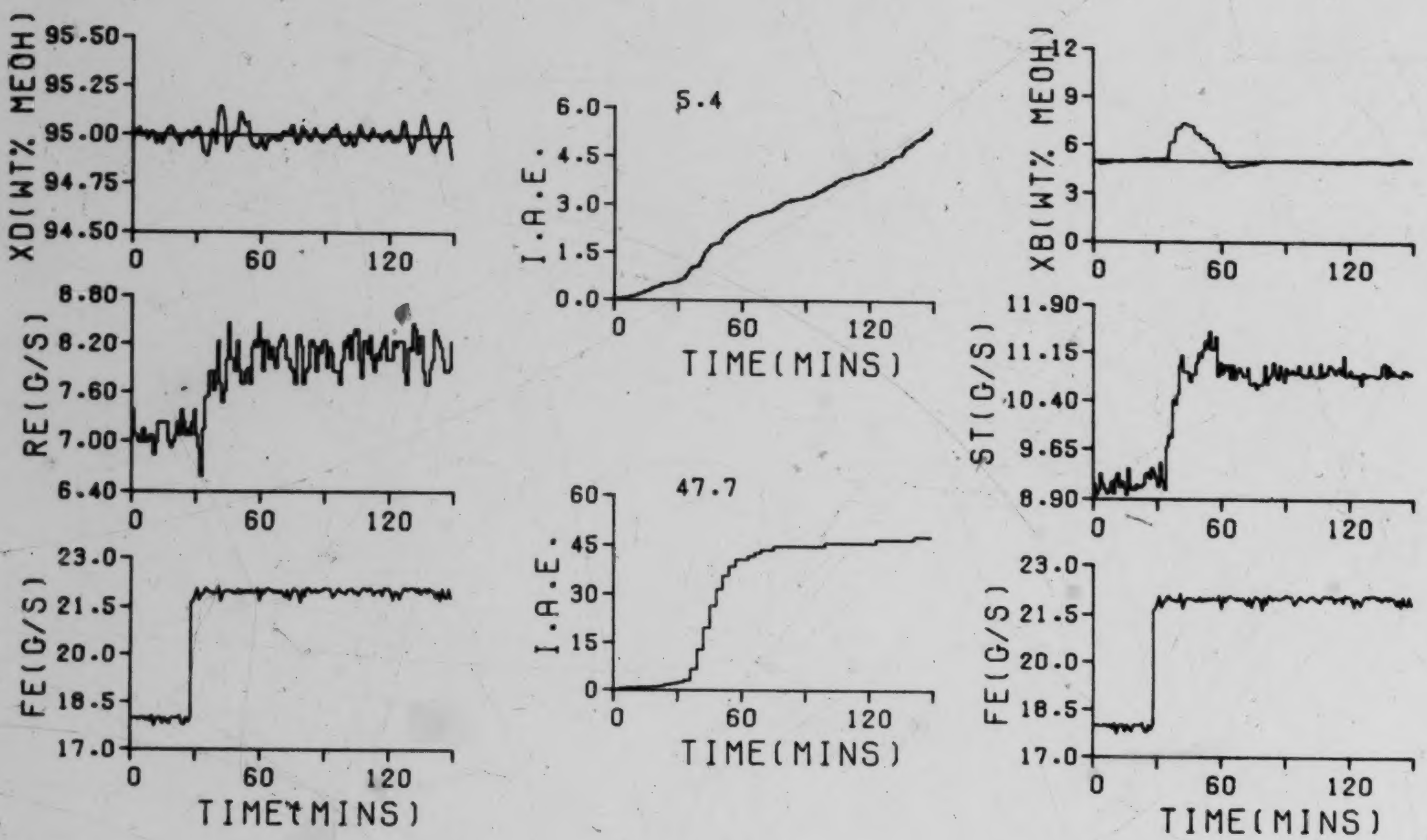

FIGURE 7.93 MR KINC ST MFF/Q(PB=5.2.TI=107.6.TD=0.0)/TS=60.0/4.3.3.0.4/
Q(PB=50.0.TI=150.0.TD=0.0)/TS=180.0/5.3.3.0.6/

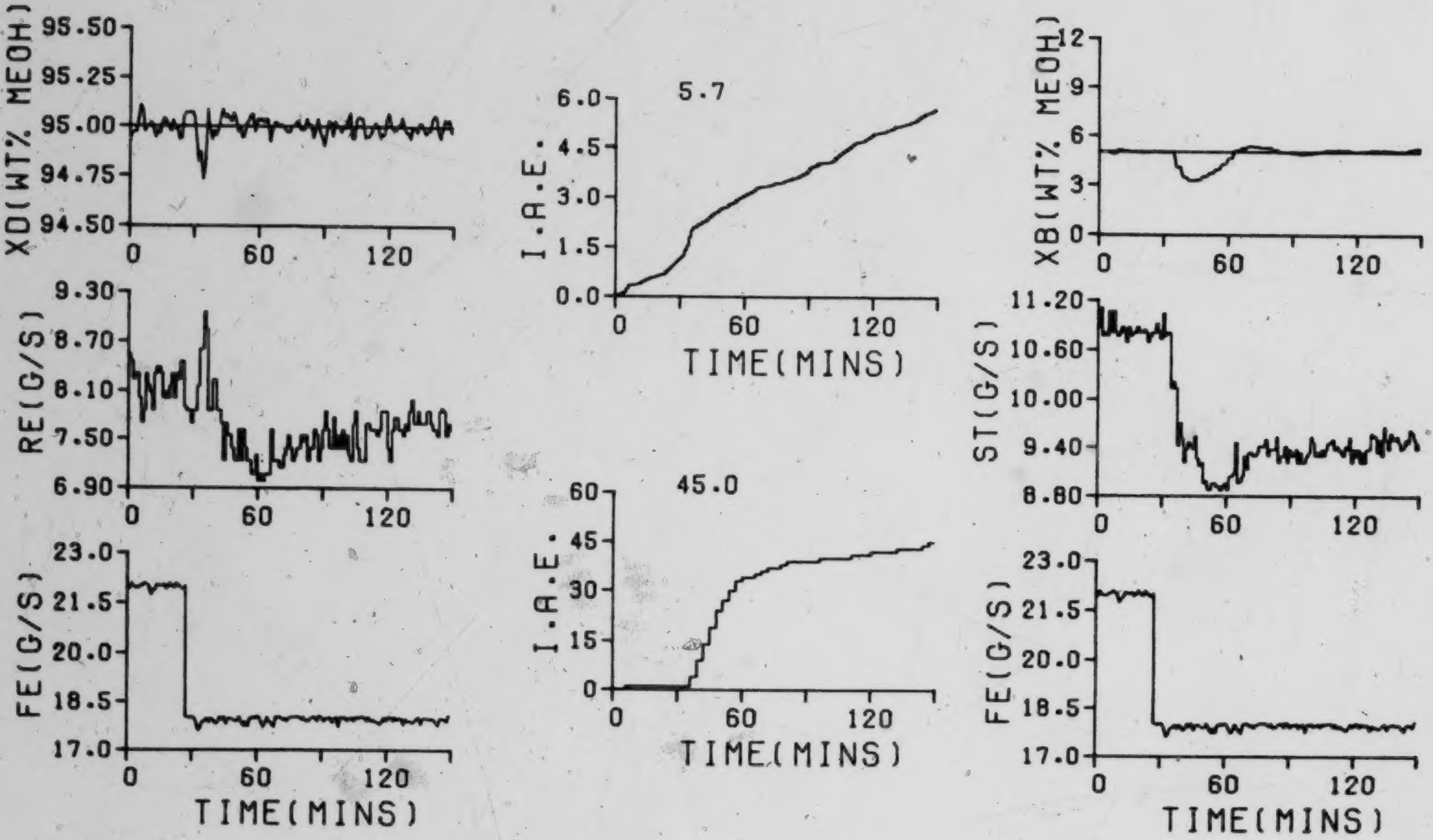

FIGURE 7.94 MR KINC ST MFF/Q(PB=5.2.TI=107.6.TD=0.0)/TS=60.0/4.3.3.0.4/
Q(PB=50.0.TI=150.0.TD=0.0)/TS=180.0/5.3.3.0.6/

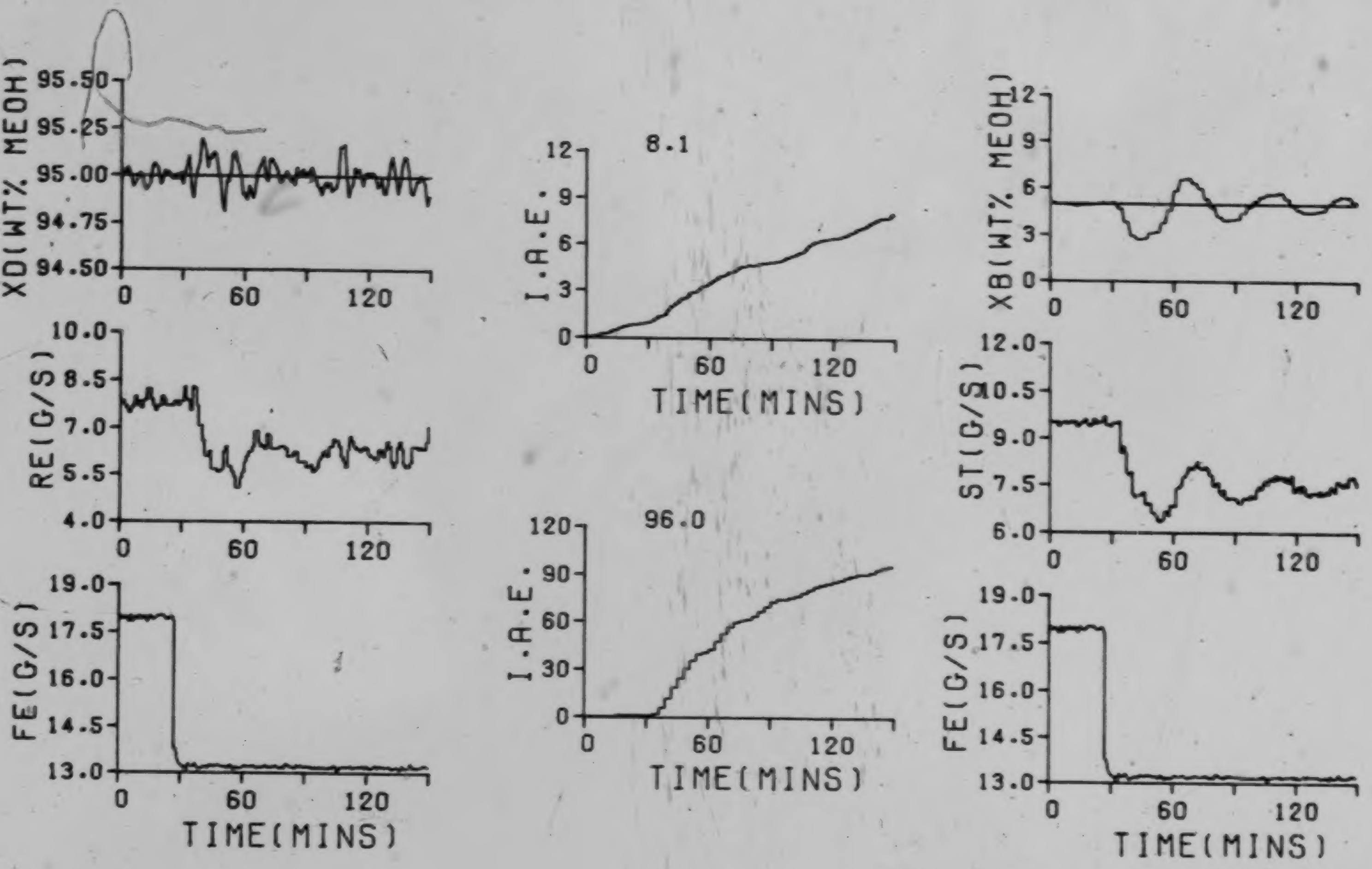

FIGURE 7.95 MR KINC ST MFF/Q(PB=5.2,TI=107.6,TD=0.0)/TS=60.0/4.3.3.0.4/
Q(PB=50.0,TI=150.0,TD=0.0)/TS=180.0/5.3.3.0.6/

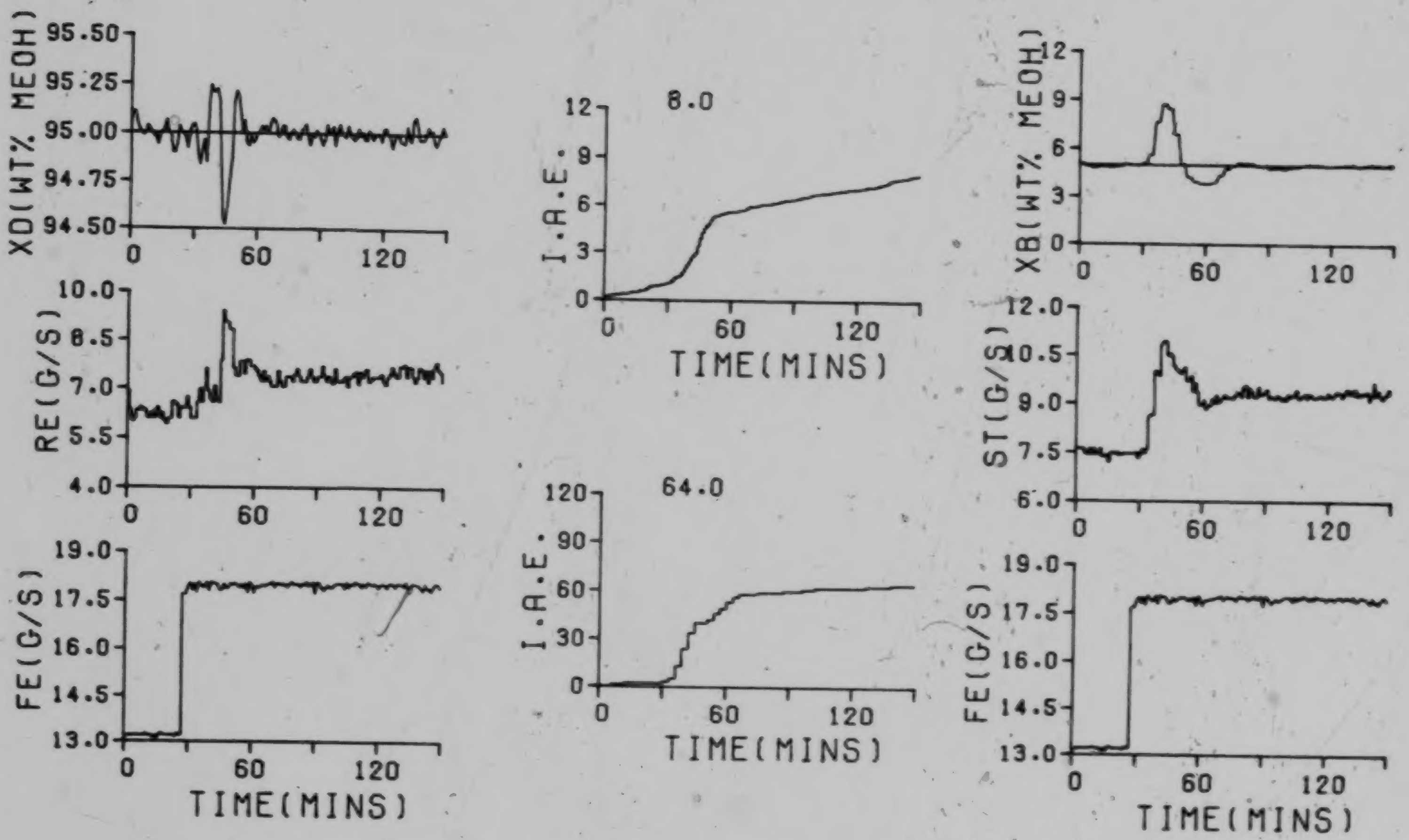

FIGURE 7.96 MR KINC ST MFF/Q(PB=5.2.TI=107.6.TD=0.0)/TS=60.0/4.3.3.0.4/
Q(PB=50.0.TI=150.0.TD=0.0)/TS=180.0/5.3.3.0.6/

Table 7.8.2
Column Performance Using Multirate K-Incremental Self-Tuning Control With Tuned Q Weighting Constants

	IAE Values	
Step	TOP	BOTTOM
increase from steady state	5.4	47.7
decrease to steady state	5.7	45.0
decrease from steady state	8.1	96.0
increase to steady state	8.0	64.0
total	27.2	252.7

steady state flow rate, the top composition IAE values of 8.1 and 8.0 are the lowest IAE values achieved for any control strategy and controller settings evaluated in this study.

Results have been presented for multivariable, multirate self-tuning control and the k-incremental self-tuning controller (K-INC) formulation, all using measured feedforward compensation. A summary of the IAE values obtained for the tests conducted using the measured feedforward compensation is given in Table 7.8.3.

Examination of the results indicate that control of top composition was improved using the k-incremental form of the algorithm for both single rate sampling and multirate sampling. However, regulation of the bottom composition by use of the k-incremental form of the self-tuning controller only improved for the single rate sampling.

Table 7.8.3
Summary of Measured Feedforward Compensation IAE Totals

		Single Rate Sampling		Multirate Sampling	
STEP	loop	STC	K-INC	STC	K-INC
increase from SS	top	7.9	6.8	6.1	5.4
	bottom	50.9	36.2	30.2	47.7
decrease to SS	top	7.4	4.8	5.8	5.7
	bottom	39.2	42.5	35.7	45.0
decrease from SS	top	14.0	13.5	9.4	8.1
	bottom	59.8	62.4	53.8	96.0
increase to SS	top	9.3	8.4	10.2	8.0
	bottom	60.2	50.9	53.5	64.0
Top composition IAE total		38.6	33.5	31.5	27.2
Bottom composition IAE total		210.1	192.0	173.2	252.7
Total		248.7	225.5	204.7	279.9

On the basis of these results it is not possible to reach any general conclusion on the improvement of control behavior that results by use of the incremental form of the algorithm as the Q weighting parameters were the same as used for the tests with the positional form of the algorithm. It is to be expected that adjustment of the Q weighting parameters for tests performed using the k-incremental algorithm and multirate sampling would result in a bottom composition IAE value lower than 173.2, thus showing the same improvement trend as was evident from the tests performed using only single rate sampling.

8. Conclusions

This work has been primarily concerned with the experimental evaluation of the control performance that can be achieved using multivariable self-tuning control strategy for single and multirate sampling. In the evaluation of this strategy, comparison with conventional PID control with no decoupling or feedforward compensation was used. The comparison was accomplished in two stages:

The first stage presented a comparison of the distillation column responses under multiloop PID control, with that of multivariable self-tuning control where controller parameter selections were based on four parameter selection methods.

The second stage compared the performance obtained using the multiloop PID control strategy with tuned controller settings with the behaviour obtained using the multivariable self-tuning control strategy with tuned Q weighting parameters.

Of the four methods used to calculate the PID controller settings, the calculated settings using the Cohen-Coon(3-C) method, resulted in the best control performance for both single and multirate sampling.

Tests of the multivariable self-tuning control strategy using calculated Q weighting parameters for the single rate sampling revealed that the Cohen-Coon method resulted in the lowest overall IAE values for the selection of the Q weighting parameters for the self-tuning controller. For multirate sampling, the IAE selection technique was found to result in the lowest overall IAE value.

Control of the distillation column using the multivariable self-tuning control strategy with Q weighting parameters based on initial selection methods has been shown to provide superior performance for disturbance rejection when compared with multiloop PID control, for both single and multirate sampling studies.

Multirate sampling versus single rate sampling for both the PID and self-tuning control strategies resulted in improved top composition regulation, with minimal reduction in the effectiveness of bottom composition control due to the increased interaction.

The change in column responses due to the adjustment of the Q weighting parameters (effectively altering the amount of proportional and integral action) followed the pattern observed for adjusting the PID controller constants. Significant improvement in terms of an overall IAE value was obtained from tuning, of the PID controller constants for both single and multirate sampling. Using the multiloop PID control strategy with the controller settings adjusted to obtain the lowest overall IAE value, virtually identical total IAE values resulted using both the single rate and multirate sampling. It can be concluded, that for the multiloop PID control strategy there appears to be no significant benefit to be derived by multirate sampling for control of the distillation column.

Tests of column control using the multirate self-tuning control strategy with Q weighting based on initial selection methods showed that superior results for disturbance rejection is possible compared with results achieved using tuned PID controls with a multiloop control strategy.

Measured feedforward compensation improves the disturbance rejection capabiltities of the self-tuning controller, for both the single rate and multirate forms of the algorithms. Furthermore it was shown that including feedforward compensation action resulted in improved controller performance and did not require tuning of the Q weighting of the self-tuning controllers as would be the case if feedforward control was included with the multiloop PID control strategy. The multivariable self-tuning control strategy evaluated in this work provides good disturbance rejection for both measured and unmeasured disturbances. The multirate application provides superior regulation compared to the multivariable form. The self-tuning control strategy with feedforward compensation can be regarded as an effective means of including the benefits of feedforward compensation without the drawbacks associated with the implementation using conventional PID control strategies and their need for periodic tuning.

The column control performance that resulted when the k-incremental form of the self-tuning control strategy was tested, for single rate sampling, shows promise in providing improved disturbance rejection capabilities when compared with multivariable (positional) self-tuning control strategy results. However no improvement was observed from using multirate sampling from the tests that were conducted. The results do indicate that additional testing to fully evaluate the potential of the k-incremental form of the algorithm is warranted.

9. Recommendations

9.1 Recommended Changes and/or Additions to the Equipment

As a consequence of the numerous experimental tests performed to study column control behaviour, the following equipment modifications are suggested:

(a)The effect of changes in cooling water flow on the steady state operation of the distillation column was documented in Chapter 4. It is recommended that a cascade control loop be established between the column pressure control loop and the cooling water flow control loop. Control of the column pressure loop should be accomplished with a proportional plus integral controller with its output as a setpoint to the temperature control of the cooling water discharge. The temperature control loop should be added as proportional control only. It is recommended that the setpoint range of the temperature controller be limited to a range of 20°C to 30°C. Since the desired normal operating temperature of the cooling water discharge is approximately 25°C. Setpoints larger than 30°C would alter the column's steady state operating charateristics by a significant amount, as noted in Chapter 4.

(b)In several of the tests, the nonlinear dynamics of the condenser level control required the duplication of several experiments. This was due mainly to the nonlinear nature of the level response of the condenser level. The nonlinearity is due to the reduced glass section of the vessel where the level is maintained. At times top composition control required a large change in reflux flow to occur, resulting in a sudden drop in condenser level. Since the level controller is a low gain controller, condenser level was at times lost resulting in loss of reflux flow to the column. This loss of reflux flow resulted in a loss of top composition measurement, necessitating that the test be aborted!. In order to correct this situation, it is recommended that a straight 3 inch diameter, 12 inch length glass section be added to the 3 inch diameter reducer section of the condenser receiver. The level controller would therefore have a linear system to control and could be tuned to provide quicker response, thereby ensuring the completion of the test runs. The capacitance probe and associated level transmiting equipment would require relocation to the bottom of the 12 inch section as well as the reference leg of the level transmitter would require extension to enable proper control.

(c)It is also recommended that the existing pneumatic controllers and transmitters be replaced with electronic transmitters and microprocessor based controllers. This would eliminate the need for P/I converters between the transmitters and the analog input boards of the computer.

9.2 Recommendations for Future Research Work

It is recommended that in planning future experimental testing of the different control strategies and algorithms that consideration be given to the following areas of research:

(a)Simulation studies [Tham, 1985] have shown some improvement in disturbance rejection abilities for the k-incremental self-tuning controller when compared with the positional form of the self-tuning control strategy evaluated in this work. Experimental evaluation of the robustness of this control strategy and comparison with the self-tuning controller presented in this work is recommended.

(b)Evaluation of hybrid self-tuning control [Gawthrop, 1980] to determine if the control strategies performance results in any improvement in the regulatory control of the inverse behavior and nonlinear characteristics of the column used in this study.

(c)An investigation on the effect of over and under parameterization on the quality of control to determine reasonable limits and bounds on the number of parameters required for self-tuning control without significant loss in controller performance.

(d)An experimental investigation and comparison of the recursive least squares identification method using recursive upper diagonal factorizatrion with variable forgetting factor [Fortescue et al., 1981] as opposed to a fixed forgetting factor used in this study.

(e)An investigation of the effect of varying the sample time, for top composition control to other than the two sample times studied in this work. The investigation of a further reduction in top loop sample time below 1 minute would determine if product composition control for the step changes below the normal feed rate could be improved.

(f)Evaluation of the multivariable self-tuning control strategy has shown superior disturbance rejection abilities when compared to the conventional multiloop PID control strategy. It is recommended that an investigation of the servo control behaviour of the self-tuning control strategy be undertaken to compare its performance to that of multiloop PID control with and without dead time compensation.

(g)In most industrial processes, output data may be lost temporarily, and if this happens it may cause a major upset or even an accident. It is proposed that the effect on the steady state and servo tracking capabilities of the self-tuning controller, when output data is temporarily missing, should be studied. Wong and Bayoumi [1982] suggested a method which may provide a starting point for this investigation.

(h)With the recommended changes for measurement of the condenser level, studies could be conducted to determine the effect of varying condenser steady state holdup. This would determine if condenser holdup could be used as a means of assisting in modifying the open or closed loop behaviour of the column.

(i)The methods applied in this work to determine controller settings and Q weighting parameters were based on a knowledge of open loop response behaviour which requires the system to be available for an extensive period of testing unless the system dynamic behaviour is known. Yuwana and Seborg, [1982] have suggested a means of determining conventional PID controller settings from closed loop operation. This technique as well as others should be investigated for establishing controller settings and parameters without a knowledge of open loop behaviour.

References

Åström, K.J., "Introduction to Stochastic Control Theory", Academic Press, New York (1970).

Åström, K.J., U. Borrison, L. Ljung and B. Wittenmark, "Theory and Applications of Self-Tuning Regulators", Automatica, Vol 13, pp457 (1977).

Åström, K.J. and B. Wittenmark, "On Self-Tuning Regulators", Automatica, Vol 9, pp185 (1973).

Bierman, G.J., "Brief Paper, Measurement Updating Using U-D Factorization", Automatica, Vol 12, pp375 (1976).

Bierman, G.J., "Factorization Methods for Discrete Sequential Estimation", Academic Press, New York (1977).

Brooks, J.D., Y. Nazer and L.B. Schryer, "Self-Tuning Control Applied to an Industrial Distillation Column", Preprints of the 33rd Canadian Chemical Engineering Conference, Toronto, (1983).

Chien, I.L., D.A. Mellichamp and D.E. Seborg, "Adaptive Control Strategies for Distillation Columns", Proceedings 1983 American Control Conference, San Francisco (1983).

Clarke, D.W., "Introduction to Self-Tuning Controllers", Chapter 2 in "Self-Tuning and Adaptive Control: Theory and Applications", C.J. Harris and S.A. Billings (Eds.), Peter Peregrinus Ltd., London (1981).

Clarke, D.W. and P.J. Gawthrop, "Self-Tuning Controller", Proceedings IEE, Vol 122, pp929 (1975).

Clarke, D.W. and P.J. Gawthrop, "Self-Tuning Control", Proceedings IEE, Vol 126, pp633 (1979).

Clarke, D.W., A.J.F. Hodgson and P.S. Tuffs, "Offset Problem and K-Incremental Predictors in Self-Tuning Control", IEE Proceedings, Vol 130, pp217 (1983).

Cohen, G.H. and G.A. Coon, "Theoretical Consideration of Retarded Control", Taylor Technical Data Sheet, No TDS-10A100, Taylor Instrument Companies, Rochester, New York, (1953).

Coppus, G.W.M.,"Robust Control of Distillation Column", MSc Thesis, University of Alberta, Edmonton (1980).

Dahlin, E.B., "Designing and Tuning Digital Controllers", Instruments and Control Systems, Vol 41, No 4, pp77 (1968).

De Keyser, R.M.C. and A.R. van Cauwenberghe, "Self-Adjusting Control of Multivariable Nonstationary Processes", Internal Report, Automatic Control Laboratory, University of Ghent, Belgium, (1978).

Deshpande, P.B. and R.H. Ash, "Elements of Computer Process Control With Advanced Control Applications", Instrument Society of America, (1981).

Fortesque, T.R., L.S. Kershenbaum and B.E. Ydstie, "Implementation of Self-Tuning Regulators with Variable Forgetting Factors", Automatica, Vol 17, No 6, pp831 (1981).

Gawthrop, P.J., "Hybrid Self-Tuning Control", IEE Proceedings, Vol 127, pp229 (1980).

Haalman, A., "Adjustment of Continuous Controllers", Revue A, Vol VIII, nr 4, pp181 (1966).

Harris, C.J. and S.A. Billings (Eds.),"Self-Tuning and Adaptive Control: Theory and Applications", Peter Peregrinus Ltd., London (1981).

Harris, T.J., J.F. MacGregor and J.D. Wright, "An Application of Self-Tuning Regulator to a Catalytic Reactor Control", Proceedings 1978 JACC, Philadelphia, pp43 (1978).

Kalman, R.E., "Design of a Self-Optimizing Control System", Trans. ASME 80, pp468 (1958).

Kan, H.W., "Binary Distillation Column Control; Evaluation of Digital Control Algorithms", MSc Thesis, University of Alberta, Edmonton (1982).

Keviczky, L. and J. Hetthessy, "Self-Tuning Minimum Variance Control of MIMO Discrete Time Systems", Automatic Control Theory and Applications, Vol 5, No 1, pp11 (1977).

Keviczky, L., J. Hetthessy, M. Hilger and J. Kolostori, "Self-Tuning Adaptive Control of a Cement Raw Material Blending", Automatica, Vol 14, pp525 (1978).

Koivo, H.N., "A Multivariable Self-Tuning Controller", Automatica, Vol 16, pp351 (1980).

Koivo, H.N., J.T. Tanttu and J. Penttinen, "Experimental Comparison of Self-Tuning Controller Methods in Multivariable Case", Proceedings 8th IFAC World Congress(Control Science and Technology for the Progress of Society), ppVII-53, Kyoto (1981).

Lieuson, H.Y., "Experimental Evaluation of Self-Tuning Control of a Binary Distillation Column", MSc Thesis, University of Alberta, Edmonton (1980).

Lopez, A.M., J.A. Miller, C.L. Smith and P.W. Murrill, "Tuning Controllers with Error Integral Criteria", Instrumentation Technology, Vol 14, pp57, November (1967).

Lopez, A.M., P.W. Murrill and C.L. Smith, "Tuning PI and PID Digital Controllers", Instrument and Control Systems, Vol 42, pp89 (1969).

Miller, J.A., A.M. Lopez, C.L. Smith and P.W. Murrill, "A Comparison of Controller Tuning Techniques", Control Engineering, Vol 14, No 12, pp72 (1967).

Moore, C.F., C.L. Smith and P.W. Murrill, "Simplifying Digital Control Dynamics for Controller Tuning and Hardware Lag Effects", Instrument Practice, pp45, January (1969).

Morris, A.J., T.P. Fenton and Y. Nazer, "Application of Self-Tuning Regulators to the Control of Chemical Processes", Proceedings 5th IFAC/IFIP Conference on Digital Computer Application to Process Control, The Hague, Netherlands, pp447 (1977).

Morris, A.J., Y. Nazer and K. Chisholm, "A Comparison of Identification Techniques for Robust Self-Tuning Control", Department of Chemical Engineering, University of Newcastle, Newcastle upon Tyne, England, (1982).

Morris, A.J., Y. Nazer, R.K. Wood and H. Lieuson, "Evaluation of Self-Tuning Contollers for Distillation Column Control", Proceedings 6th IFAC/IFIP Conference on Digital Computer Application to Process Control, pp345 (1981).

Morris, A.J., Y, Nazer and R.K. Wood, "Multivariate Self-Tuning Process Control", Optimal Control Applications and Methods, Vol 3, pp363 (1982).

Nazer, Y., "Single and Multivariable Self-Tuning Controllers", PhD Thesis, University of Newcastle upon Tyne, England (1981).

Ogunnaike, B.A., J.P. Lemaire, M. Morari and W.H. Ray, "Advanced Multivariable Control of a Pilot Plant Distillation Column", AIChE Journal, Vol 29, No 4, pp632 (1983).

Pacey, W.C., "Control of a Binary Distillation Column; An Experimental Evaluation of Feedforward and Combined Feedforward-Feedback Control Scheme", MSc Thesis, University of Alberta, Edmonton (1973).

Pemberton, T.J., "PID; The Logical Control Algorithm", Control Engineering, Vol 19, No 5, pp66 (1972).

Sastry, V.A., D.E. Seborg and R.K. Wood, "Self-Tuning Regulator Applied to a binary Distillation Column", Automatica, Vol 13, pp417 (1977).

Seborg, D.E., S.L. Shah and T.F. Edgar, "Adaptive Control Strategies For Process Control: A Survey", AIChE Journal, vol 32, pp881 (1986).

Stephanopolous, G., "*Chemical Process Control, An Introduction to Theory and Practice*", Prentice Hall, New Jersey, (1984).

Svercek, W.Y., "Binary Distillation Column Dynamics", PhD Thesis, University of Alberta, Edmonton (1967).

Tanttu, J.T. and H. Koivo, "A Multivariable Self-Tuning Controller: Different Delays in the Control Input", Proceedings Applied Control and Identification, pp26-14, Copenhagen, Denmark (1983).

Tham, M.T., "Some Aspects of Self-Tuning Control", PhD Thesis, University of NewCastle upon Tyne, England (1985).

Verbruggen, H.B., J.A. Peperstaete and H.D. Debruyn, "Digital Controllers and Digital Control Algorithms, The Digital Version of Analogue Controllers", Journal A, Vol 16, No 2, pp53 (1975).

Wong, K.Y. and M.M. Bayoumi, "Self-Tuning Control for Systems with Temporary Missing Output Data", Proceedings American Control Conference, pp869 (1982).

Wong, K.Y., M.M. Bayoumi and S. Nuyan, "Comparative Study of some Estimator Algorithms for Self-Tuning Control of Time Varying Systems", Proceedings Applied Control and Identification, pp18-12, Copenhagen, Denmark (1983).

Wong, T., "Multicomponent Simulation of Distillation Column Dynamics", MSc Thesis, University of Alberta, Edmonton (1985).

Yuwana, M. and D.E. Seborg, "A New Method for On-Line Controller Tuning", AIChE Journal, Vol 28, No 3, pp434 (1982).

Appendices

Appendix A

Differentiation of Cost Function

The multivariable control law formulation of section 3.3.1 required the minimization of the performance index represented by equation 3.53. Based on the approach of Clarke [1975] the expectation operator is removed and the performance index becomes:

$$J_1 = [PY^*(t+k_{ii}|t) - RW(t)]^t\,[PY^*(t+k_{ii}|t) - RW(t)] + [Q'U(t)]^t\,[Q'U(t)] + \sigma^2_{t+k_{ii}} \qquad (A.1)$$

Minimization of equation A.1 is accomplished by setting the derivative to zero ($dJ_1/dU(t)=0$).

Differentiation of the cost function of equation A.1 will be accomplished in several parts. First some basic matrix differentiation is presented.

1. If:

$$f = y^t A z \qquad (A.2)$$

where

$$y = y(x,t)$$
$$A = A(x,t) \qquad (A.3)$$
$$z = z(x,t)$$
$$x = x(t)$$

Then

$$\frac{df}{dx} = \left[\frac{dy'}{dx}\right]Az + \left[\frac{dz'}{dx}\right]A'y + y'\left[\frac{dA}{dx}\right]'z \qquad (A.4)$$

2. If:

$$F = AB \qquad (A.5)$$

where

$$\begin{aligned} A &= A(x,t) \\ B &= B(x,t) \qquad (A.6) \\ x &= x(t) \end{aligned}$$

then:

$$\frac{dF}{dx} = B'\frac{\partial A}{\partial x} + \frac{\partial B A'}{\partial x} \qquad (A.7)$$

The above two relations were extracted from Appendix A of Optimum System Control, A. P. Sage, Prentice Hall Inc., 1968.

With the above matrix differentiation relations the cost function can now be minimized.

Using relation 1 and setting:

$$\begin{aligned} [\mathbf{PY}^*(t+k_{ii}|t) - \mathbf{RW}(t)]' &= y' \\ I &= A \qquad (A.8) \\ [\mathbf{PY}^*(t+k_{ii}|t) - \mathbf{RW}(t)] &= z \end{aligned}$$

Then the first portion of the differentiation becomes:

$$\frac{\partial J_i}{\partial U(t)} = \frac{\partial}{\partial U(t)}[PY^*(t+k_{ii}|t) - RW(t)]^t[PY^*(t+k_{ii}|t) - RW(t)]$$

$$+ \frac{\partial}{\partial U(t)}[PY^*(t+k_{ii}|t) - RW(t)]^t\ I^t\ [PY^*(t+k_{ii}|t) - RW(t)]$$

$$+ [PY^*(t+k_{ii}|t) - RW]^t\left[\frac{\partial I}{\partial U(t)}\right]^t[PY^*(t+k_{ii}|t) - RW(t)] \tag{A.9}$$

Since $\dfrac{\partial I}{\partial U(t)} = 0$ (A.10)

therefore, equation A.3 is composed of only the first two terms, requiring the evaluation of:

$$\frac{\partial}{\partial U(t)}[PY^*(t+k_{ii}|t) - RW(t)]^t \tag{A.11}$$

Since the term RW(t) is not a function of U(t), it's partial derivative is zero and the derivative is evaluated based on substitution of equation 3.49 into equation 3.52 given below.

$$PY(t+k_{ii}) = C^{-1}P_d^{-1}FY(t) + z^{k_{ii}-k_{ij}}C^{-1}EBU(t)$$
$$+ z^{k_{ii}-d_{ij}}C^{-1}EDV(t) + E\Xi(t+k_{ii}) \tag{3.49}$$

and

$$PY^{*}(t+k_{ii}|t) = PY(t+k_{ii}) - E\Xi(t+k_{ii}) \qquad (3.52)$$

which results in the following equation:

$$PY^{*}(t+k_{ii}|t) = C^{-1}P_{d}^{-1}FY(t) + z^{k_{ii}-k_{ij}}C^{-1}EBU(t) + z^{k_{ii}-d_{ij}}C^{-1}EDV(t) \qquad (A.12)$$

performing the partial differentiation of equation A.12 leaves only the term containing U(t), all other elements of the right hand side of the equation disappear after the differentiation, resulting in:

$$\frac{\partial PY^{*}(t+k_{ii}|t)}{\partial U(t)} = \frac{\partial}{\partial U(t)}\left[C^{-1}EBU(t)\right]' \qquad (A.13)$$

Since E, B and C are polynomial matrices of z^{-1}, the only elements which are functions of U(t) are the first terms of the polynomials. The result of the right hand side of equation A.13 becomes:

$$\frac{\partial}{\partial U(t)}\left[C^{-1}EBU(t)\right]' = C(0)^{-1}E(0)'B(0)' \qquad (A.14)$$

so, the first term of equation A.9 is expressed as:

$$C(0)^{-1}E(0)'B(0)'[PY^{*}(t+k_{ii}|t) - RW(t)] \qquad (A.15)$$

Now, using relation 1 for the second term of equation A.1, the following variables are defined as:

$$\begin{aligned} [Q'U(t)]' &= y' \\ I &= A \\ [Q'U(t)] &= z \end{aligned} \qquad (A.16)$$

with

$$\begin{aligned} \frac{\partial}{\partial U(t)} &= \frac{\partial}{\partial U(t)} [Q'U(t)]'[Q'U(t)] \\ &+ \frac{\partial}{\partial U(t)} [Q'U(t)]' \; I' \; Q'U(t)] \\ &+ [Q'U(t)]' \left[\frac{\partial I}{\partial U(t)} \right]' [Q'U(t)] \end{aligned} \qquad (A.17)$$

The last term of equation A.17 is zero since the partial derivative of I is zero (c.f. equation A.10).

We must therefore evaluate the following expression:

$$\frac{\partial [Q'U(t)]'}{\partial U(t)} \qquad (A.18)$$

Since Q' is a diagonal matrix of z^{-1}, only the first term of the product is involved in the differentiation, with the result:

$$\frac{\partial[Q'U(t)]'}{\partial U(t)} = Q'(0)' \qquad (A.19)$$

Since the noise term was assumed to be of constant covariance. Then:

$$\frac{\partial \sigma^2_{t+k_i|t}}{\partial U(t)} = 0 \qquad (A.20)$$

combining the results of A.14, A.15, A.19 and A.20 yields the following minimization:

$$\frac{dJ_1}{dU(t)} = C(0)^{-1}E(0)'B(0)' \, [PY^*(t+k_i|t) - RW(t)] \qquad (A.21)$$

$$+ \, Q'(0)'Q'U(t)$$

Equation A.21 represents the final result of the minimization and is presented as equation 3.57 in Chapter 3.

Appendix B

Source Code PROFIT.FOR

```
C
C    PROGRAM  PROFIT.FOR
C
C    THIS PROGRAM FITS A SECOND ORDER PLUS DEAD TIME
C     MODEL TO A SET OF INPUT-OUTPUT DATA OF A PROCESS.
C     A NONLINEAR REGRESSION IS USED TO SOLVE THE PROBLEM.
C
C    REF: DESHPANDE P B & ASH R H
C    "ELEMENTS OF COMPUTER PROCESS CONTROL WITH ADVANCED
C         CONTROL APPLICATIONS"
C         INSTRUMENT SOCIETY OF AMERICA, 1981
C
C
C    THE FOLLOWING NOMENCLATURE IS USED:
C         K = PROCESS GAIN
C         T1 = PROCESS TIME CONSTANT 1
C         T2 = PROCESS TIME CONSTANT 2
C         N = PROCESS DEAD TIME
C         INUM = NUMBER OF INPUT OUTPUT POINTS
C         U(I) = PROCESS INPUT
C         X(I) = PROCESS OUTPUT
C         T    = SAMPLING PERIOD
C
C    THE ORIGINAL PROGRAM FROM THE ABOVE REFERENCE
C     IS MODIFIED TO HAVE ANOTHER I/O STRUCTURE.
C
C     ALSO THE PROGRAM FIXED A MAXIMUM POSSIBLE TIME DELAY
C     DECLARATION OF 8 SAMPLE INTERVALS.
C     THAT HAS BEEN MODIFIED
C     TO TAKE 'N' SAMPLE DELAY INTERVALS PROVIDED THAT THE
C     NUMBER OF DATA POINTS DO NOT EXCEED ( 200 - N - 1 )
C     IF MORE DATA POINTS ARE REQUIRED, THEN THE DIMENSIONS
OF THE
C     APPROPRIATE ARRAYS' MUST BE ENLARGED.
C     THIS PROGRAM READS IN A MAXIMUM OF 6 COLUMNS OF DATA.
C  TO INCREASE THIS, DIMENSIONS OF 'D' AND 'FACTOR' MUST BE
C  CHANGED TOGETHER WITH THE END LIMITS OF I/O 'DO' LOOPS.
C
C
C             U. OF A.                         U. OF A.
C              VAGI                              MING
C             APR-84                          17-OCT-82
C
      REAL K
      DIMENSION D(200,6), FACTOR(6)
      COMMON/BLK1/X(200),U(200),XP(200),F(200),INUM,T,N,J,
     1       PINDEX
      COMMON/BLK2/XAOPT(3),XBOPT(3),XCOPT(3),XSOPT(3),
     1 FBOPT(3),FCOPT(3),FSOPT(3),XMM2,XMM1,XM,XMP1,FMM2,
     2 FMM1,FM,FMP1,DK,K,T1,T2,PREOPT,FREOPT,FAOPT(3)
C
      DATA IYES /'Y'/
C
      IDATA = 1
      IWIO = 6
      IRIO = 5
      PINDEX = 0.0
      READ (IDATA,220) (FACTOR(J),J=1,6)
      REWIND IDATA
C
C ... READ AND NORMALIZE DATA SET
C
      DO 15 I = 1, 200
        READ (IDATA,220,END=20) (D(I,J),J=1,6)
C
        DO 10 J = 1, 6
          D(I,J) = D(I,J) - FACTOR(J)
   10   CONTINUE
C
        INUM = I
   15 CONTINUE
C
   20 CONTINUE
C
C .. SEPERATE OUT THE INPUT-OUPUT VARIABLES TO BE USED
C
      WRITE (IWIO,225)
      READ (IRIO,230) IPERT
      WRITE (IWIO,235)
      READ (IRIO,230) IOUT
C
C  ... IF INPUT-OUTPUT RELATION IS OF NEGATIVE GAIN TYPE
C      CONVERT THE NORMALIZED OUTPUT VECTOR SET TO HAVE
C      THE OPPOSITE SIGN. THE INITIAL GUESS FOR 'K' MUST
C      THEREFORE BE A POSITIVE REAL NUMBER.( THE ORIGINAL
C      PROGRAM DOES NOT SEEM TO WORK FOR NEGATIVE
C      GAIN IDENTIFICATION, HENCE THIS ADDITION)
C
C
C ... INITIALIZE GAIN PARITY FLAG
C
C      SIGN = 1.0 FOR +VE GAIN RELATION
C      USED TO GIVE PROPER SIGN IN FINAL PRINTOUT
C
      SIGN = 1.0
      WRITE (IWIO,215)
      READ (IRIO,290) IANS
      IF (IANS .EQ. IYES) SIGN = -1.0
C
      DO 25 I = 1, INUM
        D(I,IOUT) = SIGN * D(I,IOUT)
   25 CONTINUE
C
```

```
C ... GET SAMPLING INTERVAL AND INITIAL ESTIMATES
C
      WRITE (IWIO,240)
      READ (IRIO,245) T, N
      WRITE (IWIO,250)
      READ (IRIO,255) K, T1, T2
C
C  ... ENSURE THAT ALL ENTRIES FOR INITIAL ESTIMATES
C      ARE +VE NUMBERS
C
      K = ABS(K)
      T1 = ABS(T1)
      T2 = ABS(T2)
C
C .... INCLUDE SAMPLING DELAY OF '1' TO PURE PROCESS DELAY
C
      N = N + 1
C
C  ..  RESERVE SPACE FOR TIME DELAY SHIFTS IN SUBSEQUENT
C       CALCULATIONS
C
      DO 30 I = 1, N
        U(I) = 0.0
        X(I) = 0.0
        XP(I) = 0.0
   30 CONTINUE
C
C  .. PLACE THE APPROPRIATE DATA INTO THEIR RESPECTIVE
C     VECTORS
C
      DO 35 I = 1, INUM
        U(I + N) = D(I,IPERT)
        X(I + N) = D(I,IOUT)
   35 CONTINUE
C
C     'IC' IS THE CYCLE NUMBER
C
      IC = 1
C
      WRITE (IWIO,260)
      WRITE (IWIO,265)
C
C     IN THE NEXT 3 SECTIONS OF THE PROGRAM, K, T1, T2 ARE
C     OPTIMIZED SEPARATELY USING A DSC-POWELL SEARCH.
C
   40 P1 = K
      P2 = T1
      P3 = T2
C
C   PRINT THE VALUE OF GAIN WITH ITS PROPER SIGN
C
      SIGNK = K * SIGN
      WRITE (IWIO,270) SIGNK, T1, T2, PINDEX
      WRITE (IWIO,275) IC
```

```
C
C     OPTIMIZATION OF K
C     DSC SEARCH
C
      L = 1
      DK = 0.001
      J = 1
      PREOPT = K
      F(J) = ERROR(K,T1,T2)
      IW1 = J + 1
      F(J + 1) = ERROR(K + DK,T1,T2)
      IF (F(J + 1) .GE. F(J)) DK = -DK
      IF (K + DK .LE. 0.0) GO TO 60
   45 IW1 = J + 1
      F(J + 1) = ERROR(K + DK,T1,T2)
      IF (F(J + 1) .GT. F(J)) GO TO 55
      OLDDK = DK
      K = K + DK
      PREOPT = K
      FREOPT = F(J + 1)
      DK = 2.0 * DK
      IF (DK .GT. 0.5) DK = 0.5
      IF (DK .LT. - 0.5) DK = -0.5
      IF (K + DK .LT. 0.0) GO TO 50
      J = J + 1
      GO TO 45
   50 DK = OLDDK
      K = K - DK
   55 XM = K + DK
      XMM1 = K
      XMM2 = K - 0.5 * DK
      XMP1 = K + 0.5 * DK
      FM = F(J + 1)
      FMM1 = F(J)
      FMM2 = ERROR(XMM2,T1,T2)
      FMP1 = ERROR(XMP1,T1,T2)
      CALL DSC(1)
      K = XSOPT(L)
      GO TO 100
C
C     OPTIMIZATION OF T1 ... DSC SEARCH
C
   60 L = 2
      DK = 0.01
      J = 1
      PREOPT = T1
      F(J) = ERROR(K,T1,T2)
      IW1 = J + 1
      F(J + 1) = ERROR(K,T1 + DK,T2)
      IF (F(J + 1) .GE. F(J)) DK = -DK
      IF ((T1 + DK)/T .LT. 0.0145) GO TO 80
   65 IW1 = J + 1
      F(J + 1) = ERROR(K,T1 + DK,T2)
      IF (F(J + 1) .GT. F(J)) GO TO 75
      OLDDK = DK
      T1 = T1 + DK
      PREOPT = T1
      FREOPT = F(J + 1)
      DK = 2.0 * DK
      IF (DK .GT. 0.5) DK = 0.5
      IF (DK .LT. - 0.5) DK = -0.5
      IF (T1 + DK .LT. 0.0) GO TO 70
      IF ((T1 + DK)/T .LT. 0.0145) GO TO 70
      J = J + 1
      GO TO 65
   70 DK = OLDDK
      T1 = T1 - DK
   75 XM = T1 + DK
      XMM1 = T1
      XMM2 = T1 - 0.5 * DK
      XMP1 = T1 + 0.5 * DK
      FM = F(J + 1)
      FMM1 = F(J)
      FMM2 = ERROR(K,XMM2,T2)
      FMP1 = ERROR(K,XMP1,T2)
      CALL DSC(2)
      T1 = XSOPT(L)
      GO TO 100
C
C  OPTIMIZATION OF T2 ...DSC SEARCH
C
   80 L = 3
      DK = 0.01
      J = 1
      PREOPT = T2
      F(J) = ERROR(K,T1,T2)
      IW1 = J + 1
      F(J + 1) = ERROR(K,T1,T2 + DK)
      IF (F(J + 1) .GE. F(J)) DK = -DK
      IF ((T2 + DK)/T .LT. 0.0145) GO TO 205
   85 IW1 = J + 1
      F(J + 1) = ERROR(K,T1,T2 + DK)
      IF (F(J + 1) .GE. F(J)) GO TO 95
      OLDDK = DK
      T2 = T2 + DK
      PREOPT = F(J + 1)
      DK = 2.0 * DK
      FREOPT = F(J + 1)
      IF (DK .GT. 0.5) DK = 0.5
      IF (DK .LT. - 0.5) DK = -0.5
      IF (T2 + DK .LT. 0.0) GO TO 90
      IF ((T2 + DK)/T .LT. 0.0145) GO TO 90
      J = J + 1
      GO TO 85
   90 DK = OLDDK
      T2 = T2 - DK
   95 XM = T2 + DK
      XMM1 = T2
      XMM2 = T2 - 0.5 * DK
      XMP1 = T2 + 0.5 * DK
      FM = F(J + 1)
      FMM1 = F(J)
      FMM2 = ERROR(K,T1,XMM2)
      FMP1 = ERROR(K,T1,XMP1)
      CALL DSC(3)
      T2 = XSOPT(L)
C
C      POWELL SEARCH:
C      THIS SECTION OF THE PROGRAM CALCULATES 'XSTAR'
C     WHICH IS THE OPTIMUM VALUE OF ONE OF THE VARIABLES.
C
  100 IF (XSOPT(L) .EQ. PREOPT) GO TO 200
      PREOPT = XSOPT(L)
      FREOPT = FSOPT(L)
      XA = XAOPT(L)
      XB = XBOPT(L)
      XC = XCOPT(L)
      XSTAR = XSOPT(L)
      FA = FAOPT(L)
      FB = FBOPT(L)
      FC = FCOPT(L)
      FSTAR = FSOPT(L)
  105 XACCUR = 0.005
      I1 = INT(FA*1.0E6+0.5)
      I2 = INT(FB*1.0E6+0.5)
      I3 = INT(FC*1.0E6+0.5)
      I4 = INT(FSTAR*1.0E6+0.5)
      IF(I1.EQ.I2 AND.I2.EQ.I3.AND.I3.EQ.I4)GOTO 200
  110 IF (FA .GE. FB .AND. FA .GE. FC) GO TO 115
      IF (FB .GE. FA .AND. FB .GE. FC) GO TO 130
      IF (FC .GE. FA .AND. FC .GE. FB) GO TO 140
  115 FBIG = FA
      XBIG = XA
      IF (FB .LE. FC) GO TO 125
  120 FSMALL = FC
      XSMALL = XC
      GO TO 145
  125 FSMALL = FB
      XSMALL = XB
      GO TO 145
  130 FBIG = FB
      XBIG = XB
      IF (FA .GT. FC) GO TO 120
  135 FSMALL = FA
      XSMALL = XA
      GO TO 145
  140 FBIG = FC
      XBIG = XC
      IF (FA .LE. FB) GO TO 135
      GO TO 125
  145 ABEROR = ABS(XSTAR - XSMALL)
      IF (ABEROR .LE. XACCUR) GO TO 200
      IF (FSTAR .LT. FBIG) GO TO 150
      XSTAR = XSMALL
      GO TO 200
  150 IF (FBIG .NE. FB) GO TO 155
      GO TO 200
  155 IF (FBIG .EQ. FC) GO TO 160
      AB1 = ABS(XC - XB) - ABS(XC - XSTAR)
      IF (AB1) 165, 170, 170
  160 AB1 = ABS(XA - XB) - ABS(XA - XSTAR)
      IF (AB1) 170, 165, 165
  165 XC = XB
      FC = FB
      XB = XSTAR
      FB = FSTAR
      GO TO 175
  170 XA = XB
      FA = FB
      XB = XSTAR
      FB = FSTAR
  175 ANUM=(XB**2-XC**2)*FA+(XC**2-XA**2)*FB+(XA**2-XB**
     1   2) * FC
      DENOM=(XB-XC)*FA+(XC-XA)*FB+(XA-XB)*FC
      XSTAR = (ANUM/DENOM) / 2.0
      IF (XSTAR .LT. 0.0) XSTAR = PREOPT
      IF(L-2.GE.0.0.AND.XSTAR/T.LT.0.0145)XSTAR=PREOPT
      IF (L - 2) 180, 185, 190
  180 FSTAR = ERROR(XSTAR,T1,T2)
      K = XSTAR
      IF (FSTAR .GE. FREOPT) K = PREOPT
      GO TO 195
  185 FSTAR = ERROR(K,XSTAR,T2)
      T1 = XSTAR
      IF (FSTAR .GE. FREOPT) T1 = PREOPT
      GO TO 195
  190 FSTAR = ERROR(K,T1,XSTAR)
      T2 = XSTAR
      IF (FSTAR .GE. FREOPT) T2 = PREOPT
  195 IF (K .EQ. PREOPT) GO TO 200
      IF (T1 .EQ. PREOPT) GO TO 200
      IF (T2 .EQ. PREOPT) GO TO 200
      GO TO 105
  200 IF (L - 2) 60, 80, 205
C
C     THIS SECTION OF THE PROGRAM DETERMINES IF ALL
C     3 OF THE VARIABLES ARE WITHIN THE PRESCRIBED ACCURACCY
C       (YACCUR) OF THE PREVIOUS CYCLE VALUES.
C       IF THEY ARE NOT, THEN THE OPTIMIZATION IS REPEATED.
C
  205 IC = IC + 1
      YACCUR = 0.001
      IF (ABS(K - P1) .GT. YACCUR) GO TO 40
      YACCUR = YACCUR * 2.0
      IF (ABS(T1 - P2) .GT. YACCUR) GO TO 40
      IF (ABS(T2 - P3) .GT. YACCUR) GO TO 40
      WRITE (IWIO,280)
C
      SIGNK = K * SIGN
      WRITE (IWIO,270) SIGNK, T1, T2, PINDEX
C
C  .. RESET PINDEX TO ZERO
C
      PINDEX = 0.0
C
C  .. RESET OUTPUT DATA TO ORIGINAL FORM
C
      DO 210 I = 1, INUM
        D(I,IOUT) = SIGN * D(I,IOUT)
  210 CONTINUE
C
      WRITE (IWIO,285)
      READ (IRIO,290) IANS
      IF (IANS .EQ. IYES) GO TO 20
C
      STOP
C
  215 FORMAT (1X, ' IS RESPONSE OF -VE GAIN TYPE (Y/N)?')
  220 FORMAT (6G12.5)
  225 FORMAT (1X, ' ENTER COLUMN NUMBER OF PERTURBATION
     1 VARIABLE:')
  230 FORMAT (I2)
  235 FORMAT (1X, ' ENTER COLUMN NUMBER OF OUTPUT
     1 VARIABLE:')
  240 FORMAT (1X, ' ENTER SAMPLING INTERVAL AND APPROXIMATE
     1 TIME DELAY:')
  245 FORMAT (G12.5, I3)
  250 FORMAT (1X, ' ENTER INITIAL GUESS FOR K, T1 AND T2 :')
  255 FORMAT (3G12.5)
  260 FORMAT ('0STARTING VALUES')
  265 FORMAT (10X, 'K', 14X, 'T1', 13X, 'T2', 11X, 'PINDEX')
  270 FORMAT (4F15.6)
  275 FORMAT (1X, ' CYCLE =', I3)
  280 FORMAT ('0OPTIMUM VALUES')
  285 FORMAT (1X, ' MORE (Y/N) ?')
  290 FORMAT (A1)
      END
```

```
C
C
C       THIS SUBPROGRAM CALCULATES "ERROR"
C      WHICH IS A MEASURE OF HOW WELL THE VALUES
C        OF K, T1, T2 FIT THE DATA
C       XP(I) = THE PREDCTED PROCESS OUTPUT
C
      FUNCTION ERROR(K, T1, T2)
      REAL K
      COMMON/BLK1/X(200),U(200),XP(200),F(200),INUM,T,N,J,
     1       PINDEX
C
      PINDEX = 0.0
      A1 = EXP(-T/T1) + EXP(-T/T2)
      A2 = EXP(-T/T1) * EXP(-T/T2)
      B1=K*(1.0-A1+(T1*EXP(-T/T2)-T2*EXP(-T/T1))/(T1-T2))
      B2=K*(A2-(T1*EXP(-T/T2)-T2*EXP(-T/T1))/(T1-T2))
C
      ISTART = N + 2
      IFIN = INUM + N
C
C     NOTE THAT THE DELAY TERM HAS ALREADY
C     INCLUDED THE SAMPLE DELAY
C     OF '1'
C
      DO 10 I = ISTART, IFIN
       XP(I)=A1*XP(I-1)-A2*XP(I-2)+B1*U(I-N)+B2*U(I-N-1)
        E = X(I) - XP(I)
        PINDEX = PINDEX + E * E
   10 CONTINUE
C
      ERROR = PINDEX
C
      RETURN
      END
```

```
C
C
C   THIS IS PART OF THE DSC SEARCH..
C
C      THIS SUBROUTINE FINDS "XSOPT(L)"
C    WHICH IS THE PSEUDO-OPTIMUM VALUE
C      OF THE PARTICULAR VARIABLE BEING SEARCHED
C           L=1 ( K IS THE SEARCHED VARIABLE )
C           L=2 ( T1 IS THE SEARCHED VARIABLE )
C           L=3 ( T2 IS THE SEARCHED VARIABLE )
C
      SUBROUTINE DSC(L)
      REAL K
      COMMON/BLK1/X(200),U(200),XP(200),F(200),INUM,T,N,J,
     1       PINDEX
      COMMON/BLK2/XAOPT(3),XBOPT(3),XCOPT(3),XSOPT(3),
     1 FBOPT(3),FCOPT(3),FSOPT(3),XMM2,XMM1,XM,XMP1,FMM2,
     2 FMM1,FM,FMP1,DK,K,T1,T2,PREOPT,FREOPT,FAOPT(3)
C
      IF (FMM1 .GE. FMP1) GO TO 10
      XAOPT(L) = XMM2
      XBOPT(L) = XMM1
      XCOPT(L) = XMP1
      FAOPT(L) = FMM2
      FBOPT(L) = FMM1
      FCOPT(L) = FMP1
      GO TO 15
   10 XAOPT(L) = XMM1
      XBOPT(L) = XMP1
      XCOPT(L) = XM
      FAOPT(L) = FMM1
      FBOPT(L) = FMP1
      FCOPT(L) = FM
   15 ANUM = (DK/2.0) * (FAOPT(L) - FCOPT(L))
      DENOM = 2.0 * (FAOPT(L) - 2.0*FBOPT(L) + FCOPT(L))
      XSOPT(L) = XBOPT(L) + (ANUM/DENOM)
      FSOPT(L) = 1.0E6
      IF (XSOPT(L) .LE. 0.0) GO TO 40
      IF(L-2 .GE. 0 .AND. XSOPT(L)/T .LT. 0.0145)GOTO 40
      IF (L - 2) 20, 25, 30
   20 FSOPT(L) = ERROR(XSOPT(L),T1,T2)
      GO TO 35
   25 FSOPT(L) = ERROR(K,XSOPT(L),T2)
      GO TO 35
   30 FSOPT(L) = ERROR(K,T1,XSOPT(L))
   35 IF (FSOPT(L) .LE. FREOPT) GO TO 45
   40 XSOPT(L) = PREOPT
   45 RETURN
      END
```

Appendix C

Figure Nomenclature

The figures presented in this work were labeled with a standard set of nomenclature. Refering to Figure C.1 the plots are identified as:

A Controlled variable, top composition weight percent methanol (XD(WT% MEOH)).

B Manipulated variable, for top loop control; reflux flow (RE(G/S)).

C Disturbance, feed flow grams/second (FE(G/S)).

D Performance criteria, top loop integral of absolute error (IAE).

E Controlled variable, bottom composition weight percent methanol (XB(WT% MEOH)).

F Manipulated variable, for bottom loop control; steam flow grams/second (ST(G/S)).

G Disturbance, feed flow grams/second (FE(G/S)).

H Performance criteria, bottom loop integral of absolute error (IAE).

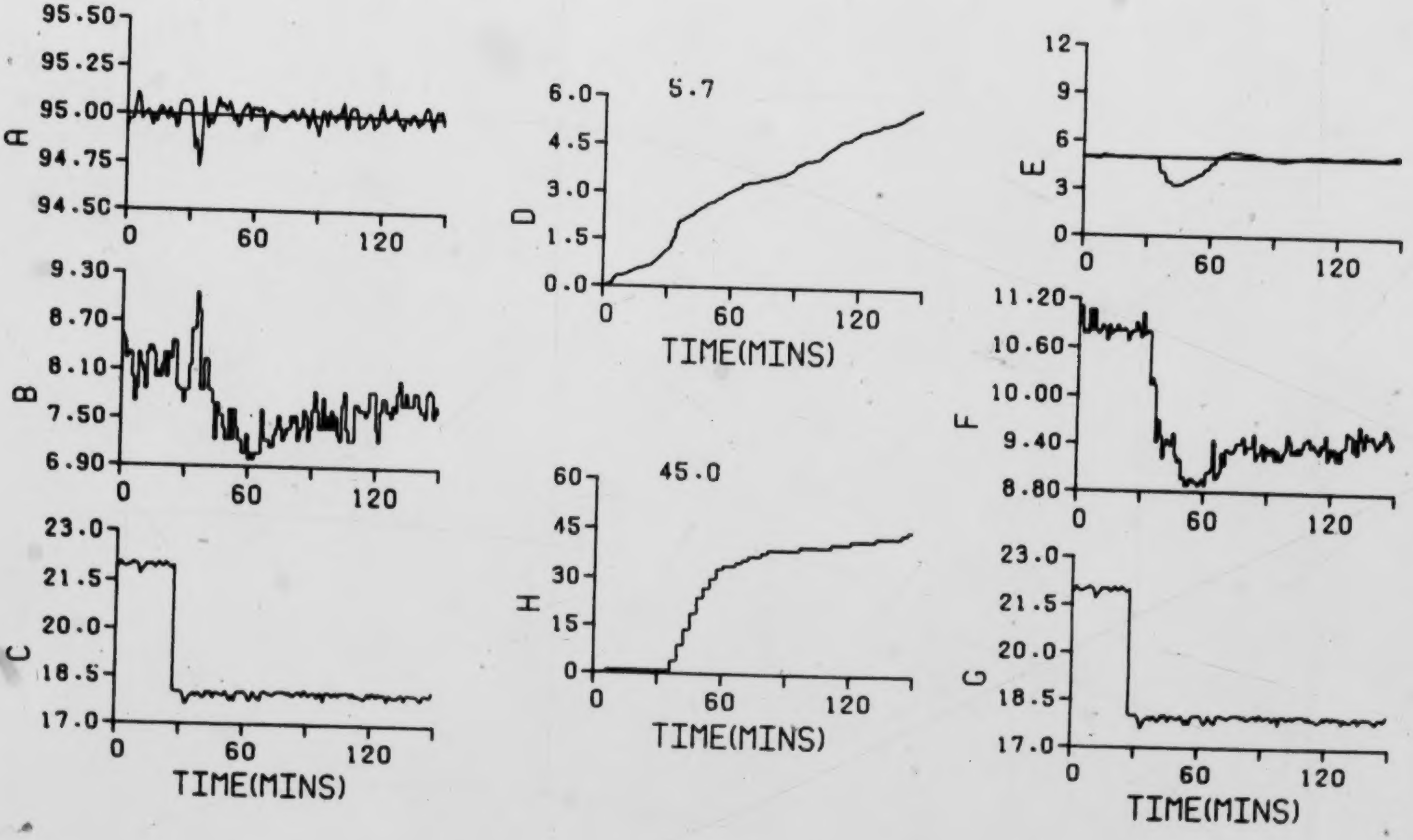

FIGURE C.1 TITLE AREAS (1) / (2) / (3) / (4) /
(5) / (6) / (7) /

Refering to Figure C.1 the title of the plots are defined in the following format, with each of the seven areas of the title defined by:

1. This area indicates the figure number and description of the control used for the particular plot. The following abbreviations were used:

ML	Multiloop Control Strategy: Single rate sampling
MV	Multivariable: Single rate sampling
MR	Multirate Sampling

Design Method:

Z-N	Ziegler-Nichols
3-C	Cohen-Coon
IAE	Integral of Absolute Error
ITAE	Integral of the Time Multiplied by the Absolute Error

Where no design method is indicated, the results presented are for tuned control.

Type of control:

PID	Conventional proportional integral derivative control
ST	Self-tuning control
KINC ST	K-Incremental self-tuning control
MFF	Measured feedforward compensation added

The title is presented in a two line format. The first line presenting the type of control used for the column as well as information regarding the control of the top loop. The second line indicates the information for the bottom loop control.

Refering to Figure C.1 the information in the title for areas 2 through 7 are defined by:

2 and 5 Controller settings for PID control, specifically the values of the proportional band(PB), integral time(TI), and derivative time(TD). For self-tuning control these values indicate the parameters used for the Q weighting.

3 and 6 Sample time for top and bottom loops respectively.

4 and 7 For self-tuning controllers only. This area specifies the number of parameters used in each of the controller polynomials. 5 integers are specified, with their associated polynomials in left to right order:

$\mathbf{G}_{ii}$ parameters
$\mathbf{F}_{i}$ parameters
$\mathbf{L}_{i}$ parameters
$\mathbf{H}_{i}$ parameters
$\mathbf{G}_{ij}$ parameters

For PID control areas 4 and 7 are ommitted.